ABSTRACT

Title of dissertation: EFFECTS OF AGING AND MODERATE CALORIE RESTRICTION ON THE REPRODUCTIVE AXIS OF THE MALE RHESUS MACAQUE (MACACA MULATTA)

Brandon Dale Sitzmann, Doctor of Philosophy, 2007

Dissertation directed by: Professor Mary Ann Ottinger
Department of Animal and Avian Sciences

Calorie restriction (CR) has been established as the only non-genetic method of altering longevity and attenuating biological changes associated with aging. This nutritional paradigm has been effective in nematodes, flies, rodents, dogs and possibly non-human primates. Its long history notwithstanding, little is known regarding the exact mechanism(s) of CR action or its potential impact on the hypothalamic-pituitary-gonadal (HPG) axis. The objectives of this project were to: 1) analyze neuroendocrine changes to the HPG axis that occur with aging and 2) evaluate the effects of moderate CR on reproductive function in male rhesus macaques.

Pituitary gene expression profiling, semi-quantitative RT-PCR (sqRT-PCR) and immunohistochemistry showed circadian clock mechanism components present in three age categories of macaques, demonstrated age differences in expression for *Per2*, indicated differential expression of *Per2* and *Bmal1* at

opposing time points and revealed daily rhythmic expression of REV-ERBα protein. These data indicate the ability of the macaque pituitary to express core-clock genes, their protein products, and to do so in a 24-hour rhythm.

Young Adult CON and CR pituitary gene expression profiles detected potential differential expression in <150 probesets. A decline in *TSHR* and *CGA* was detected in CR macaques as measured by sqRT-PCR. Other genes investigated showed no diet-induced changes.

Young Adult CON and CR testicular gene expression profiles detected potential differential expression in <300 probesets although mRNA expression was not altered based on sqRT-PCR and real-time RT-PCR. Age-related and/or diet-induced changes in *HSD17β3*, *INSL3*, *CSNK1E* and *CGA* were observed in a separate experiment with *CGA* in Old Adult CR subjects returning to youthful levels.

Semen samples were collected from Young Adult CON and CR macaques. Normal spermiogram measures, ZP-binding, AR assay and SCSA® were conducted and indicated no differences between CON and CR-treated animals. Both groups exhibited similar daily testosterone profiles with no differences in mean or maximum levels; however, daily minimum testosterone levels were lower in CON animals.

It appears that moderate CR had limited impact on neuroendocrine or reproductive function in male rhesus macaques based on our selected endpoints. Thus, advantageous CR health benefits can be achieved without obvious negative consequences to the HPG axis.

EFFECTS OF AGING AND MODERATE CALORIE RESTRICTION ON THE REPRODUCTIVE AXIS OF THE MALE RHESUS MACAQUE (MACACA MULATTA)

By

Brandon Dale Sitzmann

Dissertation submitted to the Faculty of the Graduate School of the
University of Maryland, College Park, in partial fulfillment
of the requirements for the degree of
Doctor of Philosophy
2007

Advisory Committee:

Professor Mary Ann Ottinger, Chair
Dr. Donald K. Ingram
Professor Tom E. Porter
Dr. Henryk F. Urbanski
Professor Gerald S. Wilkinson

For Holly, who never stopped believing.

Acknowledgements

My wife, Holly, and I like to say that this year was my 25th anniversary. Not our anniversary, but mine. As I finish this dissertation I end a 25 year path of formal education. What began in kindergarten has now been completed with this degree; and except for four years where, as my friends tell me, I actually worked, I have been 'in school' that entire time. Holly knows this better than anyone since in the 16 years we have been together I have been working toward a degree of some kind for 12 of them. The last few years I found it incredibly funny to call her at the beginning of each school year and laugh that it was another first day of school. I don't think she found the joke as funny as I did. Despite my bad sense of humor she has been my partner throughout and always given me nothing less than her enduring faith, limitless understanding, constant encouragement, saintly patience and everlasting love. That is why I thank her first and foremost; without her I could never have achieved this or any other goal in my adult life. She has been my greatest supporter and my harshest critic, and for that I thank her. I love you, Holly.

Next, I must thank my parents, who instilled in me the importance of education and supported me along whatever path I chose. More than that, however, they taught me that passing through adversity gives you strength as a person. For all my flaws I have always tried to grow during the good and bad situations in my life and have become a better individual for it.

To the rest of my very extended family, you have all brought me great strength and happiness in my life. From sibling to grandparent to in-law, each of you has contributed to the person I have become and for that I am eternally grateful. While everything else may change in my life, family is forever.

I have been very fortunate to have had two outstanding advisors during my doctoral labors, Dr. Mary Ann Ottinger and Dr. Henryk Urbanski. As mentors and friends you have encouraged me every step of the way and in the process enabled me to become a more confident and competent scientist. You have given me opportunities, your trust, and most importantly, the freedom to pursue a path that many students never enjoy.

I want to acknowledge my committee. Dr. Donald Ingram, for entrusting such a large component of his life's work to me and always expecting the best in return. Dr. Jerry Wilkinson, for keeping me grounded in the big picture and asking the good questions. Dr. Tom Porter for reminding me that research should be fun. Thank you for your willingness, recommendations and advice during this long journey.

Throughout my academic career I have been exposed to many wonderful educators and it would be a great injustice if I did not mention a few who helped me at crucial times in my life. Mr. Richard Sievert, for his unconventional approach and innate ability to connect with students. Dr. Richard Kowles, for his wit and presence in the classroom; I could not have asked for a better mentor or example of what it means to be a teaching professor. Dr. Arthur and Mrs. Rosamond Spring, who showed me how to connect all things great and small.

Dr. Alan Hunter, for befriending me at a difficult time and enabling me to complete my masters degree. Dr. Mark Varner, who challenged me as a teaching assistant and broadened my approach to working with students.

A special note of thanks to the incredible people I have met while working in Oregon; I have grown professionally and personally under your influence. Dr. Mary Zelinski, the most optimistic person I have ever known; Dr. Jodi Downs, who can always find good in any situation; Dario and Lula Lemos, true examples of finding balance in life; Bill Garyfallou, my debating partner with whom I may never agree but always respect; Nigel Noriega, whose laugh can light up a room; and Roberto Curilovic and Nick Wallingford, your comraderie and our Wednesday night (into Thursday morning) card games meant a great deal to me while so far away from home. These meager words can not adequately express how much you all mean to me.

Finally, to all my past and present lab colleagues, especially Dr. Mike Quinn, Dr. Julie Wu and Sara Pollack. I escaped my fourth floor exile only to leave for St. Louis and Oregon, but I will always be grateful for your friendship and support.

Thank you all.

Table of Contents

List of Tables

List of Figures

Abbreviations

ACTH	adrenocorticotropic hormone
AD	Alzheimer's disease
AGPAT3	1-acylglycerol-3-phosphate O-acyltransferase 3
AR	acrosome reaction
ART	assisted reproductive technologies
BMI	body mass index
BN	Brown Norway
BSA	bovine serum albumin
CART	cocaine- and amphetamine-regulated transcript
CCND2	cyclin D_2
CGA	glycoprotein hormone common alpha subunit
CK1E	casein kinase 1 epsilon
CON	control
COX2	cyclooxygenase 2
CR	calorie restriction
cDNA	copy deoxyribonucleic acid
cRNA	copy ribonucleic acid
CRY	Cryptochrome proteins
CSNK1E	casein kinase 1 epsilon
CYP11A1	cytochrome P450, family 11, subfamily A, polypeptide 1; side-chain cleavage; $P450_{scc}$
CYP17A1	cytochrome P450, family 17, subfamily A, polypeptide 1; $P450_{c17}$
dbcAMP	dibutyryl adenosine 3',5'-cyclic monophosphate
DFI	DNA fragmentation index
DNA	deoxyribonucleic acic
FITC	fluorescein isothiocyanate
FSH	follicle-stimulating hormone
$GABA_A$ β_1	gamma-aminobutyric acid
GH	growth hormone

GnRH	gonadotropin-releasing hormone
hnRNP-K	heterogeneous nuclear ribonucleoprotein K
HOS	hypo-osmotic swelling
HPA	hypothalamic-pituitary-adrenal
HPG	hypothalamic-pituitary-gonadal
HSD3β2	hydroxysteroid (3-beta) dehydrogenase 2
HSD17β3	hydroxysteroid (17-beta) dehydrogenase 3
ICSI	intracytoplasmic sperm injection
IGF-1	insulin-like growth factor 1
IHC	immunohistochemistry
INSL3	insulin-like factor 3
IVF	*in vitro* fertilization
J	Juvenile
LH	luteinizing hormone
LHCGR	luteinizing hormone/choriogonadotropin receptor
MAR	microwave antigen retrieval
mRNA	messenger ribonucleic acid
NCBI	National Center for Biotechnology Information
NHP	non-human primates
NIA	National Institute on Aging
NIH	National Institutes of Health
OA	Old Adult
OACR	Old Adult Calorie Restricted
OHSU	Oregon Health and Science University
ONPRC	Oregon National Primate Research Center
PER	Period proteins
PES	penile electrostimulation
PFK	phosphofructokinase
POMC	proopiomelanocortin
qRT-PCR	quantitative real-time reverse transcriptase polymerase chain reaction

RHT	retinohypothalamic tract
RMA	robust multi-array average
RNA	ribonucleic acid
RIA	radioimmunoassay
ROR	retinoic acid-related orphan receptors
RORE	retinoic acid-related orphan receptor response elements
ROS	reactive oxygen species
RT	room temperature or reverse transcriptase
SCN	suprachiasmatic nucleus
SCSA®	sperm chromatin structure assay
SEM	standard error of the mean
SER	smooth endoplasmic reticulum
SOD	superoxide dismutase
sqRT-PCR	semi-quantitative reverse transcriptase polymerase chain reaction
SSFA2	sperm-specific antigen 2
StAR	steroidogenic acute regulatory protein
T	testosterone
T_3	triiodothyronine
TSH	thyroid-stimulating hormone
TSHR	thyroid-stimulating hormone receptor
UCP2	uncoupling protein 2
YA	Young Adult
YACON	Young Adult Control
YACR	Young Adult Calorie Restricted
ZP	zona pellucida

CHAPTER 1

GENERAL INTRODUCTION

The past two decades have seen an upward trend in the average age of couples having children (Buwe et al., 2005). The average age of motherhood in the United States has increased from 21.4 years in 1971 to an all time high of 25.1 years. Although some of this demographic shift can be attributed to lower teen birth rates, much of it is due to an increase in older women having children. Women between the ages of 35-45 years now have children at the highest levels in three decades (Thacker, 2004). Paralleling this rise, since 1980 there has been a 16-24% increase in the birth rate for U.S. fathers over age 35 years (Buwe et al., 2005; Eskenazi et al., 2003; Kidd et al., 2001). The increase in older adults having children can be traced to a number of factors. The two biggest contributors, however, are socioeconomic pressures and the implementation of assisted reproductive technologies (ART) (Plas et al., 2000). This reality has driven a subsequent interest in understanding better the consequences of normal reproductive aging in both genders.

The hypothalamic-pituitary-gonadal axis (HPG) is central to reproductive function and retains remarkable similarity across higher order taxa (Everett, 1994). After a period of latency early in life, the axis becomes activated at puberty. A period of reproductive maturity and activity follows, after which there is a period (variable in length) of reproductive senescence and loss of function. Reproductive decline during aging is observed in a wide variety of species

including fish, mollusks, rodents, rabbits, dogs, whales, elephants, domestic livestock and non-human primates. This decline, however, is not uniform and can vary depending on species and gender (Austad, 2001; Kirkwood and Austad, 2000; Packer et al., 1998).

The male primate HPG axis (Figure 1.1) appears particularly resilient and overt reproductive decline is almost negligible, as compared to females who undergo menopause. Subtle alterations do occur, however, resulting in decreased testosterone (T) levels and increased sperm abnormalities over time. Using rhesus macaques as a model, it was our intention to investigate these age-related changes in order to gain a better understanding of overall decline to the system. In addition, we were interested in examining the potential effects of calorie restriction on normal reproductive function and its subsequent decline with age.

General Aging

The original search for a unifactorial cause of aging such as a gene or decline of a major body system has since been replaced with the view that aging is a complex multifactorial process (Weindruch and Walford, 1988; Weinert and Timiras, 2003). The cascade of events that leads to normal aging may interact simultaneously at the molecular, cellular and systemic level. When these physiological systems go awry, the result is a disruption of functional organization that inhibits the organism's ability to respond to stress. Aging then becomes the manifestation of this gathering disarray of systemic function leading to

homeostatic imbalance, pathology and ultimately death (Weindruch and Walford, 1988). Put another way, aging is the progressive loss of function (including reproductive capacity) accompanied by increasing incidence of disease and mortality (Kirkwood and Austad, 2000).

A few examples of age-related homeostatic imbalance include decreased stress response, increased pathology, decline in memory function and documented alterations in circadian organization, such as changes in hormonal rhythms, core body temperature, sleep/wake cycles, and response to the phase-shifting effects of light (Asai et al., 2001; Hofman and Swaab, 2006; Oster et al., 2003). Although the physiological underpinnings remain unclear for many of these parameters, studies of circadian function suggest that the amplitude of the hypothalamic circadian pacemaker is decreased in older animals (Kolker et al., 2003) while some findings have shown deterioration of transcription and rhythmicity in peripheral tissues, including lung and aortic/cardiac muscle cells (Kunieda et al., 2006; Yamazaki et al., 2002).

There are a host of theories that attempt to explain normal aging. They can often be categorized into evolutionary, molecular, cellular and systemic theories. Several of them will be briefly summarized, including the Disposable Soma Theory, Gene Regulation Theory, Free Radical Theory and Neuroendocrine Theory. Each may adequately describe some or all of the observed aging processes alone or in combination with other theories (Kirkwood and Austad, 2000; Weinert and Timiras, 2003).

Disposable Soma Theory

The Disposable Soma Theory proposes that lifespan is dictated by life history trade-offs involving optimal allocation of metabolic resources between somatic maintenance and reproduction (Kirkwood and Austad, 2000). Selective pressures have incredible power to shape life history patterns over evolutionary time, especially when imposed during juvenile or early adult development. These forces can ultimately lead to large species differences in the age of sexual maturation, size and spacing of litters and the age at which fecundity begins to fall. Genetic loci responsible for these parameters are likely to be important mediators that allow organisms to adapt to situations where changes in intrinsic mortality rate permit a decelerated life history schedule. In other words, animals may have the innate ability to shift metabolic resources from growth and reproduction to improved somatic maintenance and repair when forces of extrinsic mortality are lessened (Kirkwood and Austad, 2000; Miller et al., 2002). Such a shift would effectively slow aging and prolong disease resistance and health. Lifespan thus becomes a species specific function of survivability and reproductive strategy in a competitive environment; the balance of resources invested in longevity versus reproduction determines lifespan. Organisms that die primarily from predation and environmental interactions will evolve a lifespan optimal for their own particular niche (Weinert and Timiras, 2003). The Disposable Soma Theory explains why an organism lives for a given period of time, but it makes no attempt to explain the underlying molecular nature of aging. It may be that the genes responsible for regulating key life history events may

exact their effect through hormonal and other developmental pathways (Miller et al., 2002; Weinert and Timiras, 2003). In this regard, this theory overlaps with the second theory, Gene Regulation.

Gene Regulation Theory

The Gene Regulation Theory proposes that senescence results from changes in gene expression. Selective pressures would give an organism a distinct advantage if it was able to utilize genes that promote longevity (Weinert and Timiras, 2003). The recent development of microarray technology has allowed for the transcriptional profiles of normal aging in a wide variety of species. The resulting data can then be compared to profiles generated by interventions intended to slow or accelerate aging. By making such comparisons gene expression changes can be identified which may help unlock the key genetic components to aging systems. One example of this is the identification of an insulin-like signaling pathway or its homolog that can modify lifespan in yeast, nematodes, flies and mice (Kenyon, 2001; Weinert and Timiras, 2003). Lifespan extension results from the activation of a conserved transcriptional factor following insulin-like signaling reduction. This model indicates that gene expression can regulate lifespan. Whether this system or an analogous system is conserved in longer lived model organisms remains to be determined. And while regulation of gene expression may start the cascade, lifespan extension in this system may actually be the result of delayed reproduction and stress resistance,

particularly to reactive oxygen species (ROS). Both these responses are observed in these models (Kenyon, 2001).

Free Radical Theory

The Free Radical Theory proposes that aging is caused by cumulative oxidative damage generated by free radical-containing ROS produced during normal cellular respiration (Koubova and Guarente, 2003; Weinert and Timiras, 2003). Free radicals are highly reactive molecules that carry an unpaired electron on their surface. They are prone to indiscriminately and destructively oxidize any compound they encounter. Because approximately 90% of cellular oxygen is consumed in the mitochondria, and 3% of molecular oxygen reduced by mitochondria is not reduced to water, mitochondria may be the major intracellular contributor to superoxide ($O_2^{-\cdot}$) generation and to oxidative stress in general (Huang and Manton, 2004). The Mitochondrial Theory of aging, a variant to the Free Radical Theory, suggests that accumulation of damage to mitochondria, mitochondrial DNA, and RNA specifically leads to aging in humans and animals (Weinert and Timiras, 2003). A growing body of evidence and experimental support implicates mitochondrial derived ROS as a major cause of cellular decline. A direct relationship between individual age, species longevity and rate of mitochondrial ROS production has been documented (Gredilla and Barja, 2005; Kirkwood and Austad, 2000; Weinert and Timiras, 2003). Production results from leakage of the mitochondrial electron transport chain under normal aerobic conditions in the cell. Usually the organism's own antioxidant defenses

eliminate the resulting superoxide anion by converting it into hydrogen peroxide (H_2O_2) via superoxide dismutase (SOD). Catalase then converts H_2O_2 to molecular oxygen and water. This defense, however, is not always completely effective. Excessive ROS production may overwhelm the antioxidant capacity of cells thereby initiating a pathogenic cascade of events. In addition, age-related impairment in respiratory enzymes decreases ATP synthesis and enhances ROS production by increasing electron leakage in the respiratory chain (Huang and Manton, 2004).

Neuroendocrine Theory

The Neuroendocrine Theory proposes that aging is a result of neural and endocrine functional changes which are crucial for 1) coordinated communication and response of an organism to its environment, 2) programming physiological responses to that environment, and 3) maintaining an optimal functional state to balance reproduction and survival while responding to environmental needs (Weinert and Timiras, 2003). A major component of this theory is the perception of the hypothalamus and pituitary gland as critical pacemakers of the system. These two organs occupy a unique niche within the neuroendocrine system by acting as a connecting point between reproduction (via the HPG axis) and stress response (via the hypothalamic-pituitary-adrenal axis; HPA). In this regard the neuroendocrine theory is really a more holistic approach which recognizes that aging must depend more on interrelations between hormonal and neural signals than on isolated endocrine reactions. The interplay between the components of

the HPG/HPA axes, in which aging may change responses but where it is difficult to decide which comes first, is a good example of the quandary of neuroendocrine aging. It illustrates why studies of reproductive senescence, which at first may seem of rather secondary interest with respect to 'true' senescence, remains a fertile field for aging research (Weindruch and Walford, 1988).

Overview of Reproductive Decline

In humans, female fertility can begin to decline in early thirties and culminates with complete reproductive quiescence at approximately 50 years of age (Buwe et al., 2005; Kidd et al., 2001). Thus, female aging leads to complete elimination of reproductive potential thought to stem from the dramatic loss of ovarian follicles. Reproductive aging in men typically follows a more gradual course than in females. The age-related demise seen in male reproduction may be due to functional deterioration of the system at several sites including testosterone synthesis in the Leydig cells, hypothalamic production of gonadotropin-releasing hormone (GnRH), pituitary gland release of gonadotropins and/or other integrative neuroendocrine components that impact the HPG axis as a whole (Harman et al., 2001; Moffat et al., 2002; Ottinger, 1998). Still, men generally do not undergo an unavoidable and distinct cessation of reproductive capacity as spermatogenesis continues well into old age with no known critical threshold with respect to sperm production (Buwe et al., 2005; Henkel et al., 2005; Kidd et al., 2001). The oldest documented paternity has been

reported in a 94-year-old man (Plas et al., 2000). This does not mean, however, that there are no physiological changes.

One consequence of reproductive decline in men and women can be infertility, which has a major impact on public health. In the United States approximately 15% of couples of reproductive age will experience difficulty conceiving and approximately 7% of married couples are not able to conceive after trying for a year (Eskenazi et al., 2003; Kidd et al., 2001). Depending on the figures used, the proportion of infertility that is attributable to male factors ranges from 25-50%, making it the single most common cause of infertility in clinical cases (Agarwal and Said, 2003; Eskenazi et al., 2003; Kidd et al., 2001; Larson-Cook et al., 2003). In addition, the risk of spontaneous abortion is almost twice as high among men older than 45 years of age than among those aged less than 25 years, even after adjusting for maternal age (Slama et al., 2005). The question of how paternal age influences fertility and reproductive outcome is not easily defined nor easily answered since there are no longitudinal studies. Instead, the alterations of semen parameters in the aging male are almost always described on the basis of cross-sectional sampling (Plas et al., 2000). Several recent studies, however, have shown that many aspects of male fertility are affected by aging (Henkel et al., 2005; Kidd et al., 2001; Zubkova and Robaire, 2006).

In addition to age, external cues such as nutrition can have a substantial impact on the HPG axis of both genders. The recent phenomenon of increased average body mass index (BMI) experienced by the Western world has resulted in an increased incidence of obesity (BMI>25 kg/m^2). The risk for increased BMI

typically increases as people get older so that reproductive capacity is not only impacted negatively by age but also by the pathologies often associated with obesity. In women, excessive amount and distribution of body fat has been previously linked to reduced fertility with prolonged time to pregnancy, increased risk of irregular menstrual cycles, preterm delivery, spontaneous abortion, stillbirths and birth defects (Fejes et al., 2005; Jensen et al., 2004; Kort et al., 2006). Men with BMI>25 kg/m^2 had lower sperm concentration and total sperm count compared to men with non-obese BMI (Jensen et al., 2004) while another study looked at 520 normal, healthy men, age 26-45 and found an inverse relationship between BMI and total number of motile sperm cells and a positive relationship between BMI and sperm DNA fragmentation per subject (Kort et al., 2006).

Male Reproductive Aging

First and foremost, there is a documented decline in testosterone (T) production beginning after 30 years of age and continuing gradually for life (Hardy and Schlegel, 2004; Henkel et al., 2005; Ottinger, 1998; Stocco and Wang, 2006; Zirkin and Chen, 2000). Observations from the Massachusetts Male Aging Study show that total testosterone, often called the male hormone because of its ability to masculinize an organism, decreases 0.4-0.8% annually while biologically active free T serum levels decrease by 1.2-1.7% per year starting at the age of 50 (Henkel et al., 2005; Plas et al., 2000). In men, testosterone is responsible for regulation of gonadotropin secretion by the hypothalamic-pituitary

system and predominantly drives production of spermatozoa. Consequently there is the potential for a cascade effect to the entire reproductive system with its fall. Testosterone decline can also result in weakening muscle function, bone density and other physiological parameters related to overall aging (Harman et al., 2001; Moffat et al., 2002).

The decline in circulating testosterone levels would be expected to stimulate increased GnRH production by the hypothalamus followed by increased production of luteinizing hormone (LH) at the level of the pituitary gland. Yet despite the loss of negative feedback, LH levels can reportedly respond with slight non-significant increases, unchanged levels, or non-significant decreases (Hardy and Schlegel, 2004; Ottinger, 1998; Zirkin and Chen, 2000). In contrast, follicle-stimulating hormone (FSH) increases due to loss of gonadal inhibin feedback from the Sertoli cells (Ottinger, 1998; Zirkin and Chen, 2000). Although T declines it may not be the best measure of general male aging since differences between young and old men are not always significant due to individual variation (Black and Lane, 2002). Such variation is normal and is often observed in biological parameters of this nature (Henkel et al., 2005).

Other parameters of reproductive function and fertility of elderly men have traditionally focused strictly on semen analysis. Classical spermiograms include ejaculate volume, concentration, motility, morphology and count (Plas et al., 2000). For these measures of semen quality, the weight of scientific evidence

suggests that increased male age is associated with decreased reproductive potential.

The majority of studies suggest that there is a significant inverse relationship between semen volume and age (Zubkova and Robaire, 2006). The relative decrease reportedly ranges between 3% and 30% when comparing men ≤30 years of age to men 50 years of age or older (Henkel et al., 2005; Kidd et al., 2001). One small study reported a decrease in semen volume of 0.03 mL per year for men between the ages of 22 and 80 (Eskenazi et al., 2003). Conversely, the weight of evidence from the literature suggests that sperm concentration remains constant or even increases with age (Henkel et al., 2005; Kidd et al., 2001). These two observations, decreased volume and increased concentration, may be due to insufficient functioning of the accessory sex glands, particularly the seminal vesicles, in elderly men (Henkel et al., 2005).

There are very consistent reports of significantly lower sperm motility in the range of 3-37% when comparing men ≥50 years to men ≤30 years of age (Kidd et al., 2001; Zubkova and Robaire, 2006). Overall, motility can decline 0.7-4.7% per year depending on whether motility, progressive motility, or total progressive motility is measured (Eskenazi et al., 2003). The decrease in overall motility may be correlated with the observed decline of testosterone in older men. The epididymis, which is dependent on testosterone for its function, is intimately involved in sperm maturation and induction of sperm motility. Consequently, decreased concentrations of bioactive free T will lead to epididymal dysfunction and decreased motility (Henkel et al., 2005).

Normal sperm morphology also appears to be negatively correlated with age (Zubkova and Robaire, 2006). In men ≥50 years morphologically abnormal sperm increased 4-22% compared to men ≤30 years old (Kidd et al., 2001). In another retrospective study of 1655 men between the ages of 17 and 66, normal sperm morphology was found to decline 0.47% annually (Henkel et al., 2005).

Sperm count, which is a standard measure in most spermiograms, is generally not considered as good a measure of age as concentration or motility since sperm production is almost always in excess of that needed to realize fertility potential. Subfecund sperm counts are usually the result of some pathological condition. Additionally, there are high intra-individual variations in spermiogram measures obtained on different occasions, consequently cross-sectional studies on single semen parameter determinations must be interpreted with caution (Plas et al., 2000). In general, however, most measures of male reproductive health exhibit no evidence of an age 'threshold' but rather display gradual changes over time (Eskenazi et al., 2003).

More recently a new measure of male fertility that deals with DNA integrity has been investigated. This new assay sets quantifiable levels for reproductive success that are highly correlated with age. The assay takes advantage of the difference between male and female gamete meiotic potential to measure DNA integrity, an essential component for the accurate transmission of genetic information to the offspring. Since spermiogenesis is a continuous process starting during puberty, spermatagonia undergo high numbers of replications and DNA duplications, reaching roughly 150 divisions at the age of 20 years with a

linear increase of ~23 divisions per year thereafter. Thus, spermatogonia of a 28-year-old father may have already undergone ~380 mitoses and DNA replications, which increases to 540 in a 35-year-old male. In contrast, complete oogenesis in female primates occurs prior to birth with relatively constant 22 cell divisions. Due to these high numbers, the risk of transcriptional DNA errors during sperm production increases (Buwe et al., 2005; Plas et al., 2000; Zubkova and Robaire, 2006). The sperm chromatin structure assay (SCSA®) is a flow cytometric technique that uses semen to determine the susceptibility of sperm nuclear DNA to acid-induced DNA denaturation *in situ*. The resulting ratio of denatured single-stranded DNA to total DNA gives a DNA fragmentation index (DFI) expressed as a percentage (Agarwal and Said, 2003; Evenson and Wixon, 2006). In multiple studies DFI levels $\geq$30% have proven incompatible with *in vivo* fertility and *in vitro* ART procedures (Bungum et al., 2004; Larson-Cook et al., 2003). Sperm susceptibility to DNA fragmentation increases with age so the importance of this assay cannot be understated. Overall, about one of 200 human livebirths possess a numerical or structural aberration which may severely affect the mental and physical integrity of a child (Buwe et al., 2005). Paternal (and maternal) age only increases the incidence of these disorders. There are approximately 20 different known genetic disorders correlated with paternal age (Thacker, 2004; Zubkova and Robaire, 2006), while children born to men 50 years or older are three times more likely to develop schizophrenia than children born to men in their early 20's (Thacker, 2004).

Models of Reproductive Aging in Males

The study of aging systems in humans can be very prohibitive due to cost, complex variables in lifestyle and time requirement. Therefore, there is a great need to find appropriate, alternative animal models. The ideal model of male reproductive aging would have similar endocrine and neuroendocrine aspects to human testicular biology. Additionally, if possible, the model should have reproductive traits which can be manipulated in the laboratory, i.e. transgene or natural mutations resulting in accelerated or delayed examples of testicular aging. It is important to be able to compare normal aging to accelerated and/or delayed models as a way of elucidating the aging process as well as the underlying mechanisms contributing to it. Two model systems, each with their own benefits and deficits, have made up the majority of studies.

Rodent Models

The reasons for using rodent models in reproductive aging research are numerous. They are relatively short-lived, inexpensive to maintain and the availability of homogenous laboratory strains permit controlled research experiments. Overall life history, including health and reproductive parameters in rodents, are well characterized. Furthermore, genetic manipulation of specific genes has made it possible to study aspects of reproductive decline in transgenic models. Rodents also parallel many of the normal reproductive deficits observed in aged men.

In the Brown Norway (BN) rat, decreased serum and intratesticular testosterone levels as a result of impaired Leydig cell steroidogenesis have been reported (Chen et al., 2002; Syntin et al., 2001; Zirkin and Chen, 2000). Decline in steroidogenic pathway production within these cells appears to be due to malfunction of the pathway itself rather than a loss of Leydig cell numbers (Chen et al., 1996; Chen and Zirkin, 1999; Zirkin, 2006). Serum LH levels do not decline as a result of steroid loss, but there are measurable changes in LH pulse and interval (Chen et al., 2002). In both humans and rodents, age-related loss in the numbers of spermatogenic cells within the seminiferous tubules begins focally with atrophic tubules often adjacent to tubules exhibiting normal spermatogenesis. Eventually the loss of germ cells will spread throughout the testis causing a progressive loss of testis weight in the rat (Syntin et al., 2001). With increasing age rodent epididymal epithelium acquires morphological hallmarks of decay (Jervis and Robaire, 2003) including significantly greater levels of reactive oxygen species produced by Leydig cell mitochondria when compared to younger males (Chen et al., 2001; Chen et al., 2004). Finally, spermatozoa from older rats have altered chromatin packaging and integrity (Zubkova and Robaire, 2006).

Also of importance is the neurological impact of reproductive decline, specifically of testosterone loss. Recently it has been understood that the brain is androgen-responsive and exhibits age-related T depletion, thus making it vulnerable to senescent effects of androgen loss. Studies show that men with Alzheimer's disease (AD) have significantly lower T levels than aged men without

AD. Importantly, testosterone depletion appears to occur well before clinical and pathological diagnosis of AD, suggesting that low T contributes to AD pathogenesis rather than results from it. This has been verified in 3xTg-AD mice (a triple transgenic mouse model of AD) in which androgen depletion accelerated the development of AD-like neuropathology, both in deposition of β-amyloid plaques and behavioral impairment. These effects were prevented with androgen treatment (Rosario et al., 2006).

There are two reasons, however, why rodents may not be appropriate for the analysis of aging in mammals. Laboratory-adapted stocks of rodents experience selected pressures for rapid maturation and large body size. Along with genetic homogeneity, as a result of decades of structured breeding, the resulting stocks may have lost natural alleles that slow the aging process. As a result, the genetic and physiological mechanisms against late-life diseases and which time mammalian aging may have disappeared (Miller et al., 2002). Secondly, given the complexity of human physiology, it may be more advantageous to study organisms more phylogenetically similar. The best alternative for aging research applicable to human health may then be the use of non-human primates (NHP).

Non-Human Primate Models

The ideal model for investigating reproductive senescence would be actual human subjects since it would permit the most direct application of research into practice. In the past few decades, the increased demand for human

assisted reproductive technology has indeed supported the rapid advancement of research in human reproduction. Unfortunately, much of the demand is the result of postponement of childbearing and the increased incidence of infertility with age. Consequently, much of the information gained is collected at later life stages when reproductive senescence is more advanced. To understand the normal progression of reproductive decline, studies must be undertaken that can follow the entire aging process. In this regard non-human primates, in particular the rhesus macaque (*Macaca mulatta*), make very good models.

Rhesus macaques adapt well to laboratory settings and have been used for the better part of a century in a number of research endeavors. A great deal is known about their general husbandry, nutritional requirements, breeding practices and veterinary care. As normal, healthy rhesus macaques get older, values for routine hematological and blood chemistry variables exhibit notable and likely biologically relevant variations. These age effects most likely reflect normal patterns of change associated with the aging process (Smucny et al., 2001). Most importantly, the rhesus macaque shares 97.5% genetic homology to humans (Gibbs et al., 2007). This close genetic relationship produces a highly similar aging phenotype to humans and has been extensively reviewed elsewhere by Roth et al. (2004). Important parallels exist with regards to metabolism, body composition, cardiopulmonary system, reproduction and behavior. Disadvantages to rhesus macaques as research models include limited availability, cost of procurement and maintenance, risk of disease transmission and welfare requirements. There is also the possible confounding problem of

sub-species designation as there are Chinese-origin and Indian-origin rhesus macaques. And with a maximum lifespan of 40 years, or roughly three times the rate of aging for humans, large investments of time, money and effort are still required for longitudinal studies with this species (Ingram et al., 1990; Roth et al., 2004).

Many fields of human health have indeed benefited from the use of rhesus macaques in research, including the study of female reproductive aging. There is, however, surprisingly little known about the effect of senescence on the male rhesus macaque system. Longitudinal studies are very few and when performed have focused on other systems of interest such as metabolism, immune function or cognitive and neural aging. Some of this can be attributed to the long held misperception that human males do not experience reproductive decline of any consequence.

While there are several reports of semen collection in a number of NHP species (Ji et al., 2001; Morrell, 1997; Platz et al., 1980; Ramesh et al., 1998; Schaffer et al., 1992; Tollner et al., 1990; VandeVoort et al., 1993; Yeoman et al., 1997), these studies are usually cross-sectional in nature. Often they are the result of single or short time-point measures with small sample sizes. Very often such reports come from zoos or research facilities maintaining breeding colonies of animals for ART development. Normally the goal in these settings is successful pregnancy and birth with female gametes receiving higher priority. When there is a problem on the male side, whether due to mate incompatibility, disease, behavior or age, another male is utilized or alternative sperm employed

through the use of cryopreservation. While this may be the most effective way to manage time and resources in these circumstances, it does little to illuminate the problems and mechanisms behind male reproductive decline.

There have been sporadic studies of testosterone measurement in rhesus macaques, but even these are contradictory. Some reports claim non-significant declines in testicular mass, serum T levels and pulsatile T release in aged animals (Black and Lane, 2002; Roth et al., 2004), while others show no evidence of different T levels with age (Mattison et al., 2003; Mattison et al., 2001). This can perhaps be attributed to poor sampling and/or the fact that T levels vary widely amongst individuals, throughout the day and even from day-to-day. It seems, however, that despite the value of rhesus macaques in investigating human systems of health, the area of male reproductive senescence remains wide open for study.

Evaluating Reproductive Aging in Males

When it comes to evaluating male reproductive potential there is no single measure which correlates perfectly with age. Although some, such as the sperm chromatin structure assay, can be highly predictive it is not necessarily an age specific test. And others, such as testosterone measures, take an enormous amount of effort to monitor long term as needed to draw any conclusions. What we are left with is the need for a comprehensive battery of tests which, when taken as a whole, can provide a general idea of reproductive health and ability. Many of these measures and the rationale for them have been previously

mentioned in the section on male reproductive aging or in Table 1.1 on page 40. They include count, concentration, weight, volume, pH, motility and morphology. These are typical spermiogram measures of semen production that are part of any standard fertility clinic or research protocol. There are also dozens of other more extensive tests which are not usually performed unless absolutely necessary due to cost and time constraints. For a review of these techniques see Jeyendran (2003). Four that are worth mentioning specifically, however, include the hypo-osmotic swelling (HOS) assay, sperm chromatin structure assay (SCSA®), zona pellucida binding and acrosome reaction assay (ZP binding and AR), and seminal plasma constituent analysis.

Hypo-osmotic Swelling Assay

One property of any cell membrane is to selectively regulate the movement of molecules across its surface. When exposed to hypo-osmotic conditions the cell will allow water to enter the cytoplasm in an attempt to reach osmotic equilibrium. Spermatozoa display this same ability. It can be assumed that the capacity of sperm to swell in the presence of a hypo-osmotic solution is a sign that membrane integrity and normal functional activity are intact. Membrane integrity is not only important for sperm metabolism, but critically timed changes in membrane properties are required for successful sperm activation, acrosome reaction and binding to the oocyte. Whereas histological techniques and 'live-dead' morphology stains only measure whether the membrane is morphologically intact, the HOS assay evaluates the functional integrity of the sperm membrane

(Jeyendran et al., 1984). This assay is simple to run and demonstrates a high correlation between the percentage of sperm in an ejaculate that are capable of swelling and their ability to undergo activation and/or oocyte binding. As a result, the assay has been applied clinically in human fertility clinics as well as research settings with non-human primates (Jeyendran, 2003; Kholkute et al., 2000; Rutllant et al., 2003).

Sperm Chromatin Structure Assay

The sperm chromatin structure assay (SCSA®) mentioned earlier is the most statistically robust tool used to measure sperm nuclear DNA fragmentation and has proven highly effective in predicting fertility outcome both *in vivo* and *in vitro* (Larson-Cook et al., 2003). Sperm chromatin is normally a highly organized and compact structure. Consisting of DNA and heterogeneous nucleoproteins, it is condensed and insoluble to protect genetic integrity and allow for transport through the male and female reproductive tracts. Accumulating data suggest that alterations in genomic organization of the sperm nuclei are negatively correlated with the fertility potential of sperm. Recent reports by Evenson et al. (2006) have indicated that natural pregnancy is not possible when $\geq$30% of sperm DNA is damaged. It has also been suggested that sperm DNA integrity may be a more objective measure of sperm function compared to standard semen analysis, which can be very subjective and prone to intra- and inter-observer variability (Agarwal and Said, 2003). This is the case with *in vitro* fertilization (IVF) and intracytoplasmic sperm injection (ICSI), where basic semen parameters are not

sufficient to evaluate with precision sperm performance and may result in failure to form viable embryos even though sperm could fertilize the oocyte and trigger early preimplantation development. Findings such as these suggest that pathologically increased sperm DNA fragmentation is one of the main paternally derived causes of repeated assisted reproductive failures with ICSI (Tesarik et al., 2006).

Of particular interest is the ability for SCSA® to distinguish between normal DNA degradation and that caused by exposure to ROS. Programmed cell death (apoptosis) is a physiological process in the seminiferous tubules and appears necessary for normal spermatogenesis, probably because it maintains an optimal cell number ratio between individual germ cell stages and Sertoli cells. In one study of 36 normal men between the ages of 53 and 88, accelerated apoptosis of primary spermatocytes was determined to be one of the causes of germ cell loss with aging (Kimura et al., 2003). Unlike apoptotic activity found in aging, the mechanisms of DNA damage detected in ejaculated sperm is related to oxidative damage brought about by ROS present in the fluid filling the male genital tract. Antioxidant treatment orally has been shown to reduce the percentage of DNA fragmented sperm markedly (Tesarik et al., 2006).

Zona Pellucida Binding and Acrosome Reaction Assay

Eutherian spermatozoa cannot penetrate the zona pellucida (ZP), or glycoprotein membrane surrounding the oocyte, immediately after ejaculation. Instead, a final stage of maturation, termed capacitation in which sperm acquire

the ability to undergo the acrosome reaction, is required (Mortimer, 1994; Yanagimachi, 1994). Capacitation regulates the induction of the acrosome reaction and is marked by hyperactivation in motility of the sperm. The sequence of events leading to *in vivo* fertilization can thus be expressed as: ejaculation → capacitation → ZP binding → acrosome reaction →

oocyte penetration → fertilization. An *in vitro* assay has been developed which quantifies the ability of collected sperm to complete this sequence (Jeyendran, 2003; VandeVoort et al., 1992).

In vivo capacitation normally occurs within the female reproductive tract, and while human sperm will spontaneously activate *in vitro*, rhesus macaque spermatozoa will not. Capacitation of rhesus macaque sperm *in vitro* is facilitated by exposure to two activators: caffeine and dbcAMP (VandeVoort et al., 1994). When capacitated sperm are exposed to whole oocytes or zona pellucida membranes *in vitro*, ZP binding will occur. This binding acts as a signal to induce the sperm acrosome reaction.

The acrosome is a membrane bound, hydrolytic enzyme-containing organelle that overlies the anterior end of the sperm head. Following ZP binding but prior to actual fertilization, the outer acrosomal membrane fuses with the surrounding sperm plasma membrane resulting in formation of vesicles. The hydrolytic contents of the acrosome are then released through holes between the fused membranes and allow the underlying plasma membrane to fuse with the inner vitelline membrane of the oocyte. This fusion allows the sperm to eventually penetrate and fertilize the oocyte.

Almost all rhesus macaque sperm are intact upon ZP binding and although they will bind when exposed to heterologous or homologous ZP proteins *in vitro*, they will only acrosome react when exposed to a homologous sperm-ZP interaction (VandeVoort et al., 1992; VandeVoort et al., 1994). The ZP-induced acrosome reaction occurs rapidly (VandeVoort et al., 1994), and unlike humans where acrosome-reacted sperm can still bind, if rhesus macaque sperm acrosome react prior to interaction with the oocyte, their binding capacity is significantly reduced (VandeVoort et al., 1997). Because zona pellucida binding and the acrosomal reaction occur on the external surface of the oocyte and activated sperm head, respectively, these processes can be microscopically observed and quantified using dual fluorescent staining.

Seminal Plasma Constituent Analysis

Much effort has focused on measures of sperm integrity and yet sperm only make up 1% to 5% of the total volume of an ejaculate (Owen and Katz, 2005). The remaining volume consists of a large number of varied constituents secreted by the accessory sex glands; mainly the bulbourethal gland, seminal vesicles and prostate. These constituents include potassium, semenogelin, bicarbonate, fructose, magnesium, prostaglandins, ascorbic acid and proteins from the seminal vesicles and calcium, zinc, citric acid, prostate-specific antigen and albumin from the prostate (Jeyendran, 2003; Mortimer, 1994). In the primate the bulbourethal gland contributes minimally to overall semen volume but is

believed to aid in the lubrication of the urethra in the first stage of ejaculation (Harrison and Lewis, 1986).

Since the seminal vesicles and prostate contribute approximately 60% and 25% of the seminal plasma volume, respectively, it is of great interest to determine if these glands are functioning properly (Gonzales, 2001; Owen and Katz, 2005). Seminal vesicle secretion is important for sperm metabolism, semen coagulation, sperm motility, stability of chromatin and suppression of immune activity in the female reproductive tract (Gonzales, 2001; Lewis-Jones et al., 1996). Specifically fructose, the major carbohydrate in human semen, has been reported to be a source of energy for the motile sperm (Elzanaty et al., 2002; Lewis-Jones et al., 1996). As a result, the measurement of seminal fructose has been used in most fertility labs worldwide and by the World Health Organization as a marker of seminal vesicle function (Gonzales, 2001; Harrison and Lewis, 1986).

In the rhesus macaque, secretion from the cranial lobe of the prostate mixes with fluid from the seminal vesicles to bring about coagulation of the seminal plasma following ejaculation (Harrison and Lewis, 1986). Prostate derived citrate is one of the most important anions present in human semen and is probably responsible for regulating ionized calcium levels in the seminal plasma. It may also be responsible for the high buffering capacity of semen which allows sperm to survive in the acidic vaginal environment until it can enter the neutral pH cervical mucus (Owen and Katz, 2005). Determination of fructose

and citric acid concentration is, therefore, one of the major methods for evaluating human seminal vesicle and prostatic function.

Finally, reference should be made to gene microarray technology. For many years the theoretical application of microarray technique held great promise, but only in the last few years has its practical application expanded as genetic sequencing of whole species genomes has been achieved. It has been less than two years since the rhesus macaque microarray chip became available to investigators. While not specifically a method for evaluating reproductive measures, it is nonetheless a very powerful tool for determining changes to gene expression profiles. Using high-density oligonucleotide expression arrays, researchers can quickly screen thousands of transcripts to determine genes of interest. This technology has been used to investigate gene expression in components of the HPG axis including the anterior pituitary gland, epididymis, Leydig cells and spermatogenic cells (Chen, 2004; Chen et al., 2004; He et al., 2006; Jervis and Robaire, 2003; Syntin et al., 2001; Wrobel and Primig, 2005). Biologically relevant variations can then be further verified using semi-quantitative reverse transcriptase polymerase chain reaction (sqRT-PCR), quantitative real-time RT-PCR (qRT-PCR), *in situ* hybridization, immunohistochemistry (IHC), or various other techniques. In the case of the HPG axis tissues can be evaluated for the effect of age, chemical exposure, disease pathology or nutrition.

Calorie Restriction

Calorie restriction (CR) can be defined as undernutrition without malnutrition (Black et al., 2001; Dhahbi et al., 2004; Hursting et al., 2003; Koubova and Guarente, 2003; Lane et al., 1999b). In this paradigm essential nutrients and vitamins are provided to an organism while limiting total energy (calorie) intake. Often various other terms are used interchangeably, and incorrectly, when referring to similar manipulation of energy intake in the context of diet. Other methodologies, in addition to calorie or caloric restriction, include energy restriction, diet restriction, dietary energy restriction, total dietary restriction, food or feed restriction, fasting, underfeeding and starvation. The fundamental distinction between these paradigms is whether restriction is achieved by feeding a reduced amount of food without any adjustment in nutrient density, or if formulation of dietary nutrient density is adjusted upwards to compensate. Without adjustments the investigator cannot know if the results are due to energy restriction only or are the result of nutrient insufficiency. Adjusting nutrient density allows for investigation of energy restriction effects without the confounding effect of variation in the amount of nutrients or other dietary factors ingested (Thompson et al., 2002). In this regard, CR falls into the former category and results in lower energy input without sacrificing nutritional competence.

In their pioneering experiments, McCay et al. (1935) reduced caloric input to white rats and successfully demonstrated the effect of retarding growth upon the total length of life. Individuals of both sexes attained extreme ages beyond those of either sex that grew normally. Besides showing lifespan extension, their

studies also demonstrated lower incidences of tumors and certain other diseases. The fact that a number of disease incidences can be substantially altered by variation in both type and quantity of certain dietary components independent of calorie effect, without influencing lifespan, serves to underscore that disease is distinct from aging (Weindruch and Walford, 1988).

Since McCay's initial studies in rats, moderate calorie restriction has been established as the only non-genetic method of altering longevity and attenuating biological processes associated with aging. Successful CR does not lead to malnutrition, but instead provides the essential nutrients in adequate amounts while restricting calorie intake to a range 30-70% below the *ad libitum* level. The lifespan extending effects seem to depend very specifically on energy (calorie) restriction since restriction of fat, protein, or carbohydrate without energy restriction does not increase the maximum lifespan of rodents. It is also not increased by general vitamin supplementation, supplementation with vitamin E or other antioxidants, or alteration of the type of fat, protein, or carbohydrate in the diet (Lane et al., 1995; Roth et al., 2000; Weindruch and Sohal, 1997; Weindruch and Walford, 1988).

Aging and Calorie Restriction

Moderate calorie restriction extends lifespan by slowing the rate of physiological decline and retarding age-related chronic diseases in a variety of species. To date this nutritional paradigm has been found to be effective in protozoa, yeast, rotifers, fleas, nematodes, spiders, flies, mollusks, fish, mice,

rats, dogs and possibly non-human primates such as squirrel monkeys and cynomolgus and rhesus macaques (Ingram et al., 1990; Lane et al., 1999b; Roth et al., 1999; Weindruch and Walford, 1988). Calorie restriction is not only effective for extending lifespan but exhibits great consistency across species and demonstrates widespread, beneficial health effects on almost every physiological system within the organism. Researchers have shown that CR can reduce body mass and adiposity, lower body temperature and initially reduce metabolic rate, lower blood pressure, and significantly slow growth and skeletal maturation. It has been successful in reducing glucose and fasting plasma insulin levels while increasing insulin sensitivity and levels of high density lipoproteins. In addition, CR alters neuorendocrine and sympathetic nervous system function by lowering levels of growth hormone (GH), thyroid-stimulating hormone (TSH) and thyroid hormones, insulin-like growth factor 1 (IGF-I), and gonadotropins while increasing glucocorticoid and catecholamine levels. It has also been shown to reduce oxidative stress and alter gene expression profiles (Gredilla and Barja, 2005; Gresl et al., 2001; Heilbronn and Ravussin, 2003; Koubova and Guarente, 2003; Lane et al., 1997).

The longer the duration and the greater the degree of calorie restriction (within the limits tolerated by the species) following the post-weaning period of life the greater the effect on survival and the rate of aging (Merry, 2002). Although the exact mechanism(s) of action explaining how this occurs is still largely unknown, it is believed to be evolutionarily conserved and acts by altering and/or improving the function of a variety of physiological systems (Hursting et

al., 2003). This is evidenced by the wide range of biological parameters, mentioned above, that are simultaneously affected in species put under this paradigm.

While data on life extension in a wide range of species strongly suggests that CR mechanisms are universal across species, the paradigm had not been studied in an animal model living longer than four years until the late 1980's. In 1987, to address the relevance of this nutritional intervention to human health, the National Institute on Aging (NIA) began the first study of CR and aging in non-human primates (NHP) using rhesus macaques to determine its potential application in humans (Ingram et al., 1990). Definitive evidence showing that CR extends life span in these animals is not yet available because of a maximal life expectancy of 40 years; however, the emerging data from the study as well as ongoing studies of rhesus and cynomolgus macaques at the University of Wisconsin-Madison, University of Maryland, and Wake Forest University School of Medicine strengthens the possibility that the diverse beneficial effects of CR seen in other lower species will also apply to NHP and ultimately humans.

Animals in the NIA study were gradually restricted until a 30% calorie restricted diet had been reached. By definition, the diet was supplemented with additional vitamins and minerals to guard against malnutrition (Ingram et al., 1990; Mattison et al., 2005). Several endpoints have since been investigated in studying the long-term effects of CR on aging in these animals. Results parallel those listed above and show CR-induced attenuation of age changes in plasma triglycerides, oxidative damage, and glucose regulation (Roth et al., 2002).

Treatment animals weigh less, have less body fat, and lower body temperatures than their matching control counterparts. These data provided early evidence of the potential benefit of CR for the risk for diabetes and cardiovascular disease (Lane et al., 1999a; Mattison et al., 2003). Additionally, tumor incidence is lower and mortality in the calorie restricted animals is about half that observed in controls (Mattison et al., 2003; Roth et al., 2002). For the most part, the Wisconsin Regional Primate Research Center study confirms these findings in their own calorie restricted animals despite a slightly different experimental implementation of the CR treatment (Gresl et al., 2001).

Potential Impact of Moderate CR on Reproduction in Females and Males

The effects of moderate calorie restriction on the HPG axis are mixed and adjustments must be made for level of calorie restriction and the species utilized. Data from rats and mice are inconsistent with regard to CR effect on female reproduction. In mice, restriction disrupts normal cycling; however, when returned to an *ad libitum* diet, CR mice will resume normal reproductive function and can cycle longer than continuously *ad libitum* fed mice (Weindruch and Walford, 1988). Rats maintained at 50% body weight (as compared to control littermates) still achieved sexual maturation, albeit delayed, with onset of puberty observed once the animals reached body weights similar to pubertal controls (Gredilla and Barja, 2005; Holehan and Merry, 1985). Calorie restriction has also been proven to significantly increase reproductive longevity without disrupting normal cycling in rats (Holehan and Merry, 1985). In this regard, CR may delay reproductive

senescence in rodents either by delaying puberty or initiating a period of ovarian 'rest'.

More recent data suggest that calorie restriction affects reproductive longevity at the level of the hypothalamus and/or pituitary gland. Investigators have found that female rats restricted to 60% of *ad libitum* food after the onset of puberty did not experience any interruption of normal cycling, but delayed cessation of estrous cycles was still observed (McShane and Wise, 1996). Therefore, they concluded that calorie restriction affected the HPG axis in rats by a mechanism other than simply delaying puberty or disrupting normal cycling. They hypothesized that calorie restriction may actually preserve the reproductive neuroendocrine axis, allowing for prolonged reproductive ability in these animals.

Preliminary data in female rhesus macaques aged 7-27 years suggests no adverse effects of long-term CR with regard to reproductive hormones (Black et al., 2001; Mattison et al., 2003). Researchers have also documented no interruption of normal ovarian cyclicity in young and menopausal restricted subjects, suggesting that long-term energy restriction does not negatively affect the animals (Lane et al., 2001; Mattison et al., 2003). More recently it has been demonstrated that young female rhesus macaques continue to cycle normally under short-term, moderate calorie restriction (Wu, 2006).

Initiation of short-term, moderate CR in old females, however, has had mixed results. Embryonic development was improved *in vitro* using oocytes collected from older macaques maintained on a calorie restricted diet compared to old controls. Specifically, only embryos from old CR macaques progressed

beyond the blastocyst stage and no old control embryos were observed at expanded blastocyst or hatched blastocyst stages (Wu, 2006). In the first 1-2 years under the dietary regiment however, even though no adverse effects were observed, there was a trend to advance cycle irregularity after three years on the treatment. Parallel work in long-term old CR macaques has not been completed so it remains to be seen if they will continue to function similarly to the old control animals, or if they will also begin to show advanced signs of menstrual cycle irregularity (Wu, 2006). Despite these investigations effects of CR on normal female reproductive parameters in the rhesus macaque are still poorly understood.

In the male reproductive axis, early onset CR in rats results in delayed pubertal peak of serum testosterone and a 30% reduction in peak height once puberty is reached. Later in life, however, T levels are similar and remain elevated longer in CR males while LH levels are consistently higher throughout life when compared to control animals. Although capable of successful breeding, young calorie restricted male rats experience slightly reduced fertility which recovers later in life (Weindruch and Walford, 1988). Generally speaking, evidence for male reproductive senescence in rodents is unconvincing so most work has been done in females where precipitous reproductive decline is a hallmark of aging. Overall, male rats appear less sensitive than females, however, with regards to reproductive development and the impact of calorie restriction.

In male rhesus macaques, as with rats, moderate calorie restriction implemented prior to puberty can delay the maturational increase in circulating testosterone concentrations, indicative of reproductive activation, by approximately one year (Lane et al., 1997; Roth et al., 2000). Concomitantly, skeletal growth was also limited in these animals (Mattison et al., 2003; Roth et al., 2000). In total, however, there have been very few investigations into the effects of calorie restriction on male rhesus macaque reproduction and no reports of its impact on semen analysis or sperm function parameters. With only four known studies underway using approximately 160 males, only 75 of them calorie restricted, there has been little opportunity to pursue such investigations until now.

As part of the ongoing study being undertaken by the NIA, a detailed panel of measurements was added in order to ascertain the impact of calorie restriction on male rhesus macaque reproductive fitness. Sixty animals are designated as part of the longevity aspect of the study so measurements and procedures are extremely limited in these males; general health measures have been previously summarized by Roth et al. (2004). Fortunately, 23 young adult and old adult males (CON=11, CR=12) were designated as part of the short-term (i.e. terminal) aspect of the study. These animals form the focus of the work reported here.

Summary

The average lifespan of humans can be prolonged and has in fact been markedly increased by improving environmental conditions, as demonstrated by advancements in health care technology. In contrast, maximal lifespan is thought to be increased by actually decreasing the rate of aging and has remained largely unchanged in modern times (Weindruch and Sohal, 1997). Calorie restriction in short-lived species has demonstrated that CR regimens extend lifespan, retard age-related disease, and maintain the vitality of a wide range of organisms. Numerous laboratories worldwide have repeated, in various forms, this work first reported by McCay et al. (1935). What this nutritional paradigm does to the reproductive axis in these organisms, however, is still unclear.

In the preceeding sections I have attempted to establish a framework from which the interaction between aging and calorie restriction can be understood. I have also established the need for detailed investigations into the impact of this nutritional paradigm on the HPG axis, particularly in higher order species. It is my goal then to pursue these investigations through analysis of rhesus macaque aging with particular focus on the neuroendocrine component since these neuroendocrine changes may coordinate the life prolonging response of animals to CR. The nervous system likely plays an important role in the initial response to altered caloric intake by sensing the change. This sensation of reduced food most likely occurs within the GI tract or CNS. Although all cells within the organism could respond directly and independently to reduced calories via metabolic signals, it is unlikely that coordinated cellular responses could be

achieved without the systemic control mediated by neural and endocrine factors. These CR effects presumably involve the same neural and endocrine driven mechanisms that coordinate metabolic adaptation to such environmental perturbations as starvation, thermal stress, and exercise. An example is the reduction in gonadotropin levels and gonadal function in response to reduced leptin levels caused by less food (Heilbronn and Ravussin, 2003; Koubova and Guarente, 2003).

The collaborative effort between the National Institute on Aging, the Oregon Health and Science University-Oregon National Primate Research Center (OHSU-ONPRC) and the University of Maryland has made possible a comprehensive analysis of the effects of moderate calorie restriction on reproductive function in young and old male rhesus macaques. Therefore, the objectives of this project were to: 1) analyze general neuroendocrine changes to the HPG axis that occur with aging and 2) evaluate the effects of moderate (30%) CR on reproductive function and decline in male rhesus macaques.

Age is an issue of mind over matter. If you don’t mind, it doesn’t matter.

- Mark Twain, 1835 - 1910

How old would you be if you didn’t know how old you are?

- Leroy ‘Satchel’ Paige, 1906 - 1982

When you stop seeing beauty you start growing old
The lines on your face are a map to your soul
When you stop taking chances you'll stay where you sit
You won't live any longer but it'll feel like it

- U2, 1978 - present

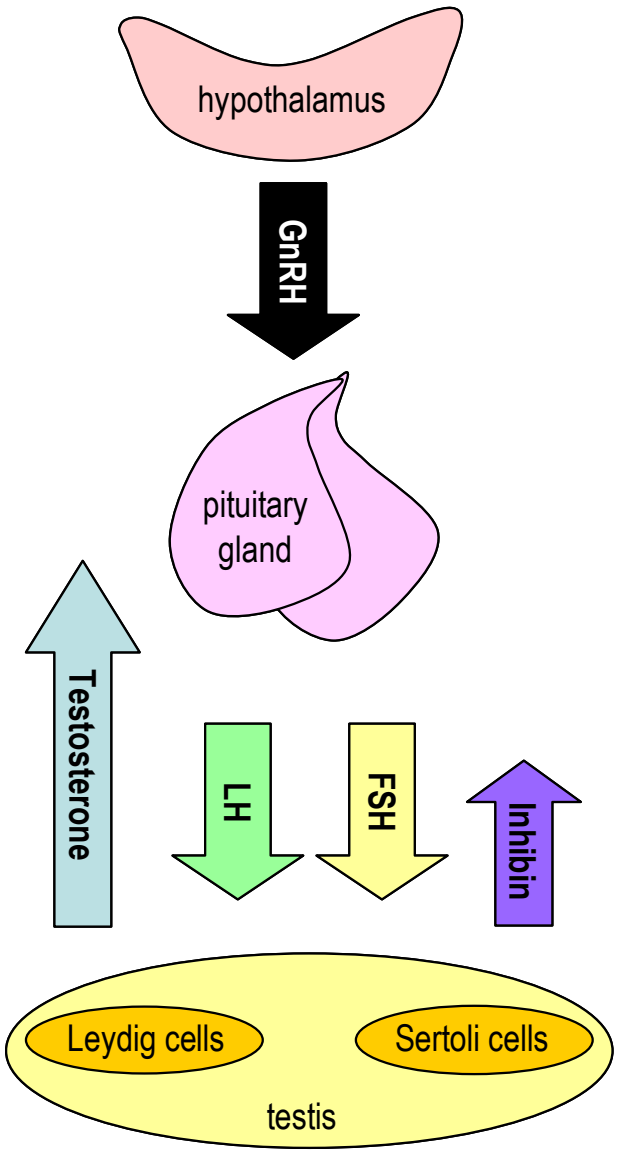

Figure 1.1 Hypothalamic-Pituitary-Gonadal Axis Schematic representation of the male hypothalamic-pituitary-gonadal axis and the major hormones involved. Hypothalamic production of gonadotropin-releasing hormone (GnRH) stimulates pituitary gland production of gonadotropins luteinizing hormone (LH) and follicle-stimulating hormone (FSH). Testicular response to LH stimulates the release of testosterone (T) from Leydig cells while FSH acts on Sertoli cells to stimulate inhibin production.

Table 1.1 Summary of Semen Measurements

Measure	Rationale
Ejaculate appearance	Indicative of cell (sperm) numbers
Ejaculate weight	Indicative of accessory sex gland production and secretion
Ejaculate color	Abnormal color may indicate accessory sex gland or other clinical pathology
Ejaculate volume	Low volume may indicate retrograde semen flow into the bladder or accessory sex gland pathology
Osmolarity/osmolality	Indicative of ionic composition
pH	Indicative of ratio of alkaline seminal vesicle secretions and acidic prostatic secretions
Count	Indicative of overall spermatogenesis success
Concentration	Indicative of successful spermatogenesis and accessory sex gland production
Motility	Indicative of sperm ability to reach the ova
Morphology	Indicative of cell maturation status
Activation (capacitation)	Indicative of sperm ability to reach the ova and then penetrate the zona pellucida
Agglutination	May indicate possible surface antigen problems
Zona pellucida (ZP) binding	Sperm binding to the ZP outer surface is a prerequisite for oocyte vitelline membrane binding and penetration
Acrosome reaction	Prior to fertilization the outer acrosomal membrane fuses with the surrounding plasma membrane
Hypo-osmotic swelling assay	Indicative of intact sperm membrane. Membrane integrity can influence motility, activation, acrosome reaction and is required for successful fusion with the ova
Seminal plasma composition	Overall measure of accessory sex gland contribution
Sperm chromatin structure assay (SCSA®)	Indicative of DNA packaging and sperm development capabilities

CHAPTER 2

EFFECTS OF AGE ON CORE-CLOCK GENE EXPRESSION IN THE MALE RHESUS MACAQUE (*MACACA MULATTA*) PITUITARY GLAND

INTRODUCTION

Biological organisms exhibit a wide range of natural rhythms, including endogenous circadian oscillations with a periodicity of approximately 24 hours (Takahashi et al., 2001). These intrinsic, elemental rhythms regulate diverse physiological processes including metabolism, stress response, thermoregulation, and reproduction. The hypothalamic suprachiasmatic nucleus (SCN) acts as a master circadian pacemaker to synchronize, coordinate and sustain circadian physiology and function in mammals (Refinetti, 2005; Takahashi et al., 2001). Because the intrinsic period of the SCN oscillator is not exactly 24 hours, it will drift out of phase with the solar day unless synchronized or 'entrained' by sensory input (zeitgebers), such as temperature changes, food intake or light-dark cycles. Light (photic information) is by far the most important external entraining cue in mammals. Visual light is transmitted primarily from the eye via the retinohypothalamic tract (RHT) and terminates in the ventral part or core of the SCN (Abizaid et al., 2004; Hofman and Swaab, 2006; Reppert and Weaver, 2002). The nucleus responds to timing signals received from these afferent pathways and drives overt circadian rhythms throughout the body via its own efferent connections and neuroendocrine outputs (Lowrey and Takahashi, 2004; Morse and Sassone-Corsi, 2002; Stehle et al., 2003).

The molecular clock mechanism consists of core circadian clock genes and appears to be highly conserved at the intracellular level. Core genes are those whose mRNA translates into protein products which are necessary components for the generation and regulation of circadian rhythms, that is, proteins which form the primary molecular circadian oscillatory mechanism within individual cells throughout the organism (Lowrey and Takahashi, 2004). The system involves interconnected cyclic transcriptional/translational feedback loops that autoregulate the expression of both positive and negative oscillator components as well as their respective output proteins (Figures 2.1 and 2.2).

In mammals the positive components that comprise the transcriptional activators are CLOCK and BMAL1. These proteins dimerize and bind constitutively to E-box *cis*-regulatory enhancer sequences in the promoter regions of various genes, including the negative components of the feedback loop (Figure 2.3). The negative components include the Period proteins (PER1, PER2) and Cryptochrome proteins (CRY1, CRY2) which act to disrupt activity of the bound CLOCK/BMAL1 transcriptional complex, and subsequently generate a circadian rhythm in their own transcription. The positive and negative feedback loops are connected by the product of another core-clock gene, REV-ERBα. This gene codes for an orphan nuclear receptor, and like the PER and CRY genes, is activated by CLOCK/BMAL1 heterodimers binding to E-box enhancers. REV-ERBα protein inhibits BMAL1 gene transcription by functionally competing with retinoic acid-related orphan receptors (ROR) at the retinoic acid-related orphan receptor response elements (RORE) in the promoter region of BMAL1. Thus,

BMAL1 activation of REV-ERBα attenuates its own transcription. Finally, significant posttranslational modifications play a critical role in generating 24-hour rhythms of mRNA and protein levels. Phosphorylation of PER proteins (especially PER2) by casein kinase 1 epsilon (CSNK1E) activates their degradation and is the rate limiting step in their accumulation. Only after there is adequate PER present in the cytoplasm to overwhelm CSNK1E-mediated degradation, does enough PER persist to dimerize with CRY. Casein kinase then phosphorylates the dimer to allow for nuclear translocation and disruption of the positive CLOCK/BMAL1 complex. These inherent transcription, translation, and posttranslational modifications give the clock its own natural rhythmicity approximately equal to one terrestrial day (Glossop and Hardin, 2002; Guillaumond et al., 2005; Lowrey and Takahashi, 2004; Okamura et al., 2002; Reppert and Weaver, 2002).

Genetic components of this clock mechanism are also expressed in various peripheral tissues, raising the possibility that circadian physiology is ultimately regulated by a coordinated network of oscillators rather than by the single master circadian clock of the suprachiasmatic nucleus (Balsalobre, 2002; Balsalobre et al., 1998; Glossop and Hardin, 2002). Revision of the circadian paradigm, whereby mammalian circadian rhythms are coordinated by a network of subordinate, peripheral oscillators located in multiple tissues throughout the body and synchronized by the SCN, allows each of these oscillators to regulate circadian expression of a portion of the tissue genome and to coordinate tissue-specific functions. Gene microarray, RT-PCR, *in situ* hybridization and

immunohistochemistry experiments with a number of species have shown that circadian transcriptional mechanisms temporally regulate biochemical pathways in various tissues throughout the body including hypothalamus, pineal, liver, heart, kidney and adrenal (Balsalobre, 2002; Chappell et al., 2003; Jilg et al., 2005; Lemos et al., 2006; Morse and Sassone-Corsi, 2002; Stehle et al., 2003; von Gall et al., 2002). These constituent clock mechanisms work by driving the circadian expression of specific sets of genes. These studies demonstrate that many proteins involved in general cellular and tissue-specific pathways can accumulate in a circadian manner and appear to be controlled by clock mechanisms in many cases.

Throughout life and during specific life stages the hypothalamic-pituitary-gonadal axis is responsible for a number of circadian activities in mammals including rhythmic release of gonadotropin-releasing hormone (GnRH), luteinizing hormone (LH), growth hormone (GH) and adrenocorticotropic hormone (ACTH) (Griffin and Ojeda, 2000; Knobil et al., 1994). In fact, the levels of most reproductive hormones, such as testosterone (T), are regulated in a circadian fashion in mammals (Jilg et al., 2005; Sehgal, 2004). Intuitively this makes sense since the pituitary, as the master endocrine gland, is ideally situated in the axis to exert direct control over such neuroendocrine functions (Everett, 1994). Experimental evidence in the rat pituitary gland has shown that at least some components of the circadian mechanism (Per1, Per2, Cry1) are present in the adenohypophysis but not the neurohypophysis (Shieh, 2003). It may be that while receiving signals from the suprachiasmatic nucleus, the

pituitary gland works to fine-tune and regulate physiological events within its domain.

In view of the experimental evidence, our goal was to examine whether the pituitary gland of the rhesus macaque expresses core-clock genes and their protein products; to quantify expression levels of selected genes; to determine if expression follows a 24-hour rhythmic pattern; and to reveal any age-related alterations in the system.

MATERIALS AND METHODS

Animals and Diet

All experiments made use of banked rhesus macaque (*Macaca mulatta*) tissues from previous unrelated studies and were approved for use by the Institutional Animal Care and Use Committees at the University of Maryland and the Oregon National Primate Research Center. Animals were individually housed in a temperature-controlled environment under 12L:12D photoperiod (lights on 7 h -19 h) and allowed auditory, visual and olfactory interaction with male and female conspecifics in the vivarium. Food was provided in two meals at 8 h and 15 h daily; water was available *ad libitum*. Diet consisted of primate chow (Purina Mills, Inc.; St. Louis, MO) supplemented with fresh fruits and vegetables. Animals were sacrificed according to the NIH *Guide for the Care and Use of Laboratory Animals*.

Experiment 1: Gene Expression Profiling and Age Characterization

Four Juvenile (1 – 2 years), four Young Adult (7 – 12 years), and four Old

Adult (18 – 26 years) male rhesus macaques were sacrificed between 11 h and 15 h. Pituitary glands had either been kept whole or sectioned sagittally and placed in RNAlater® (Ambion, Inc.; Austin, TX) and then frozen in liquid nitrogen or simply flash frozen in liquid nitrogen.

Experiment 2: Phase Shift Characterization

Six ovariectomized female rhesus macaques (8 – 11 years) were sacrificed at either 1 h or 13 h. Pituitary glands had either been kept whole or sectioned sagittally and placed in RNAlater® (Ambion, Inc.; Austin, TX) and then frozen in liquid nitrogen or simply flash frozen in liquid nitrogen.

Experiment 3: 24-hour Gene Expression

Five additional ovariectomized females (7 – 12 years) were sacrificed in 4-hour intervals at 3 h, 7 h, 15 h, 19 h, and 23 h; tissue was unavailable for 11 h. Pituitary glands had been kept whole and fixed in 4% paraformaldehyde.

RNA Extraction and Gene Microarrays

Whole pituitary glands or ½ sagittally cut sections were homogenized using a PowerGen rotor-stator homogenizer (Fisher Scientific; Pittsburgh, PA). Total RNA was isolated using RNeasy columns (QIAGEN; Valencia, CA); concentration and integrity were assessed by microcapillary electrophoresis using a model 2100 Agilent Bioanalyzer (Santa Clara, CA; see Appendix A for more detail). Only male samples from experiment 1 (n=3 for each age group) were sent for analysis to the Affymetrix Microarray Core of the OHSU Gene Microarray Shared Resource.

Analysis was performed in accordance with the manufacturer's instructions (Affymetrix GeneChip® Analysis Technical Manual; Santa Clara, CA). Labeled target cRNA was prepared from total RNA samples and hybridized to human arrays (Affymetrix HG_U133A) detecting a total of 18,400 transcripts. Image processing and expression analysis were performed using Affymetrix GCOS v1.2 software. A number of quality control metrics were utilized as a measure of probe quality and included chip background, chip noise, total fluorescent intensity, number of genes detected and the 3'/5' ratio of the housekeeping genes β-actin and GAPDH. These metrics are assessed to determine the validity of the data obtained from the scanned GeneChip®. Data were normalized to an average intensity on each chip which enabled direct comparisons between the nine different arrays.

Semi-quantitative RT-PCR

PrimerExpress® software (Applied Biosystems; Foster City, CA) was used for all primer and probe design (Appendix G). Specific primers were designed for each transcript using the human sequences and then BLASTed against the macaque sequences available at the Human Genome Sequencing Center at Baylor College of Medicine (http://www.hgsc.bcm.tmc.edu/projects/rmacaque/) to obtain, whenever possible, the macaque sequences. The primers were purchased from Invitrogen (Carlsbad, CA) and the sequences are given in Table 2.1.

Total RNA (1 µg) was used to synthesize cDNA using the Omniscript kit (QIAGEN) and oligo $d(T)_{15}$ primers (Promega Corp; Madison, WI). The reaction was performed following the manufacturer's instructions in a 20 µl volume at 37^{o}C for 1 hour. The linear range of amplification was calculated for each pair of primers using pooled samples and reactions were performed in duplicate. sqRT-PCR amplifications were performed using 1 µl of cDNA, 200 µM deoxynucleotide triphosphates (Promega), 0.5 µM of each primer, and 2.5 U of HotStarTaq® polymerase (QIAGEN) in a 25 µl reaction volume. The reactions were performed using the following program: 95^{o}C, 15 min; 94^{o}C, 1 min; specific annealing temperature for each primer set (Table 2.1), 1 min and 72^{o}C, 1 min (see Appendix H for specific details).

Aliquots (7 µl) of reaction product were resolved by electrophoresis on 2% agarose gels with ethidium bromide and photographed under ultraviolet light. Subsequent image analysis was performed using ImageJ software 1.37v (NIH; Bethesda, MD; http://rsb.info.nih.gov/ij/). Briefly, a single rectangle was drawn horizontally around all bands in a selected gel image and a plot profile of signal intensities was generated. Area selections were created under the peak for each band using the 'straight lines selection' tool. Area under the curves was then measured and provided area statistics for analysis. Appendix I discusses troubleshooting for primer design, sqRT-PCR and gel imaging.

Taqman® Quantitative Real-Time RT-PCR

cDNA was prepared by random-primed reverse transcription using

random hexamer primers (Promega), 200 ng of RNA and the Omniscript kit (QIAGEN). The RT reaction was then diluted 1:100 for PCR analysis. The PCR mixtures contained 5 µl of Taqman® Universal PCR Master Mix (Applied Biosystems), 300 nM Rev-Erbα primers (Invitrogen), 50 nM human β-actin primers (Applied Biosystems), 250 nM Rev-Erbα probe (Sigma; St. Louis, MO) and 2 µl cDNA. Reactions were run in triplicate for higher accuracy. The amplification was performed as follows: 2 min at 50°C, 10 min at 95°C, and then 40 cycles each at 95°C for 15 sec and 60°C for 60 sec in an ABI/Prism 7700 Sequences Detector System (Applied Biosystems). The β-actin standard curve was used to convert the critical threshold values (i.e. above background) into relative RNA concentrations for each sample. The Rev-Erbα primers and probe were designed using the rhesus macaque sequence available in the GenBank database (accession no. BV208705) and are listed in Table 2.1.

Immunohistochemistry

Fixed pituitary glands were sectioned (25 µM) horizontally from inferior to superior orientation using a frozen-stage sliding microtome. Three continuous sections from three different areas at approximately ¼, ½ and ¾ of the way through the gland were utilized for each animal to give broad sampling. All sections were subjected to 20-second microwave antigen retrieval (MAR) in 2X Antigen Retrieval Citra (BioGenex; San Ramon, CA) prior to staining; this improved considerably the accessibility of antigens in the tissue. Sections were processed for single-label immunohistochemistry using a primary polyclonal

antibody against human REV-ERBα (Lifespan Biosciences; Seattle, WA), ABC amplification (Vector Laboratories; Burlingame, CA), and DAB chromogen (Sigma; St. Louis, MO). As a control, tissue that was not MAR-treated or was not exposed to primary antibody during incubation was included. This served as a validation of both the primary antibody and the method as well as to rule out any false-positive results or altered immunostaining patterns. Sections were mounted onto Fisherbrand Superfrost Plus microscope slides (Fisher Scientific) and coverslipped with DPX mountant (Fisher Scientific) for imaging. (See Appendix J for more detail.)

Statistical Analysis

Data are expressed as mean $\pm$ SEM for each parameter measured in each group. Signal intensity and mRNA expression levels were analyzed by Student's *t*-test or one-way ANOVA. In order to control for experiment-wide false positives while still maintaining statistical power, each Student's *t*-test was treated as an independent test and, therefore, alpha was adjusted to correct for multiple comparisons. To accomplish this sequential Bonferroni with Simes-Hochberg correction was used (Hochberg, 1988). If group differences were revealed by ANOVA, differences between individual groups were determined with the Tukey-Kramer post-hoc analysis using GraphPad Prism (GraphPad; San Diego, CA). Power analysis was performed using Statistical Analysis System (SAS Institute; Cary, NC). For all analyses significant differences were established at $P<0.05$ unless otherwise adjusted by Bonferroni correction.

Results

Experiment 1: Gene Expression Profiling and Age Characterization

Mean signal intensity values from the Affymetrix GeneChip® microarray for three age categories of rhesus macaques are listed in Table 2.2. All probesets for the six core-clock genes investigated are shown as well as *Clock* which was not investigated further. Because we were specifically interested in core-clock genes we did not perform a comprehensive screening and filtering of the microarray data, as was done for experiments discussed in Chapters 3 and 4. Instead we searched the probeset library for the seven genes of interest in order to compile Table 2.2. A significant difference was observed between *Per2* expression in Young Adults and the other two age groups. A significant difference was also detected between Juvenile *Bmal1* expression and Young Adult mRNA levels.

Figure 2.4 provides validation information for the microarray data which was conducted by showing sqRT-PCR amplification of all six core-clock genes in the three age groupings of macaques. Amplicons were detected between 26-28 cycles at 65-66^{o}C (Table 2.1).

The sqRT-PCR expression levels for the core-clock genes within the three age groups of macaques are shown in Figures 2.5 A-F. Significant differences were detected between Juvenile animals and the other two groups for *Per2* expression (Graph A). In both instances a negative fold-change resulted, with a 37% decline in Young Adult mRNA expression and a 42% decline in Old Adults as compared to Juvenile animals. Due to large variation within some groups

Csnk1ε and *Bmal1* expression (Graphs B-C) were not statistically significant but did trend in a similar direction as the microarray data.

Experiment 2: Phase Shift Characterization

Semi-quantitative RT-PCR expression levels for the rhythmically expressed core-clock genes are demonstrated at two opposing time-points (1h and 13h) in Figure 2.6. *Csnk1ε* was not measured because it is constitutively expressed throughout the 24-hour cycle.

The sqRT-PCR expression levels for the five rhythmically expressed core-clock genes are depicted in Figures 2.7 A-E. Significant differences were identified in Per2 and Bmal1 mRNA expression at the opposing time-points with both being expressed more highly at 13h. *Per2* exhibited a 1.33 ($\pm$0.05) fold-increase in expression while *Bmal1* levels increased 1.82 ($\pm$0.34) fold from the 1h time point.

The results of Taqman® quantitative real-time RT-PCR of *Rev-Erbα* are given in Figure 2.8. Expression levels were not significantly different at these two time-points.

Experiment 3: 24-hour Gene Expression

A representative section of rhesus macaque pituitary gland is shown in Figure 2.9 with immunostaining for REV-ERBα. Staining can clearly be seen in the anterior and intermediate pituitary but not the posterior pituitary gland, demonstrating regional specificity in distribution of the nuclear protein.

Representative single-label immunohistochemistry staining for REV-ERBα in the anterior pituitary gland of the rhesus macaque is depicted in Figure 2.10. Temporal changes in staining intensity are clearly observed across the 24-hour cycle providing evidence of rhythmic expression of a core-clock gene.

Discussion

Biological organisms exhibit endogenous circadian rhythms which regulate a diverse array of physiological processes, such as temperature regulation, energy metabolism, blood pressure and sleep/wake cycle (Takahashi et al., 2001). The hypothalamic suprachiasmatic nucleus (SCN) acts as the master circadian pacemaker to synchronize, coordinate and sustain circadian activity (Refinetti, 2005; Takahashi et al., 2001). Sensory input (zeitgebers) to the SCN from afferent pathways drives circadian rhythms throughout the body via efferent connections and humoral outputs (Lowrey and Takahashi, 2004; Morse and Sassone-Corsi, 2002; Stehle et al., 2003). The molecular clock mechanism consists of highly conserved core circadian clock genes and, in mammals, includes *Per1*, *Per2*, *Cry1*, *Bmal1*, *Clock*, *Rev-Erbα* and *Csnk1ε*. Together these genes form an interconnected cyclic transcriptional/translational feedback loop that autoregulates the expression of oscillator components and their respective output genes (Reppert and Weaver, 2002).

Genetic components of this clock mechanism are also expressed in various peripheral tissues including pineal, liver, heart, kidney, adrenal and hypothalamus (Balsalobre, 2002; Chappell et al., 2003; Jilg et al., 2005; Lemos

et al., 2006; Morse and Sassone-Corsi, 2002; Stehle et al., 2003; von Gall et al., 2002). It is known that immortalized GT1-7 mouse hypothalamic GnRH neurons contain a functional circadian clock mechanism and that they exhibit pulsatile GnRH secretion *in vitro*. These cells exhibit significant rhythmic gene expression of *Bmal1*, *Per1*, and *Per2* (Gillespie et al., 2003). Experimental findings have also established a direct connection of primary visual afferents to GnRH and dopamine-producing neuroendocrine cells of the vervet monkey hypothalamus (Abizaid et al., 2004). This retinal connection is outside of the predominant retinohypothalamic tract to the SCN. These hormone producing neurons are regulators of pituitary gland gonadotrophs and lactotrophs and reveal for the first time in primates that light stimuli can reach the HPG axis, providing a direct and independent pathway from the SCN master circadian clock for the photic modulation of hormone release. Throughout life and during specific life stages the hypothalamic-pituitary-gonadal axis is responsible for a number of circadian activities in mammals. All of this leads to the distinct possibility that the pituitary gland may also contain its own circadian clock mechanism.

At least some of the molecular clock components have been shown to exist in the rat pituitary gland. *In situ* hybridization experiments mapped Per1, Per2 and Cry1 mRNA to areas of the anterior pituitary, pars tuberalis/median eminence and intermediate pituitary gland. No signals for mRNA expression were detected in the posterior pituitary gland (Shieh, 2003). Early work investigated the possibility that the pituitary gland functions as an autonomous clock capable of generating rhythmic luteinizing hormone release independent of

hypothalamic control (Lewy et al., 1996). The results, in mice, indicated that pituitary gland gonadotrophs are capable of producing rhythms of LH release for a long duration *in vitro*. More recently data demonstrated *in vitro* release patterns of prolactin, which are affected by photoperiod and age *in vivo*. They demonstrated in the rat model that both mean levels and rhythmic prolactin release are determined by the age of the animal, the circadian time of pituitary gland isolation, and the photoperiodic conditions in which the animal was housed (Lewy et al., 2005).

Our experimental data build on the published literature and demonstrate that mRNA and protein core-clock components are indeed expressed in the rhesus macaque pituitary gland at measurable levels; that mRNA levels are significantly different at two specific, opposing time points; that protein synthesis and turnover of at least one component oscillated with a 24-hour rhythmic pattern; and that at least one mRNA component of the clock mechanism was affected by age.

Experiment 1: Gene Expression Profiling and Age Characterization

GeneChip® microarrays were used to identify expression of seven core-clock genes in the rhesus macaque pituitary gland: *Per1, Per2, Bmal1, Cry1, Clock, Rev-Erbα* and *Csnk1ε*. Microarray results showed small but significant changes in mRNA expression across the three age categories of interest. Specifically, *Per2* expression in Young Adults was significantly less than the other two age groups while Bmal1 mRNA expression levels were higher in Young

Adults compared to Juvenile animals (P<0.05). At the time of the experiments the rhesus macaque GeneChip® was unavailable so the human chip (Affymetrix HG_U133A) was utilized. Given the high similarity between non-human primate (NHP) and human genomes [e.g. 98.77% similarity between chimpanzee and human, (Dillman and Phillips, 2005); 97.5% between rhesus macaque and human (Gibbs et al., 2007)], it was reasonable to expect that the human GeneChip® could successfully hybridize with NHP samples. This has in fact been determined in multiple studies (Dillman and Phillips, 2005; Wang et al., 2004).

Overall, few age-related changes in pituitary gland gene expression were detected utilizing the 18,400 transcripts on the Affymetrix HG_U133A human array. This finding correlates well with other reports that the pituitary gland exhibits a high consistency of mRNA expression with aging, indicating that this may be a fundamental characteristic of the gland. Previous microarray experiments have revealed few hypothalamic and pituitary gland changes in gene expression in 3, 15, and 24 month old Sprague-Dawley male rats (Kappeler et al., 2003). Out of a total of 1183 genes on the microarray, only 454 were detected in the hypothalamus and 115 in the pituitary gland, representing 38% and 10% of the detectable RNAs, respectively. More importantly, in the pituitary gland, only six genes were differentially expressed in an age dependent manner [$GABA_A$ β_1, cocaine- and amphetamine-regulated transcript (CART), heterogeneous nuclear ribonucleoprotein K (hnRNP-K), GH, phosphofructokinase (PFK) and cyclin D_2 (CCND2)]. Kappeler et al. concluded that age-associated modifications in rat hypothalamic and pituitary gland gene

expression appeared to be restricted to rather modest number of genes. Finally, it should be noted that there were only one or two probesets for each circadian gene as compared to most other genes which may have as many as 11-16 probesets. Fundamentally and most important, however, our array data did indicate that the clock mechanism was present in the rhesus macaque pituitary gland.

Microarray data were validated using sqRT-PCR. Experimental findings showed that all six of the investigated genes (*Clock* was not analyzed) were present. *Per2* expression again showed a significant difference ($P<0.05$) between age categories, with expression 60% higher in Juvenile animals as compared to Young Adult but also Old Adult animals, which was not detected by the microarray data alone. This further emphasizes the need for additional experiments to support microarray data of any kind.

Of the other non-significant transcripts, *Csnk1ε* and *Bmal1* were close to statistical significance, possibly due to large variation within some groups. Based on our experimental means and standard deviations, power analysis indicated we would have needed to double our sample size to nine animals per group in order to have had a 90% chance of detecting a difference in *Csnk1ε* expression. The trend for *Bmal1* was not as strong, as even this larger sample size would have only achieved a 60% chance of detecting significant differences. Both of these transcripts, however, did trend in the direction of the microarray data with *Csnk1ε* mRNA expression declining with age and *Bmal1* increasing.

While the changes may have been subtle this line of investigation is still very important since age changes have the potential to cause temporal dysregulation of gene expression, a principal factor in cellular malfunction and disease. It's worth noting, too, that the pituitary gland is also a very heterogeneous tissue consisting of multiple cell types (gonadotrophs, lactotrophs, somatotrophs) and each may have its own inherent circadian timing mechanism. The pars tuberalis, for example, expresses clock genes which are entrained by melatonin (Stehle et al., 2003). Melatonin activation results in modulation of prolactin levels (Jilg et al., 2005; von Gall et al., 2002) and would be activated at a very different time than gonadotropin-releasing cells. Such cellular variation may have inhibited our ability to detect gland-wide mRNA expression changes.

Experiment 2: Phase Shift Characterization

Pituitary gland samples from ovariectomized females obtained at 1h and 13h provided opposing times in the circadian cycle and therefore were useful in verifying circadian changes. Additionally, since hormone variation can influence gene expression, this tissue allowed demonstration of universal circadian changes across gender by eliminating the fluctuating hormone environment. Five rhythmically expressed core-clock genes were measured using sqRT-PCR. Expression of *Per2* and *Bmal1* levels were significantly different ($P<0.05$), with *Per2* displaying a fold-change of 1.33 ($\pm$0.05) from 1h to 13h and *Bmal1* showing a similar shift in direction with a 1.82 ($\pm$0.34) fold-change. No differences were

observed for Rev-Erbα mRNA levels at 1h vs 13h using Taqman® quantitative real-time PCR.

The fact that *Per2* and *Bmal1* both increased at 13h compared to 1h was somewhat surprising. In the SCN these two transcripts would be in antiphase to one another at these sampling times (Figure 2.11). While *Per2* should be high during circadian day (13h) and low at circadian night (1h), *Bmal1* would be the exact opposite. Our findings in the pituitary gland are most likely attributed to the nature of this peripheral tissue. There are reports that peripheral tissues exhibit a 3-9 hour phase shift in mRNA core-clock oscillation compared to the SCN, suggesting that peripheral tissues might be receiving timing cues from the master oscillator in a delayed fashion (Morse and Sassone-Corsi, 2002). If such a phase shift is occurring in the pituitary gland, our sampling times would be capturing the circadian rhythms at very different expression points. In this case, it appears that the pituitary gland was shifted by 8-9 hours in production of mRNA.

These data lead to the interesting question of rhythms in gene expression for organs that are in communication via hormonal signals. For example, Lemos et al. (2006) found core-clock gene expression in the rhesus macaque adrenal using real-time PCR of *Rev-Erbα* to investigate phase shift. Their adrenal samples came from the same animals and time-points as our pituitary glands and the probes and primers were the same as in our analysis. Their results revealed *Rev-Erbα* expression was significantly lower ($P<0.05$) at 13h than 1h. These findings support the contention that each peripheral tissue, although receiving

signals from the SCN, may regulate its own circadian expression of genes within the limits of its physiological constraints and demands.

Experiment 3: 24-hour Gene Expression

Pituitary gland tissue from ovariectomized females collected at 4-hour intervals across the day was analyzed to determine if core-clock protein expression followed a 24-hour rhythmic pattern. REV-ERBα was targeted using immunohistochemical staining as it is localized to the nucleus and because it links the positive and negative feedback loops of the molecular clock mechanism. Staining for REV-ERBα protein revealed a temporal change in expression within the anterior and intermediate pituitary gland of the rhesus macaque. As with mRNA expression, there may be a noticeable phase shift in protein expression levels compared to the SCN as the peripheral tissues receive timing cues from the master oscillator in a delayed fashion (Figure 2.12).

Our staining technique proved very successful in detecting the circadian protein. Future work involving double-staining of the pituitary gland for REV-ERBα and FSH/LH is particularly appealing. DAB immunohistochemistry identified the nuclear REV-ERBα and combined with NiCl staining for cytoplasmic FSH/LH could potentially demonstrate colocalization of the proteins. This would give added weight to the theory that core-clock gene expression is of physiological relevance in the pituitary gland, particularly with regard to daily hormonal rhythms.

Taken together, the data from these experiments supports the presence of an intrinsic clock mechanism which may contribute to the rhythmic physiology of the pituitary gland and that expression of selected genes may become altered during aging. There are well documented alterations in circadian organization during aging, including changes in hormonal rhythms, core body temperature, sleep/wake cycles, activity and locomotor patterns, behavioral responses, and response to the phase-shifting effects of light (Asai et al., 2001; Hofman and Swaab, 2006; Oster et al., 2003). Despite these overt signs, however, the physiological underpinnings for the circadian dysregulation remain unclear.

Studies suggest that the amplitude of the central circadian pacemaker is decreased in older animals. It has recently been reported that *Clock* and *Bmal1* expression in the SCN decreased with age in hamsters, but that there was no difference between young and old hamsters in the expression of either *Per1* or *Per2* (Kolker et al., 2003). The change in *Clock*/*Bmal1* expression was not enough to disrupt the overall cycle as the circadian mechanism continued to exhibit a normal phase profile (Hofman and Swaab, 2006; Kolker et al., 2004). Similar results were found in rats where *Per* and *Cry* expression levels in the SCN were not dampened or disrupted by aging (Asai et al., 2001; Hofman and Swaab, 2006; Yamazaki et al., 2002). It appears then that the daily rhythm of expression of core-clock genes is similar in the SCN of young and old rodents and that oscillation of the master pacemaker remains remarkably stable.

Within peripheral tissues there appears to be more variation in aging impaired circadian expression of core-clock genes. While some findings have

shown deterioration of transcription and rhythmicity in peripheral tissues, including lung and aortic/cardiac muscle cells (Kunieda et al., 2006; Yamazaki et al., 2002), other research has found no age-related decline in liver, pineal, kidney or pituitary gland rhythmicity (Hofman and Swaab, 2006; Yamazaki et al., 2002). It may be that some peripheral tissues, like the pituitary gland, are more resilient with regard to circadian changes brought about by cellular senescence. In this way they may mirror the stability seen in the suprachiasmatic nucleus.

Finally, there may be a biological significance to the trend observed in the decline of *Csnk1ε* in the pituitary gland with age. Hamsters harboring the naturally occurring *tau* mutation possess a mutated *Csnk1ε* that is unable to fully phosphorylate its physiologically relevant substrate, *Per2* (Eide and Virshup, 2001). Because limited phosphorylation leads to less *Per2* degradation it is able to build up quicker in the cytoplasm. With higher *Per2* content the Per/Cry dimer forms faster causing the negative loop of the cycle to progress more rapidly. That is to say, a shorter circadian cycle persists which is closer to 20-22 hours in the *tau* mutant (Eide and Virshup, 2001; Morse and Sassone-Corsi, 2002). In addition, the *tau* hamster exhibits accelerated LH pulse frequencies suggesting that the underlying GnRH pulsatility may be fundamentally altered by this circadian mutation (Chappell et al., 2003).

We have observed parallel findings in the testes of aging rhesus macaques with significant decreases in *Csnk1ε* expression as measured by sqRT-PCR (Chapter 4). How this deficiency in a core-clock gene component impacts the circadian cycle is unclear. Studies have shown that *Csnk1ε*

mutations have no effect on Per mRNA expression or the nuclear accumulation of PER proteins in the SCN. The mutation does, however, have unanticipated consequences for circadian timing in the periphery, including tissue-specific phase advances and/or reduced amplitude of circadian gene expression. The reprogrammed output from the clock is associated with peripheral desynchrony, which in turn could account for the physiological manifestations of the mutation (Dey et al., 2005). These actions of *Csnk1ε* may partially explain the altered expression levels in other core-clock genes such as *Per2* and *Bmal1* within the tissue. Each tissue type may be very different and it would take more experimental evidence before the mysteries of circadian mechanisms in each will be unlocked. A central unresolved issue is to what extent age-related changes in circadian behavior are the result of effects on the central SCN pacemaker, on peripheral oscillators, or on the mechanisms providing synchronization among contributing oscillators.

Summary

Genome-wide expression profiling of rhesus macaque pituitary gland was performed and showed that several of the genetic components of the circadian clock mechanism (*Per1, Per2, Cry1, Bmal1, Clock, Rev-Erbα* and *Csnk1ε*) were clearly present in all pituitary glands, regardless of age. Semi-quantitative RT-PCR (sqRT-PCR) confirmed the presence of these core-clock genes and also indicated significant age differences in expression for at least one component (*Per2*). In an additional experiment, sqRT-PCR corroborated the microarray data

by showing differential expression of core-clock genes at two opposite time-points. Specifically, we found that expression of *Per2* and *Bmal1* were significantly higher (P<0.05) at 1300 h as compared to 0100 h. Expression levels of *Rev-erbα* as measured with qRT-PRC were not found to be significantly different at these two time-points. In a final experiment, however, immunohistochemistry performed on pituitary gland tissue collected across a 24-hour period demonstrated rhythmic expression of REV-ERBα protein in the anterior pituitary gland of ovariectomized females. Taken together these data indicate the ability of the rhesus macaque pituitary gland to express core-clock genes, their protein products, and to do so in a 24-hour rhythmic pattern. To our knowledge, these findings are the first demonstration of a potential molecular clock mechanism in a primate pituitary gland. It remains to be elucidated whether this mechanism is expressed in all pituitary gland cells or only in specific cell types, and whether they play a physiological role in circadian endocrine function.

Acknowledgments

Research was supported by NIH Grants AG-19914, HD-29186, RR-00163 and U01-AG21380-03. Additional support provided by: Research Assistantship from the Department of Animal and Avian Sciences at the University of Maryland; the Intramural Research Program of the National Institutes of Health; and the National Institute on Aging. We would also like to thank the members of the Oregon National Primate Research Center: Dario Lemos, Dr. Jodi Downs, Vasilios (Bill) Garyfallou, Laura James, Luciana Tonelli Lemos and the entire

animal care staff. Statistical support graciously provided by Erin Hoerl Leone at the University of Maryland.

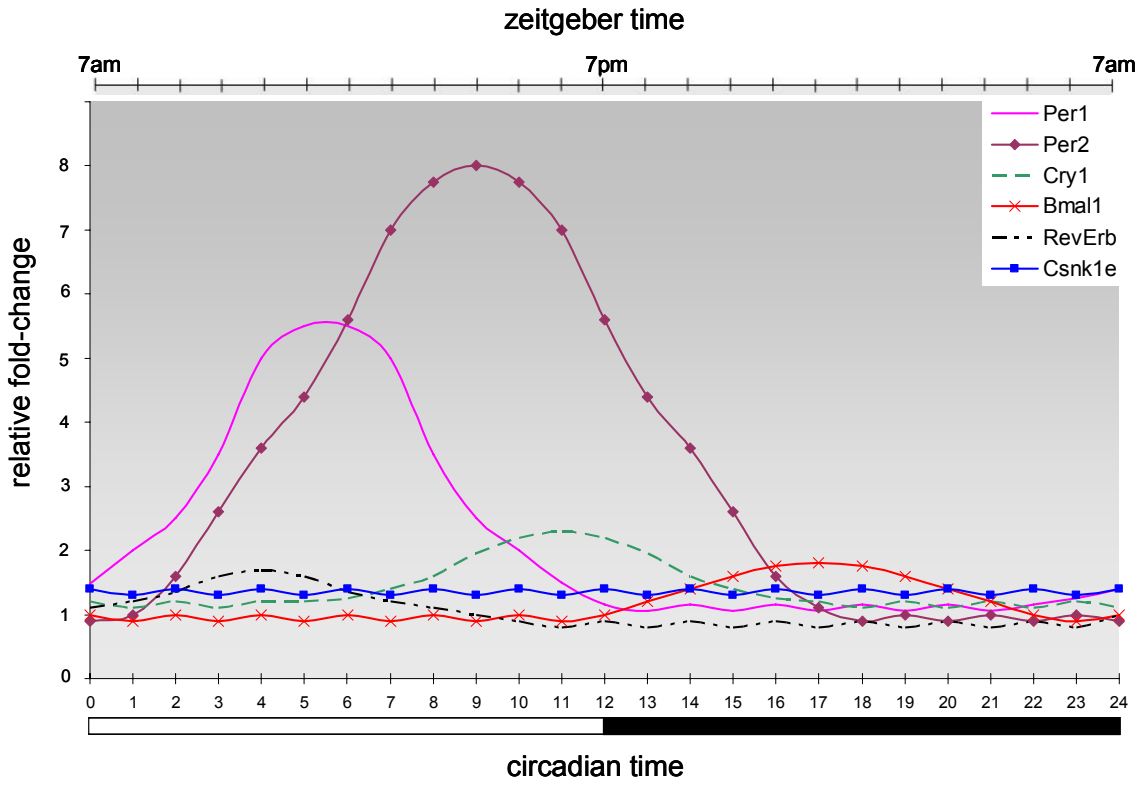

Figure 2.1 Mammalian Circadian Clock Model (mRNA Expression) Schematic presentation of core-clock mRNA expression within the suprachiasmatic nucleus (SCN). Circadian time represents the endogenous phases of the intracellular clock mechanism which in this example is entrained and reset by the daily light cycle (zeitgeber). With a 12L:12D photoperiod relative mRNA expression levels would follow this pattern. *Bmal1* transcript peaks in the middle of circadian night and is the driving force behind the clock mechanism. *Per* and *Rev-Erbα* (and to a lesser extent *Cry*) transcript levels peak during the mid to late circadian day antiphase to the *Bmal1* peak. *Csnk1ε* and *Clock* (not shown) are both constitutively expressed throughout the day. Data used to create this graph was compiled from Glossop and Hardin, 2002, and Lowrey and Takahashi, 2004.

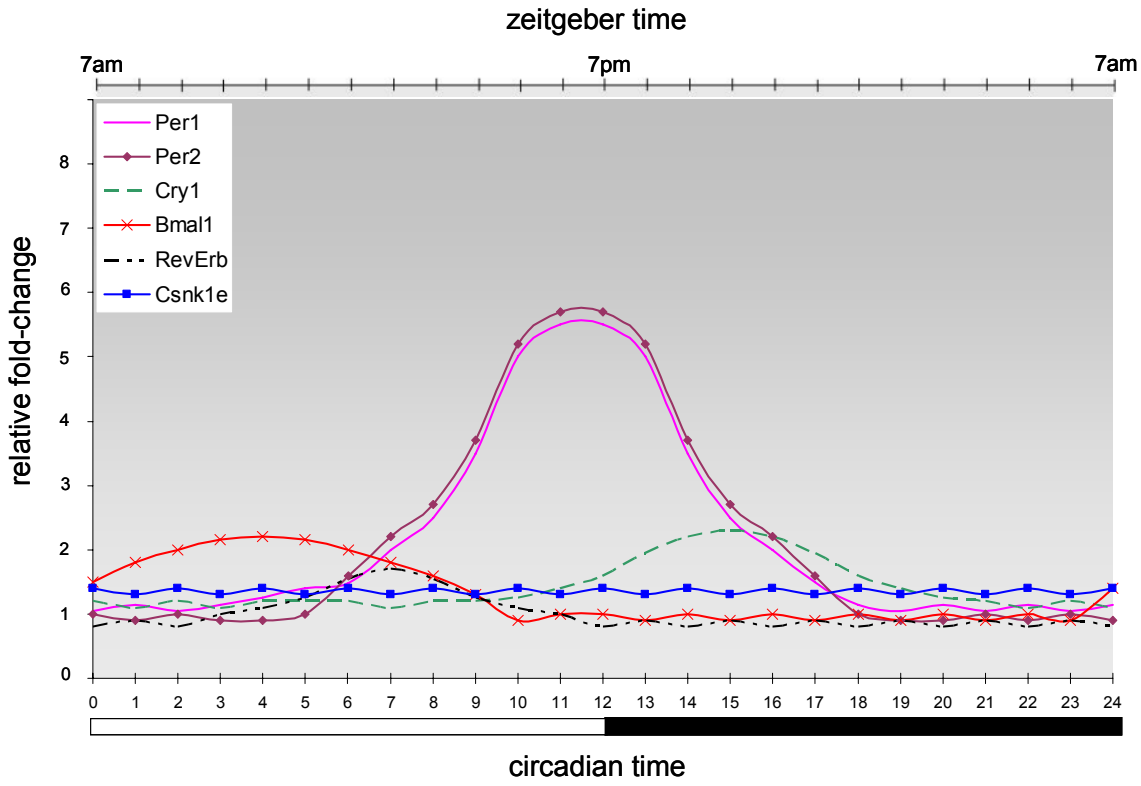

Figure 2.2 Mammalian Circadian Clock Model (Protein Expression) Schematic presentation of core-clock protein expression within the suprachiasmatic nucleus (SCN). Circadian time represents the endogenous phases of the intracellular clock mechanism which in this example is entrained and reset by the daily light cycle (zeitgeber). With a 12L:12D photoperiod relative protein expression levels would follow this pattern. Observe the variable shift in peak translation levels for each gene compared to its mRNA expression in Figure 2.1. Data used to create this graph was compiled from Glossop and Hardin, 2002, and Lowrey and Takahashi, 2004.

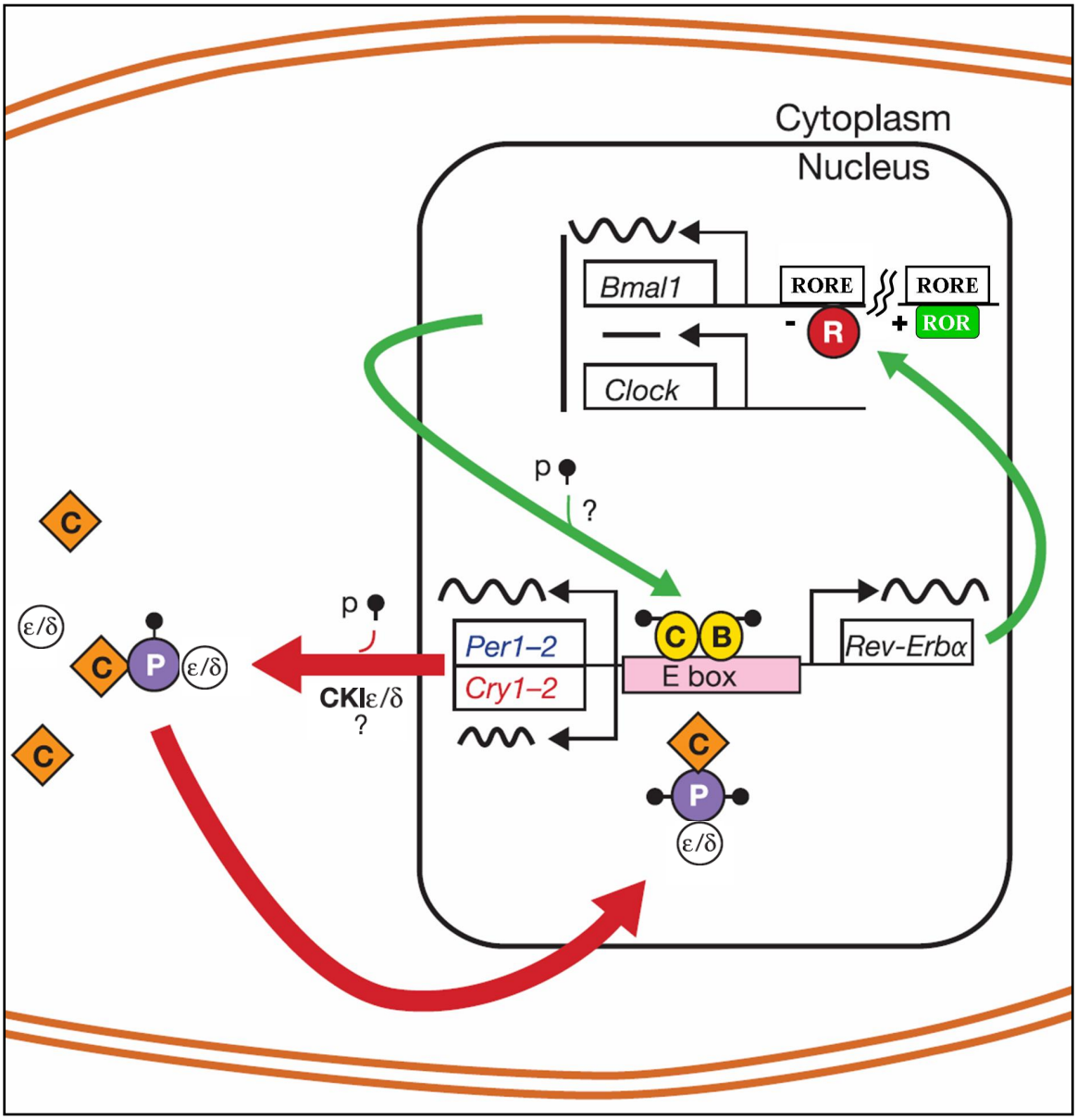

Modified from: Reppert, S. M. and Weaver, D. R. (2002). Coordination of circadian timing in mammals. Nature. *418*, 935-941.

Figure 2.3 Mammalian Circadian Clock Model The clock mechanism consists of positive (green, or light grey) and negative (red, or dark grey) feedback loops. CLOCK (C, oval) and BMAL1 (B, oval) form heterodimers and constitutively activate transcription of the *Per*, *Cry*, and *Rev-Erbα* genes through E-box enhancers in their promoter regions. As the levels of PER (P, circle) and CRY (C, diamond) proteins increase they form complexes that are phosphorylated by casein kinase 1 epsilon (CKIε or CSNK1E) and translocate into the nucleus. Once in the nucleus these complexes associate with the CLOCK-BMAL1 heterodimers to shut down transcription while the heterodimer remains bound to DNA, forming the negative feedback loop. For the positive feedback loop, increasing REV-ERBα levels (R, circle) functionally compete with retinoic acid-related orphan receptors (ROR) at the retinoic acid-related orphan receptor response elements (RORE) in the *Bmal1* promoter to repress transcription. PER-CRY mediated inhibition of CLOCK-BMAL1 mediated transcription activates *Bmal1* by lowering REV-ERBα levels.

sqRT-PCR primers	Forward sequence	Reverse sequence	Amplicon	Cycles	Temp
Per1	GCCAGCATCACTCGCAGCAGC	GTGGGTCATCAGGGTGACCAGG	~400 bp	27	65°C
Per2	CATCCACTGGTGGACCTCGCG	GGCTCACTGGGCTGCGACGC	~325 bp	27	65°C
Cry1	GCCTGTCCTAAGAGGCTTCCCTG	ACTGAGACCAGTGCCCATGGAGC	~375 bp	28	65°C
Bmal1	CACAGCATGGACAGCATGCTGC	GCCACCCAGTCCAGCATCTGC	~450 bp	26	65°C
Rev-Erbα	TGGCGCTTACCGAGGAGGAGC	TCCACCCGGAAGGACAGCAGC	225 bp	26	66°C
Csnk1ε	AAGTATGAGCGGATCAGCGAGA	CCGAATTTCAGCATGTTCCAGT	218 bp	28	65°C
β-actin	CATTGCTCCTCCTGAGCGCAAG	GGGCCGGACTCGTCATACTCC	~300 bp	22	65°C
Taqman® qRT-PCR β-actin primers	Human ACTB (beta actin) Endogenous Control (Applied Biosystems; Foster City, CA)		N/A	40	60°C
Taqman® qRT-PCR β-actin probe			N/A	40	60°C
Taqman® qRT-PCR Rev-Erbα primers	ACCCTGAACAACATGCATTCC	GGAGAGAGAAGTGCAGAGTTCGA	~100	40	60°C
Taqman® qRT-PCR Rev-Erbα probe	5'-6FAM-CTGCCGCTGCCCCCTTGTACA-TAMRA-3'		N/A	40	60°C

Table 2.1 Core-Clock Gene Primers and Probes Forward and reverse primer sequences (5' to 3') used for sqRT-PCR and qRT-PCR are shown along with the expected amplicon sizes, annealing temperatures and number of cycles run for each reaction. Primers and qRT-PCR probes were designed using human or rhesus macaque gene sequences and PrimerExpress® software (Applied Biosystems). All were successful in detecting core-clock mRNA gene expression.

probeset	gene	Juvenile	Young Adult	Old Adult
202861_at	***Per1***	765 ± 185	553 ± 44	735 ± 103
36829_at	***Per1***	1301 ± 254	1037 ± 115	1038 ± 46
205251_at	***Per2***	1881 ± 57	1283 ± 327	1460 ± 101
208518_s_at	***Per2***	311 ± 27[a]	186 ± 15[b]	317 ± 25[a]
209674_at	***Cry1***	314 ± 62	309 ± 63	360 ± 124
209824_s_at	***Bmal1***	500 ± 30[a]	792 ± 71[b]	630 ± 69[a,b]
210971_s_at	***Bmal1***	298 ± 31	355 ± 80	444 ± 123
31637_s_at	***Rev-Erbα***	1989 ± 232	2617 ± 203	2188 ± 282
202332_at	***Csnk1ε***	207 ± 13	184 ± 16	148 ± 18
204980_at	***Clock***	280 ± 16	365 ± 38	357 ± 41
217563_at	***Clock***	142 ± 25	172 ± 18	142 ± 15

Table 2.2 Gene Expression Profiles of Core-Clock Genes in the Rhesus Macaque Pituitary Gland Mean signal intensity values (±SEM) of core-clock gene expression across three age categories (n=3) of rhesus macaques (Juvenile = 1 - 2 years, Young Adult = 7 - 12 years, and Old Adult = 18 - 26 years) as measured by GeneChip® microarray (Affymetrix). Significant differences were observed in *Per2* and *Bmal1* expression using one-way ANOVA and Tukey-Kramer post-hoc analysis (letter notations, $P<0.05$).

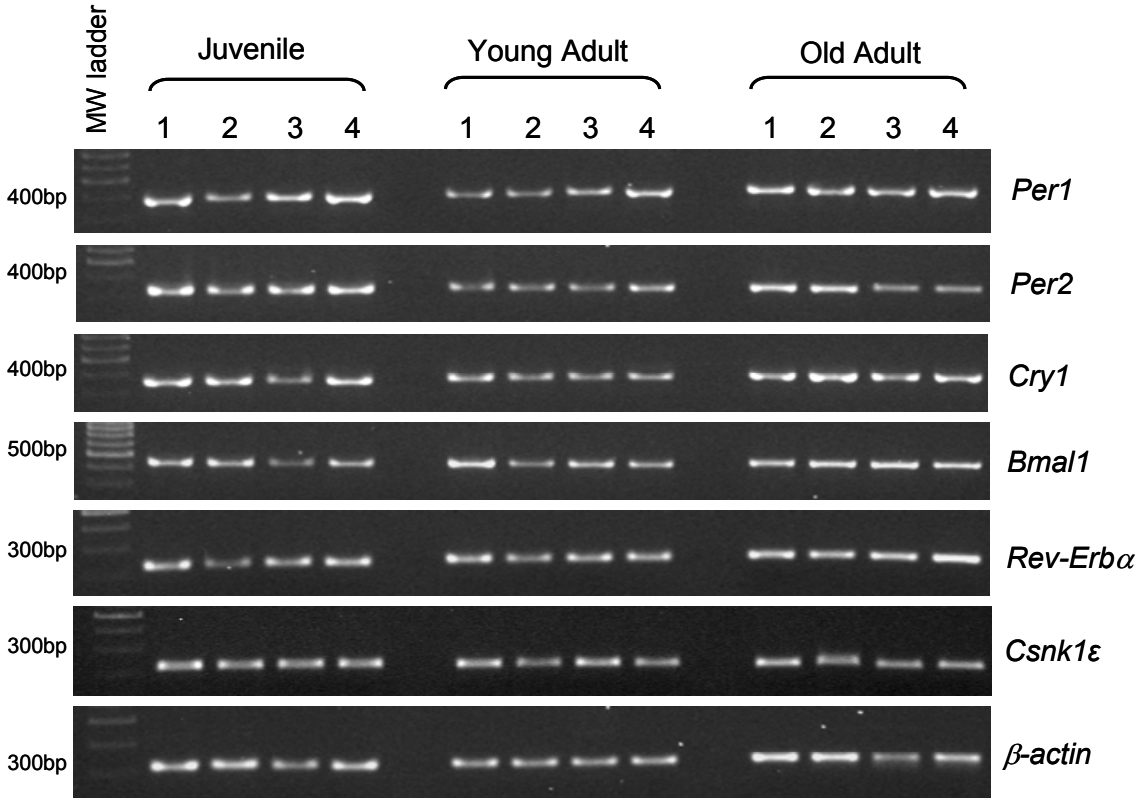

Figure 2.4 Age Distribution of Core-Clock Genes in the Rhesus Macaque Pituitary Gland Representative sqRT-PCR results validating the microarray data and demonstrating expression of clock genes across three age categories (n=4) of rhesus macaques (Juvenile = 1 - 2 years, Young Adult = 7 - 12 years, and Old Adult = 18 - 26 years). The housekeeping gene β-actin was used as a positive control and for normalizing images for analysis.

Figures 2.5 A-F sqRT-PCR Expression Levels of Core-Clock Genes Across Age Categories in the Rhesus Macaque Pituitary Gland Each bar, along with SEM, represents mean, normalized fluorescence data from four animals. Statistical comparisons were made using one-way ANOVA and Tukey-Kramer post-hoc analysis ($P<0.05$). Significant differences were observed in *Per2* expression (Graph A) between Juvenile animals and the other two groups, resulting in a negative fold-change of 0.63 ($\pm$0.05) and 0.58 ($\pm$0.06), respectively. *Csnk1ε* and *Bmal1* expression (Graphs B-C) did not reach significant levels due to large variation within some groups, but trends were observed that correlated with microarray data. The other transcripts were not significantly different across age categories.

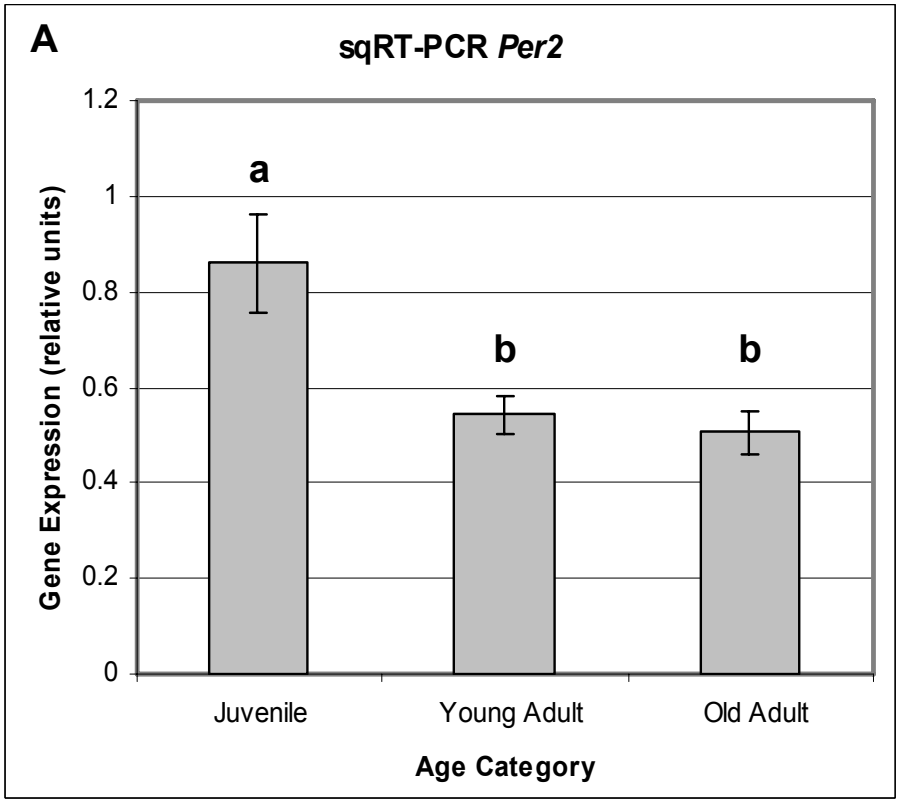
A
sqRT-PCR Per2
1.2
1
0.8
0.6
0.4
0.2
0
Gene Expression (relative units)
a
b
b
Juvenile
Young Adult
Old Adult
Age Category

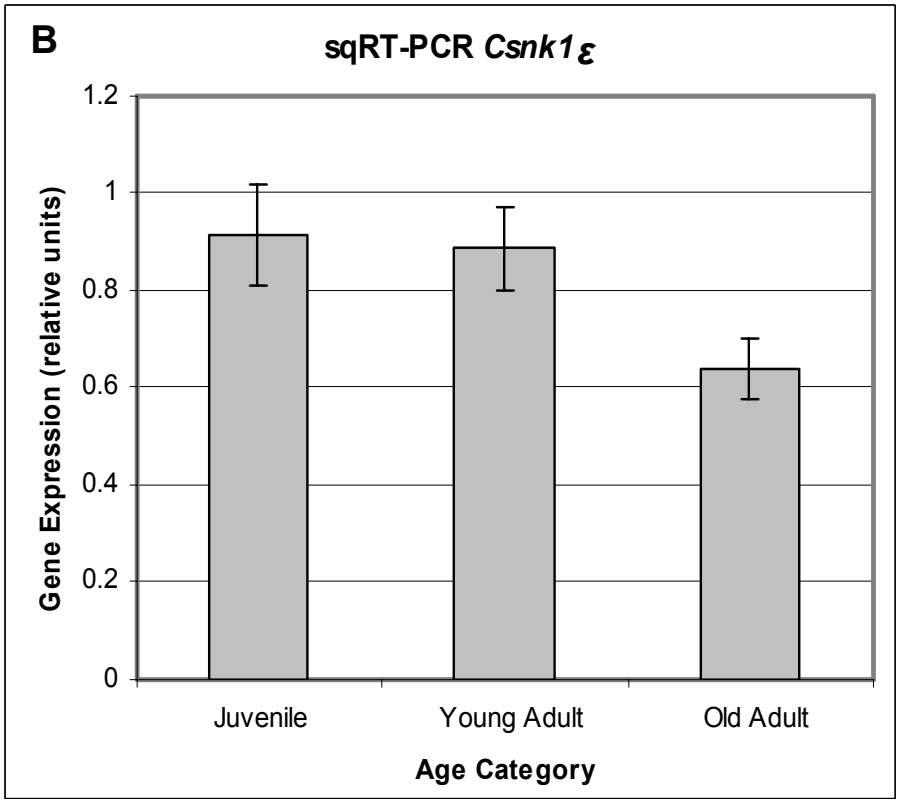
B
sqRT-PCR Csnk1ε
1.2
1
0.8
0.6
0.4
0.2
0
Gene Expression (relative units)
Juvenile
Young Adult
Old Adult
Age Category

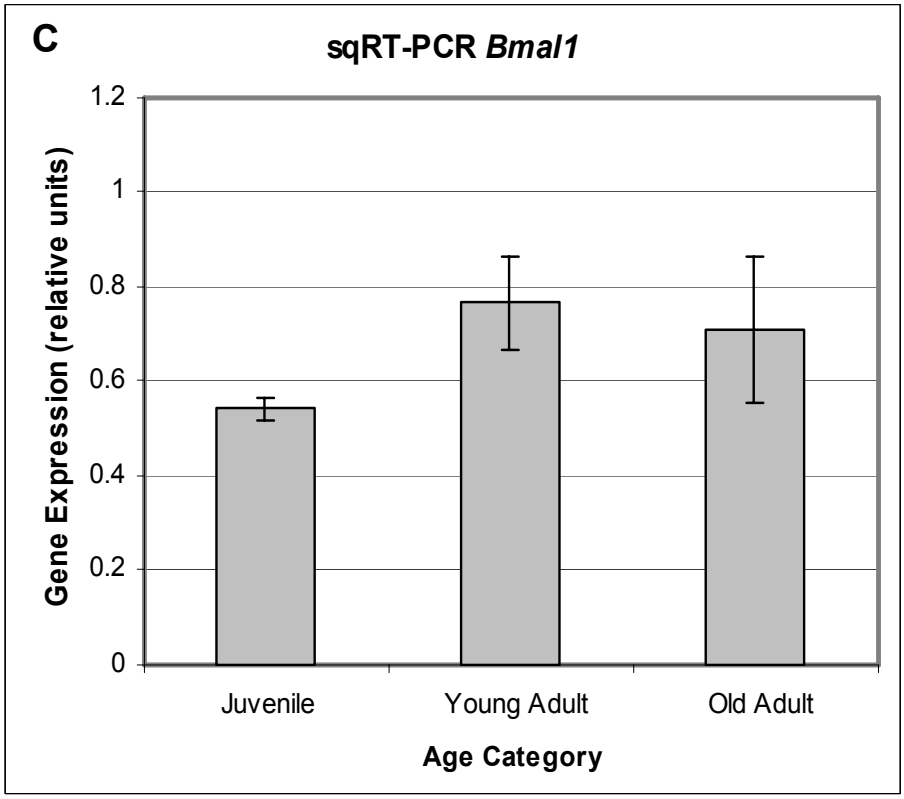
C
sqRT-PCR *Bmal1*
Gene Expression (relative units)
1.2
1
0.8
0.6
0.4
0.2
0
Juvenile
Young Adult
Old Adult
Age Category

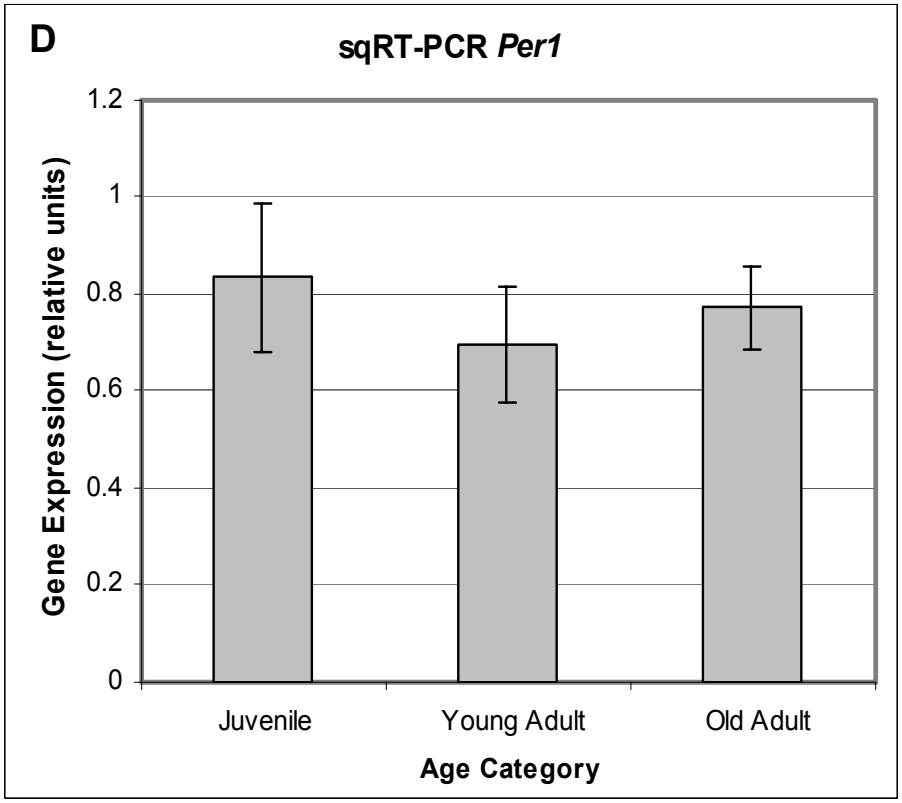
D
sqRT-PCR *Per1*
Gene Expression (relative units)
1.2
1
0.8
0.6
0.4
0.2
0
Juvenile
Young Adult
Old Adult
Age Category

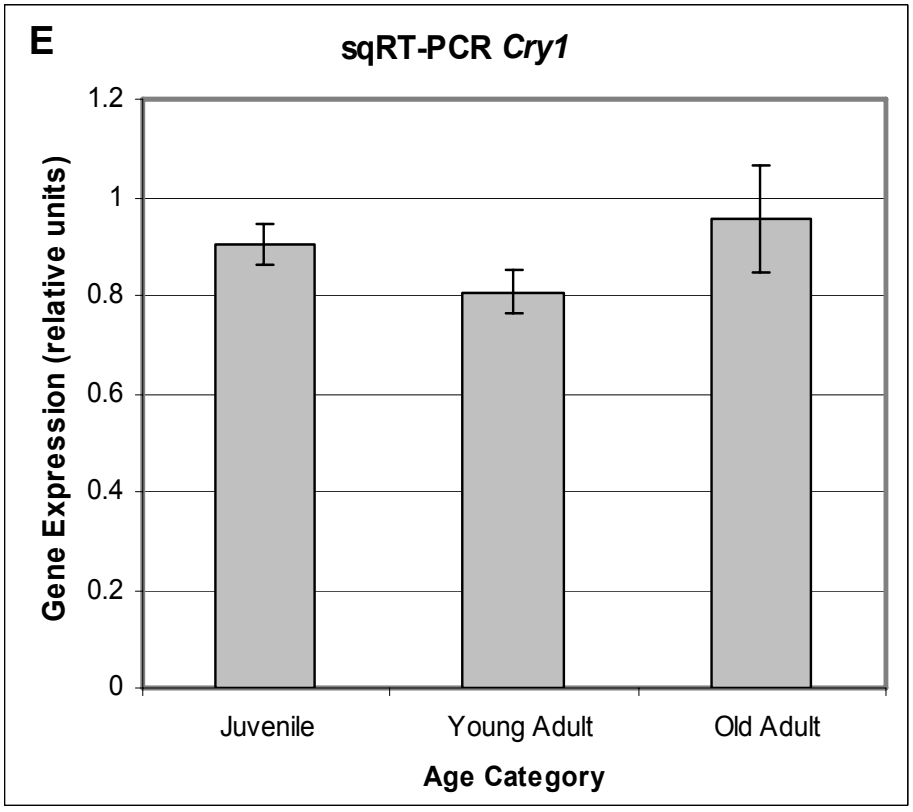
E
sqRT-PCR *Cry1*
Gene Expression (relative units)
1.2
1
0.8
0.6
0.4
0.2
0
Juvenile
Young Adult
Old Adult
Age Category

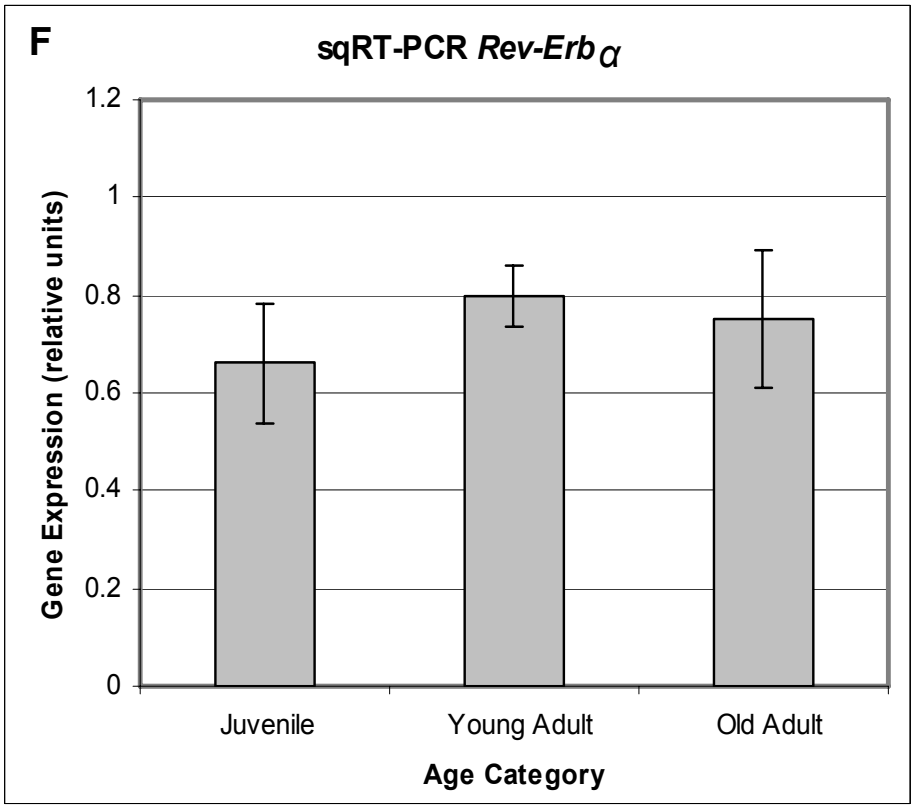
F
sqRT-PCR *Rev-Erb*α
Gene Expression (relative units)
1.2
1
0.8
0.6
0.4
0.2
0
Juvenile
Young Adult
Old Adult
Age Category

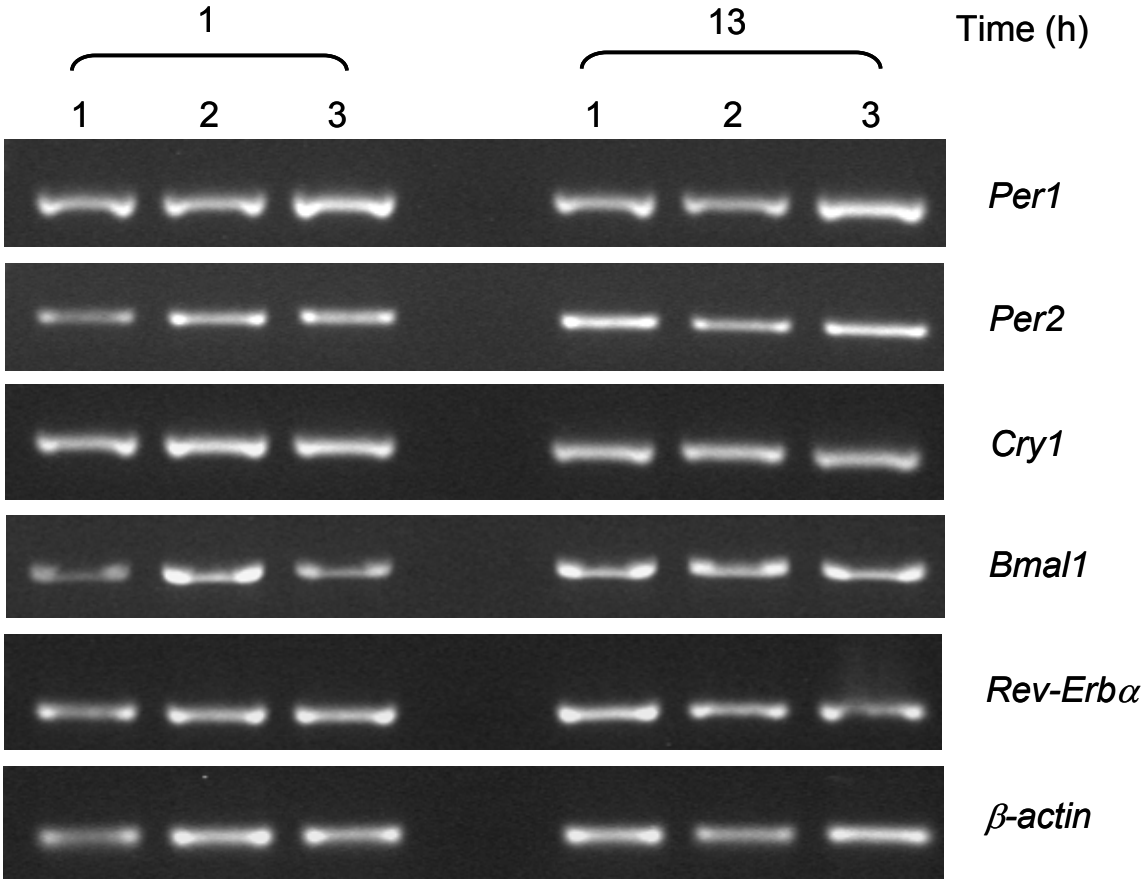

Figure 2.6 Phase Shift Expression of Core-Clock Genes in the Rhesus Macaque Pituitary Gland Representative sqRT-PCR results demonstrating expression of core-clock genes at 1 h (lanes 1-3) and 13 h (lanes 4-6). The housekeeping gene β-actin was used as a positive control and for normalizing images for analysis. *Csnk1ε* was not measured because it is constitutively expressed across the 24-hour cycle.

Figures 2.7 A-E sqRT-PCR Expression Levels of Core-Clock Genes at 0100 h and 1300 h in the Rhesus Macaque Pituitary Gland Each bar, along with SEM, represents mean, normalized fluorescence data from three animals. Statistical comparisons were made using Student's *t*-test (*, $P<0.05$). Significant differences were observed in expression levels between time points and resulted in a fold-change of 1.33 ($\pm$0.03) for *Per2* and 1.82 ($\pm$0.17) for *Bmal1*.

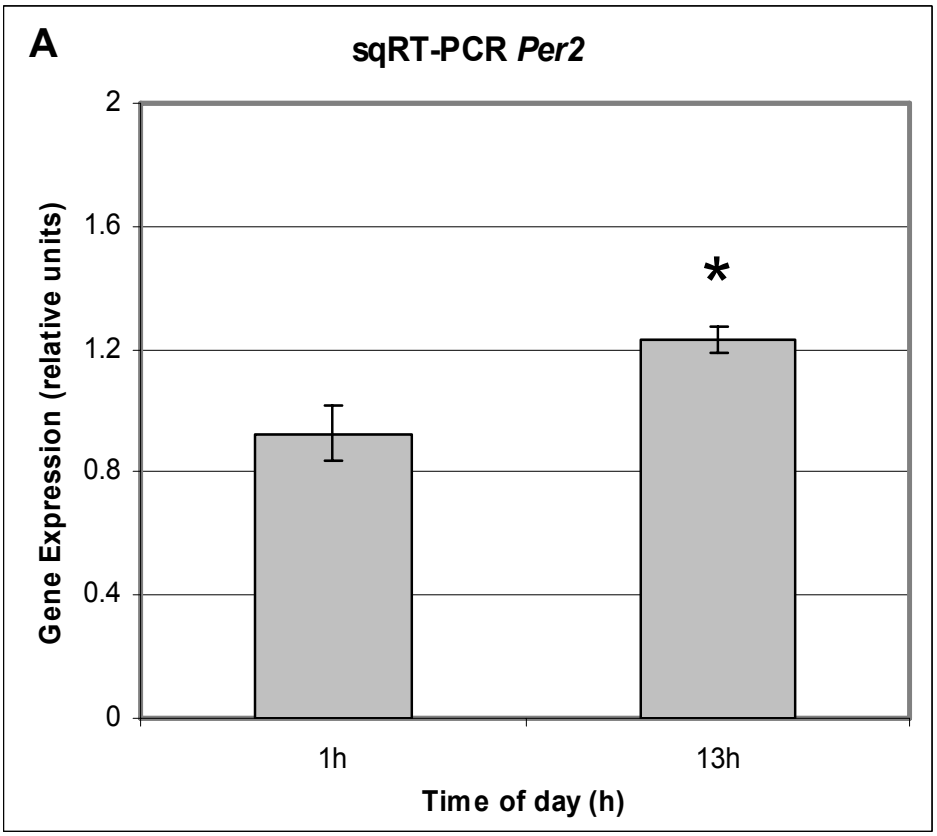

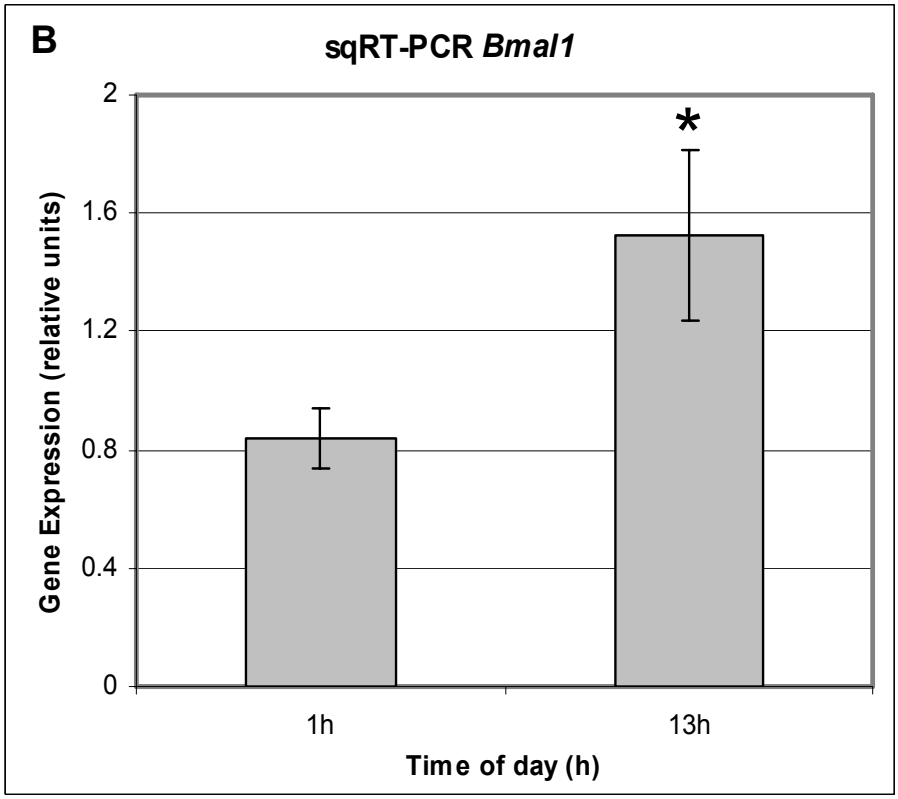
B
sqRT-PCR *Bmal1*
Gene Expression (relative units)
2
1.6
1.2
0.8
0.4
0
*
1h
13h
Time of day (h)

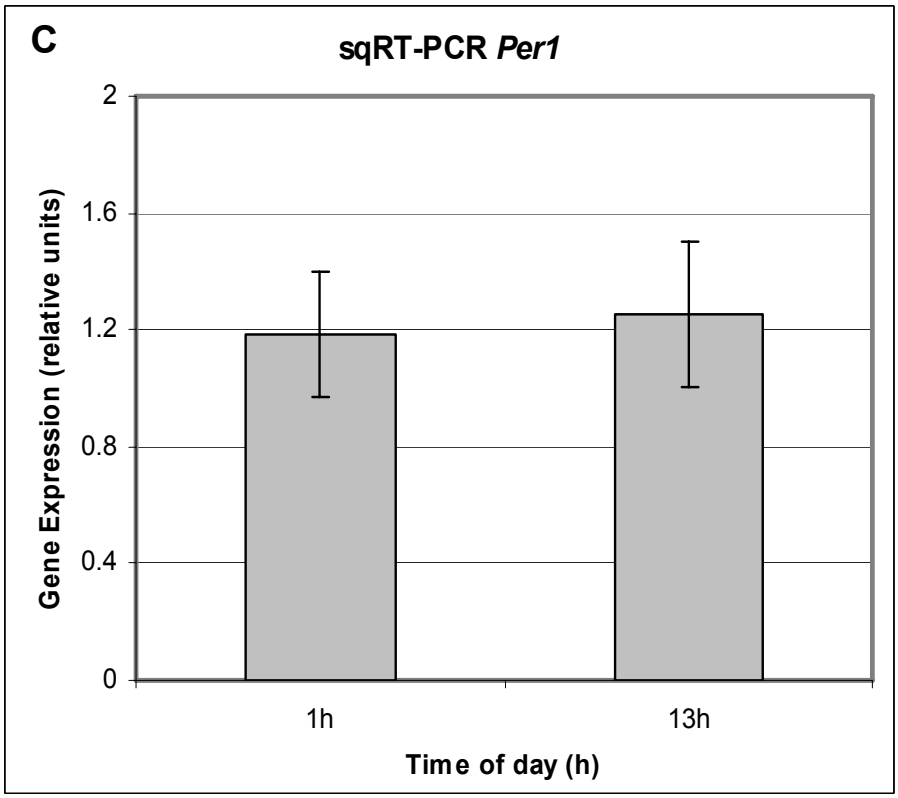
C
sqRT-PCR *Per1*
Gene Expression (relative units)
2
1.6
1.2
0.8
0.4
0
1h
13h
Time of day (h)

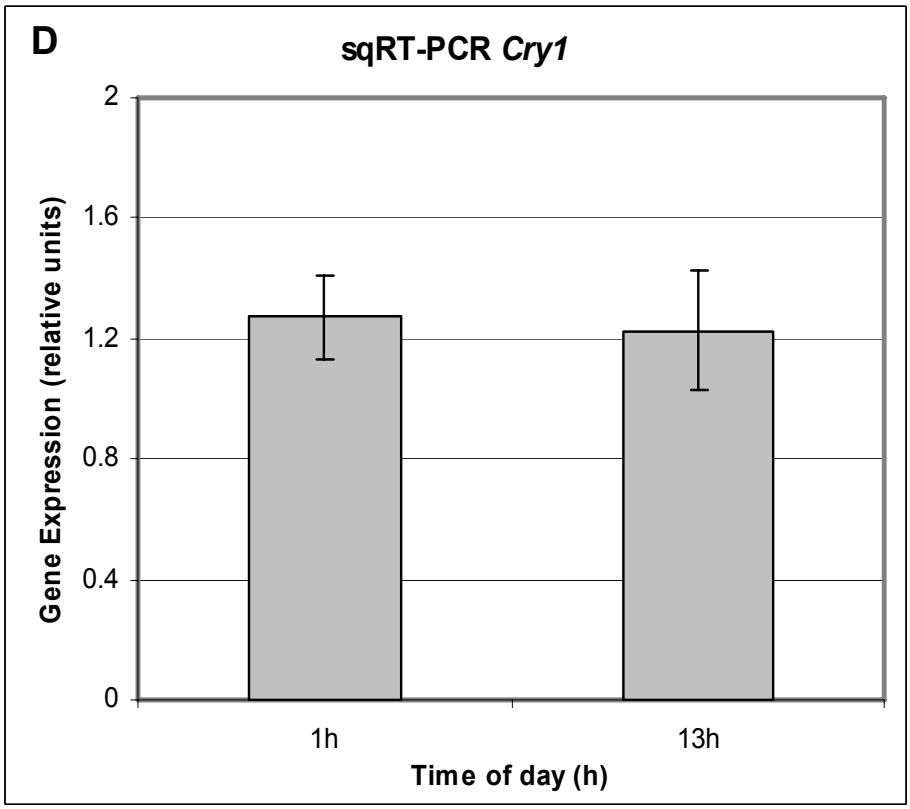
D
sqRT-PCR *Cry1*
Gene Expression (relative units)
2
1.6
1.2
0.8
0.4
0
1h
13h
Time of day (h)

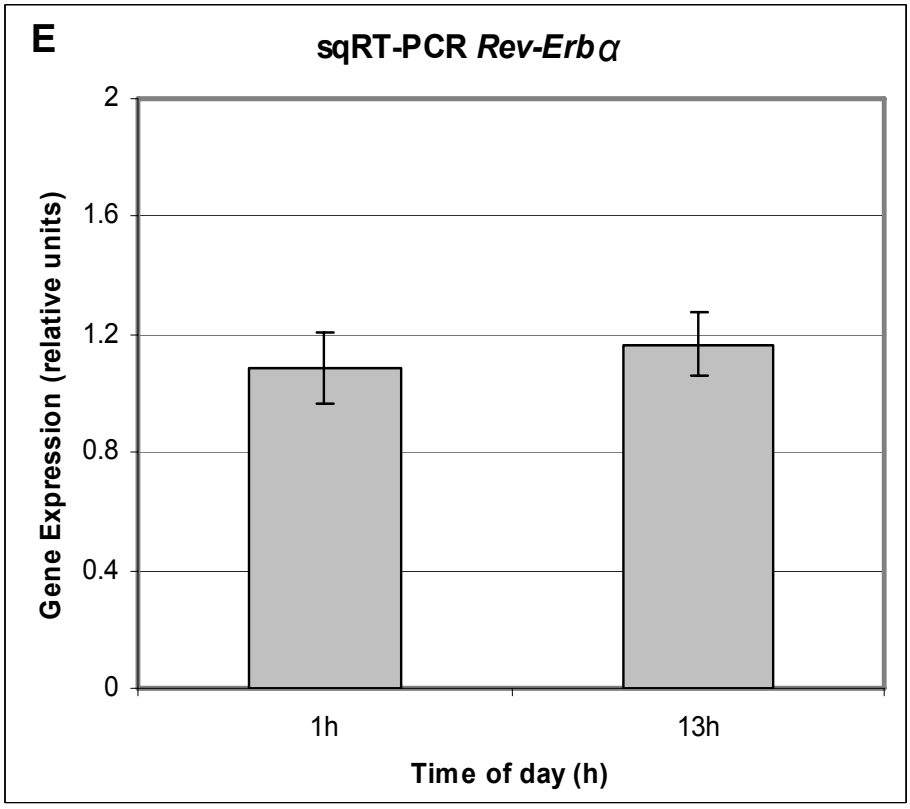
E
sqRT-PCR *Rev-Erbα*
Gene Expression (relative units)
2
1.6
1.2
0.8
0.4
0
1h
13h
Time of day (h)

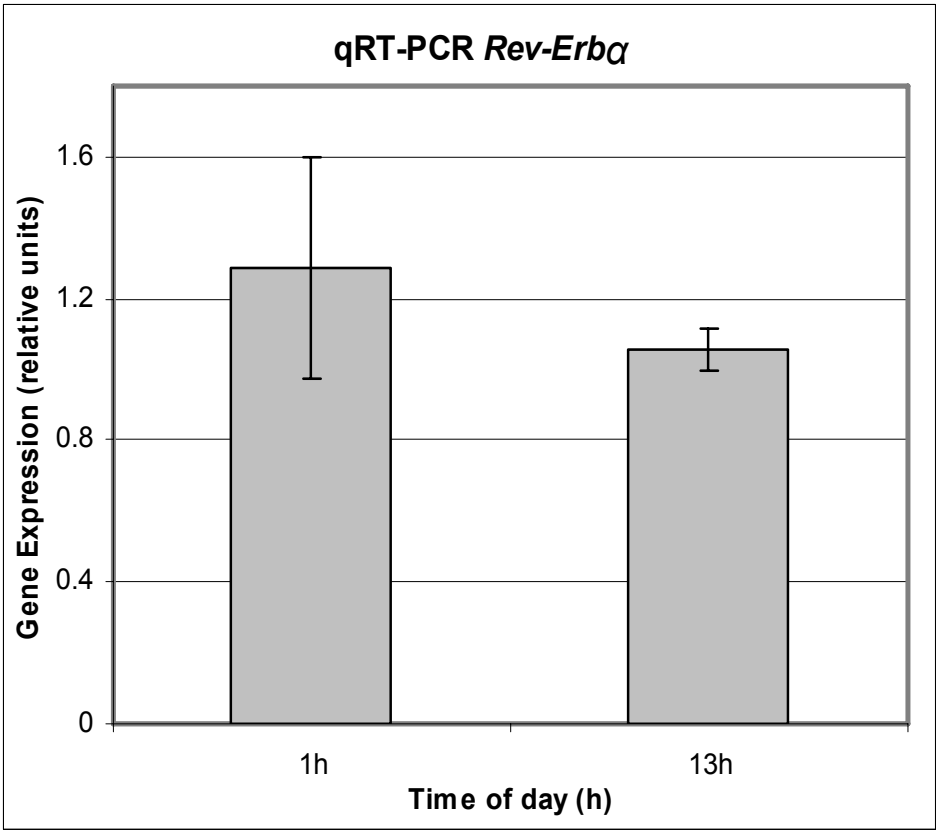

Figure 2.8 Taqman® Quantitative Real-Time PCR of *Rev-Erbα* in the Rhesus Macaque Pituitary Gland Each bar, along with SEM, represents mean, normalized fluorescence data from three animals. Statistical comparisons were made using Student's *t*-test ($P<0.05$).

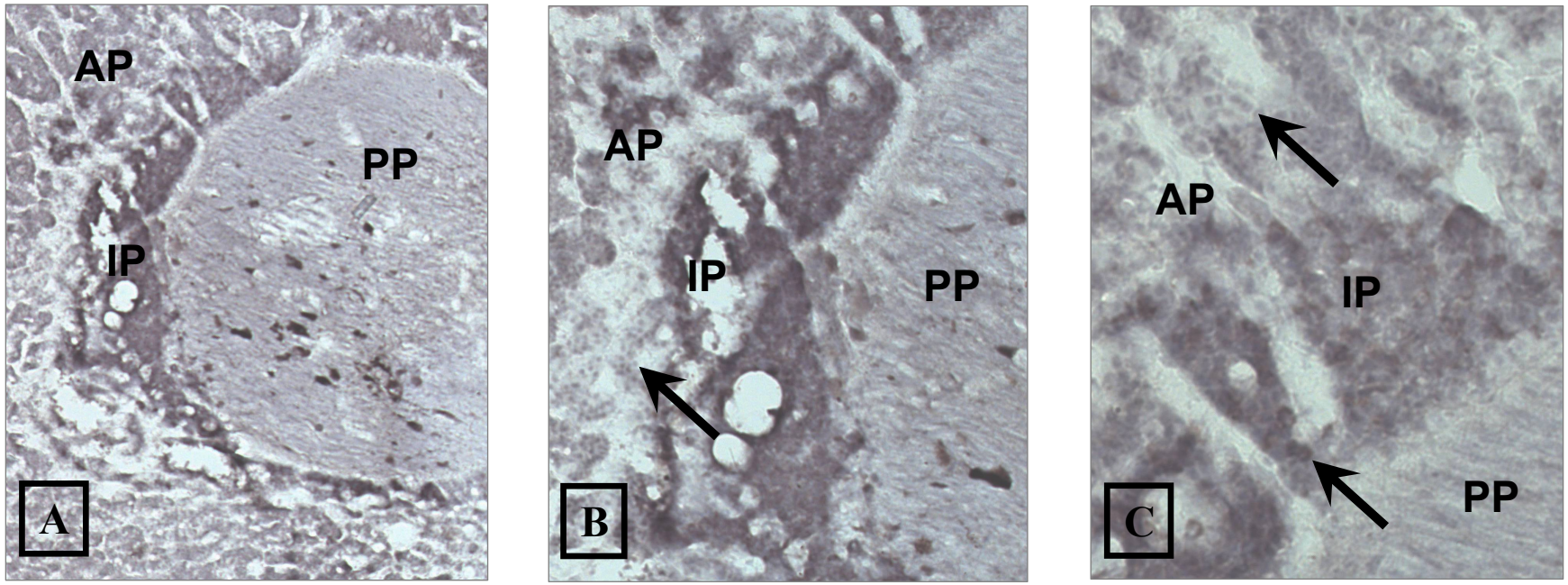

Figure 2.9 Immunohistochemistry of REV-ERBα Distribution Within the Rhesus Macaque Pituitary Gland REV-ERBα nuclear immunostaining in the pituitary gland demonstrating regional variation in protein expression. A) very low power magnification of entire pituitary gland (anterior pituitary=AP, posterior pituitary=PP, intermediate pituitary=IP). B) all three regions at low magnification. C) all three regions under moderate magnification. Black arrows indicate nuclear staining.

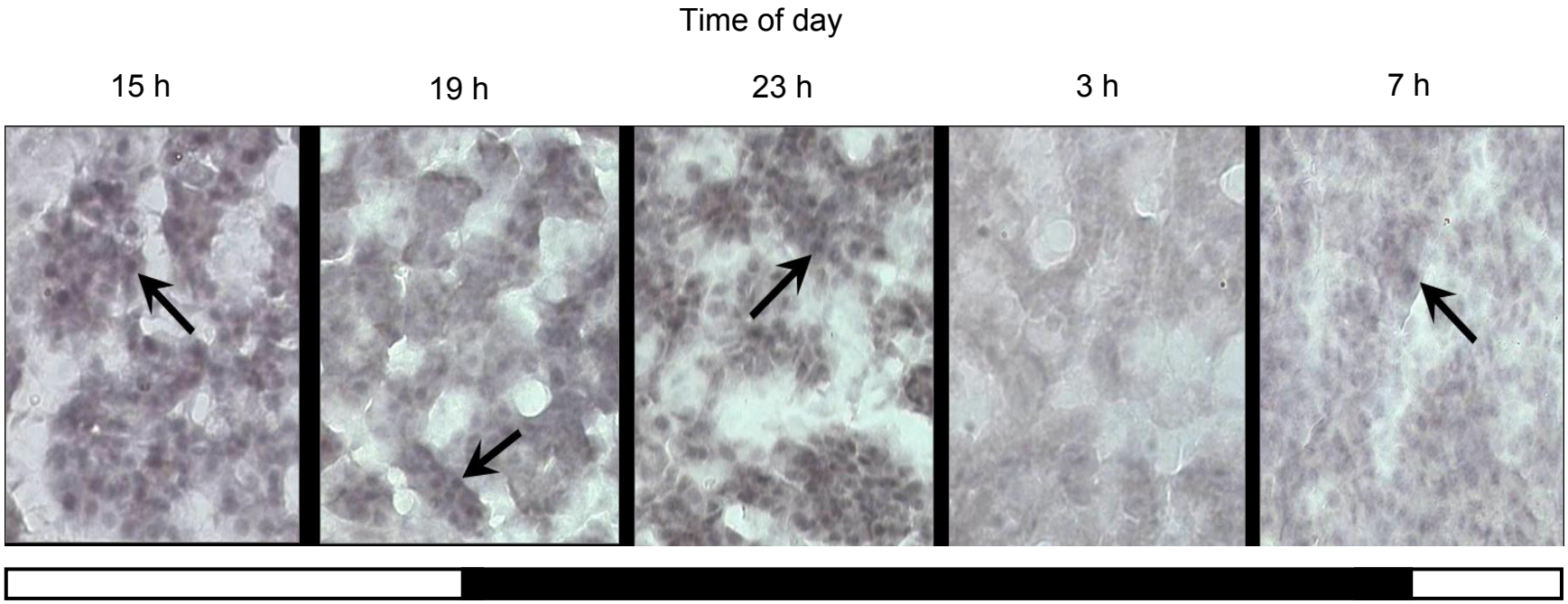

Figure 2.10 Immunohistochemistry of Circadian Expression of REV-ERBα in the Rhesus Macaque Pituitary Gland
REV-ERBα nuclear immunostaining (black arrows) in the anterior pituitary gland showing temporal changes in intensity across a 24-hour cycle (400X bright-field). The horizontal white and black bar represent day and nighttime.

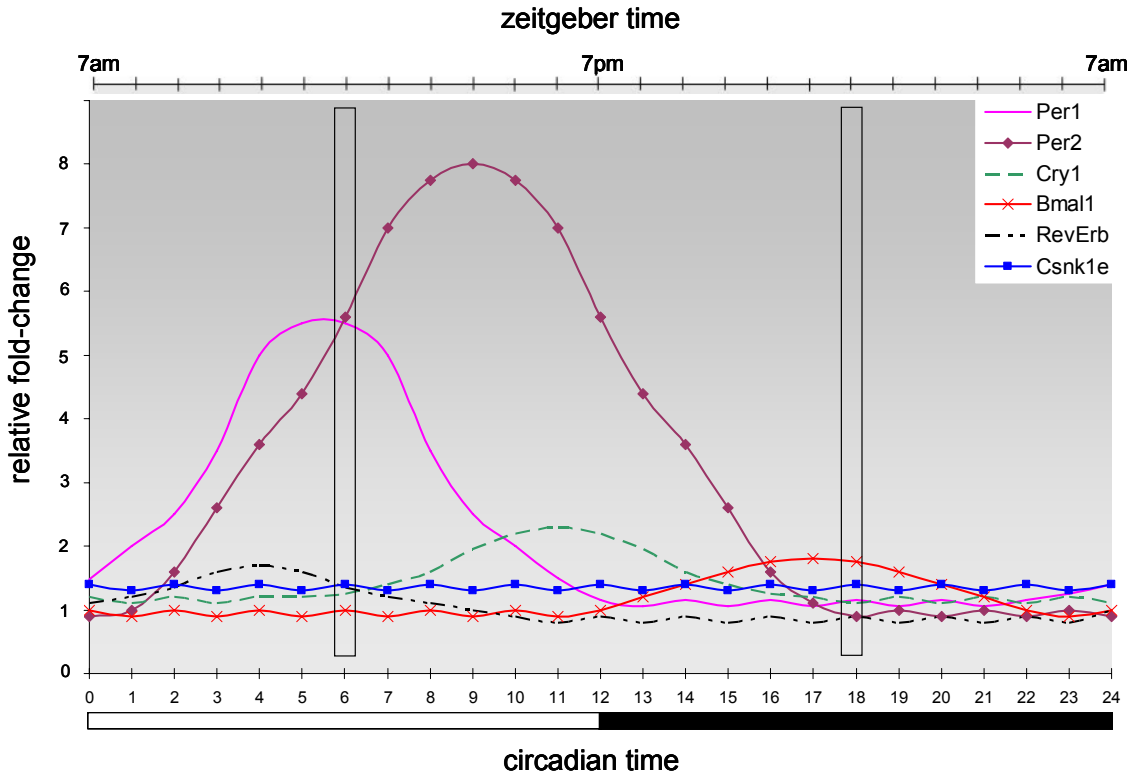

Figure 2.11 Mammalian Circadian Clock Model (mRNA Expression) with Experimental Sampling Time Points Schematic presentation of core-clock mRNA expression within the suprachiasmatic nucleus (SCN). Vertical black boxes represent the sampling time points for pituitary glands in Experiment 2: Phase shift expression of core-clock genes. Peripheral tissue presumably exhibits a similar pattern of expression but in which the mRNA peaks are phase shifted depending on the exact tissue type.

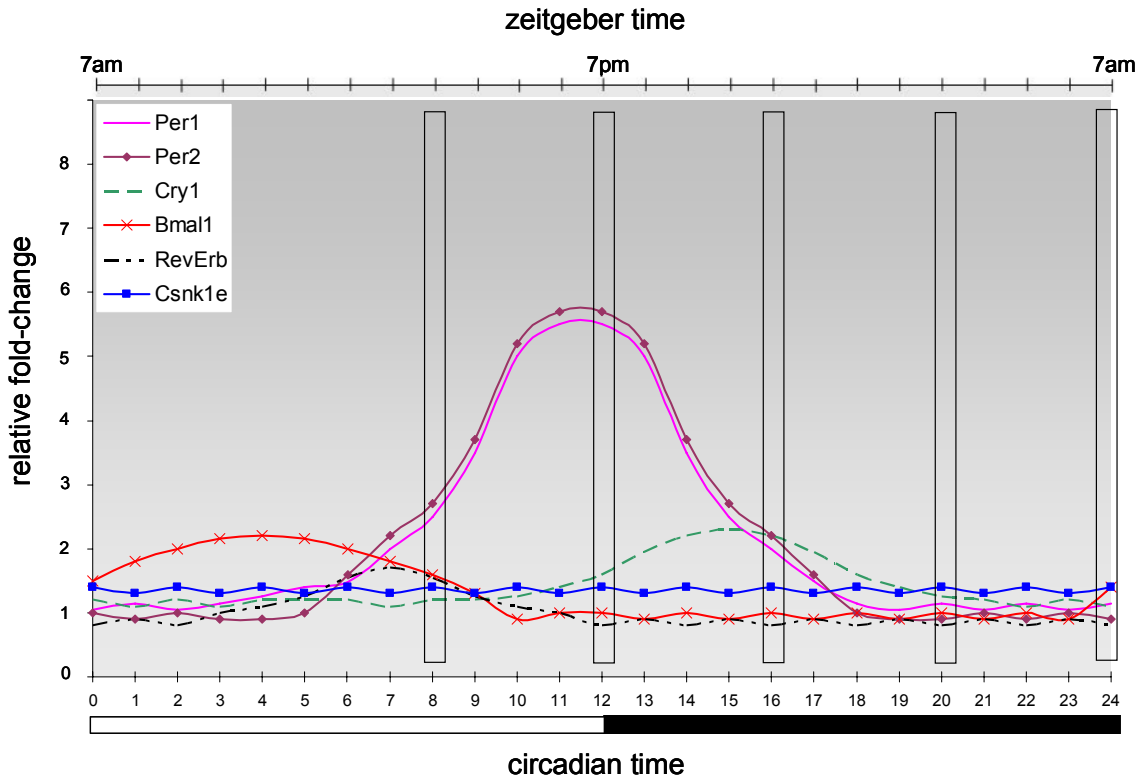

Figure 2.12 Mammalian Circadian Clock Model (Protein Expression) with Experimental Sampling Time Points Schematic presentation of core-clock protein expression within the suprachiasmatic nucleus (SCN). Vertical black boxes represent the sampling time points for pituitary glands in Experiment 3: 24-hour gene expression changes of core-clock genes. Peripheral tissue presumably exhibits a similar pattern of expression but in which the protein peaks are phase shifted depending on the exact tissue type.

CHAPTER 3

EFFECTS OF MODERATE CALORIE RESTRICTION ON PITUITARY GLAND GENE EXPRESSION IN THE MALE RHESUS MACAQUE (*MACACA MULATTA*)

INTRODUCTION

Calorie restriction (CR), defined as undernutrition without malnutrition, has been established as the only non-genetic method of altering longevity and attenuating the biological changes associated with aging (Koubova and Guarente, 2003; Lane et al., 1999b; McCay et al., 1935). Calorie restricted animals receive essential nutrients and vitamins while total calorie intake is decreased to a range 30-70% below *ad libitum* levels. The result is lower energy input without sacrificing nutritional competence (Weindruch and Walford, 1988). Some characteristic markers of CR include reduced body mass and adiposity, lower body temperature, slowed growth, delayed skeletal maturation, and decreased glucose and fasting plasma insulin levels. In addition, CR has been shown to alter gene expression profiles and modify neuorendocrine function by lowering levels of growth hormone (GH), thyroid stimulating hormone (TSH) and thyroid hormones (Gredilla and Barja, 2005; Gresl et al., 2001; Heilbronn and Ravussin, 2003; Koubova and Guarente, 2003; Lane et al., 1997). Although the exact mechanisms of action explaining CR's benefits are still elusive, this experimental paradigm has been found to be effective in a diversity of species including yeast, rotifers, nematodes, flies, fish, rodents, dogs and possibly non-

human primates (Ingram et al., 1990; Lane et al., 1999b; Roth et al., 1999; Weindruch and Walford, 1988).

Moderate calorie restriction is believed to successfully intervene in the cascade of events which lead to normal aging, thus accounting for its advantageous health benefits. These aging events occur simultaneously at molecular, cellular and systemic levels, resulting in disruption of homeostatic mechanisms and progressive loss of function (including reproductive capacity). A few examples of age-related homeostatic imbalance include decreased stress response, increased pathology, decline in memory function and documented alterations in circadian organization, such as changes in hormonal rhythms, core body temperature and sleep/wake cycles (Asai et al., 2001; Hofman and Swaab, 2006; Oster et al., 2003). In males, the age-related reproductive demise occurs with functional deterioration of the system at several sites including reduced testosterone (T) production, decreased hypothalamic gonadotropin-releasing hormone (GnRH) and altered pituitary gland release of gonadotropins (Harman et al., 2001; Moffat et al., 2002; Ottinger, 1998).

While data on life extension in a wide range of species strongly suggests that CR mechanisms are universal across species, few studies were conducted in an animal model living longer than four years until the late 1980's. In 1987, to address the relevance of this nutritional intervention to human health, the National Institute on Aging began the first study of CR and aging in non-human primates using rhesus macaques (*Macaca mulatta*) to determine its potential application in humans (Ingram et al., 1990). Several endpoints have since been

investigated in studying the long-term effects of CR on aging in these animals. Results parallel findings in other species and verified the CR-induced attenuation of age-related changes in plasma triglycerides, oxidative damage, and glucose regulation (Mattison et al., 2003; Roth et al., 2002). Treatment animals weighed less, with reduced body fat and lower body temperatures than their matching control counterparts, providing early evidence of the potential benefit of CR for individuals at risk for diabetes and cardiovascular disease (Lane et al., 1999a; Mattison et al., 2003).

As with rats, moderate calorie restriction implemented prior to sexual maturity delayed the maturation-related increase in circulating testosterone concentrations and postponed skeletal growth by approximately one year in male rhesus macaques (Lane et al., 1997; Mattison et al., 2003; Roth et al., 2000). Less is known, however, about the impact of CR on the hypothalamic-pituitary-gonadal (HPG) axis when the dietary intervention is applied post-pubertally. In light of the essential functions of the neuroendocrine system and the pituitary gland in the HPG axis, it is important to examine pituitary gland function as a critical site for CR-associated effects.

The aim of the present study was to investigate the impact of CR on pituitary gland gene expression and to quantify expression levels in adult rhesus macaques (*Macaca mulatta*). We were particularly interested in genes associated with reproduction, circadian mechanisms, metabolism, and oxidative stress.

MATERIALS AND METHODS

Animals and Diet

All experiments were approved for use by the Institutional Animal Care and Use Committees at the University of Maryland and the Oregon National Primate Research Center. The study consisted of 10 Young Adult (12 years) male rhesus macaques (*Macaca mulatta*) fed a control diet (CON; n=5) or calorie restricted at 30% CON (CR; n=5) for eight years, beginning post-pubertally. Animals were individually housed in a temperature-controlled environment under 12L:12D photoperiod (lights on 7 h -19 h) and allowed auditory, visual and olfactory interaction with male and female conspecifics in the vivarium. Food was provided in two meals at 8 h and 15 h daily; water was available *ad libitum*.

The diet consisted of individual biscuits that had been specially formulated for this study (Ingram et al., 1990) supplemented with a daily low calorie treat. The composition of the diet was 15% protein, 5% fat and 5% fiber with a caloric content of approximately 3.7 kcal/g. Biscuits included a vitamin/mineral mix that was 40% higher than the recommended allowance for rhesus macaques by a National Research Council report (NRC, 1978), but were otherwise similar to those used in many laboratory studies of rhesus macaques. This vitamin/mineral supplementation was designed to ensure sufficient availability of essential nutrients in both the CON and CR diets. Thus, it should be clear that the CON and CR groups were receiving exactly the same diet. Biochemical assays were performed periodically and with every new shipment to ensure diet content and quality (Black et al., 2001; Mattison et al., 2005).

The amount of food provided to CON animals was provided at an *ad libitum* level, originally determined with the individual leaving a few uneaten biscuits each day during regular measurements of food consumption. CR macaques were given 30% less than age- and body-weight matched controls. Food allotments were held constant other than as needed on a case-by-case basis when warranted by greater than acceptable changes in body weight (Lane et al., 1999b; Mattison et al., 2005).

Animals were sacrificed according to the NIH *Guide for the Care and Use of Laboratory Animals*. Pituitary glands were collected and sectioned sagittally. One half of each pituitary gland was flash frozen in liquid nitrogen and the other half was fixed in 4% paraformaldehyde.

RNA Extraction and Gene Microarrays

Sagittally cut, flash frozen pituitary gland sections were homogenized using a PowerGen rotor-stator homogenizer (Fisher Scientific; Pittsburgh, PA). Total RNA was isolated using RNeasy columns (QIAGEN; Valencia, CA); concentration and integrity were assessed by microcapillary electrophoresis using a model 2100 Agilent Bioanalyzer (Santa Clara, CA; see Appendix A for more detail). Three samples from both treatment groups were sent for microarray analysis at the Affymetrix Microarray Core of the OHSU Gene Microarray Shared Resource.

Analysis was performed in accordance with the manufacturer's instructions (Affymetrix GeneChip® Analysis Technical Manual; Santa Clara, CA).

Labeled target cRNA was prepared from total RNA samples and hybridized to GeneChip® Rhesus Macaque Genome Arrays detecting over 47,000 transcripts. Image processing and expression analysis were performed using Affymetrix GCOS v1.2 software. A number of quality control metrics were utilized as a measure of probe quality and included chip background, chip noise, total fluorescent intensity, number of genes detected and the 3'/5' ratio of the housekeeping genes β-actin and GAPDH. These metrics are assessed to determine the validity of the data obtained from the scanned GeneChip®. Data were normalized to an average intensity on each chip which enabled direct comparisons between the six different arrays.

Gene Microarray Filtering

Microarray data filtering was performed using Genesifter® software (vizXlabs; Seattle, WA) followed by hand analysis and determination of genes of interest (see Appendices B and C). Briefly, unscaled array data was normalized and $\log_2$ transformed using robust multi-array average (RMA) analysis. Student *t*-test ($P<0.05$) comparisons with Benjamini-Hochberg post-hoc corrections were performed. Signal quality and fold-change parameters were not set in order to allow for qualitative and quantitative hand filtering later. Probesets showing a significant change between treatments were then imported into Excel (Microsoft; Redmond, WA) and filtered for a minimum 1.5 fold-change in expression. Based on this gene discovery method, probesets meeting these criteria for significance were then considered for investigation. In addition, a keyword search of the entire

52,000+ probesets was performed to identify non-significantly changed probesets of interest. These included genes that were highly expressed and/or fell into the categories of reproduction, metabolism and oxidative stress. Table 3.1 lists the pituitary gland genes (and their probesets) that were subjected to sqRT-PCR and qRT-PCR.

Semi-quantitative RT-PCR

PrimerExpress® software (Applied Biosystems; Foster City, CA) was used for all primer and probe design (Appendix G). Specific primers were designed for each transcript using the predicted rhesus macaque mRNA sequences posted at the National Center for Biotechnology Information (NCBI) Entrez Nucleotide database. The primers were purchased from Invitrogen (Carlsbad, CA) and the sequences are given in Table 3.2.

Total RNA (1 µg) was used to synthesize cDNA using the Omniscript kit (QIAGEN) and oligo $d(T)_{15}$ primers (Promega Corp; Madison, WI). The reaction was performed following the manufacturer's instructions in a 20 µl volume at 37^{o}C for 1 hour. The linear range of amplification was calculated for each pair of primers using pooled samples and reactions were performed in duplicate. sqRT-PCR amplifications were performed using 1 µl of cDNA, 200 µM deoxynucleotide triphosphates (Promega), 0.5 µM of each primer, and 2.5 U of HotStarTaq® polymerase (QIAGEN) in a 25 µl reaction volume. The reactions were performed using the following program: 95^{o}C, 15 min; 94^{o}C, 1 min; specific annealing

temperature for each primer set (Table 3.2), 1 min and 72^{o}C, 1 min (see Appendix H for specific details).

Aliquots (7 µl) of reaction product were resolved by electrophoresis on 2% agarose gels with ethidium bromide and photographed under ultraviolet light. Subsequent image analysis was performed using ImageJ software 1.37v (NIH; Bethesda, MD). Briefly, a single rectangle was drawn horizontally around all bands in a selected gel image and a plot profile of signal intensities was generated. Area selections were created under the peak for each band using the 'straight lines selection' tool. Area under the curves was then measured and provided area statistics for analysis. Appendix I discusses troubleshooting for primer design, sqRT-PCR and gel imaging.

Taqman® Quantitative Real-Time RT-PCR

cDNA was prepared by random-primed reverse transcription using random hexamer primers (Promega), 200 ng of RNA and the Omniscript kit (QIAGEN). The RT reaction was then diluted 1:100 for PCR analysis. The PCR mixtures contained 5 µl of Taqman® Universal PCR Master Mix (Applied Biosystems), 300 nM CGA primers (Invitrogen), 50 nM human β-actin primers (Applied Biosystems), 250 nM CGA probe (IDT; Coralville, IA) and 2 µl cDNA. Reactions were run in triplicate for higher accuracy. The amplification was performed as follows: 2 min at 50^{o}C, 10 min at 95^{o}C, and then 40 cycles each at 95^{o}C for 15 sec and 60^{o}C for 60 sec in an ABI/Prism 7700 Sequences Detector System (Applied Biosystems). The β-actin standard curve was used to convert

the critical threshold values (i.e. above background) into relative RNA concentrations for each sample. The CGA primers and probe were designed using the predicted rhesus macaque sequence available in the NCBI Entrez Nucleotide database and are listed in Table 3.2.

Amplicon Sequencing

Following amplification the PCR samples contain a complex mixture of specific PCR product and residual reaction components such as primers, unincorporated nucleotides, enzyme(s), salts and non-specific amplification products. The PCR products were purified using a QIAquick Gel Extraction Kit (Qiagen). Purified samples were then submitted to the Molecular and Cell Biology Core of the Oregon National Primate Research Center. DNA sequencing was performed on an ABI 3130XL Genetic Analyzer using Dye Terminator sequencing chemistry. The resulting sequences were then BLASTed at the NCBI website (www.ncbi.nlm.nih.gov) to verify primer specificity and proper amplicon production.

Statistical Analysis

Data are expressed as mean $\pm$ SEM for each gene measured in each group. Signal intensity and mRNA expression levels were analyzed by Student's *t*-test. In order to control for experiment-wide false positives while still maintaining statistical power, each Student's *t*-test was treated as an independent test and, therefore, alpha was adjusted to correct for multiple comparisons. To accomplish

this sequential Bonferroni with Simes-Hochberg correction was used (Hochberg, 1988). For all analyses significant differences were established at $P<0.05$ unless otherwise adjusted by Bonferroni correction.

RESULTS:

Gene Microarray and Filtering

Initial Genesifter® sorting indicated ~26,000 probesets were upregulated in CR animals compared to CON while ~26,700 probesets were downregulated. Based on filter criteria (*t*-test; $P<0.05$) 1018 of these probesets were significantly different between the two treatments. When a 1.5 fold-change requirement was applied we then detected only 145 probesets with the potential to be differentially expressed. (For a complete list of these probesets see Appendix D).

Two potentially significant genes were chosen from this set to investigate further, including the TSH receptor (*TSHR*) and 1-acylglycerol-3-phosphate O-acyltransferase 3 (*AGPAT3*), a component of the triacylglycerol synthetic pathway. In addition, five other genes not meeting our filter conditions were investigated which were highly expressed and/or fell into the categories of reproduction, circadian mechanisms and oxidative stress (Table 3.1). These included sperm-specific antigen 2 (*SSFA2*), a surface antigen responsible for zona pellucida binding; glycoprotein hormone common alpha subunit (*CGA*); uncoupling protein 2 (*UCP2*); casein kinase 1 epsilon (*CSNK1E*), a core-clock gene; and cyclooxygenase 2 (*COX2*), a cellular stress marker.

sqRT-PCR and qRT-PCR

Semi-quantitative RT-PCR amplification of all six genes investigated in the two treatment groups (n=5) are demonstrated in Figure 3.1. Amplicons were detected between 22-29 cycles at 62-65.5^{o}C (Table 3.2). Consistent with the microarray data, COX2 mRNA expression was undetectable in any of the samples.

The sqRT-PCR expression levels for the genes within the two treatment groups are shown in Figures 3.2 A-F. In agreement with the microarray data, results showed a significant decline of 25% in glycoprotein hormone alpha subunit (CGA) mRNA expression in CR animals compared to CON. A significant decrease of 45% in expression of the TSH receptor was also observed in CR animals. Other genes associated with oxidative stress, circadian mechanisms and reproduction showed no significant diet-induced changes. These included *AGPAT3*, *UCP2*, *CSNK1E* and *SSFA2*.

The results of Taqman® quantitative real-time RT-PCR of *CGA* are represented in Figure 3.3. Expression levels were significantly different between treatment groups with CR animals exhibiting a negative fold-change of 0.57 ($\pm$0.10).

DNA Sequencing

The complete sequences for experimentally derived PCR products are listed in Table 3.3, as determined by DNA sequencing. The resulting sequences were BLASTed in the NCBI database to determine the sequence of best fit. In

almost every instance, the experimentally derived sequence returned a best fit for the predicted rhesus macaque mRNA sequence which had been used for primer design.

DISCUSSION

Biological aging is associated with functional decline at the cellular, organ and system levels. Conversely, gene and protein expression changes triggered by calorie restriction (CR) are also thought to alter biological response, resulting in an attenuation of the aging process (Weindruch and Walford, 1988). Given the essential functions of the neuroendocrine system, it is not surprising that more interest is being directed to this system and its role in aging. The pituitary gland, as the central organ in the HPG axis, is a key component of the neuroendocrine system. From here neurological and endocrine signals are integrated and processed before bioactive peptides/hormones are released into the body. These pituitary gland messengers play a critical role in maintaining homeostatic function and their modification has been suggested to play a part in an organism's ability to respond to the biological disruptions caused by age (Chen, 2004).

In the present study we investigated the impact of moderate CR on pituitary gland gene expression and quantified expression levels in adult male rhesus macaques (*Macaca mulatta*) subjected to eight years of post-pubertally implemented restriction. We were particularly interested in genes associated with reproduction, circadian mechanisms, metabolism and oxidative stress. Health parameters in our study animals appeared to be improved with CR, however,

overall impact on the HPG axis is difficult to assess. It would be valuable to know if calorie restriction had conferred beneficial health effects without negatively impacting the neuroendocrine capability of the pituitary gland.

Previous evidence demonstrated that depending on age, gender and species, the effects of calorie restriction on the HPG axis are mixed. Female rats restricted to 60% of *ad libitum* food after the onset of puberty did not experience any interruption of normal cycling and delayed cessation of estrous cycles was observed (McShane and Wise, 1996). Preliminary data in female rhesus macaques aged 7-27 years suggests no adverse effects of long-term CR with regard to reproductive hormones (Black et al., 2001; Mattison et al., 2003). No interruption of normal ovarian cyclicity was observed in young and menopausal calorie restricted animals, suggesting that long-term energy restriction does not negatively affect the animals (Lane et al., 2001; Mattison et al., 2003). More recently it has been demonstrated that young female rhesus macaques continue to cycle normally under short-term, moderate calorie restriction (Wu, 2006). In the male reproductive axis, young calorie restricted male rats experienced slightly reduced fertility which returned to normal levels in adults (Weindruch and Walford, 1988). Overall, male rats appear less sensitive than females with regards to reproductive development and the impact of calorie restriction.

Our investigation of the effects of CR on the HPG axis began with microarray analysis of total RNA expression in the rhesus macaque pituitary gland. To ascertain biologically relevant changes, robust multi-array average (RMA) was utilized which is preferable to other logarithmic methods for detecting

probeset significance (Irizarry et al., 2003). Based on RMA and filter criteria (*t*-test; $P<0.05$), 1018 probesets out of 52,000+ were significantly different between the two treatments. When a 1.5 fold-change requirement was applied, only 145 probesets were detected with the potential to be differentially expressed. Based on previous experiences in our laboratory we typically dropped from consideration any probesets which displayed detection levels below 100 on the array. In those instances, however, we were utilizing rhesus macaque tissue with human arrays (Affymetrix HG_U133A) and were primarily concerned with cross-hybridization and false-positives. When we attempted to remove probesets containing signals below 100 in the present study it brought the total probesets to 30. Because this would have severely limited our analysis, and because we were less concerned with cross-hybridization with the newly available GeneChip® Rhesus Macaque Genome Arrays, we decided to work with the 145 probesets.

The fact that we had only 30 probesets (and potentially fewer genes) identified following more stringent screening is not unexpected. Using similar screening techniques, researchers found 145 significantly altered probesets in the hypothalamus of 4-month-old mice exposed to short-term 30% CR (Selman et al., 2006). This was, however, without a fold-change requirement and, because they were not doing follow-up work with the RNA, they did not remove weak array signals. In a separate study of rat anterior pituitary gland gene expression (Chen, 2004), only 19 out of 542 detectable genes were identified as significantly changing in 5-month-old animals restricted at 40% for 30 days. In

rats that were restricted for 21 months they found only 18 genes that were significantly changed between treatment groups.

In addition to the 145 potentially different probesets, we also performed a keyword search of the entire microarray dataset and identified non-significantly changed probesets of interest, including genes that were highly expressed and/or fell into the categories of reproduction, circadian mechanisms, metabolism and oxidative stress. Finally, we compiled a list of probesets/genes to initially investigate (Appendix F) and designed primers for them. A complete analysis was performed on a selected subset of these genes (see Appendix I for details). Final selection for analysis of pituitary gland genes for verification of expression included: thyroid-stimulating hormone receptor (*TSHR*); 1-acylglycerol-3-phosphate O-acyltransferase 3 (*AGPAT3*), a component of the triacylglycerol biosynthesis pathway; glycoprotein hormone common alpha subunit (*CGA*); uncoupling protein 2 (*UCP2*); casein kinase 1 epsilon (*CSNK1E*), a core-clock gene; and sperm-specific antigen 2 (*SSFA2*), a surface antigen responsible for zona pellucida binding (Figure 3.1). We were not sure why SSFA2 would have been present in pituitary gland tissue, but the microarray data showed high expression levels in our samples. Cyclooxygenase 2 (*COX2*), which showed no expression on the microarray data, was also included as a negative control measure of cellular stress in the animals.

As expected, most of the pituitary gland hormones or their components were highly expressed according to the microarray data. Many of them, however, showed no substantial difference between treatments. Some high expressors

such as growth hormone (GH) and proopiomelanocortin (POMC) were not investigated beyond the microarray output, but may be of potential interest to others. Five genes that were of great interest for metabolic and reproductive function included the specific beta subunits for each of the glycoprotein hormones, *LH*, *FSH*, *CG* and *TSH*, along with the shared alpha subunit chain, *CGA*. Preliminary attempts were made to identify their expression utilizing sqRT-PCR with mixed results. In the case of the alpha subunit, the cDNA amplification worked well and single-band amplicons were successfully obtained within the linear range of amplification. In other instances, such as *TSHβ* and *LHβ*, difficulties were encountered. We were originally concerned with *LHβ* because there was no probeset on the microarray and no sequence available in the NCBI databases. The closest comparable sequence was for cynomolgus macaque (*Macaca fascicularis*) mRNA. Although it might be assumed there is high homology between these two species, after designing primers to the cynomolgus sequence we were not able to achieve positive results with our samples. Equally frustrating was our inability to remove double-banding of *TSHβ* amplicons on the gels (Appendix I). Because of these difficulties it was decided not to spend time pursuing *FSHβ* if *LH* and *TSH* beta subunits were not going to be possible. Additionally, unlike the substantial fold-change demonstrated by *CGA*, the beta glycoprotein subunits gave less indication of differential expression based on the microarray dataset. We decided instead to focus on the genes that showed the most potential for exhibiting real expression changes and for which we were able to design successful primer pairs.

Significant differences were detected between treatment groups in CGA and TSH receptor mRNA expression. Microarray data had originally shown *CGA* to be highly expressed with an incredibly large fold-change difference (Table 3.1). It was determined to be non-significant, however, due to large variation within the calorie restricted animals. As shown in Figures 3.2A and 3.3, PCR detection conducted with a sample size of five in each treatment group, including the three animals used for microarray analysis, was able to reveal significant differences between groups. Results of sqRT-PCR measurement showed a 25% lower level of *CGA* expression in CR-treated animals compared to CON subjects while qRT-PCR results showed an even larger difference in CR animals with 43% lower level of expression. Quantitative PCR calculations were based on a sample size of four in both treatments as compared to five animals for sqRT-PCR. During analysis one animal from each category was removed as an outlier because their average detection signal was more than two standard deviations away from the group mean. PCR analysis was completed by sequencing the experimentally derived amplicons. Table 3.3 shows the sequences along with the results of the NCBI database search. For both the forward and reverse sequence, the best fit result was the same predicted rhesus macaque sequence that had been used for designing the primer pair.

The other significant finding of our study was in regard to TSH receptor expression. Here again the CR treatment group showed lower expression levels compared to the CON animals with a 45% decline based on sqRT-PCR data (Figure 3.2B). These data were consistent with the microarray probeset values

which also indicated a large decline in expression among the CR-treated animals. As with all other PCR products, we are confident that we successfully detected TSHR cDNA based on our sequencing results (Table 3.3).

The question remains as to the biological relevance of these changes. The observed alterations in *CGA* expression are more difficult to interpret due to the lack of β-subunit information. It would have been advantageous to check all the β-subunits, but because of the problems mentioned earlier (i.e. no *LHβ* rhesus macaque sequence, multiple gel bands), we were not able to get a complete picture of glycoprotein hormone subunit production. To have a complete understanding would have required more time than we had available and practically we felt it more efficient and feasible to determine expression levels for the common alpha subunit first. Unfortunately, without further analysis of the unique beta subunits it is impossible to determine if the change in *CGA* is related to FSH/LH levels in the reproductive axis or, alternatively, to TSH levels in the metabolic pathway.

Because calorie restriction is a nutritional paradigm, impact on an animal's metabolism is a likely mode of action. In fact, several hypotheses related to the mechanisms of CR's biological effects are linked to reduced (or more efficient) processing of energy (Heilbronn and Ravussin, 2003; Mattison et al., 2003; Weinert and Timiras, 2003). Two manifestations of CR-induced metabolic adjustments that have been well documented in rodents, non-human primates and humans, are lower core-body temperature (Heilbronn et al., 2006; Lane et al., 1996; Mattison et al., 2003; Roth et al., 2000; Weindruch and Walford, 1988)

and suppression of the thyroid axis as measured by lower TSH and thyroid hormone levels (Gredilla and Barja, 2005; Heilbronn and Ravussin, 2003; Koubova and Guarente, 2003; Mattison et al., 2001). These two phenomena may be linked since a depression in body temperature often indicates a reduction in the rate of oxygen consumption. The hypometabolic state imposed by CR is reflected by the approximately 50% reduction in serum triiodothyronine (T_3) hormone concentrations (Weindruch and Sohal, 1997). The changes in CGA and TSHR mRNA expression in our CR animals seems to indicate a modification of the metabolic pathway and could potentially correlate with these kinds of physiological responses.

In adults the thyroid gland and its hormones maintain metabolic stability by regulating oxygen requirements, body weight and basal metabolic rate (Griffin and Ojeda, 2000). In addition to lower circulating thyroid hormone levels, the metabolic rate of both restricted rodents and primates expressed as a function of lean body mass is initially reduced during adaptation to CR. This reduction, however, is not maintained after the loss of metabolic (lean) body mass (Lane et al., 1997; Roth et al., 2000). That is to say, weight loss and reduction in lean body mass experienced by the CR animals eventually ‘catch up’ to the slower metabolism. Consequently, energy expenditure per lean mass unit is not different between diet groups. It would appear then that the mechanism of CR that extends lifespan and slows aging is not strictly dependent on a reduction in metabolic rate per unit mass but is instead indicative of greater metabolic efficiency.

An ongoing human study, however, found a metabolic adaptation (decrease in energy expenditure larger than expected on the basis of loss of metabolic mass) associated with lower thyroid hormone concentrations (Heilbronn et al., 2006). They concluded that metabolic adaptations are closely paralleled by a drop in thyroid hormone plasma concentrations, confirming the importance of the thyroid pathway as a determinant of energy metabolism. *TSHR* may even be involved at the pituitary gland level, at least in humans, where the receptors are found on folliculo-stellate cells which are known to influence neighboring endocrine cells. Here an ultra-short-loop pituitary gland feedback system may be involved in the pulsatile generation of pituitary gland hormone secretion and fine-tuning of their release by attenuating the oscillation in their serum levels (Prummel et al., 2004). The changes in *CGA* and *TSHR* expression measured in our present study may be a result of such feedback regulation.

One of the ways that moderate CR is hypothesized to improve health and extend lifespan is through a shift of metabolic strategy from growth and reproduction to life maintenance (Heilbronn and Ravussin, 2003; Roth et al., 2000). While the small, but significant decrease in core-body temperature exhibited by CR animals may not be sufficient to account for the possible increase in efficiency of energy utilization that appears to underlie the slower aging rate, it may be a symptomatic marker of more fundamental biological alterations. Although there is no direct evidence that reduced body temperature slows aging, it is consistent with indirect findings in hibernating animals (Lane et al., 1996; Mattison et al., 2003) and humans (Heilbronn et al., 2006) and has

been promoted as a potential biomarker of aging (Roth et al., 2002). In the long running Baltimore Longitudinal Study of Aging, men with lower core-body temperature have been shown to experience greater survival than their respective counterparts (Roth et al., 2002).

Beneficial effects of CR, whereby resources shift from reproduction to life maintenance, would also minimize free radical production by decreasing the number of oxygen molecules interacting with the mitochondrial electron transport chain. A growing body of evidence and experimental support implicates mitochondrial derived reactive oxygen species (ROS) as a major cause of cellular decline. A direct relationship between individual age, species longevity and rate of mitochondrial ROS production has been documented (Gredilla and Barja, 2005; Kirkwood and Austad, 2000; Weinert and Timiras, 2003), and we know that CR reduces oxidative stress damage, most likely through a reduction of ROS (Heilbronn and Ravussin, 2003; Koubova and Guarente, 2003; Merry, 2004). Usually uncoupling proteins (such as UCP2) regulate the efficicacy of oxidation and as a result suppress the generation of ROS. This mechanism could play a critical role in protecting cells against degeneration that can occur naturally during aging or during pathological conditions. The existence of robust UCP2 expression has been documented in all regions of the primate pituitary gland where its expression is higher than any other part of the central nervous system (Diano et al., 2000).

In our study we observed no significant differences between our treatment groups in terms of UCP2 expression (Figure 3.2D). Both had high levels of

presentation which is not unexpected in young animals as it is assumed that their ROS protective mechanisms would be functioning at a robust level. At the same time COX2, an indicator of inflammation and cellular damage, was undetectable on the microarrays and by sqRT-PCR analysis. Whether or not CR would attenuate the expected age-related changes in expression of these two genes by maintaining a more metabolically efficient use of oxygen would be very interesting to determine.

Other genes that showed no expression changes based on sqRT-PCR results included 1-acylglycerol-3-phosphate O-acyltransferase 3, sperm-specific antigen 2, and casein kinase 1 epsilon (Figure 3.2C,E,F). We included *AGPAT3* in our studies for two reasons. First, it is a key enzyme in the triacylglycerol (triglyceride) pathway and CR has been shown to lower triglyceride levels (Roth et al., 2002). Secondly, the GeneChip® Rhesus Macaque Genome Array contained seven probesets for *AGPAT3* and at least one probeset had been labeled as significantly changing in both the pituitary gland and testis (Chapter 4) based on our filtering parameters. There were conflicting expression changes in these probesets, however, with five of them showing decreased expression in CR animals while two others showed increased mRNA expression. Because our sqRT-PCR was unable to detect significant differences between groups it is difficult to say with any certainty what is occurring with regards to AGPAT3 mRNA expression.

With regards to *SSFA2*, we had not expected to investigate this gene in the pituitary gland until we observed that expression levels on the array were

even higher than that seen in the testis (Chapter 4, Table 4.1). Since we had the primers available we decided to investigate. It is obvious, based on microarray, sqRT-PCR and DNA sequencing results, that *SSFA2* was indeed present in the sample tissues at relatively high levels. We do not know the significance of this, however, since *SSFA2* is supposed to be a surface antigen that affects sperm binding to the zona pellucida of the oocyte.

Although expression levels may not change between treatment groups, without further analysis it is unknown whether or not morphological changes may be occurring in the pituitary gland. Even though the gland may appear to be functioning normally under calorie restricted conditions, there may be changes occurring in cell location, number, size, etc. Other quantifiable techniques, such as immunohistochemistry or *in situ* hybridization would have to be employed in order to make such a determination.

Finally, even though our microarray data revealed very few CR-induced gene expression changes in the rhesus macaque pituitary gland, there are some caveats. The pituitary gland is composed of multiple regions which lie in very close apposition, often invaginating or migrating into one another. Therefore, gross dissection of the gland and region-specific gene expression analysis may result in erroneous conclusions. Consequently, we chose to use all regions of the pituitary gland for our microarray analysis, even though this may have led to some loss of sensitivity due to normalization of each probeset's intensity to an average chip intensity value. Also, it is possible that some genes oscillate in one cell type, but not in others, or the same genes may have different phases of

expression in different cell types of the gland, resulting in a net cancellation of gene expression detection. As a consequence, it is possible that in our analysis some genes fell below the detection threshold for expression. It must also be emphasized that our microarray measurements all took place in a small window of time, as the animals were sacrificed between 11 h and 14 h. Since we know that gene expression can be rhythmic in nature (Chappell et al., 2003; Lemos et al., 2006; von Gall et al., 2002), it is possible that we measured expression during a particular peak or nadir so we cannot exclude the possibility that other timepoints would show significant differences in gene expression between treatment groups.

Based on our studies, pituitary gland gene expression appears resistant to CR-induced changes. Such stability is not necessarily unexpected as it would be disconcerting for components of a primary axis, such as the HPG, to be fluctuating too broadly under anything less than pathological conditions. With CR, however, there may be a few key components that are carefully modified in such a way as to affect multiple physiological responses simultaneously. Because thyroid hormones help regulate energy metabolism and body temperature, any modification of upstream components of their signaling pathway could influence their actions. The documented changes in glycoprotein hormone alpha subunit and TSH receptor gene expression in our experimental animals could be just such modifications.

Our studies are among the first to address the potential impact of moderate CR on pituitary gland gene expression in rhesus macaques. Findings

of limited mRNA expression changes, coupled with other measures of CR-induced attenuation of age-related changes and improved health parameters (Mattison et al., 2003; Roth et al., 2002), suggest that advantageous health benefits of calorie restriction can be achieved without negative consequences. It remains to be elucidated how the changes observed in *TSHR* and *CGA* expression levels may correlate to the physiological manifestations of this nutritional paradigm.

Summary

In the present study we investigated the impact of moderate calorie restriction on pituitary gland gene expression and quantified expression levels in adult male rhesus macaques (*Macaca mulatta*). Total RNA was isolated from the pituitary glands of Young Adult (12 years) rhesus macaques fed a control diet (CON; n=5) or calorie restricted at 30% CON (CR; n=5) for eight years, beginning post-pubertally. Gene expression profiles were obtained from 3 animals in each treatment using GeneChip® Rhesus Macaque Genome Arrays (Affymetrix). Filtering with Genesifter® (vizXlabs) and a 1.5 fold-change threshold provided fewer than 150 probesets out of 52,000+ that were different between groups. We chose two genes from this set to investigate further, including the TSH receptor (*TSHR*) and a component of the triacylglycerol synthetic pathway, along with five other genes not meeting our filter conditions. In agreement with the microarray data, results of semi-quantitative PCR (sqRT-PCR) analysis showed a significant decline in TSH receptor mRNA expression in CR animals compared to CON. We

also observed a significant decrease in expression of the glycoprotein hormone alpha subunit (*CGA*) in CR animals using sqRT and real-time PCR. Without further analysis of the unique beta subunits it is impossible to determine if this polypeptide is related to FSH/LH levels in the reproductive axis or, alternatively, to TSH levels in the metabolic pathway; changes in *TSHR* expression seem to indicate the latter. Other genes associated with reproduction, circadian mechanisms and oxidative stress showed no significant diet-induced changes. Our studies are among the first to address the potential impact of CR on pituitary gland gene expression in rhesus macaques and findings suggest that advantageous health benefits of calorie restriction can be achieved without negative consequences. It remains to be elucidated how the changes observed in TSHR and CGA expression levels may correlate to the physiological manifestations of this nutritional paradigm.

Acknowledgments

Research was supported by NIH Grants AG-19914, HD-29186, RR-00163 and U01-AG21380-03. Additional support provided by: Research Assistantship from the Department of Animal and Avian Sciences at the University of Maryland; the Intramural Research Program of the National Institutes of Health; and the National Institute on Aging. We would also like to thank the members of the Oregon National Primate Research Center: Dario Lemos, Dr. Jodi Downs, Vasilios (Bill) Garyfallou, Dr. Yibing Jia, Dr. Betsy Ferguson, Dr. Eliot Spindel and the entire animal care staff.

Pituitary													
Other ID / Probeset	CON 1	Call	CON 2	Call	CON 3	Call	Gene ID	CR 1	Call	CR 2	Call	CR 3	Call
MmugDNA.14589.1.S1_at	28.7	P	34.8	P	17.2	P	**AGPAT**	15.5	P	13.2	A	21.8	M
MmugDNA.1459.1.S1_s_at	551	P	375.6	P	402.9	P		341.3	P	458.2	P	437.8	P
MmugDNA.16471.1.S1_at	125	P	96.1	P	90.2	P		104.4	P	71.9	P	61.7	P
MmugDNA.24842.1.S1_at	230.2	P	274.9	P	283.5	P		248.8	P	176.7	P	159.2	P
MmugDNA.24844.1.S1_at	452	P	518	P	394.4	P		639.9	P	520.2	P	517.8	P
MmugDNA.39097.1.S1_at	664	P	569.6	P	555	P		461.2	P	385.9	P	503.7	P
MmugDNA.6884.1.S1_at	312	P	357.7	P	308.2	P		398.2	P	307.1	P	350.4	P
MmugDNA.13477.1.S1_at	23.2	P	17.6	A	1.8	A	**TSHR**	10.3	A	11.2	A	15.4	A
MmugDNA.32655.1.S1_at	57.2	P	33.7	P	35.9	P		20.2	P	22	A	13	A
MmugDNA.796.1.S1_at	14.2	A	9.5	A	18.7	A		3.9	A	24.3	A	5.2	A
MmugDNA.19270.1.S1_at	22.2	A	21.5	A	23.2	A	**SSFA2**	11.7	A	28.5	A	32.1	A
MmugDNA.26522.1.S1_at	340.2	P	363.2	P	308.1	P		378.4	P	124	P	133.1	P
MmugDNA.14233.1.S1_at	942.2	P	911.6	P	1051.8	P		1057	P	1126.6	P	962.9	P
MmugDNA.4648.1.S1_at	946.3	P	499.7	P	470.9	P	**CGA**	245.9	P	4.5	A	212.7	P
MmugDNA.29263.1.S1_at	13438.2	P	14371.6	P	13887.8	P		11745	P	15716.4	P	14219.6	P
MmugDNA.16174.1.S1_at	677.6	P	434.6	P	546.7	P	**UCP**	498.4	P	631.5	P	575.5	P
MmugDNA.1485.1.S1_at	571.1	P	347.6	P	364.4	P		371.7	P	491.3	P	445.8	P
MmugDNA.4494.1.S1_at	27.3	A	21.2	A	3.7	A	**COX2**	21.2	A	21.5	A	18.4	A
MmugDNA.17389.1.S1_at	16.4	A	17.6	A	29	A	**CSNK1E**	21	P	25.2	A	24.7	A
MmugDNA.29650.1.S1_at	39.6	A	42.4	A	25.4	A		69.4	A	11.5	A	58	A
MmugDNA.34870.1.S1_at	293.3	P	315.4	P	214.4	P		312.9	P	189.3	P	242.5	P
MmugDNA.4033.1.S1_at	68.6	P	52.3	P	76.2	P		68.9	P	58.7	P	48.5	P
MmuSTS.1889.1.S1_at	268.6	P	219.3	P	238.8	P		255.9	P	239.1	P	207.6	P

Table 3.1 Microarray Probeset Data for Pituitary Gland Genes Subjected to Experimental Analysis Compiled list of pituitary gland genes (and their probesets) investigated experimentally with sqRT-PCR and qRT-PCR (Young Adult CON, n=3; Young Adult CR, n=3). Data are from our GeneChip® Rhesus Macaque Genome Array output (Affymetrix).

Pituitary			
Probeset	**Gene ID**	**CON**	**CR**
MmugDNA.14589.1.S1_at	**AGPAT**	27 ± 5	17 ± 3
MmugDNA.1459.1.S1_s_at		443 ± 54	412 ± 36
MmugDNA.16471.1.S1_at		104 ± 11	79 ± 13
MmugDNA.24842.1.S1_at		263 ± 17	195 ± 27
MmugDNA.24844.1.S1_at		455 ± 36	559 ± 40
MmugDNA.39097.1.S1_at		596 ± 34 [a]	450 ± 34 [b]
MmugDNA.6884.1.S1_at		326 ± 16	352 ± 26
MmugDNA.13477.1.S1_at	**TSHR**	14 ± 6	12 ± 2
MmugDNA.32655.1.S1_at		42 ± 7 [a]	18 ± 3 [b]
MmugDNA.796.1.S1_at		14 ± 3	11 ± 7
MmugDNA.19270.1.S1_at	**SSFA2**	22 ± 1	24 ± 6
MmugDNA.26522.1.S1_at		337 ± 16	212 ± 83
MmugDNA.14233.1.S1_at		969 ± 43	1049 ± 47
MmugDNA.4648.1.S1_at	**CGA**	639 ± 154	154 ± 76
MmugDNA.29263.1.S1_at		13899 ± 270	13894 ± 1158
MmugDNA.16174.1.S1_at	**UCP**	553 ± 70	568 ± 39
MmugDNA.1485.1.S1_at		428 ± 72	436 ± 35
MmugDNA.4494.1.S1_at	**COX2**	17 ± 7	20 ± 1
MmugDNA.17389.1.S1_at	**CSNK1E**	21 ± 4	24 ± 1
MmugDNA.29650.1.S1_at		36 ± 5	46 ± 18
MmugDNA.34870.1.S1_at		274 ± 31	248 ± 36
MmugDNA.4033.1.S1_at		66 ± 7	59 ± 6
MmuSTS.1889.1.S1_at		242 ± 14	234 ± 14

Table 3.2 Gene Expression Profiles in the Rhesus Macaque Pituitary Gland
Mean signal intensity values (±SEM) of pituitary gland gene expression (Young Adult CON, n=3; Young Adult CR, n=3). These genes showed a significant (AGPAT, TSHR) or non-significant change (SSFA2, CGA, UCP2, COX2, CSNK1E) in gene expression based on GeneChip® Rhesus Macaque Genome Array detection (Affymetrix) and our Genesifter® (vixXlabs) filtering parameters (letter notations, $P<0.05$).

sqRT-PCR primers	Forward sequence	Reverse sequence	Amplicon	Cycles	Temp
CGA	GGAGAGTTTACAATGCAGGATTGC	GTCATCAAAACAGCACTTGGCA	310 bp	22	62°C
TSHR	CTTCTTTTCTGAAACTGCCAGCTC	GAGATTCCAGGTGAGTCCAGCA	302 bp	29	62°C
AGPAT	GCTGACTGTTGGCCAGTTTCA	CCTGCAGCATTTCACCAGTACA	316 bp	27	62°C
UCP2	TGCAAAGCCCTGCTGTTCA	AGATAGAGGAACTCTGCCGGAATC	301 bp	26	63°C
SSFA2	GGAAGAAAGTATTCCGAGCATCGG	ACACCTCCACCAGTGCATATCATTG	307 bp	26	65.5°C
CSNK1E	AAGTATGAGCGGATCAGCGAGA	CCGAATTTCAGCATGTTCCAGT	218 bp	28	65°C
COX2	AGAGGCTAGTGCCTCAGAGAG	GCTAGCACACAGGCCTATCC	437 bp	N/A	N/A
β-actin	CATTGCTCCTCCTGAGCGCAAG	GGGCCGGACTCGTCATACTCC	~300 bp	23	65°C
Taqman® qRT-PCR β-actin primers	Human ACTB (beta actin) Endogenous Control (Applied Biosystems; Foster City, CA)		N/A	40	60°C
Taqman® qRT-PCR β-actin probe			N/A	40	60°C
Taqman® qRT-PCR CGA primers	TGGAGAGTTTACAATGCAGGATTG	AGCAGCAGCCCATACACTGA	101 bp	40	60°C
Taqman® qRT-PCR CGA probe	5'-6FAM-AATTCTTCTCCAAGCCGGGTGCCC-TAMRA-3'		N/A	40	60°C

Table 3.3 Pituitary Gland Gene Primers and Probes Forward and reverse primer sequences (5' to 3') used for sqRT-PCR and qRT-PCR are shown along with the expected amplicon size, annealing temperatures and number of cycles run for each reaction. Primers and qRT-PCR probes were designed using human or rhesus macaque gene sequences and PrimerExpress® software (Applied Biosystems). All were successful in detecting pituitary gland mRNA gene expression.

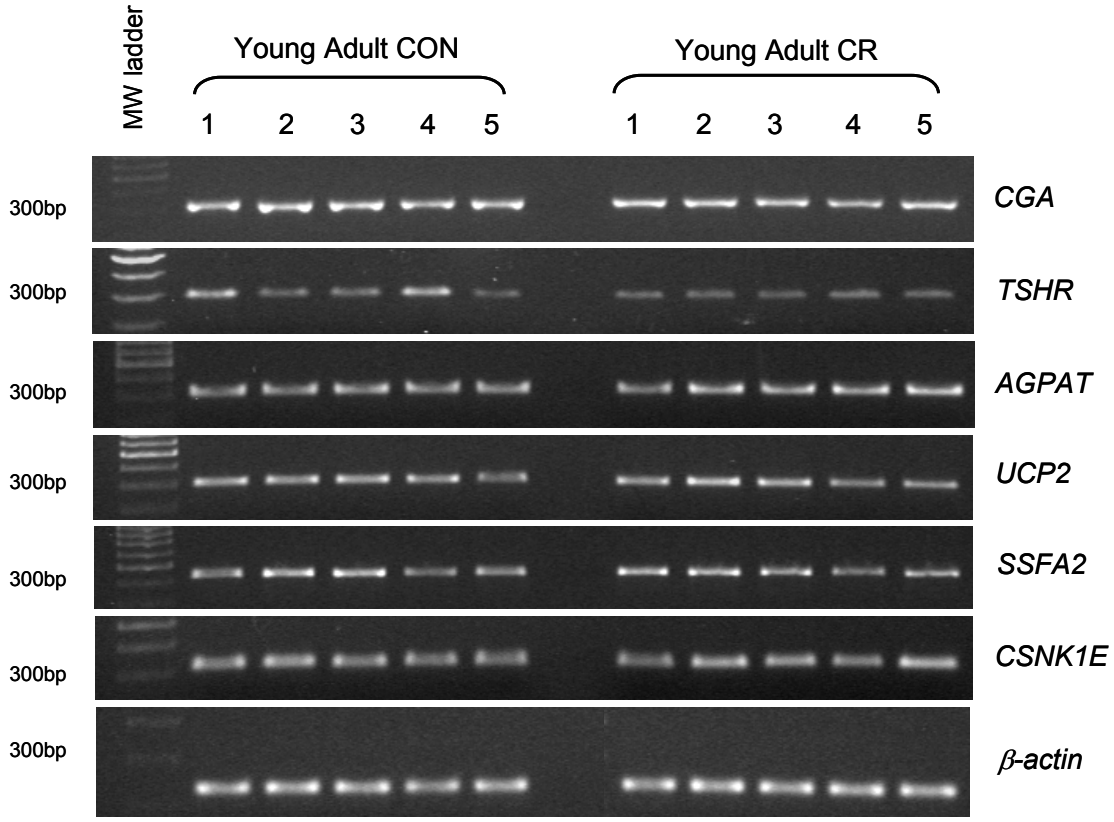

Figure 3.1 Genes in the Rhesus Macaque Pituitary Gland Representative sqRT-PCR results validating the microarray data and demonstrating expression of pituitary gland genes across the treatment groups of Young Adult rhesus macaques (12 years; CON and CR, n=5). The housekeeping gene β-actin was used as a positive control and for normalizing images for analysis.

Figures 3.2 A-F sqRT-PCR Expression Levels of Genes in the Rhesus Macaque Pituitary Gland Each bar, along with SEM, represents mean, normalized fluorescence data from five animals. Statistical comparisons were made using Student's *t*-test ($P<0.05$). Significant differences were observed in *CGA* expression (Graph A) and *TSHR* expression (Graph B) between treatment groups. In both instances, CR animals demonstrated a negative fold-change in mRNA expression of 0.75 ($\pm$0.06) and 0.55 ($\pm$0.04), respectively. The other transcripts were not significantly different between treatments.

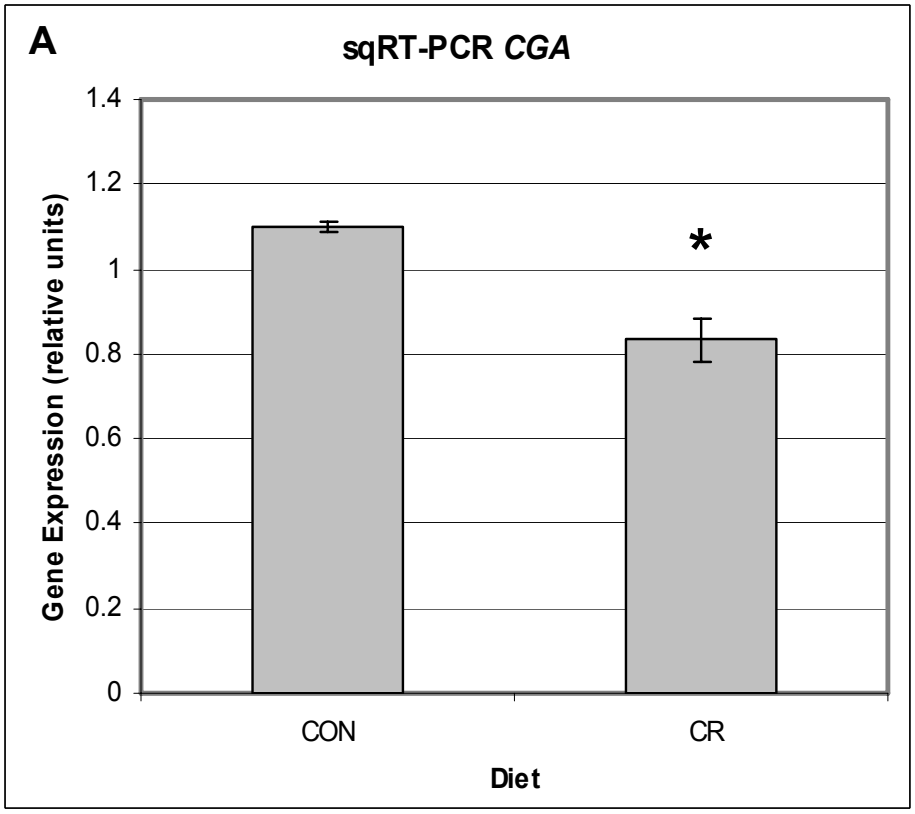
A
sqRT-PCR *CGA*
Gene Expression (relative units)
1.4
1.2
1
0.8
0.6
0.4
0.2
0
*
CON
CR
Diet

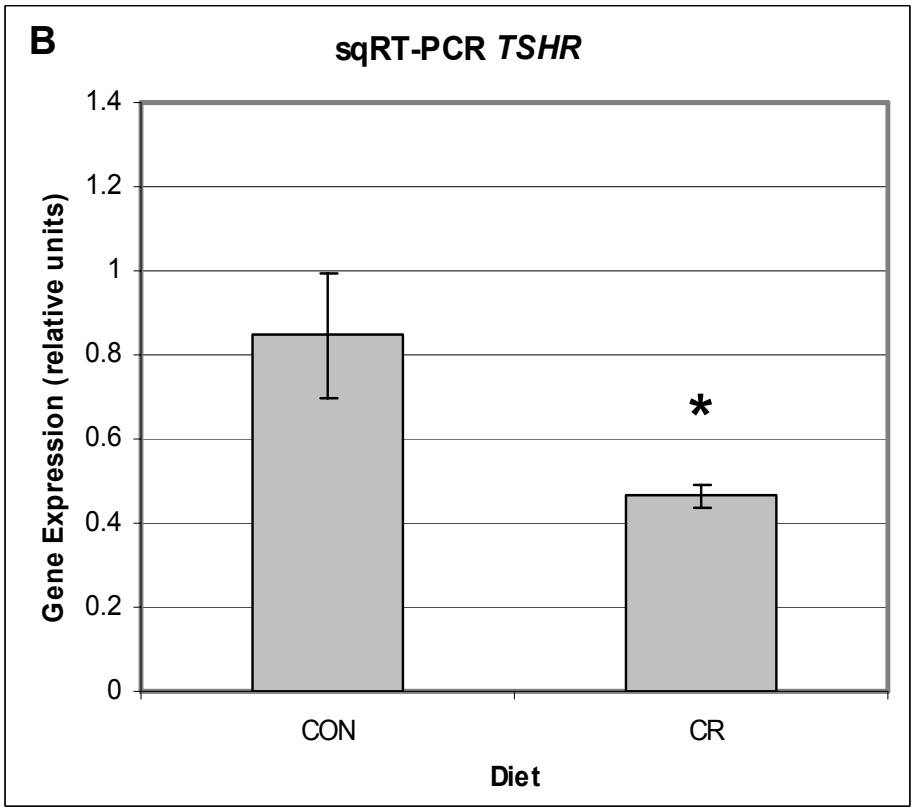
B
sqRT-PCR *TSHR*
Gene Expression (relative units)
1.4
1.2
1
0.8
0.6
0.4
0.2
0
*
CON
CR
Diet

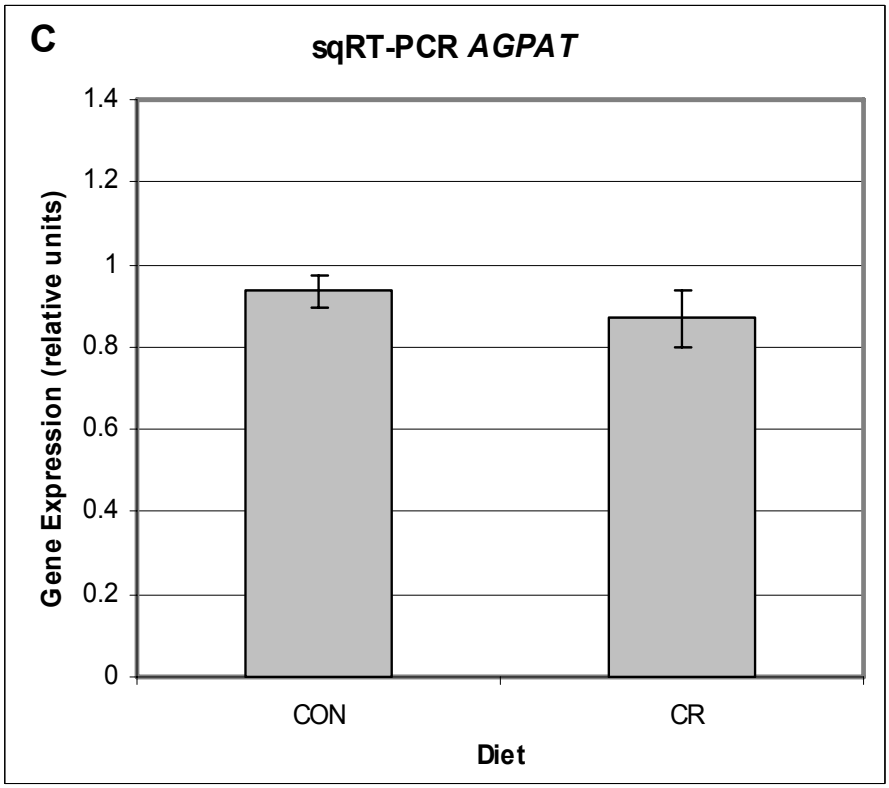
C
sqRT-PCR *AGPAT*
Gene Expression (relative units)
1.4
1.2
1
0.8
0.6
0.4
0.2
0
CON
CR
Diet

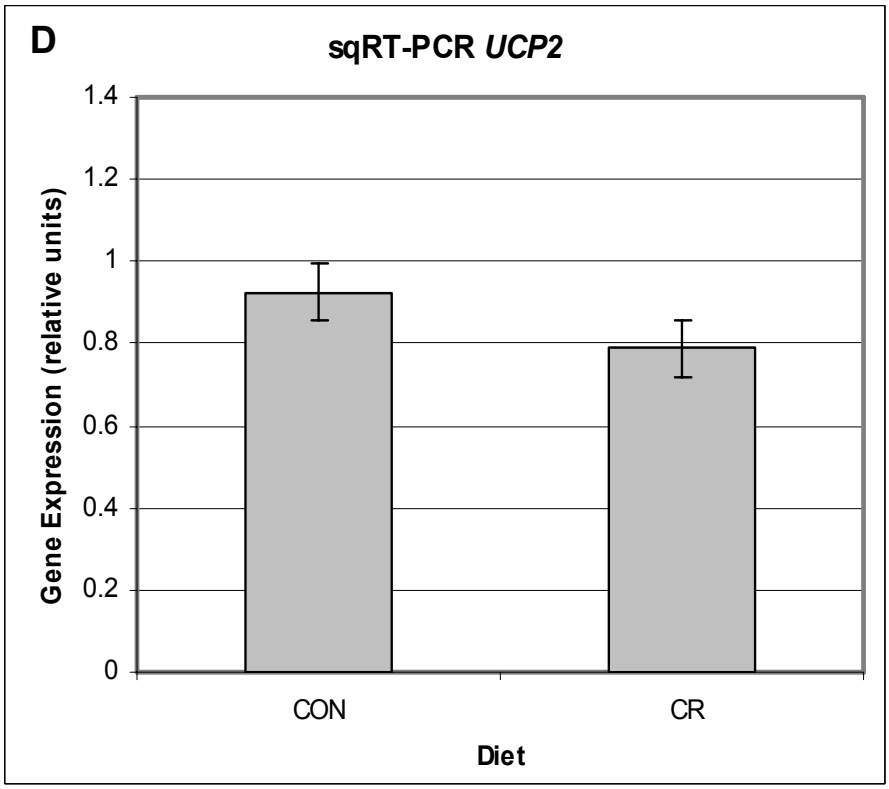
D
sqRT-PCR *UCP2*
Gene Expression (relative units)
1.4
1.2
1
0.8
0.6
0.4
0.2
0
CON
CR
Diet

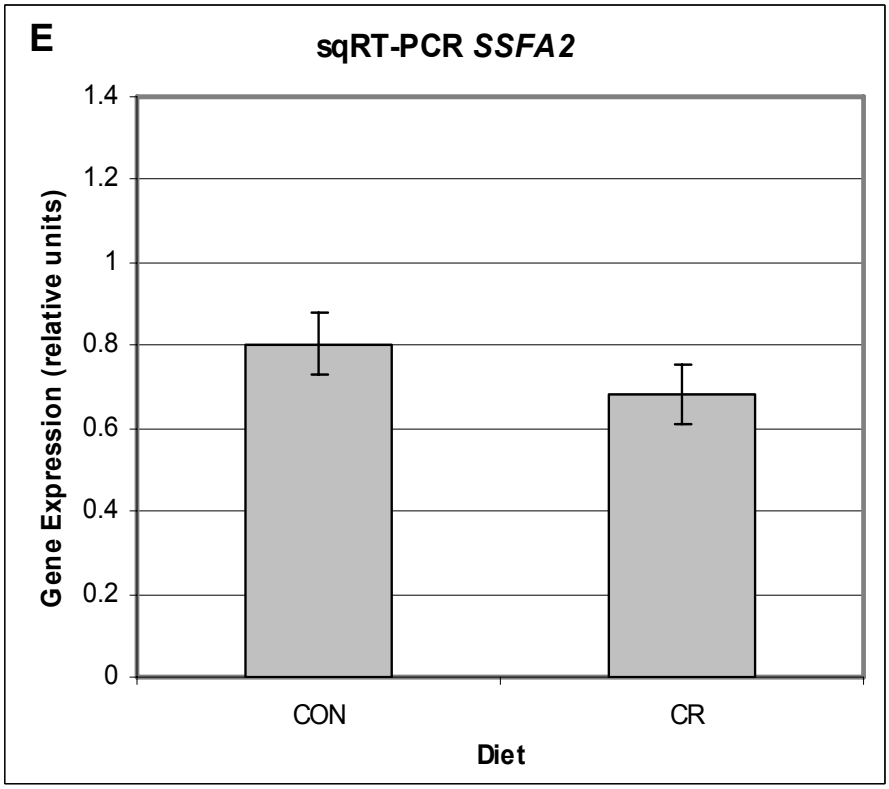
E
sqRT-PCR SSFA2
Gene Expression (relative units)
1.4
1.2
1
0.8
0.6
0.4
0.2
0
CON
CR
Diet

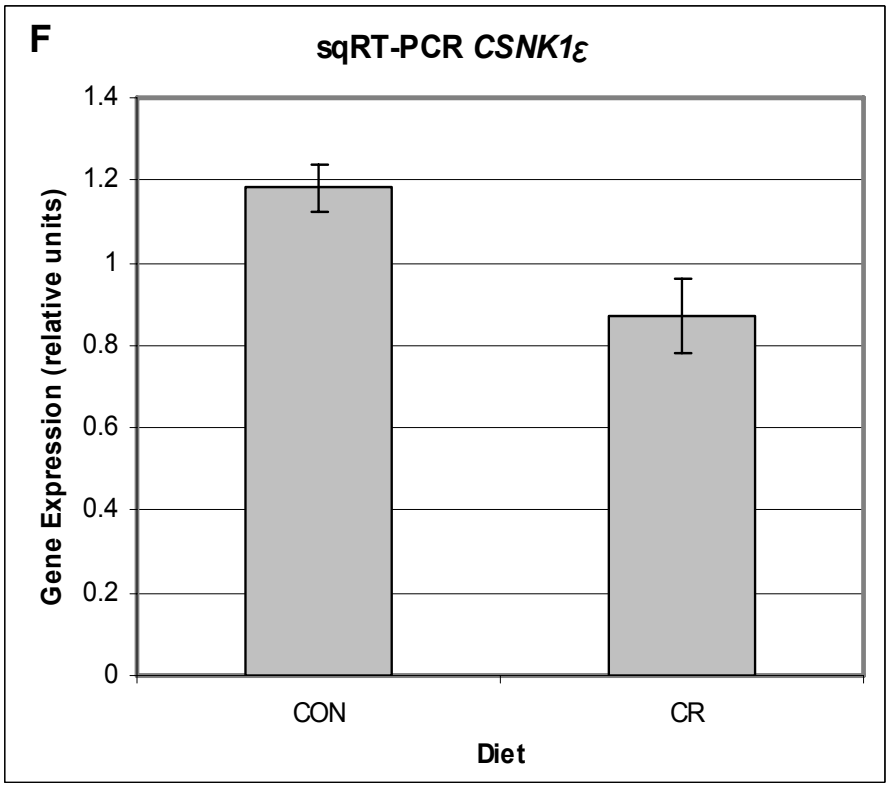
F
sqRT-PCR CSNK1ε
Gene Expression (relative units)
1.4
1.2
1
0.8
0.6
0.4
0.2
0
CON
CR
Diet

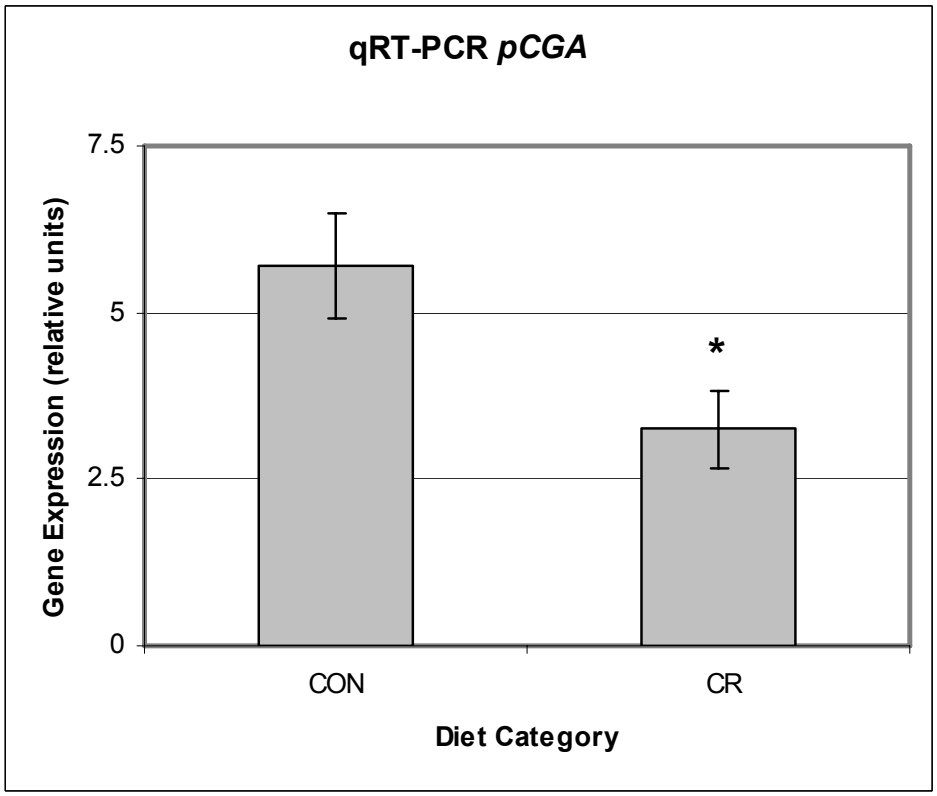

Figure 3.3 Taqman® Quantitative Real-Time PCR of *CGA* in the Rhesus Macaque Pituitary Gland Each bar, along with SEM, represents mean, normalized fluorescence data for four animals. Statistical comparisons were made using Student's *t*-test ($P<0.05$). Results corroborated our sqRT-PCR results and demonstrated a significant negative fold-change of 0.57 ($\pm$0.10) in pituitary gland *CGA* expression in the calorie restricted animals.

Table 3.4 Pituitary Gland Gene sqRT-PCR Amplicon Sequences Experimentally derived PCR amplicon sequences as determined by DNA sequencing are listed under each of the genes. Following each are the results of a BLAST search in the NCBI database to determine a best fit sequence.

A) Glycoprotein hormones, alpha polypeptide (CGA, for LH, FSH, TSH, hCG)
pCGA-Forward primer GAATCGCAGGGAACAATTCTTCTCCAGCCGGGTGCCCCAATATATCAGTGTATGGGCTGCTGCTTCTCTAGAGCATATCCCACTCCAGTAA GGTCCAAGAAGACGATGTTGGTCCAAAAAAACGTCACCTCAGAGTCCACTTGCTGTGTAGCTAAATCATTGACCAGGGTCATGGTAATGGG GAGTGTCAGAGTGTGAATGGGCAAAAGGCTTGGACAGAAGGTTTGGTTTGGTTTGCATTTTTGATGTTTTGGTTGTGTTGTACTGCAACAAG Best fit (Same as that used for primer design): gi|109071971|ref|XM_001090917.1| PREDICTED: Macaca mulatta similar to Glycoprotein hormones alpha chain precursor (Anterior pituitary glycoprotein hormones common alpha subunit) (Follitropin alpha chain) (Follicle-stimulating hormone alpha chain) (FSH-alpha) (Lutropin alpha chain) (Luteinizing hormone alpha chain) (LH-alpha), mRNA pCGA-Reverse primer ACCTAATCTAACACGGTAAGTCAATTCTTCTCCAGCCGGGTGCCCAATATCCAATCTGATACTCCCCATTACCATGAACGGGTCCCCGAGTT GATTAATCAACAAGAGGACTATGACAAAAAAAGAACCTAAATGGACAACAACTTCTTTTGGGTCTTCTAAAACATTGACCAGGGTATGGTAAA GCCCCCCTCCCCTGATAAATTGTCGCCCCGCCTCTGCATCAGGATTCATGACCA Best fit (Same as that used for primer design): gi|109071971|ref|XM_001090917.1| PREDICTED: Macaca mulatta similar to Glycoprotein hormones alpha chain precursor (Anterior pituitary glycoprotein hormones common alpha subunit) (Follitropin alpha chain) (Follicle-stimulating hormone alpha chain) (FSH-alpha) (Lutropin alpha chain) (Luteinizing hormone alpha chain) (LH-alpha), mRNA
B) Sperm specific antigen 2 (SSFA2)
pSSFA2-Forward primer GTCCAGTAAGCTCCTTCTAGAAAGGCTCTGTGCAGACACCTCCAGATTTGGAAAGTTCTGAGGAAGTTGATGCAGCTGAAGAAGCCCCAGA AGTTGTAGGACCTAAATCTGAAGTGGAAGAAAGGCATGGAAAACTCCCATTAATGCCAGCTGCTGAGGAAGTGCATAAAAATGTGGAGCAA GATGAGTTGCAGCAAGTCATACGGGAGATTAAAGAGTCTATTGTTTGGCGAAGGGCACCGCCCACTTGATTTAGGGGTCCAACTTCTGGGG CTTCTTTCCTGCGCCAACTCCTCATCATTTTAAAATTTGGAGGTGGGGCGCGTAAGGCTGTGCTCAAGGACCTGTTGGCGCTGGGGCCCCC AGGGCCGCCTATTTTTTCCCCCCATTCTAAAAA Best fit (Same as that used for primer design): gi|109100269|ref|XM_001101290.1| PREDICTED: Macaca mulatta similar to sperm specific antigen 2, mRNA pSSFA2-Reverse primer TCGCATACAGCTAATAGGATCCATGCCAACCTATAATTTCCGTTTAATGATTATCTTGCTTAGAATTAGATGCTTTACTTGAAGATACTGCTGC

CAAAAGTCCACTTACAATTTCCCGTCTGATTTCCCCAACAATAGACTCTTTAATCTCCCGTATGACTTGCTGCAACTCATCTTGCTCCACATTT
TTATGCACTTCCTCAGCAGCTGGCATTAATGGGAGTTTTCCATGCCTTTCTTCCACTTCAGATTTAGGTCCTACAACTTCTGGGGCTTCTTCA
GCTGCATCAACTTCCTCAGAACTTTCCAAATCTGGAGGTGTCTGCACAGAGCCTGTTCTAGAAGGAGCTGTTGGCGTTAGGGCCACCGATG
CTCGGAATAATTTCTTCCA

Best fit (Same as that used for primer design): gi|109100269|ref|XM_001101290.1| PREDICTED: Macaca mulatta similar to sperm specific antigen 2, mRNA

C) Uncoupling protein 2 (UCP2)

pUCP2-Forward primer
Unknown - primer did not anneal during sequencing. Poor sequencing may have been the result of impure PCR mixture or amplicons forming secondary structures due to sticky GC regions.

pUCP2-Reverse primer
GACATGCCCTTTCCGGTGAGGCCTCCAGATCAAGCTTCTCTAAAGGTGTCCCGTTCTTCAAAGCTGCCAGTGGCTATCATGGCCTGATCCC
CTTGGTTTTCCATAGAAAATGGGTGGGAGACGAAACACCTAATGGTCATACTATGTGTCCAAGCCTCAGGGAGAACACGAGAGTGCGTGCG
GCTGTGTGTATCTGCTGGAGGAGGGCGGATCTTGGAAGCCCACGGGGATTGGTTCTAATGCCTATTTTGGTCGATTTCCTAAATAAAAAAA
GGCCCGCGCTGT

Best fit (Same as that used for primer design): gi|109107894|ref|XM_001115559.1| PREDICTED: Macaca mulatta uncoupling protein 2 (UCP2), mRNA

D) Thyroid stimulating hormone receptor (TSHR)

pTSHR-Forward primer
TCCCTTTATCCTGGACTAAAACCTCTTTTCCCCAGTAATTCTTCTTTACTTAAAATAGTCAGGATCTTTATCTACAGATGTACTCTCCAGGTTA
CCTGTGATGATAGCCCTCTAACGTCCTGTTAGAAAAGTCTCCAAGCAGAGATGGCATTACTTCTGAATGCTCATAAACCACACCATGAAATA
AAAGCTCTTTGTTGTTTTCAGATTGTGGA

Best fit (Same as that used for primer design): gi|109084461|ref|XM_001104839.1| PREDICTED: Macaca mulatta thyroid stimulating hormone receptor, transcript variant 2 (TSHR), mRNA

pTSHR-Reverse primer
Unknown - primer did not anneal during sequencing. Poor sequencing may have been the result of impure PCR mixture or amplicons forming secondary structures due to sticky GC regions.

E) 1-acylglycerol-3-phosphate O-acyltransferase 3 (AGPAT3)

pAGPAT-Forward primer
ACTCTCCGGGGACCCCGGCTTCCTGAGAGGCTAGGGTCTGCCCCTCCAGTTAGAAGTTAGGGGGCCAAAACAAAAGAGGGGTTGGAACTA
AAAATCCCCAAAGAGCGTCCCCG

Did not return any macaque sequences in the list of 14 Best fit.

pAGPAT-Reverse primer
AGAATTGCGCTTGGGCGGCGCACACCTGCCTGTGTACACAGGTCCTCGCACAGCACGGCAAACGCAGCCAGGCCTTCGGGACACAGGCC
TTCGAAGAGTAAGTTAGCAGCCCTCACCCCAACAAGCTTCTAAAGACCAAAAATACCTCTATCCTCCACTACATAAAGCTTGTGAGTAGCAA
AACTTGTAAAAATGAAGCGTACAAAAGGAAACATCCATATAATACATTTGCACCCTGTATACAATGGGTCCCTTTGAAACTGGCAACAGTCAG
CA

Best fit (Same as that used for primer design): gi|109065161|ref|XM_001104367.1| PREDICTED: Macaca mulatta 1-acylglycerol-3-phosphate O-acyltransferase 3 (AGPAT3), mRNA

F) Casein kinase 1, epsilon (CSNK1E)

pCSNK1E-Forward primer
GTTCGCCCCATTGAGGTCCTCTGCAAGGCTATCCCTCCGAATTCTCAACATACCTCAACTTCTGCCGCTCCCTGCGGTTTGACGACAAGCC
CGACTACTCTTACCTACGTCAGCTCTTCCGCAACCTCTTCCACCGGCAGGGCTTCTCCTATGACTACGTCTTCGACTGGAACATGCTTCGGT
TCG

Best fit (Same as that used for primer design): ref|XM_001093672.1| PREDICTED: Macaca mulatta casein kinase 1 epsilon (CSNK1E), mRNA

pCSNK1E-Reverse primer
TAGCTTCATTTTGTAAGTTGTGCTAGCCGGTGGAAGAGGTACAGCTCCCAAAAAATACCTCATTAACTTCTGTTGAAGCGAGGTGAAGAGAG
GCGGACTACTTCTTACTACCTTTATATTACGGAACCTTTCCCCGGAGGGCTTCTCCTATGAATACCCTTCACTGGACCTGCTGAAATTCCCC
CAAAC

Did not return any macaque sequences in the list of 5 Best fit.

CHAPTER 4

EFFECTS OF MODERATE CALORIE RESTRICTION AND AGE ON TESTICULAR GENE EXPRESSION IN THE MALE RHESUS MACAQUE (*MACACA MULATTA*)

INTRODUCTION

First reported in the mid-1930's (McCay et al., 1935), calorie restriction (CR) remains the only proven non-genetic paradigm for extending lifespan and does so by slowing the rate of physiological decline and retarding age-related chronic diseases. Moderate CR also has consistent effects across vertebrate classes with beneficial health effects on many physiological systems. To date, CR has been found to be effective in a variety of species including nematodes, spiders, flies, mollusks, rodents, dogs and possibly non-human primates (Ingram et al., 1990; Lane et al., 1999b; Roth et al., 1999; Weindruch and Walford, 1988). Researchers have shown that CR can reduce body mass and adiposity, lower body temperature and initially reduce metabolic rate, lower blood pressure, and significantly slow growth and skeletal maturation. It has been successful in reducing glucose and fasting plasma insulin levels while increasing insulin sensitivity and levels of high density lipoproteins (Gredilla and Barja, 2005; Gresl et al., 2001; Heilbronn and Ravussin, 2003; Koubova and Guarente, 2003; Lane et al., 1997). Its long history notwithstanding, however, very little is known with regard to the exact mechanism(s) of action of CR.

For all of its apparent health benefits, the potential impact of CR on the hypothalamic-pituitary-gonadal (HPG) axis is also not very well understood. Could moderate CR possibly improve reproductive health parameters as it does with other systems within the body? Alternatively, could it have no impact or even a negative effect on reproductive outcome? Preliminary data in female rhesus macaques (*Macaca mulatta*) aged 7-27 years suggests no adverse effects of long-term CR with regard to reproductive hormones (Black et al., 2001; Mattison et al., 2003). Researchers have also documented no interruption of normal ovarian cyclicity in young and menopausal restricted subjects, suggesting that long-term energy restriction does not negatively affect the animals (Lane et al., 2001; Mattison et al., 2003). More recently it has been demonstrated that young female rhesus macaques continued to cycle normally under short-term, moderate calorie restriction (Wu, 2006). When implemented prior to sexual maturity, CR delays the maturation-related increase in circulating testosterone concentrations and postpones skeletal growth by approximately one year in male rhesus macaques (Lane et al., 1997; Roth et al., 2000). Generally, less is known about post-pubertal implementation of the paradigm on the male HPG system.

Reproductive aging in men typically follows a more gradual course than in females. The age-related demise seen in male reproduction appears to involve declining function at several sites including testosterone (T) synthesis in the Leydig cells, hypothalamic production of gonadotropin-releasing hormone (GnRH), pituitary gland release of gonadotropins and/or other integrative neuroendocrine components that impact the HPG axis as a whole (Harman et al.,

2001; Moffat et al., 2002; Ottinger, 1998). This makes determining reproductive senescence difficult because spermatogenesis continues well into old age. This does not mean, however, that there are no physiological ramifications of aging, especially in humans where decreasing testosterone levels, metabolic and circadian changes, and increasing body weight are generally associated with aging.

The recent phenomenon of increased average body mass index (BMI) experienced by the Western world has resulted in an increased incidence of obesity (BMI>25 kg/m^2) (Hursting et al., 2003). In women, excessive amount and distribution of body fat have been linked to reduced fertility with prolonged time to pregnancy, increased risk of irregular menstrual cycles, preterm delivery, spontaneous abortion, stillbirths and birth defects (Fejes et al., 2005; Jensen et al., 2004; Kort et al., 2006). Men with BMI>25 kg/m^2 had lower sperm concentration and total sperm count compared to men with lower, non-obese BMI levels (Jensen et al., 2004). In another study, BMI and total number of motile sperm cells in 520 normal, healthy men, age 26-45 was inversely related and a positive relationship was seen between BMI and DNA fragmentation in each subject (Kort et al., 2006). Thus, BMI typically increases during aging so reproductive capacity is not only impacted negatively by age, but also by the pathologies associated with obesity.

Since CR is capable of reducing body mass and adiposity and improving general health parameters, it would be of great benefit to know if CR could also maintain reproductive fitness and attenuate age-related changes. The National

Institute on Aging is currently conducting a study of CR and aging in rhesus macaques to determine its potential application in humans (Ingram et al., 1990). Results have shown parallel effects to those observed in other species, including attenuation of age changes in plasma triglycerides, oxidative damage, and glucose regulation (Mattison et al., 2003; Roth et al., 2002). Treatment animals weigh less, have reduced body fat and lower body temperatures than their matching control counterparts, providing early evidence of the potential benefit of CR for individuals at risk for diabetes and cardiovascular disease (Lane et al., 1999a; Mattison et al., 2003).

The aim of the present study was to investigate the potential impact of moderate CR on testicular gene expression and to quantify expression levels in young adult rhesus macaques. We were particularly interested in categories of reproductive, circadian, metabolic and oxidative stress genes. Using banked testis tissue and a subset of the previously investigated genes, we also performed a second experiment to investigate the potential impact and interaction of age and CR on expression levels.

MATERIALS AND METHODS

Animals and Diet

All experiments were approved for use by the Institutional Animal Care and Use Committees at the University of Maryland and the Oregon National Primate Research Center. The study consisted of two separate experiments. Experiment 1 included 10 Young Adult (12 years) rhesus macaques (*Macaca*

mulatta) fed a control diet (YACON; n=5) or calorie restricted at 30% CON (YACR; n=5) for eight years, beginning post-pubertally. Experiment 2 utilized banked tissues from previous unrelated studies and included three Juvenile (J; 1-2 years), three Young Adult (YA; 5-7 years), three Old Adult (OA; 24-30 years) and three calorie restricted Old Adult (OACR; 25-27 years) animals. OACR males had been on CR for the previous five years prior to sacrifice.

Males were individually housed in a temperature-controlled environment under 12L:12D photoperiod (lights on 7 h -19 h) and allowed auditory, visual and olfactory interaction with male and female conspecifics in the vivarium. Food was provided in two meals at 8 h and 15 h daily; water was available *ad libitum*. Diet for the J and YA males consisted of primate chow (Purina Mills, Inc.; St. Louis, MO) supplemented with limited amounts of fresh fruits and vegetables.

Diet for the YACON and YACR males and for both OA groups consisted of individual biscuits that had been specially formulated to include 15% protein, 5% fat and 5% fiber with a caloric content of approximately 3.7 kcal/g; the diet was supplemented with a daily low calorie treat (Ingram et al., 1990). Biscuits included a vitamin/mineral mix sufficient to provide 40% higher levels than the recommended allowance for rhesus macaques by a National Research Council report (NRC, 1978). Thus, the CON and CR groups were receiving exactly the same diet. Biochemical assays were performed periodically and with every new shipment to insure diet content and quality (Black et al., 2001; Mattison et al., 2005).

The amount of food provided to CON animals was provided at an *ad libitum* level, originally determined with the individual leaving a few uneaten biscuits each day during regular measurements of food consumption. CR macaques were given 30% less than age- and body-weight matched CON. Food allotments were held constant other than as needed on a case-by-case basis (Lane et al., 1999b; Mattison et al., 2005).

Animals were sacrificed according to the NIH *Guide for the Care and Use of Laboratory Animals*. A single testis was collected and sectioned, with one half flash frozen in liquid nitrogen and the other half fixed in 4% paraformaldehyde.

RNA Extraction and Gene Microarrays

Flash frozen testis sections were homogenized using a PowerGen rotor-stator homogenizer (Fisher Scientific; Pittsburgh, PA). Total RNA was isolated using RNeasy columns (QIAGEN; Valencia, CA); concentration and integrity were assessed by microcapillary electrophoresis using a model 2100 Agilent Bioanalyzer (Santa Clara, CA; see Appendix A for more detail). Testicular tissue from three individuals per treatment group in experiment 1 were sent for analysis to the Affymetrix Microarray Core of the OHSU Gene Microarray Shared Resource. All RNA extracts were used for subsequent PCR analysis.

Microarray analysis was performed in accordance with the manufacturer's instructions (Affymetrix GeneChip® Analysis Technical Manual; Santa Clara, CA). Labeled target cRNA was prepared from total RNA samples and hybridized to GeneChip® Rhesus Macaque Genome Arrays detecting over 47,000 transcripts.

Image processing and expression analysis were performed using Affymetrix GCOS v1.2 software. A number of quality control metrics were utilized as a measure of probe quality and included chip background, chip noise, total fluorescent intensity, number of genes detected and the 3'/5' ratio of the housekeeping genes β-actin and GAPDH. These metrics are assessed to determine the validity of the data obtained from the scanned GeneChip®. Data were normalized to an average intensity on each chip which enabled direct comparisons between the six different arrays.

Gene Microarray Filtering

Microarray data filtering was performed using Genesifter® software (vizXlabs; Seattle, WA) followed by hand analysis and determination of genes of interest (see Appendices B and C). Briefly, unscaled array data was normalized and $\log_2$ transformed using robust multi-array average (RMA) analysis. Student *t*-test ($P<0.05$) comparisons with Benjamini-Hochberg post-hoc corrections were performed. Signal quality and fold-change parameters were not set in order to allow for qualitative and quantitative hand filtering later. Probesets showing a significant change between treatments were then imported into Excel (Microsoft; Redmond, WA) and filtered for a minimum 1.5 fold-change in expression. Based on this gene discovery method, probesets meeting these criteria for significance were then considered for investigation. In addition, a keyword search of the entire 52,000+ probesets was performed to identify non-significantly changed probesets of interest. These included genes that were highly expressed and/or fell into the

categories of reproduction, circadian mechanisms, metabolism and oxidative stress. Table 4.1 shows the list of testicular genes (and their probesets) that were investigated experimentally with sqRT-PCR and qRT-PCR.

Semi-quantitative RT-PCR

PrimerExpress® software (Applied Biosystems; Foster City, CA) was used for all primer and probe design (Appendix G). Specific primers were designed for each transcript using the human or predicted rhesus macaque mRNA sequences posted at the National Center for Biotechnology Information (NCBI) Entrez Nucleotide database. The primers were purchased from Invitrogen (Carlsbad, CA) and the sequences are given in Table 4.2.

Total RNA (1 µg) was used to synthesize cDNA using the Omniscript kit (QIAGEN) and oligo $d(T)_{15}$ primers (Promega Corp; Madison, WI). The reaction was performed following the manufacturer's instructions in a 20 µl volume at 37^{o}C for 1 hour. The linear range of amplification was calculated for each pair of primers using pooled samples and reactions were performed in duplicate. sqRT-PCR amplifications were performed using 1 µl of cDNA, 200 µM deoxynucleotide triphosphates (Promega), 0.5 µM of each primer, and 2.5 U of HotStarTaq® polymerase (QIAGEN) in a 25 µl reaction volume. The reactions were performed using the following program: 95^{o}C, 15 min; 94^{o}C, 1 min; specific annealing temperature for each primer set (Table 4.2), 1 min and 72^{o}C, 1 min (see Appendix H for specific details).

Aliquots (7 µl) of reaction product were resolved by electrophoresis on 2% agarose gels with ethidium bromide and photographed under ultraviolet light. Subsequent image analysis was performed using ImageJ software 1.37v (NIH; Bethesda, MD). Briefly, a single rectangle was drawn horizontally around all bands in a selected gel image and a plot profile of signal intensities was generated. Area selections were created under the peak for each band using the 'straight lines selection' tool. Area under the curves was then measured and provided area statistics for analysis. Appendix I discusses troubleshooting for primer design, sqRT-PCR and gel imaging.

Taqman® Quantitative Real-Time RT-PCR

cDNA was prepared by random-primed reverse transcription using random hexamer primers (Promega), 200 ng of RNA and the Omniscript kit (QIAGEN). The RT reaction was then diluted 1:100 for PCR analysis. The PCR mixtures contained 5 µl of Taqman® Universal PCR Master Mix (Applied Biosystems), 300 nM of each primer (Invitrogen), 50 nM human β-actin primers (Applied Biosystems), 250 nM of each probe (IDT; Coralville, IA) and 2 µl cDNA. Reactions were run in triplicate for higher accuracy. The amplification was performed as follows: 2 min at 50^{o}C, 10 min at 95^{o}C, and then 40 cycles each at 95^{o}C for 15 sec and 60^{o}C for 60 sec in an ABI/Prism 7700 Sequences Detector System (Applied Biosystems). The β-actin standard curve was used to convert the critical threshold values (i.e. above background) into relative RNA concentrations for each sample. Luteinizing hormone/choriogonadotropin

receptor (LHCGR) and glycoprotein hormone common alpha subunit (CGA) primers and probes were designed using the predicted rhesus macaque sequence available in the NCBI Entrez Nucleotide database and are listed in Table 4.3. Steroidogenic acute regulatory protein (StAR) primers and probe sequences (Table 4.3) were graciously supplied by Dr. Jon Hennebold (ONPRC) and had been previously validated in his lab (Smith et al., 2002).

Amplicon Sequencing

Following amplification the PCR samples contain a complex mixture of specific PCR product and residual reaction components such as primers, unincorporated nucleotides, enzyme(s), salts and non-specific amplification products. The PCR products were purified using a QIAquick Gel Extraction Kit (Qiagen). Purified samples were then submitted to the Molecular and Cell Biology Core of the Oregon National Primate Research Center. DNA sequencing was performed on an ABI 3130XL Genetic Analyzer using Dye Terminator sequencing chemistry. The resulting sequences were then BLASTed at the NCBI website (www.ncbi.nlm.nih.gov) to verify primer specificity and proper amplicon production.

Statistical Analysis

Data are expressed as mean $\pm$ SEM for each gene measured in each group. Signal intensity and mRNA expression levels were analyzed by Student's *t*-test or one-way ANOVA. If group differences were revealed by ANOVA,

differences between individual groups were determined with the Tukey-Kramer post-hoc analysis using GraphPad Prism (GraphPad; San Diego, CA). For all analyses significant differences were established at $P<0.05$.

RESULTS

Gene Microarray and Filtering: Experiment 1

Initial Genesifter® sorting indicated ~21,400 probesets were upregulated in YACR animals compared to YACON while ~31,400 probesets were downregulated. Based on filter criteria (*t*-test; $P<0.05$) 1452 of these probesets were significantly different between the two treatments. When a 1.5 fold-change requirement was applied only 260 probesets with the potential to be differentially expressed were detected. For a complete list of these probesets see Appendix E.

Three genes from this set were further investigated, including a component of the triacylglycerol synthetic pathway (*AGPAT3*), a sperm-specific surface antigen (*SSFA2*), and the LHCG receptor (*LHCGR*). In addition, eleven other genes not meeting our filter conditions were investigated which were highly expressed and/or fell into the categories of steroid synthesis, oxidative stress and Leydig cell maintenance (Table 4.1).

sqRT-PCR and qRT-PCR: Experiment 1

Semi-quantitative RT-PCR amplification of all 12 genes successfully investigated in the two treatment groups (n=5) for experiment 1 are shown in Figure 4.1. Amplicons were detected between 20-29 cycles at 62-68^{o}C (Table

4.2). Consistent with the microarray data COX2 mRNA expression was undetectable in any of the samples. Primer difficulties with *CYP11A1* interfered with obtaining quantifiable results on the agarose gels.

The sqRT-PCR expression levels for the genes within the two treatment groups of experiment 1 are given in Figures 4.2 A-L. No significant diet-induced changes were detected in any of the selected genes. This is in contrast to the filtered microarray data which detected a significant difference in AGPAT3, SSFA2 and LHCGR mRNA expression between CON and CR groups.

The results of Taqman® quantitative real-time RT-PCR of *CGA, LHCGR* and *StAR* are represented in Figures 4.3 A-C. In agreement with sqRT-PCR results, no significant diet-induced changes were detected in the three transcripts even though *LHCGR* had been identified as significantly different on the microarray data.

sqRT-PCR and qRT-PCR: Experiment 2

Semi-quantitative RT-PCR amplification of all seven genes investigated in the four experimental groups (n=3) for experiment 2 are displayed in Figure 4.4. Amplicons were detected between 20-29 cycles at 63-68^{o}C (Table 4.2).

The sqRT-PCR expression levels are shown in Figures 4.5 A-G for the genes within the four treatment groups of experiment 2. Significant differences were detected in mRNA expression levels for the following three genes:

1) hydroxysteroid 17-beta dehydrogenase (*HSD17β3*, Figure 4.5E): expression was 3.13 (±0.39) fold greater in Young Adult animals compared to Juvenile subjects.
2) insulin-like factor 3 (*INSL3*, Figure 4.5F): expression in Young Adult animals was greater than Juvenile and Old Adult CR subjects, with fold-changes of 2.15 (±0.34) and 3.84 (±0.62), respectively.
3) casein kinase 1 epsilon (*CSNK1E*, Figure 4.5G): expression in Juvenile animals was greater than all other groups with a 2.85 (±0.63) fold-increase over Young Adults, a 2.93 (±0.65) fold-increase over Old Adults and a 3.86 (±0.86) fold-increase over Old Adult CR.

In addition, *LHCGR* and *StAR* expression may have shown significant differences in the Juvenile group had it not been for the large variation in the three animals. *HSD3β2* and *CYP17A1* were not differentially expressed between any of the groups.

The results of Taqman® quantitative real-time RT-PCR of *CGA*, *LHCGR* and *StAR* are shown in Figures 4.6 A-C. While no significant changes were detected in *LHCGR* and *StAR* expression across our treatment groups, *CGA* was differentially expressed in the Old Adult group compared to Juvenile and Old Adult CR animals. Expression levels in the Old Adult group were 35.11 (±10.45) fold higher than the younger animals and 4.54 (±1.66) fold higher than their age-matched CR-treated counterparts.

DNA Sequencing: Experiment 1 and 2

Complete sequences for experimentally derived PCR products are listed in Table 4.4, as determined by DNA sequencing. The resulting sequences were BLASTed in the NCBI database to determine the sequence of best fit. In almost every instance, the experimentally derived sequence returned a best fit for the predicted rhesus macaque mRNA sequence which had been used for primer design.

Discussion

Calorie restriction (CR) has been associated with life extension for over 75 years and remains the only proven non-genetic paradigm for extending lifespan and attenuating the biological processes and chronic diseases associated with aging (Heilbronn and Ravussin, 2003; McCay et al., 1935). Moderate CR also exhibits great consistency across taxa and demonstrates generalized, beneficial health effects; the potential impact of this nutritional paradigm on the hypothalamic-pituitary-gonadal axis is less clear. Could moderate CR possibly improve reproductive health parameters as it does with other systems within the body? Alternatively, could it have no impact or even a negative effect on reproductive outcome? Previous evidence suggests that depending on age, gender and species, the effects of calorie restriction on the HPG axis are mixed.

Reproductive senescence in men typically follows a more gradual course than in females. This does not mean, however, that there are no physiological ramifications of aging, especially in humans where decreasing testosterone

levels, metabolic and circadian changes, and increasing body weight are generally associated with aging. The recent phenomenon of increased average body mass index (BMI) experienced by the Western world has resulted in an increased incidence of obesity (BMI>25 kg/m^2) (Hursting et al., 2003). Men with BMI>25 kg/m^2 have lower sperm concentration and total sperm count compared to men with lower, non-obese BMI levels (Jensen et al., 2004) while BMI and total number of motile sperm cells have been shown to be inversely related (Kort et al., 2006). Thus, BMI typically increases during aging so reproductive capacity is not only impacted negatively by age, but also by the pathologies associated with obesity.

Since CR reduces body mass and adiposity and improves general health parameters, it would be of great benefit to know if CR could also maintain reproductive fitness and/or attenuate age changes in the system (Heilbronn and Ravussin, 2003; Koubova and Guarente, 2003; Lane et al., 1997). In this study we investigated the potential impact of age and moderate CR on testicular gene expression and quantified expression levels in rhesus macaques (*Macaca mulatta*). We were particularly interested in genes associated with reproduction, circadian mechanisms, metabolism and oxidative stress.

Experiment 1

Microarrays and Gene Determination

To ascertain the biologically relevant changes detected by microarray, robust multi-array average (RMA) was utilized, which is preferable to other

logarithmic methods for detecting probeset significance (Irizarry et al., 2003). Based on RMA and filter criteria (*t*-test; $P<0.05$), 1452 probesets out of 52,000+ were significantly different between the two treatments. When a 1.5 fold-change requirement was applied, 260 probesets were detected with the potential to be differentially expressed. Based on previous experiences in our laboratory we typically dropped from consideration any probesets which displayed detection levels below 100 on the array. In those instances, however, we were utilizing rhesus macaque tissue with human arrays (Affymetrix HG_U133A) and were primarily concerned with cross-hybridization and false-positives. Because this would have severely limited our analysis, and because we were less concerned with cross- hybridization with the newly available GeneChip® Rhesus Macaque Genome Arrays, we decided to work with the 260 probesets.

In addition to the 260 potentially different probesets, we also performed a keyword search of the entire microarray dataset and identified non-significantly changed probesets of interest, including genes that were highly expressed and/or fell into the categories of reproduction, circadian mechanisms, metabolism and oxidative stress. Finally, we compiled a list of probesets/genes to initially investigate (Appendix F) and designed primers for them. A complete analysis was performed on a selected subset of these genes (see Appendix I for details). Final analysis of testicular gene expression in YACON and YACR animals included 14 genes for which we were able to design successful primer pairs and which showed the most potential for exhibiting real expression changes (Figure 4.1). These included: 1-acylglycerol-3-phosphate O-acyltransferase 3 (*AGPAT3*),

a component of the triacylglycerol biosynthesis pathway; sperm-specific antigen 2 (*SSFA2*), a surface antigen responsible for zona pellucida binding; glycoprotein hormone common alpha subunit (*CGA*); thyroid-stimulating hormone receptor (*TSHR*); uncoupling protein 2 (*UCP2*); casein kinase 1 epsilon (*CSNK1E*), a core-clock gene; and insulin-like factor 3 (*INSL3*), an indicator of Leydig cell health. We also measured expression levels for all components of the testosterone biosynthetic pathway: *LHCGR*; *StAR*; cytochrome P450, family 11, subfamily A, polypeptide 1 (*CYP11A1* or side-chain cleavage or $P450_{scc}$); cytochrome P450, family 17, subfamily A, polypeptide 1 (*CYP17A1* or $P450_{c17}$); hydroxysteroid (17-beta) dehydrogenase 3 (*HSD17β3*); and hydroxysteroid (3-beta) dehydrogenase 2 (*HSD3β2*) (Figure 4.1). Also included was cyclooxygenase 2 (*COX2*), which showed no expression on the microarray data, but was used as a negative control measure of cellular stress in the animals.

Microarray vs. PCR – AGPAT3, SSFA2 and LHCGR

No significant differences in mRNA expression were detected between treatment groups in any of the genes investigated using sqRT-PCR (Figures 4.2 A-L) or qRT-PCR (Figures 4.3 A-C). This was in contrast to the microarray data which had originally shown three of the genes (*AGPAT3*, *SSFA2* and *LHCGR*) to be differentially expressed based on filter criteria. As with data from some of our previous experiments, this only further emphasized to us the need for additional experiments to support microarray data of any kind.

We were surprised to find no CR-induced changes in *AGPAT3* expression for two reasons. First, it is a key enzyme in the triacylglycerol (triglyceride) pathway, and CR has been shown to lower triglyceride levels (Roth et al., 2002). Secondly, the GeneChip® Rhesus Macaque Genome Array contained seven probesets for *AGPAT3*, and at least one probeset had been labeled as significantly changing in both the pituitary gland and testis (Chapter 3) based on filtering parameters. As with the results from our pituitary gland experiments, however, there were conflicting expression changes in these probesets with five of them showing decreased expression in CR animals while two others showed increased mRNA expression. And, as with the pituitary gland sqRT-PCR findings, no significant differences were detected between groups. Because of these conflicting results it is difficult to say with any certainty what is occurring with regards to AGPAT3 mRNA expression.

Sperm-specific fertilization antigen 1 and 2 (*SSFA1* and *SSFA2*) are sperm surface antigens that appear to affect sperm binding to the zona pellucida of the oocyte. More is known about *SSFA1* than *SSFA2*, but both may also have a role in sperm cell capacitation and/or acrosome reaction (Naz, 1999; Naz and Wolf, 1994). With regards to *SSFA2* microarray data, all three probesets showed a decrease in expression for CR animals and displayed the largest fold-change between groups of any of the testicular genes investigated. For this reason it was somewhat unusual not to detect any differences with sqRT-PCR analysis.

LHCGR is a member of the subfamily of glycoprotein hormone receptors within the superfamily of G protein-coupled receptor (GPCR)/seven-

transmembrane domain receptors. In the testis the receptor was originally thought to be restricted to Leydig cells but is now known to be present in sperm and accessory sex glands (seminal vesicles and prostate) (Ascoli et al., 2002). In the testis, luteinizing hormone acts through LHCG receptors on the Leydig cells to maintain general metabolic processes and steroidogenic enzymes and to regulate the production and secretion of androgens. Androgen production in the testis is increased solely by LH binding to its receptor via cAMP activation and is the first step in testosterone biosynthesis (Dufau, 1998).

Initial microarray data contained only two probesets for *LHCGR* with one showing significantly increased expression levels and the other at such low expression levels as to be designated 'absent' by the filter. In fact, *LHCGR* expression was surprisingly low relative to other gene transcripts considering its integral function in the male reproductive system. Originally we had hypothesized that the CR-treated animals may have been responding to lower LH levels with an increase in LHCG receptor numbers, since it has been demonstrated that CR alters neuorendocrine function by lowering gonadotropin levels (Koubova and Guarente, 2003). It appears, based on our data, that LHCGR expression is not impacted by CR in our young adult rhesus macaques.

There are several possible reasons for the discrepancies between our microarray data and our PCR results. First, it could be related to the sample sizes in each technique. Array data was based on a sample size of three for both treatments while sqRT-PCR data utilized five animals in each group. Our qRT-PCR results for YACON considered four animals versus five for YACR; one

control animal was removed as an outlier during analysis (average detection signal being more than two standard deviations away from the group mean). This was one of the YACON animals for which array hybridization had been conducted and sqRT-PCR results were within normal range.

Secondly, the heterogeneous nature of the tissue must be considered. The testis is composed of various cell types (Leydig, Sertoli, spermatagonia, spermatozoa, etc), each of which may be regulated differentially such that transcript expression may go up for a gene in one cell type while decreasing or staying the same in another. While every attempt was made to guarantee uniformity of the biopsies from the harvested testis, it may be that we simply sampled from different areas within the organ itself. Such error may have caused variation between techniques when using different animal sample sizes.

Finally, under the strictest filter requirements, there may have been as few as 76 probesets out of 52,000+ changing according to microarray analysis on the GeneChip® Rhesus Macaque Genome Array. By choosing to work with 260 probesets based on our more liberal filtering criteria we simply may have cast too wide a net in our investigation. Other researchers have also questioned the use of fold-change differences alone in concluding that a given gene has changed (Chen et al., 2004) and believe that further analytical measures are required.

Taken together, it appears that calorie restriction had limited impact on testicular gene expression in Young Adult rhesus macaques. While only 260 probesets (and potentially fewer genes) showed differential expression on the microarrays, we measured no mRNA expression differences based on semi-

quantitative and real-time PCR data for the fourteen genes investigated. These findings suggest that CR can elicit beneficial health effects without negative consequences on the gonadal portion of the HPG axis. To be completely certain, however, further analysis could be performed on the other potentially changing genes. In addition, even though expression levels may not change between treatment groups, morphological changes could be taking place. While they may appear to be functioning normally under calorie restricted conditions, changes in cell location, number or size may be occurring. Other quantifiable techniques, such as immunohistochemistry or *in situ* hybridization would have to be employed in order to make such a determination.

Experiment 2

Testosterone is a critical feedback component of the HPG axis and essential for production of spermatozoa. Although the impact of its decline on reproductive senescence is not completely understood, we know that aging brings with it a host of subtle changes to testosterone production. The Brown Norway (BN) rat, for example, experiences a significant age-related decline in T production as a result of Leydig cell dysfunction rather than a reduction in cell numbers (Chen and Zirkin, 1999; Zirkin and Chen, 2000). Overall LHCG receptor numbers and their affinity for LH also declines as a function of age in rats (Chen et al., 2002; Zirkin and Chen, 2000). In humans there is a documented decline in testosterone production beginning after 30 years of age and continuing gradually for life (Hardy and Schlegel, 2004; Henkel et al., 2005; Stocco and Wang, 2006).

Consequently there is the potential for a cascade effect to the entire reproductive system with its fall. Testosterone loss can result in weakening muscle function, bone density and other physiological parameters related to overall aging (Harman et al., 2001; Moffat et al., 2002). Also of importance is the neurological impact of testosterone loss. Men with Alzheimer's disease (AD) have significantly lower T levels than aged men without AD. Importantly, testosterone depletion appears to occur well before clinical and pathological diagnosis of AD, suggesting that low T contributes to AD pathogenesis rather than results from it (Rosario et al., 2006).

The possible effects of CR on testicular gene expression were then invstigated in an aging series of rhesus macaques. Even though limited CR-related differences in mRNA expression had been observed in the young males, could more significant age-related differences in expression be detected, and if so would they be attenuated by CR treatment? Analysis was performed on banked tissue samples available from the ONPRC using a subset of the genes previously investigated in the Young Adult males. The seven genes were separated into two categories; those for steroidogenesis and those for Leydig cell health and cell cycling.

Steroidogenesis - LHCGR, StAR, CYP17A1, HSD3β2, HSD17β3

The initial step in Leydig cell testosterone biosynthesis is the binding of LH to its receptor on the cell plasma membrane. This action begins a cascade of events that includes activation of adenylate cyclase via G proteins, increased

intracellular cAMP formation, translocation of cholesterol into the mitochondria via StAR, association of cholesterol with the cytochrome P450 side-chain cleavage enzyme (*CYP11A1*), production of pregnenolone from cholesterol, translocation of pregnenolone from the mitrochondria to the smooth endoplasmic reticulum (SER) and conversion of pregnenolone to testosterone via a series of enzymatic reactions in the SER (Figure 4.7).

The entire steroidogenic pathway was analyzed from receptor activation to testosterone formation except for one component; due to primer difficulties *CYP11A1* (*$P450_{scc}$*) was unable to be measured (Figure 4.4). No significant changes were found in *LHCGR, StAR, CYP17A1,* or *HSD3β2* in the four age categories with respect to mRNA expression as measured by sqRT-PCR (Figures 4.5 A-D). The only significant difference detected in this pathway was in *HSD17β3* expression between J animals and YA which displayed a 3.13 ($\pm$0.39) fold-change increase over the pre-pubertal group (Figure 4.5E). These findings are not very surprising since enzymatic activity for androgen production would be more prevalent following sexual maturation at puberty.

It was somewhat surprising, however, that no age-related differences were detected in the other genes since StAR protein and mRNA are reduced in older rat Leydig cells, as are P450scc activity, protein and mRNA expression (Luo et al., 2001). There has also been a demonstrated reduction in activity of each of the steroidogenic enzymes responsible for converting cholesterol to testosterone in the rat, including *P450scc*, *HSD3β*, *P450c17* and *HSD17β* (Luo et al., 1996; Zirkin and Chen, 2000). These are activity responses, however, and do not

necessarily reflect mRNA or protein levels. These data were also all derived from rat Leydig cell studies as compared to whole tissue testis biopsies which may account for the discrepancies or it may be a species-specific aging response.

Leydig cell health and cell cycling - INSL3 and CSNK1E

The peptide hormone, insulin-like factor 3 (*INSL3*), is a major secretory product of the testicular Leydig cells. It appears to be constitutively expressed due to LH stimulation and is a good serum marker for fully differentiated adult Leydig cells; its concentration reflecting the functional status of Leydig cells. It may, in fact, be a more sensitive marker of Leydig cell function than testosterone (Foresta et al., 2004; Ivell and Bathgate, 2002). *INSL3* serves an important paracrine function by binding to its receptor in seminiferous tubules and germ cells to suppress apoptosis. The receptor is not localized to the testis only, but is also localized in the pituitary gland. A functional feedback loop with LH (Foresta et al., 2004) may be involved in behavioral function (Ivell et al., 2005). Transcripts of the INSL3 gene itself represent one of the most abundant mRNAs in the Leydig cell. This was observed with the microarray data as *INSL3* was the highest expressing probeset in the selected genes of study on the testicular arrays.

When steroidogenic function of the Leydig cells deteriorates there is a marked reduction in INSL3 mRNA expression (Ivell and Bathgate, 2002; Ivell et al., 2005). For this reason we felt it would make a good age-related marker of Leydig cell function in our sqRT-PCR assay. Significant mRNA expression

differences were detected (in relative units) between YA animals (2.35±0.38) and J subjects (1.10±0.14) as well as YA and the OACR group (0.61±0.19). Expression levels for OA animals (1.40±0.32) fell between their age-matched CR-treated counterparts and the YA group, but were not significantly different from any of the other three groups (Figure 4.5F). These data show the expected age-related decline in *INSL3* expression with no apparent effect of CR.

Previous studies have found the core circadian clock components *PER1*, *CRY1*, *BMAL1*, and *CLOCK* to be present in mouse testis (Alvarez et al., 2003). None of these core-clock genes cycle in the testis as they do in other peripheral tissues, but they are expressed at very specific stages of sperm development. (i.e. *CLOCK* in round spermatids and *PER1* in spermatogonia subpopulations and condensing spermatids) (Morse et al., 2003). Casein kinase 1 epsilon (*CSNK1E*) is another core-clock gene whose product is responsible for phosphorylation of other proteins and dimers in the circadian clock molecular mechanism. It may not be strictly related to Leydig cells but perhaps to multiple cell types in the testis, including Leydig cells, Sertoli cells, and spermatogonia.

The lack of detectable cycling of circadian genes in the testis raises the question as to their function or necessity. Although circadian knockout animals are fertile (Alvarez et al., 2003), there may still be an effect on spermatogenesis. Possibly subtle affects have not been detected since a careful study of fertility and spermatogenesis has not been performed on any of the knockout mouse strains. It could also be that timing of the various spermatogenic stages are disrupted such that spermatozoa may still be produced but the proper transition

from one stage to the next is disrupted causing modifications of seminiferous tubule histology. The cumulative effect could have a negative impact on sperm quantity and/or quality.

We found a significant decline in CSNK1E mRNA expression (relative units) between J animals (2.59±0.57) and the other three age categories (YA, 0.91±0.14; OA, 0.88±0.21; OACR, 0.67±0.12) (Figure 4.5G). In a previous study we also investigated the effect of age on *CSNK1E* expression in the pituitary gland. In that tissue a more gradual age-related decline was observed; the data did not reach the same level of significance observed here in the testis. The biological significance of this possible age-related decline in either tissue is still unknown.

In experiment 2, several significant age-related changes were detected in mRNA expression of seven genes based on sqRT-PCR findings. There were, however, no observable differences in expression levels between OA animals and their age-matched CR-treated counterparts. These results seem to indicate that CR was neither beneficial nor detrimental to testicular function based on the selected endpoints. One difference between Old Adults and Old Adult CR animals was observed after completing qRT-PCR analysis on an eighth gene.

Glycoprotein hormone common alpha subunit (CGA)

Quantitative real-time RT-PCR analysis was carried out for three genes: *LHCGR*, *StAR*, and *CGA* (Figures 4.6 A-C). As with sqRT-PCR findings, no difference was observed between any of the groups for *LHCGR* and *StAR*

expression. When *CGA* was measured, however, a significant difference was found between treatments with OA subjects showing a 35.11 (±10.45) fold-change increase over J and a 4.54 (±1.66) fold-change increase over OACR animals. While investigating pituitary gland gene expression in a previous experiment, we measured *CGA* levels between Young Adult males and their age-matched restricted counterparts. In that tissue significantly different levels were observed between treatment groups with CR animals exhibiting a negative fold-change of 0.57 (±0.10). In both instances the CR-treated group exhibited significantly lower levels of *CGA* expression, and in the case of the OACR subjects, *CGA* levels were actually restored to the level of Juvenile and Young Adult expression.

Glycoprotein hormone alpha subunit levels were low in the testes compared to *LHCGR* and *StAR* measured in our experiments. Nonetheless, there may be a biological relevance to their mRNA expression in this tissue. Endogenous *CGA* has been shown to be expressed in rat ovary (Markkula et al., 1996) and testes (Zhang et al., 1995) where it is believed to perhaps play a role as a paracrine factor of gonadal function. It may be that *CGA* serves a similar function in the rhesus macaque testes.

Based on mRNA expression and semi-quantitative and real-time PCR data, we found limited impact of CR on testicular gene expression in young adult and old adult rhesus macaques based on the genes investigated. In the case of *CGA* expression in old adults, however, the nutritional paradigm returned expression levels to those observed in younger animals. Findings suggest that

CR can elicit general beneficial health effects without negative consequences on the gonadal portion of the HPG axis. Our data are also in line with findings from Chen et al. (2004) showing only 45 genes to be significantly changing in rat Leydig cells with age. In contrast to the effects seen in many other cell types and systems, the vast majority (44/45) of the Leydig cell genes that changed with age were not 'rescued' by CR intervention. The only gene that returned to younger expression levels was *tubulinα1*.

While it appears there was no protective effect of CR in our studies, with the possible exceptioin of *CGA*, there are alternative analyses that could be explored before this is determined. One potential route for further investigation would be to extend previous work in the Brown Norway rat to non-human primate models. A great deal of information has been gained from studies of BN rat Leydig cells, especially with regards to LH signal transduction in the testosterone biosynthetic pathway. It has been shown that exogenous LH stimulation of *LHCGR* alone cannot restore testosterone levels in aged Leydig cells. G protein-coupled adenylate cyclase can be stimulated with forksolin directly, however, to restore testosterone levels in the same cells. This seems to indicate that lower androgen levels are a result of inefficient signal transduction most likely due to problems in the quality of *LHCGR*, in the G proteins, and/or in their coupling (Zirkin and Chen, 2000). Thus, it may be that the aging effect on Leydig cell steroidogenesis is not caused by reduced mRNA or proteins involved in LH signaling, but rather by diminished functional activity of the proteins. This diminished function could be caused by free radical production (Chen et al.,

2002; Chen et al., 2004). Reactive oxygen species (ROS) have been shown to damage critical components of the steroid synthetic pathway and ROS have been shown to be produced during steroidogenesis itself (Chen and Zirkin, 1999). Chronic suppression of testosterone production by Leydig cells appears to prevent aging, possibly by reducing ROS formation (Zirkin and Chen, 2000) while temporary chemical destruction of old Leydig cells will allow new cells to grow which have the androgen producing ability of cells in young animals, again, possibly because they have not been ROS damaged (Chen et al., 1996; Zirkin and Chen, 2000).

It may be worth our time in future experiments to investigate the impact of CR on this much more specific route of reproductive decline. We may have even been on the right path as we had initially included glutathione and catalase in our studies and dropped them only after experiencing time constraints and primer difficulties. These two genes and their products protect against ROS and have been shown to have lower mRNA and protein expression as well as lower activity levels in aged Leydig cells (Zirkin, 2006).

Summary

In the present study we investigated the potential impact of age and CR on testicular gene expression and quantified expression levels in adult rhesus macaques (*Macaca mulatta*). Experiment 1 consisted of 10 Young Adult (12 years) rhesus macaques fed a control diet (YACON; n=5) or calorie restricted at 30% CON (YACR; n=5) for the previous eight years post-pubertally. Experiment

2 utilized banked tissues from previous unrelated studies and included three Juvenile (J; 1-2 years), three Young Adult (YA; 5-7 years), three Old Adult (OA; 24-30 years) and three calorie restricted Old Adult (OACR; 25-27 years) animals. Old Adult CR subjects in experiment 2 were on the nutritional paradigm for the previous five years prior to sacrifice. Total RNA was isolated from the testis of all animals and gene expression profiles were obtained from three animals in each treatment of Experiment 1 using Affymetrix GeneChip® arrays. Out of a potential 52,000+ probesets, we detected fewer than 300 that were different between Young Adult CON and CR animals after filtering with Genesifter® (vizXlabs) and a 1.5 fold-change threshold requirement. We chose three genes from this set to investigate further including a component of the triacylglycerol synthetic pathway, a sperm surface antigen, and the LHCG receptor. We also examined eleven other genes covering the steroidogenic pathway, oxidative stress and Leydig cell maintenance. Expression was not altered by CR in our genes of interest based on semi-quantitative and real-time PCR data. In Experiment 2 we observed age-related changes in HSD17β3, INSL3 and CSNK1E mRNA expression as measured by sqRT-PCR, but detected no significant differences in CR-treated Old Adults as compared to there age-matched controls. We did, however, detect age and CR-related changes in glycoprotein hormone common alpha subunit mRNA expression based on qRT-PCR findings, with expression levels in Old Adult CR subjects returning to youthful levels. The biological significance of this is undetermined. Our studies are among the first to address the potential impact of post-pubertal CR implementation on testicular gene expression in the rhesus

macaque. These findings suggest that CR can elicit beneficial health effects without negative consequences on the gonadal portion of the HPG axis and perhaps even return some mRNA parameters to more youthful levels. It remains to be determined whether this nutritional paradigm impacts other portions of the reproductive axis.

Acknowledgments

Research was supported by NIH Grants AG-19914, HD-29186, RR-00163 and U01-AG21380-03. Additional support provided by: Research Assistantship from the Department of Animal and Avian Sciences at the University of Maryland; the Intramural Research Program of the National Institutes of Health; and the National Institute on Aging. We would also like to thank the members of the Oregon National Primate Research Center: Dario Lemos, Dr. Jodi Downs, Vasilios (Bill) Garyfallou, Dr. Yibing Jia, Dr. Betsy Ferguson, Dr. Eliot Spindel and the entire animal care staff.

Testis													
Other ID / Probeset	CON 1	Call	CON 2	Call	CON 3	Call	Gene ID	CR 1	Call	CR 2	Call	CR 3	Call
MmugDNA.14589.1.S1_at	332.3	P	287	P	324.8	P	**AGPAT**	315.4	P	293.8	P	349.1	P
MmugDNA.1459.1.S1_s_at	222	P	239.6	P	153.9	P		159	P	164.1	P	222.8	P
MmugDNA.16471.1.S1_at	440.8	P	536.6	P	547.8	P		597.1	P	590.9	P	687.2	P
MmugDNA.24842.1.S1_at	200.2	P	218.3	P	156.4	P		124.7	P	91.8	P	63.4	A
MmugDNA.24844.1.S1_at	207.2	P	293.6	P	142.4	P		212	P	182.6	P	171.1	P
MmugDNA.39097.1.S1_at	380.8	P	532.5	P	402.7	P		321.8	P	238.6	P	295.4	P
MmugDNA.6884.1.S1_at	264.1	P	343.7	P	216	P		290.5	P	235.9	P	231.8	P
MmugDNA.13477.1.S1_at	8.5	P	21.4	A	14.6	A	**TSHR**	8.2	A	15	A	13.7	A
MmugDNA.32655.1.S1_at	22.2	P	37.3	P	49.5	P		40.8	P	42.4	P	55.6	P
MmugDNA.796.1.S1_at	12.7	A	19.3	A	5.3	A		2.1	A	4.2	A	4.5	A
MmugDNA.17932.1.S1_at	25.1	P	16.6	A	33	A	**LHCGR**	24.1	A	19	P	18.5	A
MmugDNA.21104.1.S1_at	220.6	P	133.5	P	114.4	P		357.2	P	229.4	P	243.1	P
MmugDNA.19270.1.S1_at	5.2	A	16.9	A	4.1	A	**SSFA2**	13.3	A	2.8	A	5.1	A
MmugDNA.26522.1.S1_at	171.3	P	207.3	P	131.9	P		63.5	P	47.9	P	57.8	M
MmugDNA.14233.1.S1_at	561	P	644.9	P	530.6	P		463.6	P	426.3	P	411	P
MmugDNA.4648.1.S1_at	2.1	A	0.8	A	0.9	A	**CGA**	3.9	A	1.3	A	10.9	A
MmugDNA.29263.1.S1_at	588.4	P	590.7	P	622.1	P		634	P	658.4	P	630.1	P
MmugDNA.16174.1.S1_at	280.6	P	188.6	P	260.2	P	**UCP**	393.4	P	319.2	P	307.4	P
MmugDNA.1485.1.S1_at	246.9	P	163.3	P	245.9	P		281.4	P	215.2	P	198.7	P
MmuSTS.4519.1.S1_at	342.2	P	154.6	P	184.7	P	**StAR**	163.2	P	480.3	P	109.9	P
MmugDNA.20457.1.S1_at	1398	P	646	P	1301.2	P	**HSD17B3**	902.3	P	1957.9	P	530.3	P
MmugDNA.29281.1.S1_s_at	3349.4	P	1767.8	P	1759.2	P	**INSL3**	2777.2	P	6862.8	P	2318.2	P
MmugDNA.4494.1.S1_at	9.1	M	7.6	A	15.8	A	**COX2**	2.2	A	12.3	A	36.1	P
MmugDNA.17389.1.S1_at	637.2	P	460.7	P	681.5	P	**CSNK1E**	469.4	P	419.5	P	703.9	P
MmugDNA.29650.1.S1_at	69.5	A	41.4	A	47.8	A		42.9	A	58.6	A	62.5	A
MmugDNA.34870.1.S1_at	84.1	A	119.7	A	91.6	A		79.9	A	126.4	A	102.7	A
MmugDNA.4033.1.S1_at	49.1	P	61.3	P	27.6	A		43.3	P	28.3	M	34.8	A
MmuSTS.1889.1.S1_at	66.5	P	118.9	P	52.8	A		78.4	P	70.5	P	80.1	M
MmugDNA.37726.1.S1_at	5.8	A	11.7	A	6.6	A	**CYP17A1**	8.4	A	8.2	P	6.5	A
MmuSTS.4193.1.S1_at	302	P	154.1	P	143	P		159.3	P	725.7	P	166.8	P
MmugDNA.42334.1.S1_at	15.4	A	16.2	A	30.4	A	**HSD3B2**	20.2	A	21.5	P	52.5	P
MmuSTS.601.1.S1_at	16.4	A	3.5	A	5.4	A		0.9	A	10	A	28.7	A
MmugDNA.19420.1.S1_at	722.8	P	822.6	P	551.6	P		815.4	P	695.4	P	572.5	P
MmuSTS.4192.1.S1_at	114.4	P	47.2	P	65.4	P	**CYP11A1**	44	P	142.2	P	47	P

Table 4.1 Microarray Probeset Data for Testicular Genes Subjected to Experimental Analysis Compiled list of testicular genes (and their probesets) investigated experimentally with sqRT-PCR and qRT-PCR (Young Adult CON, n=3; Young Adult CR, n=3). Data are from our GeneChip® Rhesus Macaque Genome Array output (Affymetrix).

Table 4.2 Gene Expression Profiles in the Rhesus Macaque Testis Mean signal intensity values (±SEM) of testicular gene expression (Young Adult CON, n=3; Young Adult CR, n=3). These genes showed a significant (AGPAT, LHCGR, SSFA2) or non-significant change (TSHR, CGA, UCP2, StAR, HSD17β3, INSL3, COX2, CSNK1E, CYP17A1, HSD3β2, HSD11A1) in gene expression based on GeneChip® Rhesus Macaque Genome Array detection (Affymetrix) and our Genesifter® (vixXlabs) filtering parameters (letter notations, $P<0.05$). A subset of these genes was also investigated with PCR techniques for age- and CR-induced changes in experiment 2 (Juvenile, n=3; Young Adult, n=3; Old Adult, n=3; Old Adult CR, n=3).

Testis			
Probeset	**Gene ID**	**CON mean**	**CR mean**
MmugDNA.14589.1.S1_at	**AGPAT**	315 ± 14	319 ± 16
MmugDNA.1459.1.S1_s_at		205 ± 26	182 ± 21
MmugDNA.16471.1.S1_at		508 ± 34	625 ± 31
MmugDNA.24842.1.S1_at		192 ± 18	93 ± 18
MmugDNA.24844.1.S1_at		214 ± 44	189 ± 12
MmugDNA.39097.1.S1_at		439 ± 47[a]	285 ± 25[b]
MmugDNA.6884.1.S1_at		275 ± 37	253 ± 19
MmugDNA.13477.1.S1_at	**TSHR**	15 ± 4	12 ± 2
MmugDNA.32655.1.S1_at		36 ± 8	46 ± 5
MmugDNA.796.1.S1_at		12 ± 4	4 ± 1
MmugDNA.17932.1.S1_at	**LHCGR**	25 ± 5	21 ± 2
MmugDNA.21104.1.S1_at		156 ± 33[a]	277 ± 41[b]
MmugDNA.19270.1.S1_at	**SSFA2**	9 ± 4	7 ± 3
MmugDNA.26522.1.S1_at		170 ± 22[a]	56 ± 5[b]
MmugDNA.14233.1.S1_at		579 ± 34	434 ± 16
MmugDNA.4648.1.S1_at	**CGA**	1 ± 1	5 ± 3
MmugDNA.29263.1.S1_at		600 ± 11	641 ± 9
MmugDNA.16174.1.S1_at	**UCP**	243 ± 28	340 ± 27
MmugDNA.1485.1.S1_at		219 ± 28	232 ± 25
MmuSTS.4519.1.S1_at	**StAR**	227 ± 58	251 ± 116
MmugDNA.20457.1.S1_at	**HSD17β3**	1115 ± 236	1130 ± 428
MmugDNA.29281.1.S1_s_at	**INSL3**	2292 ± 529	3986 ± 1444
MmugDNA.4494.1.S1_at	**COX2**	11 ± 3	17 ± 10
MmugDNA.17389.1.S1_at	**CSNK1E**	593 ± 67	531 ± 88
MmugDNA.29650.1.S1_at		53 ± 9	55 ± 6
MmugDNA.34870.1.S1_at		98 ± 11	103 ± 13
MmugDNA.4033.1.S1_at		46 ± 10	35 ± 4
MmuSTS.1889.1.S1_at		79 ± 20	76 ± 3
MmugDNA.37726.1.S1_at	**CYP17A1**	8 ± 2	8 ± 1
MmuSTS.4193.1.S1_at		200 ± 51	351 ± 188
MmugDNA.42334.1.S1_at	**HSD3β2**	21 ± 5	31 ± 11
MmuSTS.601.1.S1_at		8 ± 4	13 ± 8
MmugDNA.19420.1.S1_at		699 ± 79	694 ± 70
MmuSTS.4192.1.S1_at	**CYP11A1**	76 ± 20	78 ± 32

sqRT-PCR primers	Forward sequence	Reverse sequence	Amplicon	Cycles	Temp
CGA	GGAGAGTTTACAATGCAGGATTGC	GTCATCAAAACAGCACTTGGCA	310 bp	22	62°C
TSHR	CTTCTTTTCTGAAACTGCCAGCTC	GAGATTCCAGGTGAGTCCAGCA	302 bp	29	62°C
AGPAT	GCTGACTGTTGGCCAGTTTCA	CCTGCAGCATTTCACCAGTACA	316 bp	27	62°C
UCP2	TGCAAAGCCCTGCTGTTCA	AGATAGAGGAACTCTGCCGGAATC	301 bp	26	63°C
SSFA2	GGAAGAAAGTATTCCGAGCATCGG	ACACCTCCACCAGTGCATATCATTG	307 bp	26	65.5°C
CSNK1E	AAGTATGAGCGGATCAGCGAGA	CCGAATTTCAGCATGTTCCAGT	218 bp	28	65°C
COX2	AGAGGCTAGTGCCTCAGAGAG	GCTAGCACACAGGCCTATCC	437 bp	N/A	N/A
β-actin	CATTGCTCCTCCTGAGCGCAAG	GGGCCGGACTCGTCATACTCC	~300 bp	23	65°C
LHCGR	AGTGTAGACCATGACCACTGCC	TGAGACAGGGTTCCTACTCACG	610 bp	26	63°C
StAR	AACACCACAGAACAAGCAGCG	ATATTGGCCAGGATGGTCTCG	281 bp	29	68°C
HSD17β3	AGGCCCTGCAAGAGGAATATAGAG	CCTGACCTTGGTGTTGAGCTTC	302 bp	25	66°C
INSL3	CCTCTGTCCCTACTGATTCCTC	TGCACATGCAGGGAGCGGAG	313 bp	20	63°C
HSD3β2	CCACACGGTGACATTGTCAAAT	CCCACATGCACATCTCTGTCAT	211 bp	28	65°C
CYP17A1	GAGTGGCACCAGCCGGATCAG	CTCCAGGCCTGGCGCACCTTG	287 bp	25	65°C
CYP11A1	GCCATCTATGCTCTGGGCCGAG	CCATCCTCTCTGATCACTGCTGG	328 bp	N/A	N/A

Table 4.3 Testicular sqRT-PCR Gene Primers Forward and reverse primer sequences (5' to 3') used for sqRT-PCR are shown along with the expected amplicon size, annealing temperatures and number of cycles run for each reaction. Primers were designed using human or rhesus macaque gene sequences and PrimerExpress® software (Applied Biosystems). All were successful in detecting testicular mRNA gene expression.

qRT-PCR primers and probes	Forward sequence	Reverse sequence	Amplicon	Cycles	Temp
Taqman® qRT-PCR β-actin primers	Human ACTB (beta actin) Endogenous Control (Applied Biosystems; Foster City, CA)		N/A	40	60°C
Taqman® qRT-PCR β-actin probe			N/A	40	60°C
Taqman® qRT-PCR LHCGR primers	TGCTAAGAAAATGGCAATCCTCAT	CTGTGATAAGAGGCGCTTTGAA	101 bp	50	60°C
Taqman® qRT-PCR LHCGR probe	5'-6FAM-TTCACCGATTTCACCTGCATGGCA-TAMRA-3'		N/A	50	60°C
Taqman® qRT-PCR StAR primers	ACTTCCAGCCAGTGGGTGAA	CTGGCATGGCCACAGACTT	101 bp	40	60°C
Taqman® qRT-PCR StAR probe	5'-6FAM-CGGAGCACGGTCCCACTTGCAT-TAMRA-3'		N/A	40	60°C
Taqman® qRT-PCR CGA primers	TGGAGAGTTTACAATGCAGGATTG	AGCAGCAGCCCATACACTGA	101 bp	40	60°C
Taqman® qRT-PCR CGA probe	5'-6FAM-AATTCTTCTCCAAGCCGGGTGCCC-TAMRA-3'		N/A	40	60°C

Table 4.4 Testicular qRT-PCR Gene Primers and Probes Forward and reverse primer sequences (5' to 3') used for qRT-PCR are shown along with the expected amplicon size, annealing temperatures and number of cycles run for each reaction. Primers and probes were designed using rhesus macaque gene sequences and PrimerExpress® software (Applied Biosystems). All were successful in detecting testicular mRNA gene expression.

Figure 4.1 Genes in the Rhesus Macaque Testis – Dietary Effect Representative sqRT-PCR results validating the microarray data and demonstrating expression of testicular genes across the treatment groups of Young Adult rhesus macaques (12 years; CON and CR, n=5). The housekeeping gene β-actin was used as a positive control and for normalizing images for analysis.

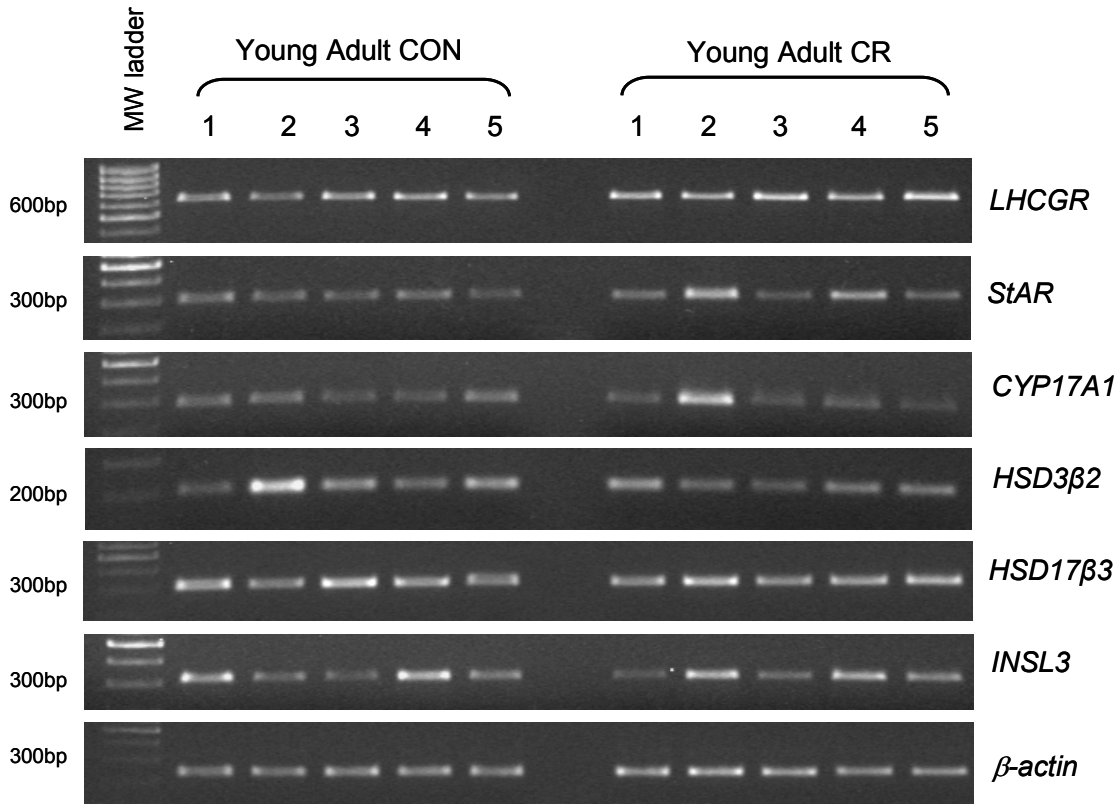
MW ladder
Young Adult CON
Young Adult CR
1 2 3 4 5
1 2 3 4 5
600bp
LHCGR
300bp
StAR
300bp
CYP17A1
200bp
HSD3β2
300bp
HSD17β3
300bp
INSL3
300bp
β-actin

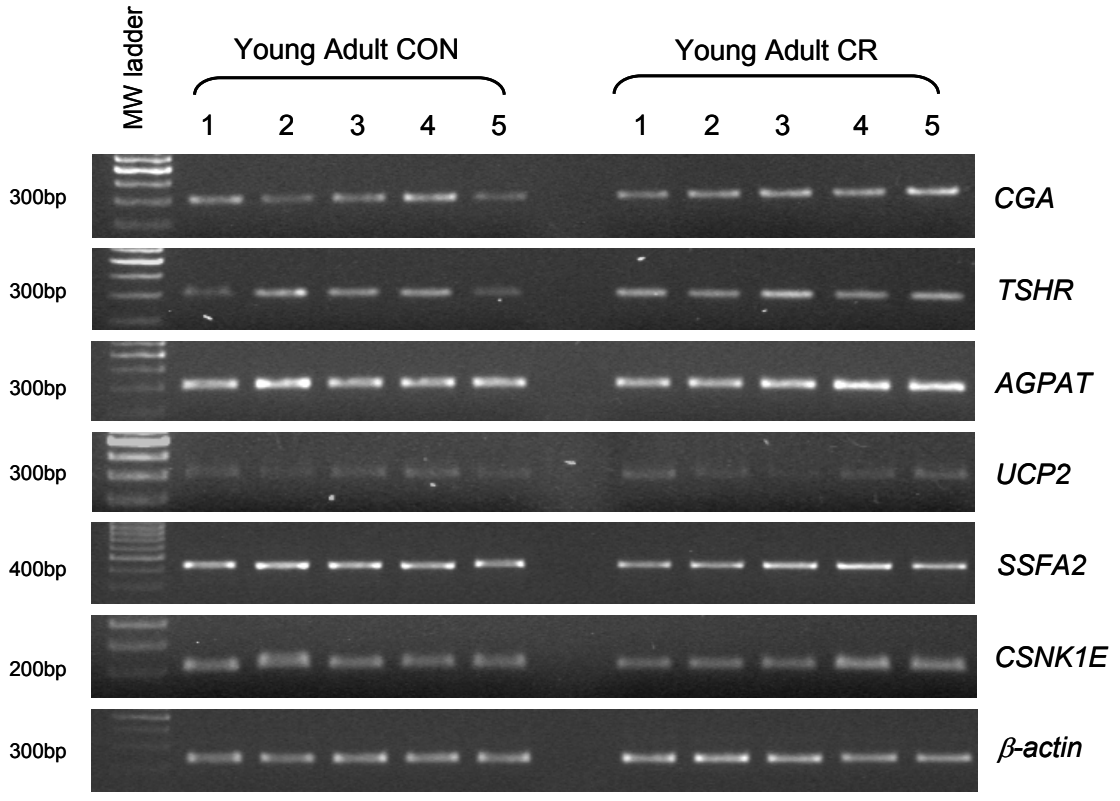
MW ladder
Young Adult CON
Young Adult CR
1 2 3 4 5
1 2 3 4 5
300bp
CGA
300bp
TSHR
300bp
AGPAT
300bp
UCP2
400bp
SSFA2
200bp
CSNK1E
300bp
β-actin

Figures 4.2 A-L sqRT-PCR Expression Levels of Genes in the Rhesus Macaque Testis – Dietary Effect Each bar, along with SEM, represents mean, normalized fluorescence data from five animals in experiment 1. Statistical comparisons were made using Student's *t*-test ($P<0.05$). None of the transcripts were significantly different between treatments.

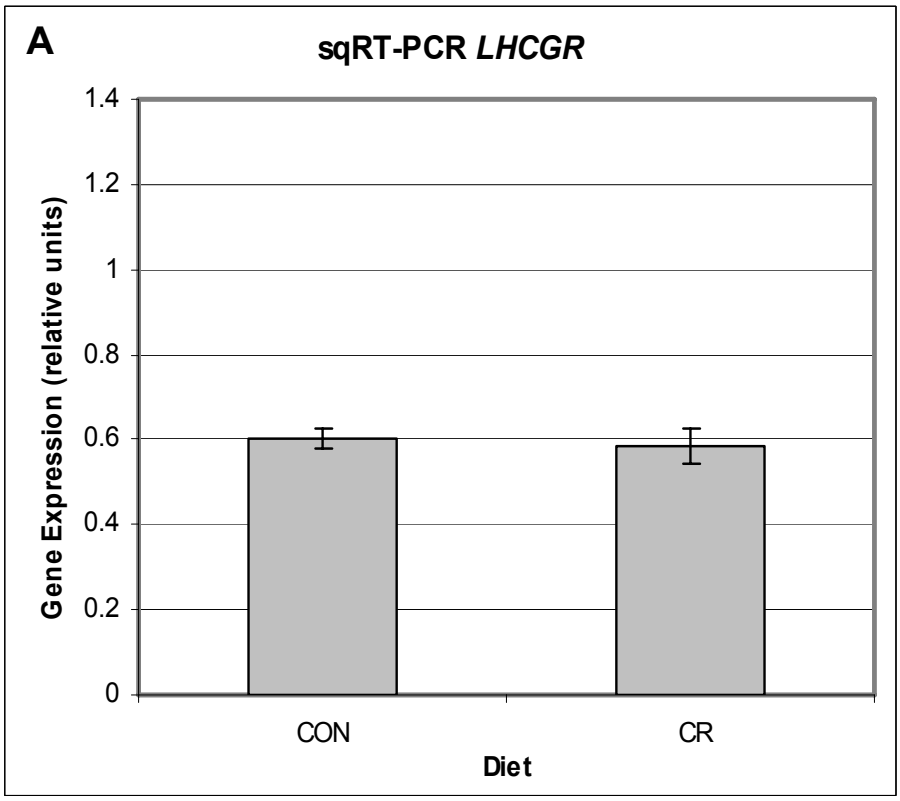
A
sqRT-PCR *LHCGR*
Gene Expression (relative units)
1.4
1.2
1
0.8
0.6
0.4
0.2
0
CON
CR
Diet

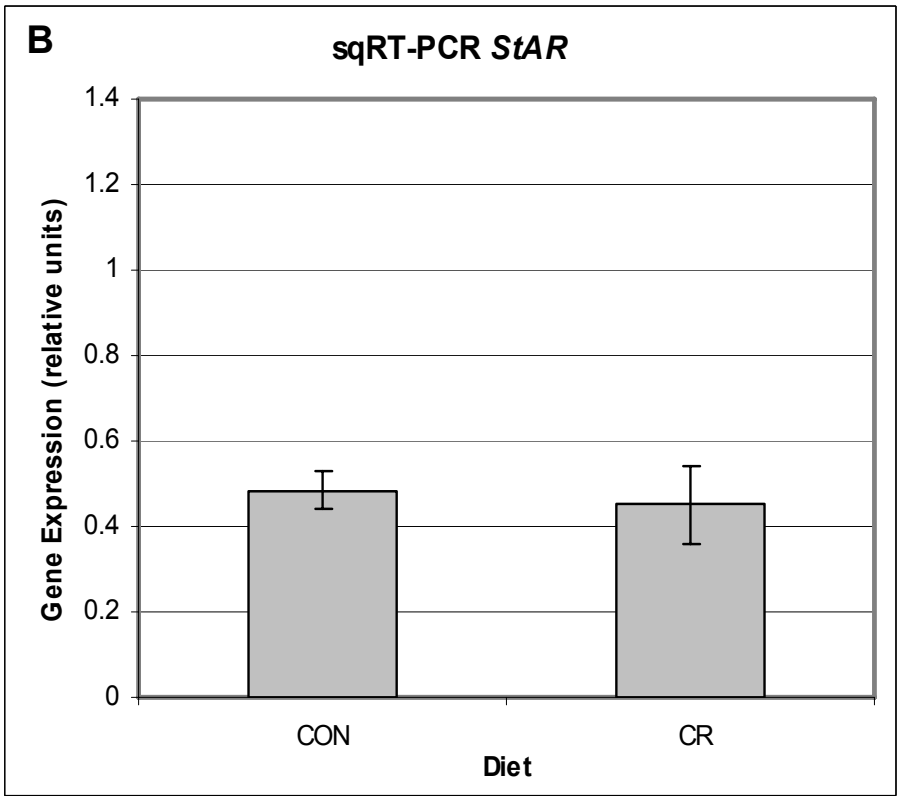
B
sqRT-PCR *StAR*
Gene Expression (relative units)
1.4
1.2
1
0.8
0.6
0.4
0.2
0
CON
CR
Diet

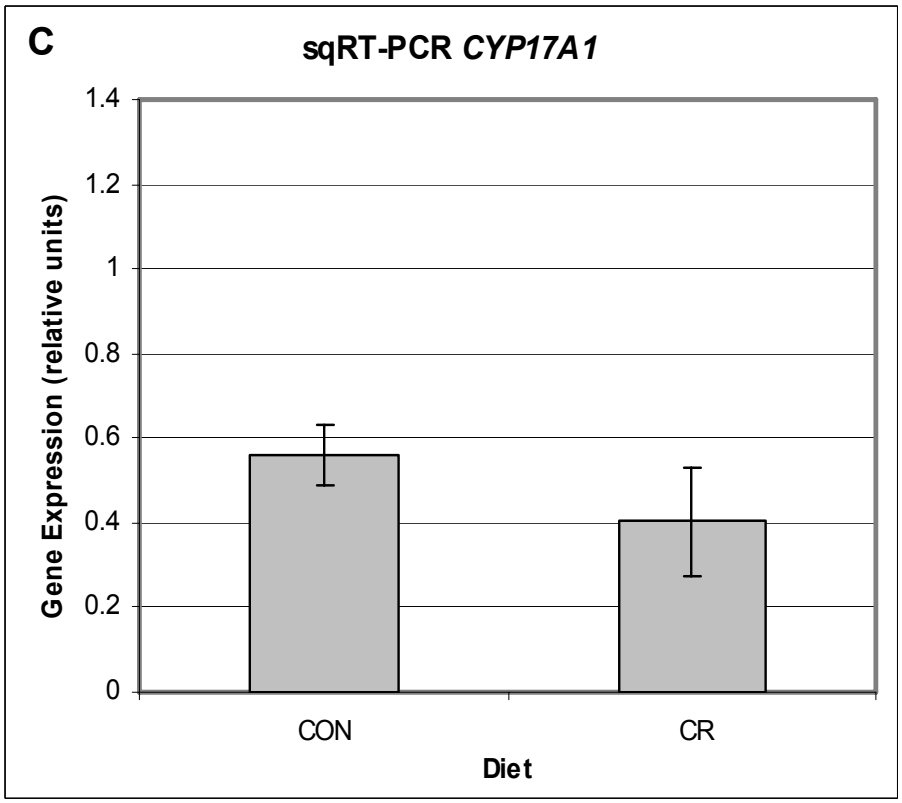
C
sqRT-PCR CYP17A1
Gene Expression (relative units)
1.4
1.2
1
0.8
0.6
0.4
0.2
0
CON
CR
Diet

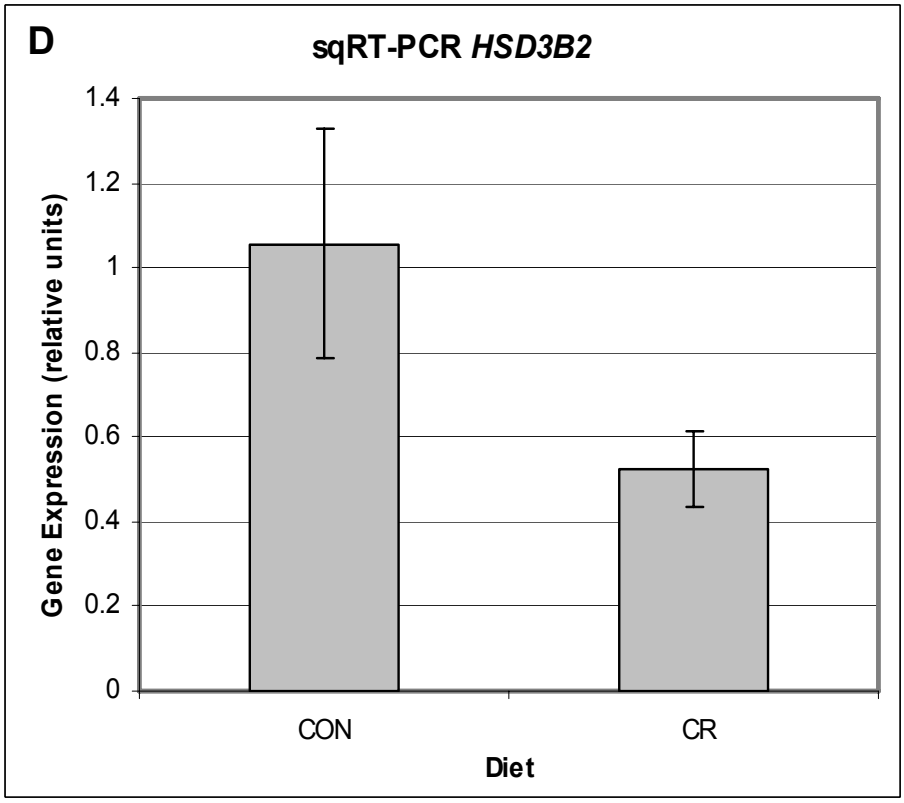
D
sqRT-PCR HSD3B2
Gene Expression (relative units)
1.4
1.2
1
0.8
0.6
0.4
0.2
0
CON
CR
Diet

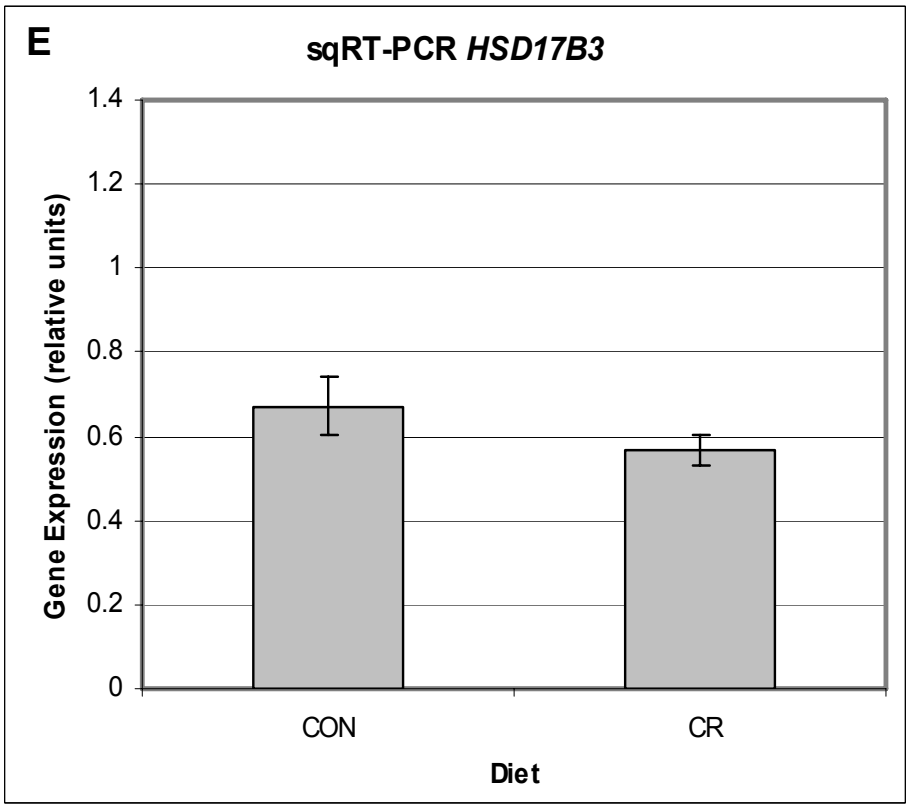
E
sqRT-PCR *HSD17B3*
Gene Expression (relative units)
1.4
1.2
1
0.8
0.6
0.4
0.2
0
CON
CR
Diet

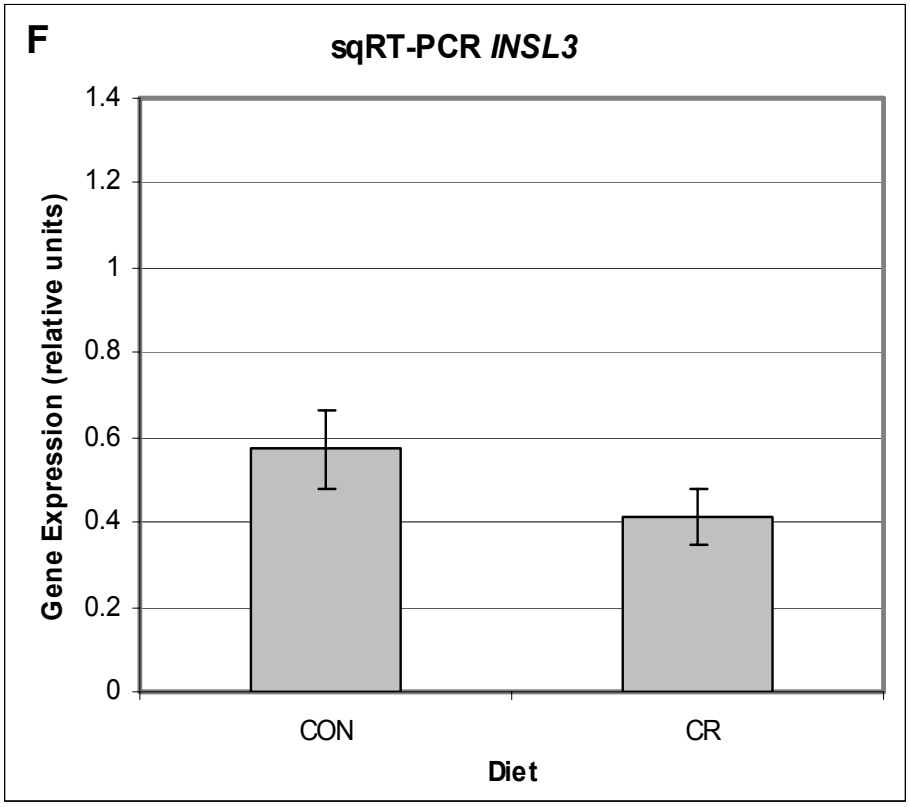
F
sqRT-PCR *INSL3*
Gene Expression (relative units)
1.4
1.2
1
0.8
0.6
0.4
0.2
0
CON
CR
Diet

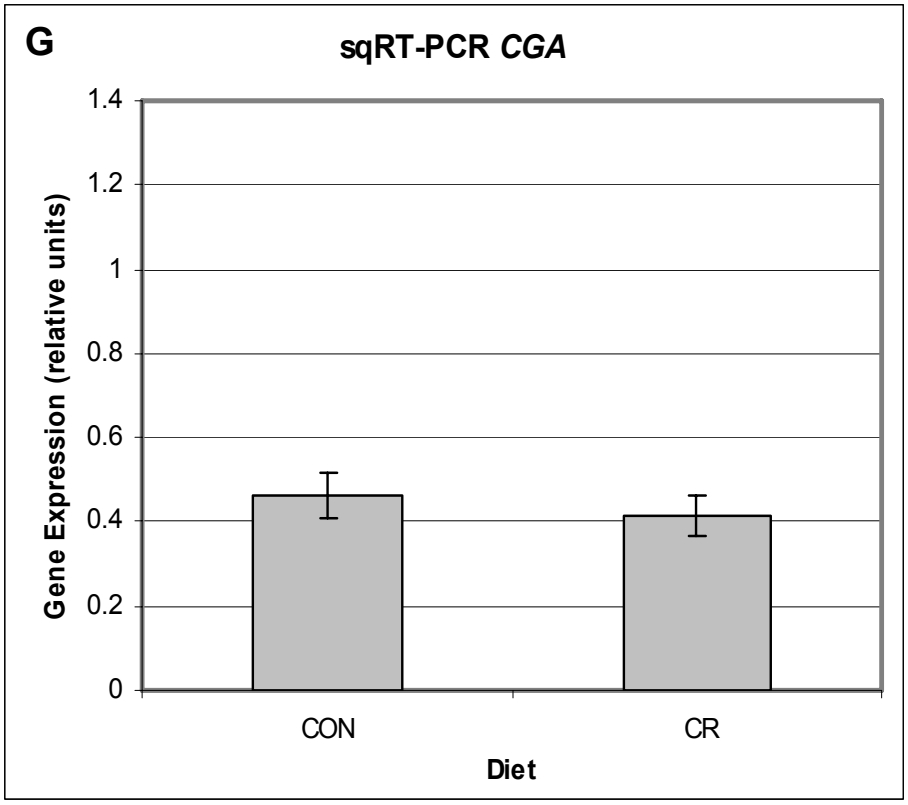
G
sqRT-PCR *CGA*
Gene Expression (relative units)
1.4
1.2
1
0.8
0.6
0.4
0.2
0
CON
CR
Diet

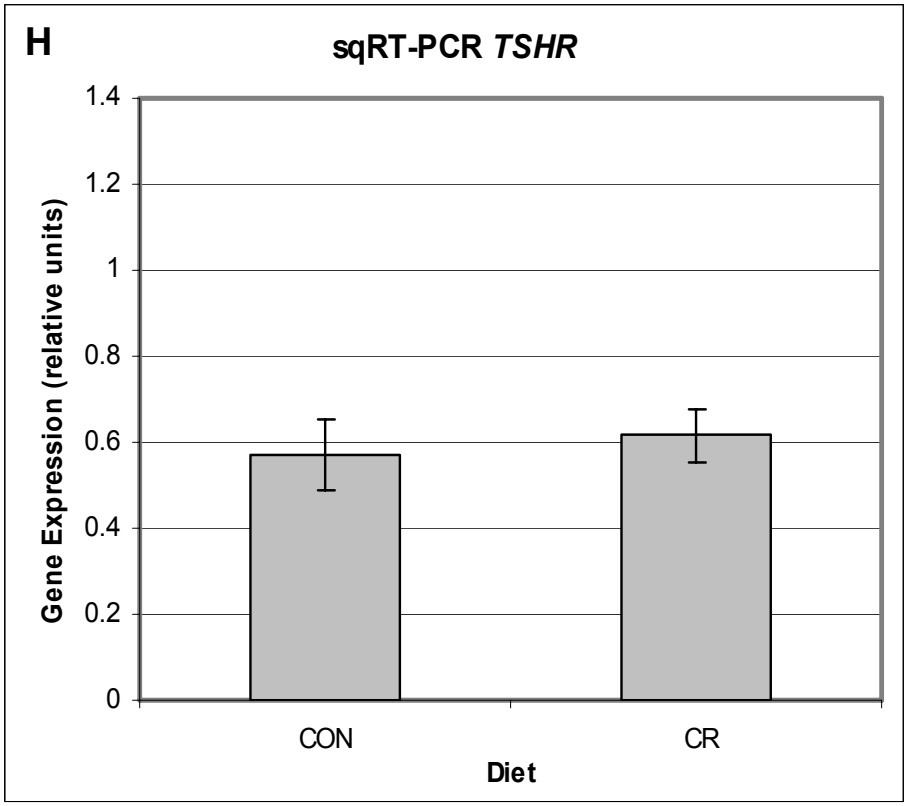
H
sqRT-PCR *TSHR*
Gene Expression (relative units)
1.4
1.2
1
0.8
0.6
0.4
0.2
0
CON
CR
Diet

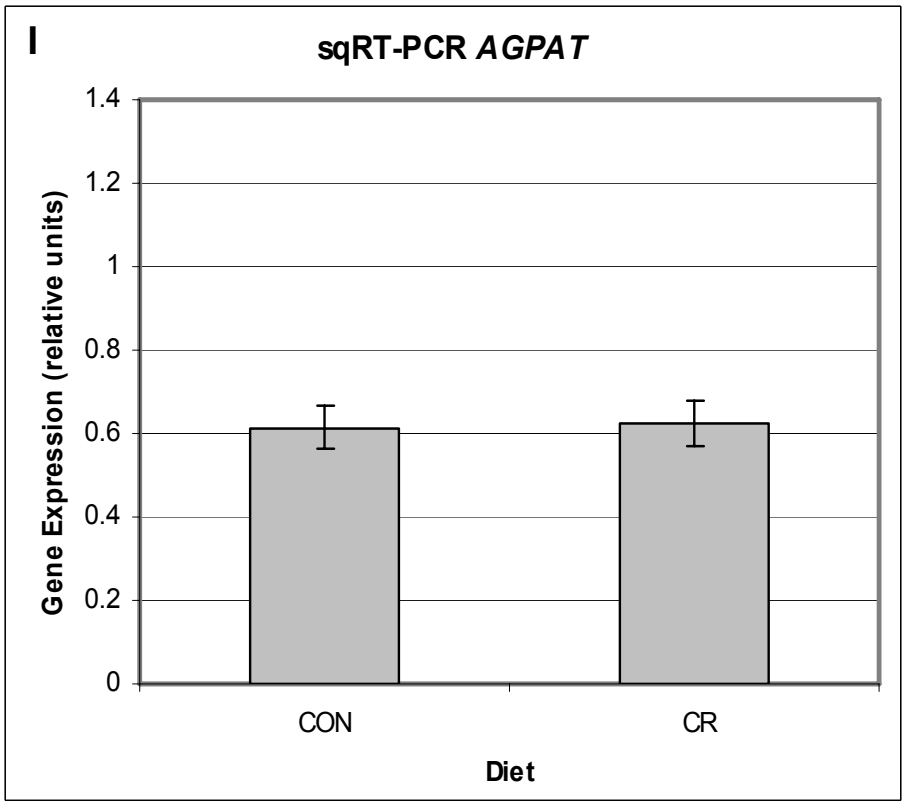
I
sqRT-PCR *AGPAT*
Gene Expression (relative units)
1.4
1.2
1
0.8
0.6
0.4
0.2
0
CON
CR
Diet

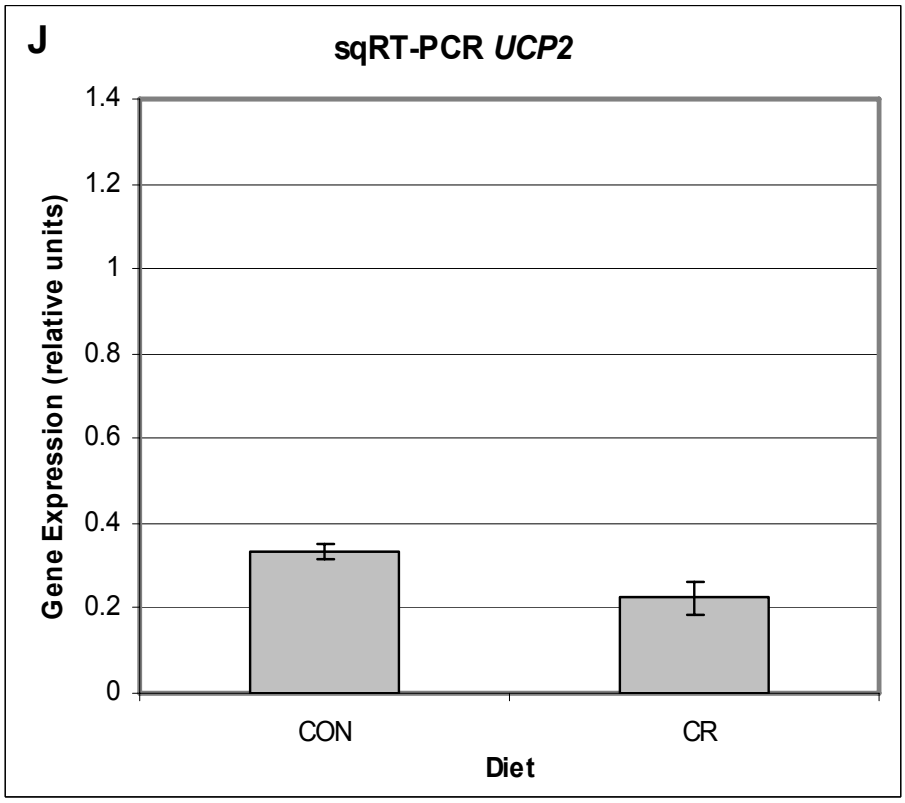
J
sqRT-PCR *UCP2*
Gene Expression (relative units)
1.4
1.2
1
0.8
0.6
0.4
0.2
0
CON
CR
Diet

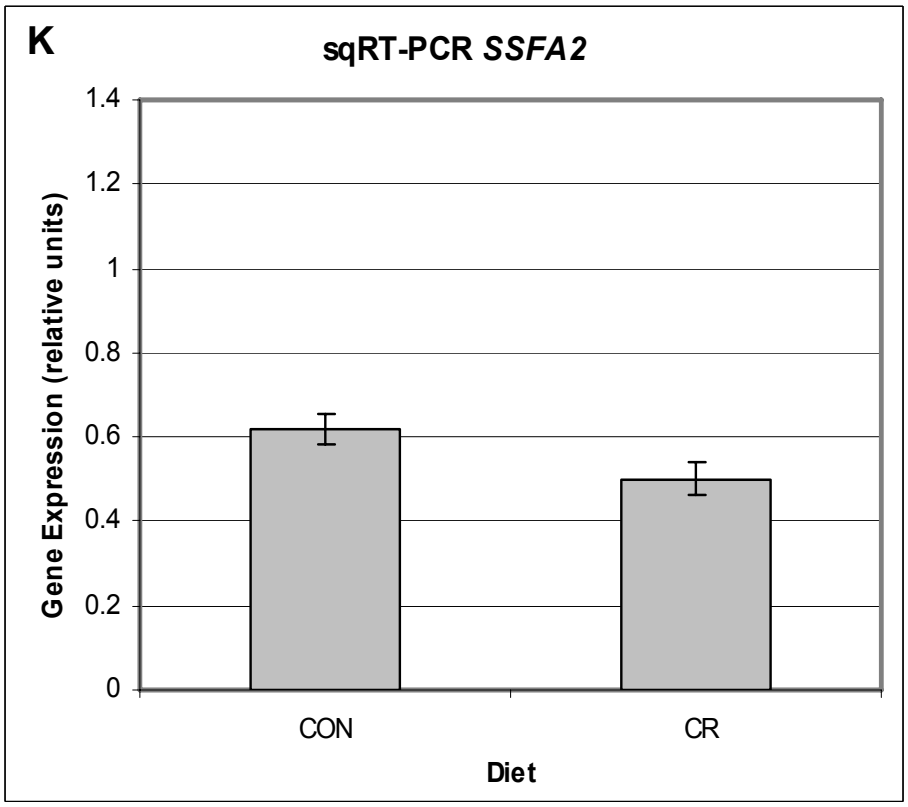
K
sqRT-PCR *SSFA2*
Gene Expression (relative units)
1.4
1.2
1
0.8
0.6
0.4
0.2
0
CON
CR
Diet

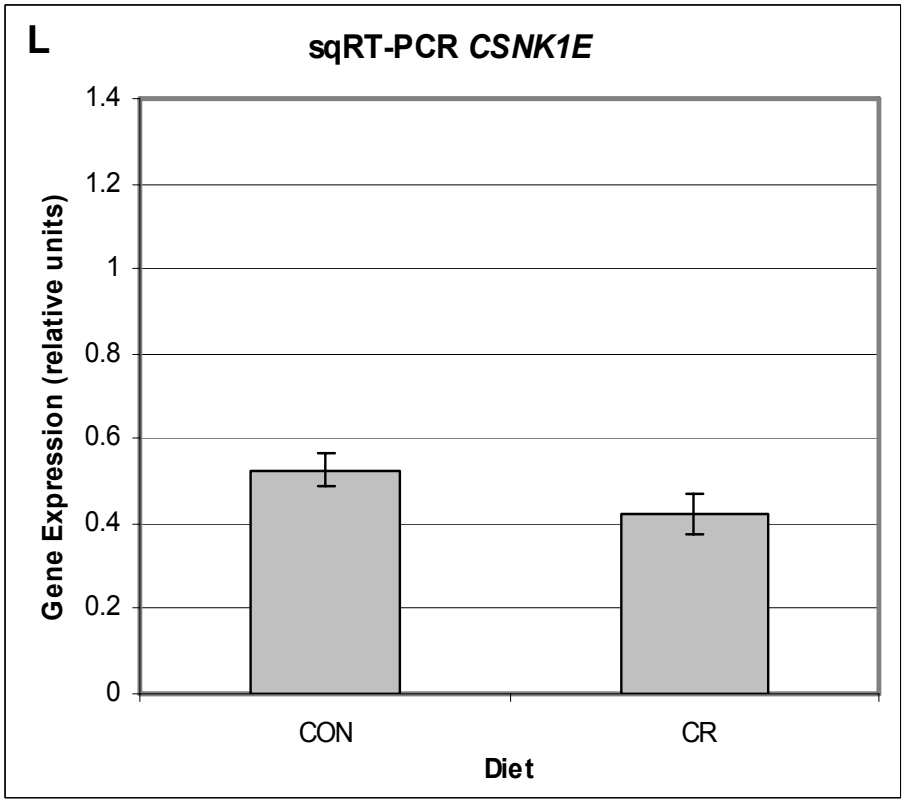
L
sqRT-PCR *CSNK1E*
Gene Expression (relative units)
1.4
1.2
1
0.8
0.6
0.4
0.2
0
CON
CR
Diet

Figures 4.3 A-C Taqman® Quantitative Real-Time PCR of Genes in the Rhesus Macaque Testis – Dietary Effect Each bar, along with SEM, represents mean, normalized fluorescence data for animals in experiment 1 (CON, n=4; CR, n=5). Statistical comparisons were made using Student's *t*-test ($P<0.05$). None of the transcripts were significantly different between treatments.

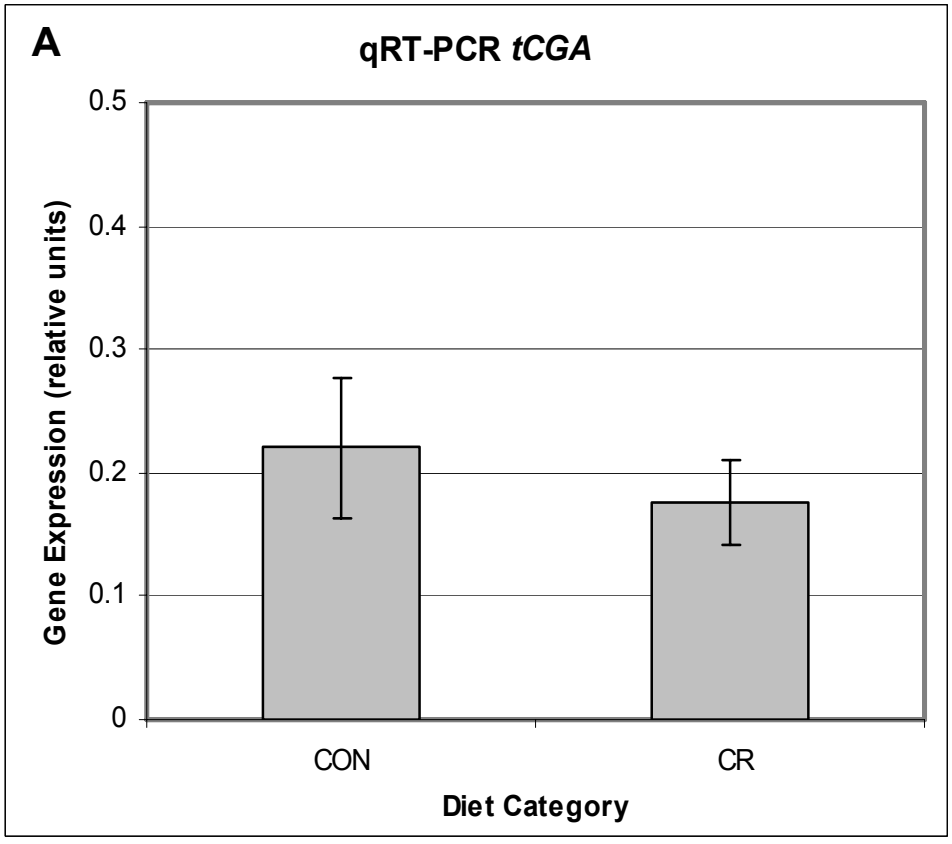

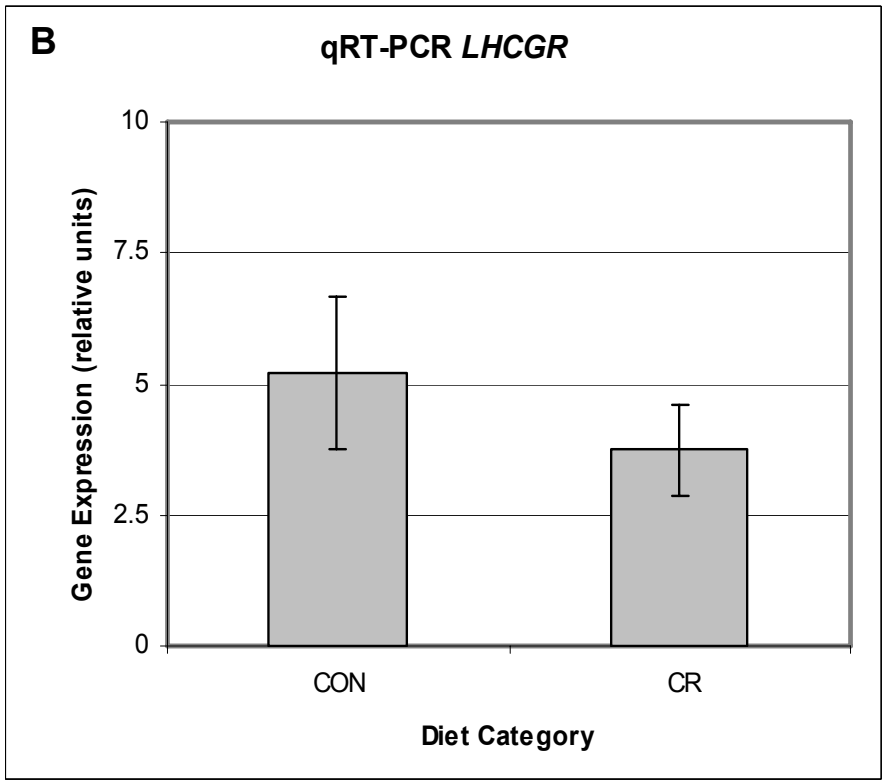
B
qRT-PCR *LHCGR*
Gene Expression (relative units)
10
7.5
5
2.5
0
CON
CR
Diet Category

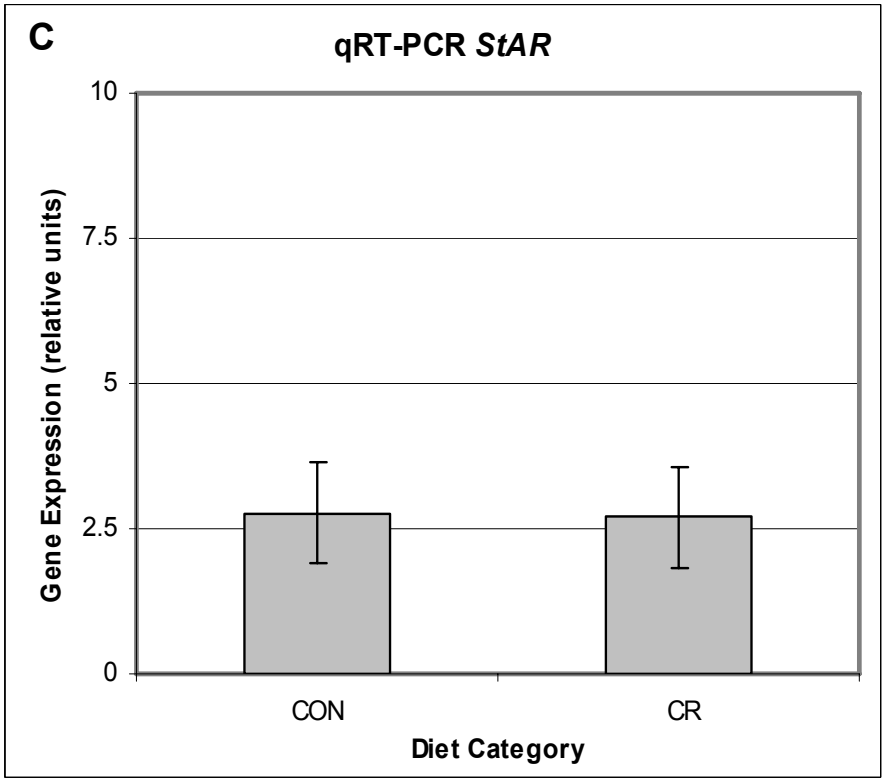
C
qRT-PCR *StAR*
Gene Expression (relative units)
10
7.5
5
2.5
0
CON
CR
Diet Category

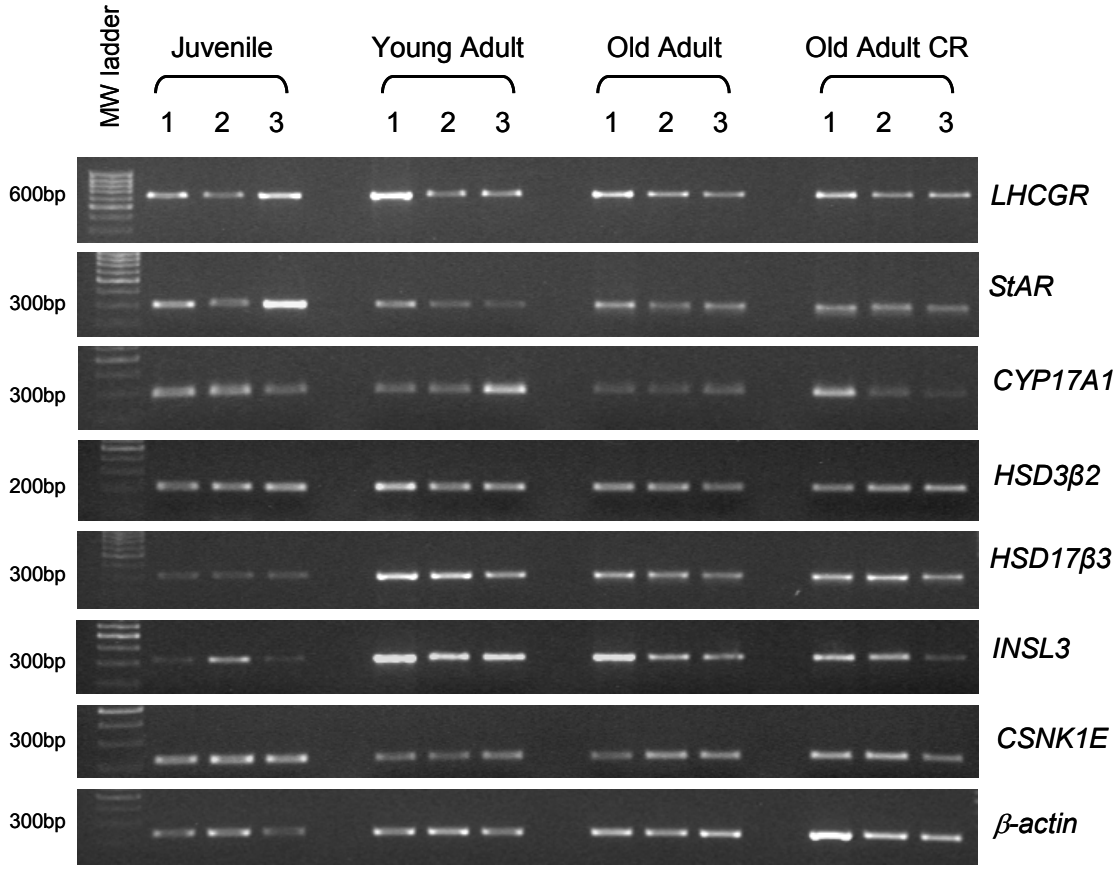

Figure 4.4 Genes in the Rhesus Macaque Testis – Age and Dietary Effect Representative sqRT-PCR results demonstrating expression of testicular genes across the treatment groups in experiment 2: Juvenile (1-2 years); Young Adult (5-7 years); Old Adult (24-30 years); and Old Adult CR (25-27 years). The housekeeping gene β-actin was used as a positive control and for normalizing images for analysis.

Figures 4.5 A-G sqRT-PCR Expression Levels of Genes in the Rhesus Macaque Testis – Age and Dietary Effect Each bar, along with SEM, represents mean, normalized fluorescence data from three animals in experiment 2. Statistical comparisons were made using one-way ANOVA and Tukey-Kramer post-hoc corrections (P<0.05).

Significant differences were observed in three of the transcripts:

1. HSD17β3 (Graph E) – YA expression was 3.13 (±0.39) fold greater than J
2. INSL3 (Graph F) – YA expression was 2.15 (±0.34) fold greater than J and 3.84 (±0.62) fold greater than OACR
3. CSNK1E (Graph G) – J expression was greater than all other groups with 2.85 (±0.63) fold-increase over YA, 2.93 (±0.65) fold-increase over OA and 3.86 (±0.86) fold-increase over OACR

The other transcripts were not significantly different between treatments.

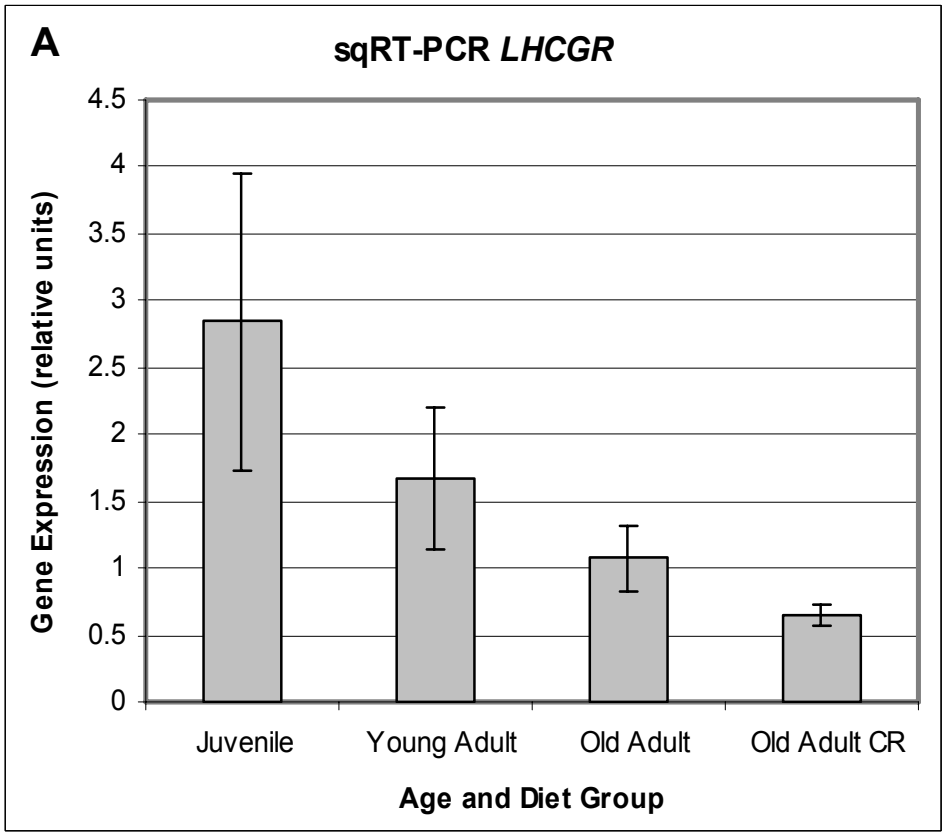

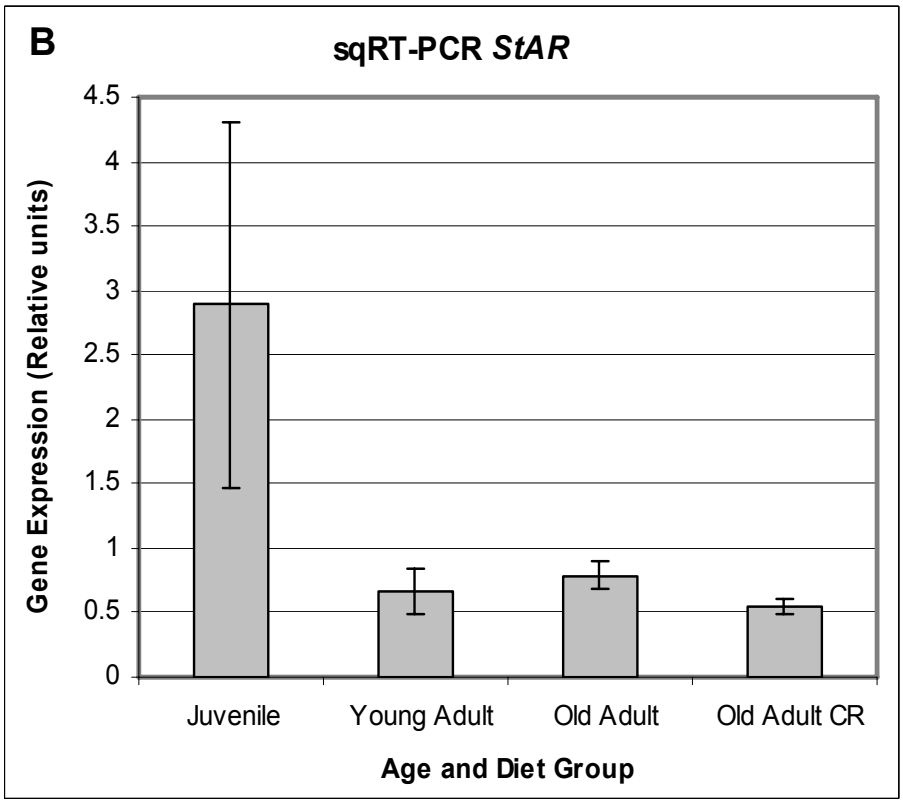
B
sqRT-PCR StAR
Gene Expression (Relative units)
4.5
4
3.5
3
2.5
2
1.5
1
0.5
0
Juvenile
Young Adult
Old Adult
Old Adult CR
Age and Diet Group

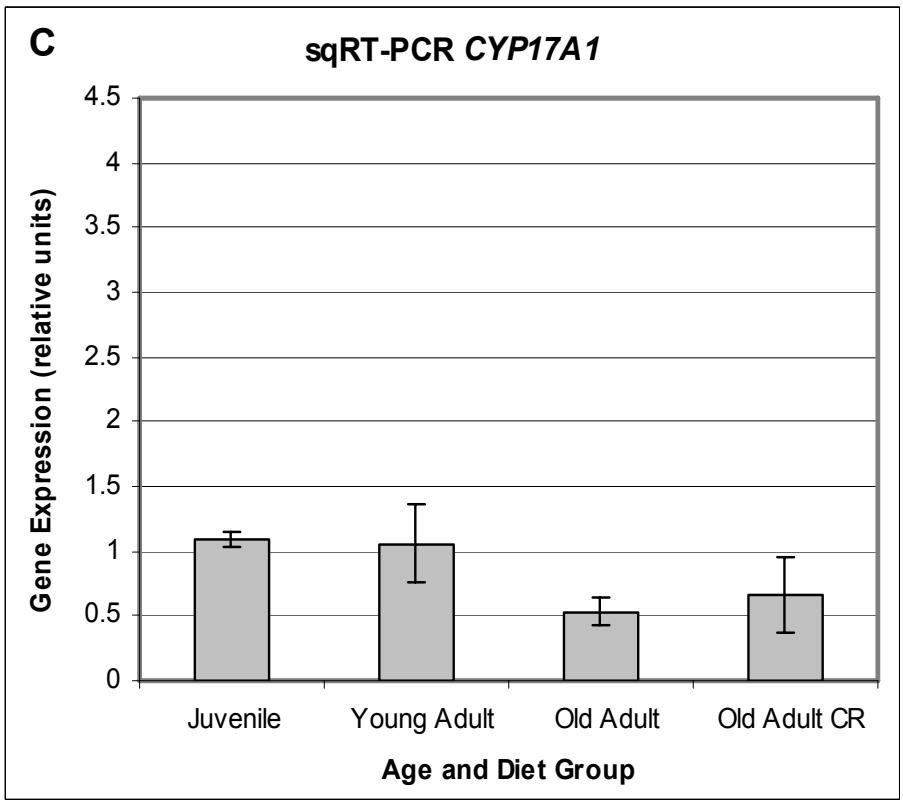
C
sqRT-PCR CYP17A1
Gene Expression (relative units)
4.5
4
3.5
3
2.5
2
1.5
1
0.5
0
Juvenile
Young Adult
Old Adult
Old Adult CR
Age and Diet Group

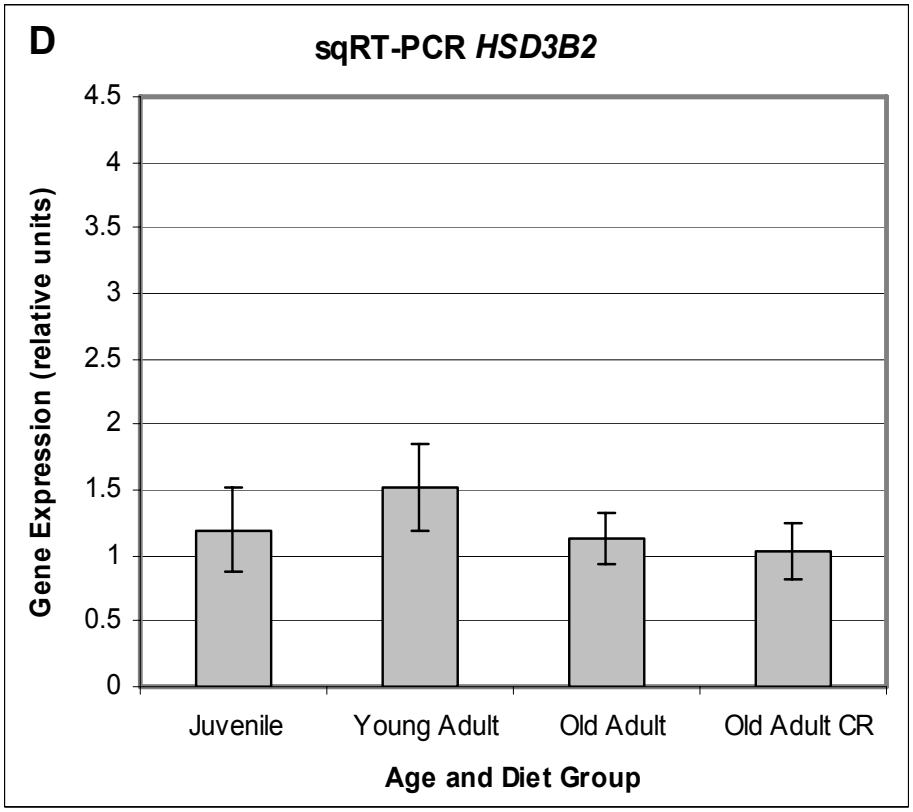
D
sqRT-PCR *HSD3B2*
Gene Expression (relative units)
4.5
4
3.5
3
2.5
2
1.5
1
0.5
0
Juvenile
Young Adult
Old Adult
Old Adult CR
Age and Diet Group

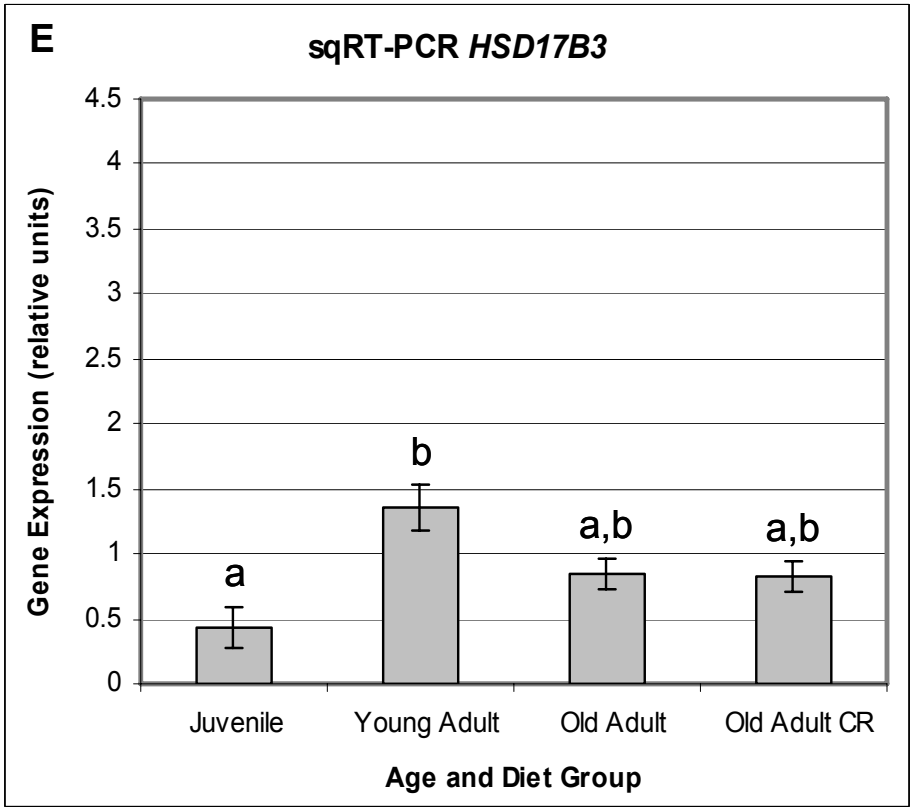
E
sqRT-PCR *HSD17B3*
Gene Expression (relative units)
4.5
4
3.5
3
2.5
2
1.5
1
0.5
0
a
b
a,b
a,b
Juvenile
Young Adult
Old Adult
Old Adult CR
Age and Diet Group

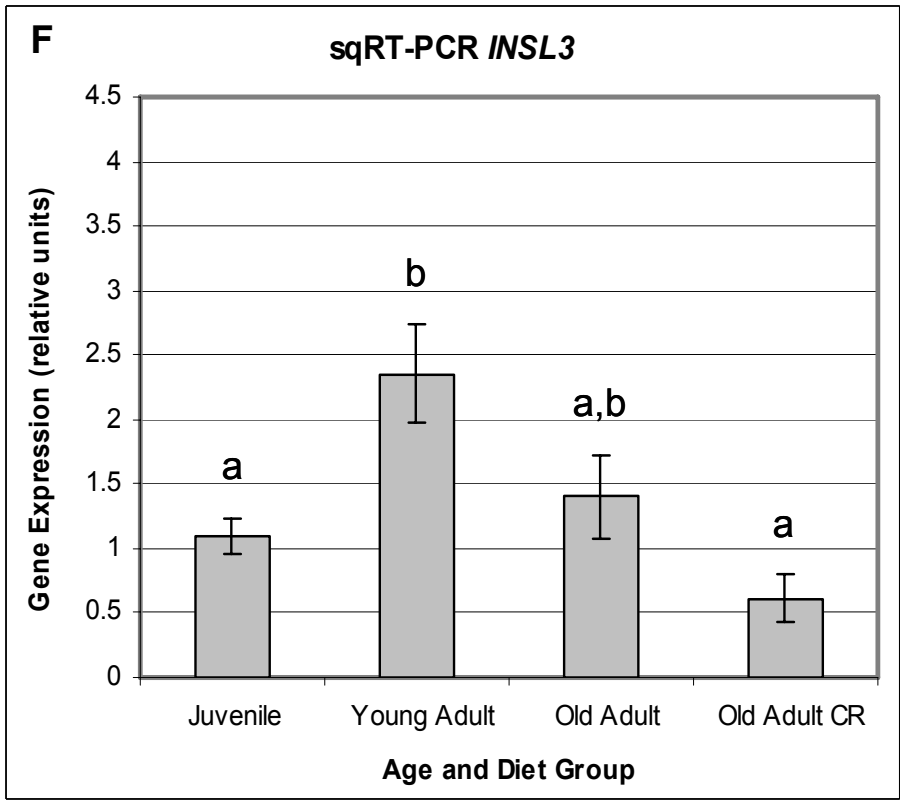
F
sqRT-PCR *INSL3*
Gene Expression (relative units)
4.5
4
3.5
3
2.5
2
1.5
1
0.5
0
a
b
a,b
a
Juvenile
Young Adult
Old Adult
Old Adult CR
Age and Diet Group

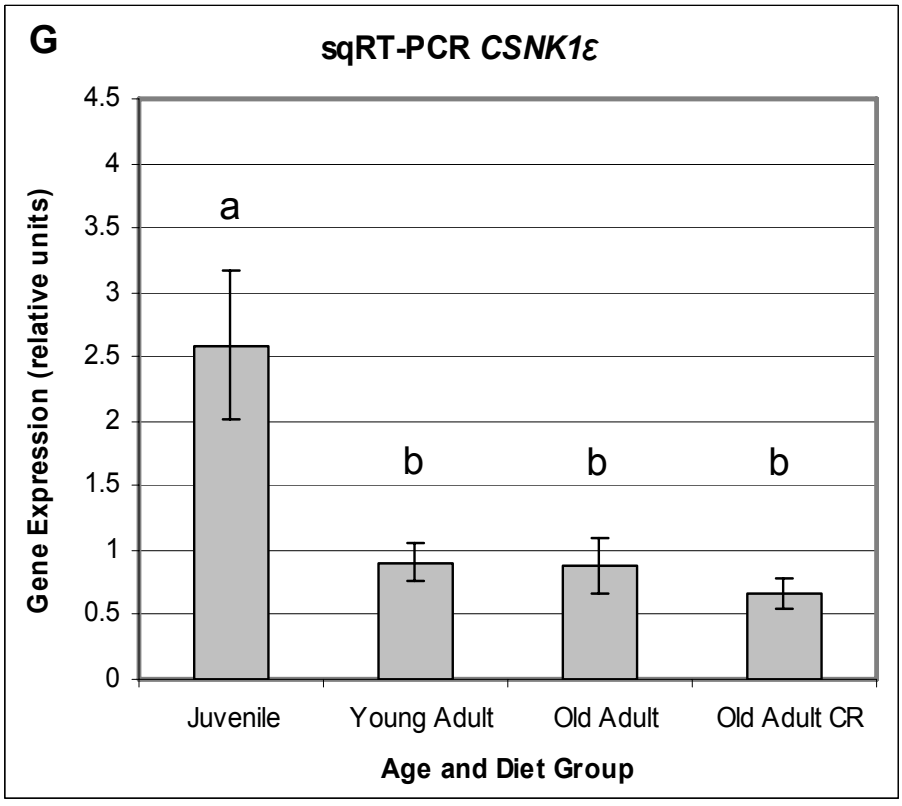
G
sqRT-PCR *CSNK1ε*
Gene Expression (relative units)
4.5
4
3.5
3
2.5
2
1.5
1
0.5
0
a
b
b
b
Juvenile
Young Adult
Old Adult
Old Adult CR
Age and Diet Group

Figures 4.6 A-C Taqman® Quantitative Real-Time PCR in the Rhesus Macaque Testis – Age and Dietary Effect Each bar, along with SEM, represents mean, normalized fluorescence data for three animals in experiment 2. Statistical comparisons were made using one-way ANOVA and Tukey-Kramer post-hoc corrections (P<0.05).

Results demonstrated significant differential expression for *tCGA* with the OA group 35.11 (±10.45) fold higher than J animals and 4.54 (±1.66) fold higher than OACR subjects.

LHCGR and *StAR* expression were not significantly different between treatments.

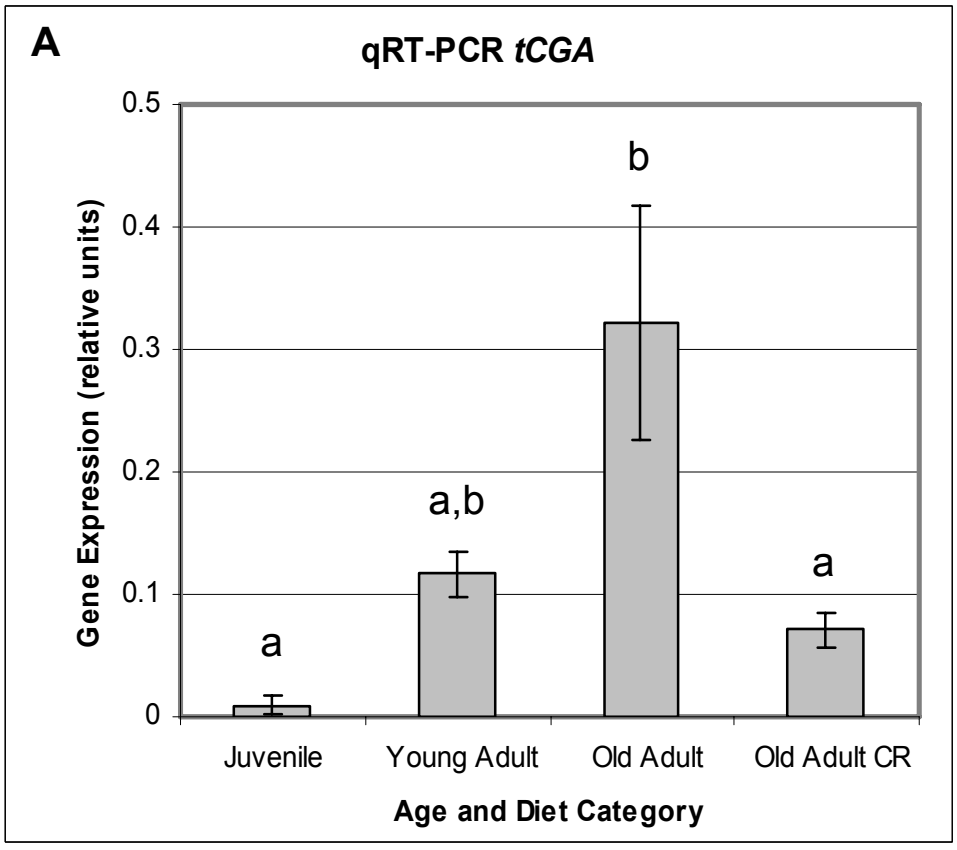

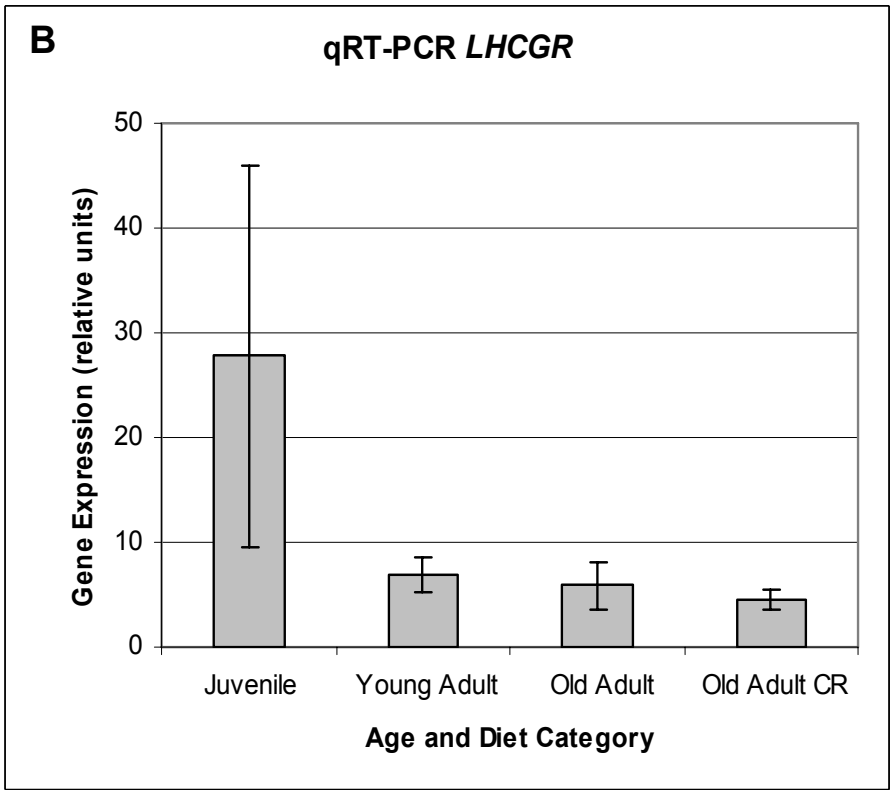
B
qRT-PCR *LHCGR*
Gene Expression (relative units)
50
40
30
20
10
0
Juvenile
Young Adult
Old Adult
Old Adult CR
Age and Diet Category

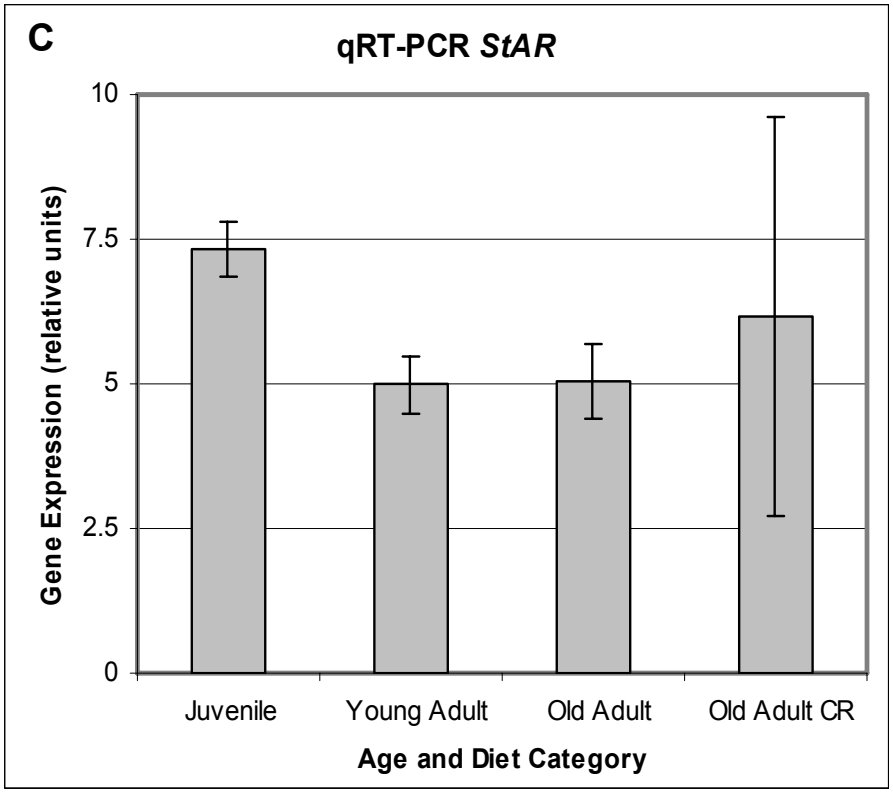
C
qRT-PCR *StAR*
Gene Expression (relative units)
10
7.5
5
2.5
0
Juvenile
Young Adult
Old Adult
Old Adult CR
Age and Diet Category

Table 4.5 Testis Gene sqRT-PCR Amplicon Sequences Experimentally derived PCR amplicon sequences as determined by DNA sequencing are listed under each of the genes. Following each are the results of a BLAST search in the NCBI database to determine a best fit sequence.

Luteinizing hormone/choriogonadotropin receptor (LHCGR)
tLHCGR-Forward primer AACGCTTTGTATTGATATAGGGCATCAATACCCAAGTTGGGAGCATTTAGAAATCTTTATAGAAATTTTACCACAGTAATTTTGTTTGATGAAT CTATTAAAAAACCGAGGAGGTATTTAGAGAGCCCGGGG Best fit (Same as that used for primer design): gi|109102901|ref|XM_001114090.1| PREDICTED: Macaca mulatta luteinizing hormone/choriogonadotropin receptor (LHCGR), mRNA tLHCGR-Reverse primer GAATGGCACGCTTATGTTTCCTAAGCAAATAGGCTGAAATGTGCTTTTAGATGTTTACCTTAAATTATAAATAAGTAGAATCCAGATAGGGGA TAGATAAAAGTCTCTATAGTATTACAAATAGAACTTTCTGTGGTGGTGAAAATATTTGGTGT Best fit (Same as that used for primer design): gi|109102901|ref|XM_001114090.1| PREDICTED: Macaca mulatta luteinizing hormone/choriogonadotropin receptor (LHCGR), mRNA
Steroidogenic acute regulatory protein (StAR)
tStAR-Forward primer AGAGTGGTACTACCGAATATAGTCCAGCTTTCTCTATGGAAAAAGACAAAACTAATTAGTAGACAGGTTTCCCTATTGCTTCCATAGGCACC CGTCAGAATAAAGAATCATAATTCACACAAAACATCAGTCTGTATGTTTTAATATTGTACTGTTAAAAAAAAATCTATGCGGCTGGGCACGGT GGCTCACGCCTGTTATCCCAGCATTTTGGGAGGCCAAGGCGGGTGGATCACAAGGTCAGGAGATCGAGACCATCCTGGCCAATAATA Best fit (Same as that used for primer design): gi|109086163|ref|XM_001090472.1| PREDICTED: Macaca mulatta similar to steroidogenic acute regulator isoform 1, transcript variant 3, mRNA tStAR-Reverse primer CTACTGTGAGACCCGCCTTGGCCTCCCAAATGCTGGGATAACAGGCGTGAGCCACCGTGCCCAGCCGCATAGATTTTTTTTTAACAGTACA ATATTAAAACATACAGACTGATGTTTTGTGTGAATTATGATTTTTTTCTTTGTACTGTTAAAAAAAAATTTATGCGGCTGGGCCGGTGGCTTTG CCCCAAAACAACAATATTTTAAGAGAGGGGGGGGGGGGGGGGGGGGAAACTCACCA Best fit (Same as that used for primer design): gi|109086163|ref|XM_001090472.1| PREDICTED: Macaca mulatta similar to steroidogenic acute regulator isoform 1, transcript variant 3, mRNA

Glycoprotein hormones, alpha polypeptide (CGA, for LH, FSH, TSH, hCG)

tCGA-Forward primer
GCGCATGACATCTCCCAGCAGTGCAATATCTGATGCTCAGTAGTCGTGTAGTCAGTCAGGTAGTCTATGCATCCTGCTGACTCTAATGCAGT
CAGACGCAATCAGTCTGCACGCTGCAGATGTGCTAGCTGATCGTAGCAGCAGTACTCCGAGTC

Did not return any macaque sequences in the list of Best fit

tCGA-Reverse primer
GCTGCGTGCTTCGTGTGTATAACAGTACTGCAGTGGCACTGCGTGTGGTTCTCCACTCTGACACTCCCCATTACCATGAACCTGGTCAATG
ATTTAGCTACACAGCAAGTGGACTCTGAGGTGACGTTTTTTTTTACCGACATCAACTTCTTTTGGATTACTTGAAGGGGGAACCCGTACAGA
AAAGGCGGGGCTTACACTGAGAATTGGGCCACCCCCGGTGGAAAAAAGTTTTTGTTTTCCTTTGATTGGGGGGGAGGGGGAGGTTGGATT
AACCCAAAAAAAA

Best fit (Same as that used for primer design): gi|109071971|ref|XM_001090917.1| PREDICTED: Macaca mulatta similar to Glycoprotein hormones alpha chain precursor (Anterior pituitary glycoprotein hormones common alpha subunit) (Follitropin alpha chain) (Follicle-stimulating hormone alpha chain) (FSH-alpha) (Lutropin alpha chain) (Luteinizing hormone alpha chain) (LH-alpha), mRNA

Insulin-like 3 (INSL3): We had to use a cloned sequence for primer design

tINSL3-Forward primer
GGAAGAAATCCTAGAGTGGACTGAGGCCCTAGGGTCTGGTCTGGTGAGCTCCTGAGGCCACACAGAACCATAAAGAGTGGTGTCTGCAAG
CTTTTGATTACCTCCTGGGATGGGGTGGTCATTAAATATCTCCCCAGAATAATGCCCCTGCAGCCTGTGAAGTCACTGCAGAATAATTACAC
CCCCTCCCTGGGTTGGTGGATCCCCCCTTCACAGATGCTGGCTCTAAAATCAAATGTGGTTGTTCCATACGCCCCCCGCACCTCCGATCCC
TGCATGAAAAAAAGGTGGAAAAGGGCCCCTAGGACACTCTGACCCTAA

Did not return any macaque sequences in the list of Best fit, but did return these two:
gi|114676076|ref|XM_001173682.1| PREDICTED: Pan troglodytes similar to Insulin-like 3 precursor (Leydig insulin-like peptide) (Ley-I-L) (Relaxin-like factor), mRNA
gi|31419621|gb|BC053345.1| Homo sapiens insulin-like 3 (Leydig cell), mRNA (cDNA clone IMAGE:5172221), partial cds

tINSL3-Reverse primer
AGAGAGGCAGAGGAGTAGAATTTGGCTCTCAGTGTCCAGCATCTGTGAAAGTGGGGATCCTCCAAGCCAGGGCTAGGGTGTGATTTATTCT
GCAGTTGACTCCACAGGCTGCAGGTGGCATTGGTCTGGGGTAGATAGTGAG

Did not return any macaque sequence in the list of Best fit, but did return these two:
gi|114676076|ref|XM_001173682.1| PREDICTED: Pan troglodytes similar to Insulin-like 3 precursor (Relaxin-like factor), mRNA
gi|31419621|gb|BC053345.1| Homo sapiens insulin-like 3 (Leydig cell), mRNA (cDNA clone IMAGE:5172221), partial cds

Hydroxysteroid (17-beta) dehydrogenase 3 (HSD17β3)
tHSD17B3-Forward primer GGGTCTCTCCGGTGCTGACCCCATATGCCGTCTCGACTGCAATGACAAAGTATCTAAATACCAATGTGATAACCAAGACTGCTGATGAGTTT GTCCAAGAGTCACTGAATTATGTCACAATCGGAGGTGAAACCTGTGGCTGCCTTGCCCATGAAATCTTGGCGGGCTTTCTGAGCCTGATCC CGGTGGGGGCCTTCTACGGCGGCGCCTTCCAAAGGCCGGACCTGAATGTTATGACCTGAACCTGAAACTCAAGTCAGGGGAAAAGAAAAA AAAAA Best fit (Same as that used for primer design): gi|109112386|ref|XM_001105829.1| PREDICTED: Macaca mulatta estradiol 17 beta-dehydrogenase 3, transcript variant 2 (HSD17B3), mRNA tHSD17B3-Reverse primer ATAGCTATGCTGTGTAGGAGCAGCCTTTGGAGGCGCCGCTGTAGAAGGCCCAGGCCGGGATCAGGCTCAAAAGCCCGCCAAGATTTCATG GGCAAGGCAGCCACAGGTTTCACCTCCGATTGTGACATAATTCAGTGACTCTTGGACAAACTCATCAGCAGTCTTGGTTATCACATTGGTAT TTAGATACTTTGTCATTGCAGGCGGTCCCTTTATGGGCTTGTGACGAATGGGGGGACCCAAATGACCTCACTCCGGGGAAGGAAAAAAAAA AAAA Best fit (Same as that used for primer design): gi|109112386|ref|XM_001105829.1| PREDICTED: Macaca mulatta estradiol 17 beta-dehydrogenase 3, transcript variant 2 (HSD17B3), mRNA
Sperm specific antigen 2 (SSFA2)
tSSFA2-Forward primer ATGTTATATGTGTTCCCTCTGGGTCCAGCTCTGTGCGGAATCTCCGGAATGGAAGTTCCGGGGGAGTTGATGCAGCTGAAGAAGCCCCAC AAGTTGTAGGACCTAAATCCGAAGCGGAAGAAAGGGAAGGAAAACCCCCCTTTGCTGACCTCCCATAC Best fit (Same as that used for primer design): gi|109100269|ref|XM_001101290.1| PREDICTED: Macaca mulatta similar to sperm specific antigen 2, mRNA tSSFA2-Reverse primer Unknown - primer did not anneal during sequencing. Poor sequencing may have been the result of impure PCR mixture or amplicons forming secondary structures due to sticky GC regions.
Uncoupling protein 2 (UCP2)
tUCP2-Forward primer AACAACGTACGCGTTGGTCCTGCTCGCCCGACGCTCCCTCCTCCAGCAGATACACACAGCCGCACGCACTCTCGTGTTCTCCCTGAGGCT TGGACACATAGTATGACCATTAGGTGTTTCGTCTCCCACCCATTTTCTATGGAAAACCAAGGGGATCAGGCCATGATAGCCACTGGCAGCTT TGAAGAACGGGACACCTTTAGAGAAGCTTGATCTTGGAGGCCTCACCGTGAGACCTTACAAAGCCAGATTCCGGCAGAGTTCCTCTATCTC AGCCTAGACATCCAGAAGATAAGCGTGTGGATTCCGGCAGAGTTCCTCTATCTGAGGGTGACGTTCGGGGGGTTCG

Best fit (Same as that used for primer design): gi|109107894|ref|XM_001115559.1| PREDICTED: Macaca mulatta uncoupling protein 2, mRNA

tUCP2-Reverse primer
TGAATTTTTCTTTAAGGGGGGGTGAAAAGGTATTGTGGGTGTAACAGGGGGGGGGGAGGGAAAGGAAAAGAAGAAAGGTGGAGGGGCGC
GCGGGAGGGGAGAAAGAAGAAACAGGCTTAAAAGAAGCGGGG

Did not return any macaque sequences in the list of 4 Best fit.

Thyroid stimulating hormone receptor (TSHR)

tTSHR-Forward primer
Unknown - primer did not anneal during sequencing. Poor sequencing may have been the result of impure PCR mixture or amplicons forming secondary structures due to sticky GC regions.

tTSHR-Reverse primer
CTTTACAATCTGGGATCAGTGTAACACTCTCCTAATCTGAAAACAACAAACAGCTTTTATTTCATGGTGTGTGAATTTAAGGGTCAGCCCGCG
GGGGGAAAGAATATTTAGGGCCCCTAAGGAGGTGGA

Best fit (Same as that used for primer design): gi|109084461|ref|XM_001104839.1| PREDICTED: Macaca mulatta thyroid stimulating hormone receptor, transcript variant 2 (TSHR), mRNA

1-acylglycerol-3-phosphate O-acyltransferase 3 (AGPAT3)

tAGPAT-Forward primer
TAGCTTCCGACTATTACCCCGTCCAACAGTGTATTATATGGATGCGGTCTCCCACCGGCAACCACCGGTTTCAGGAAACAGGCCTTCGAAG
AGTAAGTTAGCAGCCCTCACTCCAACAAGCTTCTAAAGACCAAAAATACCTCTCTATCCTCCACTACATAAAGCTTGTGAGTAACAAAACTTG
TAAAAATGAAGCGTACAAAAGGAAAATCCATATAATACATTTGTTCGTGTATACGATGGGTCCTTTTTTATGGCCAACAGTCAGCAAA

Best fit (Same as that used for primer design): gi|109065161|ref|XM_001104367.1| PREDICTED: Macaca mulatta 1-acylglycerol-3-phosphate O-acyltransferase 3 (AGPAT3), mRNA

tAGPAT-Reverse primer
ACATTGCGCTTGGGCGGCGCACACCTGCCTGTGTACACAGGTCCTCGCACAGCACGGCAAACGCAGCCAGGCCTTCGGGACACAGGCCT
TCGAAGAGTAAGTTAGCAGCCCTCACCCCAACAAGCTTCTAAAGACCAAAAATACCTCTATCCTCCACTACATAAAGCTTGTGAGTAGCAAA
ACTTGTAAAAATGAAGCGTACAAAAGGAAACATCCATATAATACATTTGCACCCTGTATACAATGGGTCCCTTTGAAACTGGCAAACAGTCAG
CA

Best fit (Same as that used for primer design): gi|109065161|ref|XM_001104367.1| PREDICTED: Macaca mulatta 1-acylglycerol-3-phosphate O-acyltransferase 3 (AGPAT3), mRNA
Casein kinase 1, epsilon (CSNK1E)
tCSNK1E-Forward primer TTTGCCCCATTGAGGTCCTCTGCAAGGCTATCCCTCCGAATTCTCAACATACCTCAACTTCTGCCGCTCCCTGCGGTTTGACGACAAGCCC GACTACTCTTACCTACGTCAGCTCTTCCGCAACCTCTTCCACCGGCAGGGCTTCTCCTATGACTACGTCTTCGACTGGAACATGCTGAAATT CGGAAAAGCCGCCGACCGGGGGGGGGGGAGGAGGAGAGGAATTTTATTATTATATATTACTCACATTCTTTTTTTTCTTTTTTACGTTA Best fit (Same as that used for primer design): ref|XM_001093672.1| PREDICTED: Macaca mulatta casein kinase 1 epsilon (CSNK1E), mRNA tCSNK1E-Reverse primer Unknown - primer did not anneal during sequencing. Poor sequencing may have been the result of impure PCR mixture or amplicons forming secondary structures due to sticky GC regions.
Hydroxysteroid (3-beta) dehydrogenase 2 (HSD3β2)
tHSD3B2-Forward primer GCGTACTTCTCTTTAGAAGGCTCAGCGAGATCTGGCATATAAGCCGCTCTACAGCTGGGAGGAAGCCAAGCAGAAAACTGTGGAGTGGGT TGGTTCCCTTGTGGACCGGCACAAGGAGACCCTGAAGTCCAAAACTCAGTGATTTAAGGATGACAGAGATGTGCATGTGGGAAA Best fit (Same as that used for primer design): ref|XM_001113717.1| PREDICTED: Macaca mulatta hydroxy-delta-5-steroid dehydrogenase, 3 beta- and steroid delta-isomerase 2, transcript variant 1 (HSD3B2), mRNA tHSD3B2-Reverse primer CCGTCTCCGTCTTGGACTTCGGGTCTCCTTGTGCCGGTCCACAAGGGAACCAACCCACTCCACAGTTTTCTGGTTGGGGGTTCCTCCCAG CTGTAGAGCGGCTTATATGCCAGATCTTGATGAAACTTCGTATAGAAAC Best fit (Same as that used for primer design): ref|XM_001113717.1| PREDICTED: Macaca mulatta hydroxy-delta-5-steroid dehydrogenase, 3 beta- and steroid delta-isomerase 2, transcript variant 1 (HSD3B2), mRNA
Cytochrome P450c_{17} (CYP17A1) These primers were designed previously in Dr. Urbanski's lab using the human sequence. They have been validated in the rhesus adrenal.
tCYP17A1-Forward primer GTCTGCGTTTCTTGATCAGCGGGGACCCAGCTTATCTCACCATCATTAAGCTACTTGCCCTTCGGAGCAGGACCTCGCTCCTGTATAGGTG AGATCCTGGCCCGCCAGGAGCTCTTCCTCATCATGGCCTGGCTGCTGCAGAGGTTCGACCTGGAGGTGCCAGATGATGGGCAGCTGCCC TCCCTGGAAGGCAACCCAAAGGTGGTCTTTCTGATCGACTCTTTCAAAGTGAAGATCAAGGTGCGCCAGGCCTGGAG

Best fit: ref|NM_001040232.1| Macaca mulatta cytochrome P450c17 (CYP17A1), mRNA

tCYP17A1-Reverse primer
Unknown - primer did not anneal during sequencing. Poor sequencing may have been the result of impure PCR mixture or amplicons forming secondary structures due to sticky GC regions.

Cytochrome P450scc (CYP11A1) These primers were designed previously in Dr. Urbanski's lab using the human sequence. They have been validated in the rhesus adrenal. As a positive control we amplified adrenal tissue and submitted the PCR samples for sequencing along with our testis PCR. We were unable to get successful single PCR bands for CYP11A1 in the testis of all our animals so no sqRT-PCR determinations could be made. In trying to determine if the problem was temperature related or due to poor probe design we cut three single bands out of the gel and sequenced them along with the adrenal control. The results show that we were successfully targeting the proper cDNA. With more time and adjustments we may have been able to get better gels and finish analysis.

aCYP11A1-Forward primer
AATTTCGTGCTCGCTGTGAGAGGTTTTGACCCAACCCGATGGCTGAGCAAAGACAAGAACATTACCTACTTCCGGAACTTGGGCTTTGGCT
GGGGTGTGCGGCAGTGTCTGGGACGGCGGATCGCCGAGCTAGAGATGACCATCTTCCTCATCAATATGCTGGAGAACTTCAGAGTTGAAA
TCCAACATCTCAGCGATGTGGGCACCACATTCAACCTCATCCTGATGCCTGAAAAGCCCATCTCCTTCACCTTCTGGCCCTTTAACCAGGAA
GCAACCCAGCAGTGATCAGAGAGGATGG

Best fit: ref|XM_001096506.1| PREDICTED: Macaca mulatta cytochrome P450, subfamily XIA, mRNA

aCYP11A1-Reverse primer
Unknown - primer did not anneal during sequencing. Poor sequencing may have been the result of impure PCR mixture or amplicons forming secondary structures due to sticky GC regions.

tCYP11A1-F
TGATTCTCTTCGACCGGAATTTTGACCCAACCCGATGGCTGAGCAAAGACAAGAACATTACCTACTTCCGGAACTTGGGCTTTGGCTGGGG
TGTGCGGCAGTGTCTGGGACGGCGGATCGCCGAGCTAGAGATGACCATCTTCCTCATCAATATGCTGGAGAACTTCAGAGGTGAAATCCT
CCCTCCC

Best fit: ref|XM_001096506.1| PREDICTED: Macaca mulatta cytochrome P450, subfamily XIA (LOC708065), mRNA

tCYP11A1-Reverse primer
GGCTTCTCCTAGGGCAGAAGGTGAAGGAGATGGGCTTTTCAGGCATCAGGATGAGGTTGAATGTGGTGCCCACATCGCTGAGATGTTGGA
TTTCAACTCTGAAGTTCTCCCCCATATTGATGAGGAAGATGGTCATCTCTAGTTCGCCGCTCCCA

Best fit: ref|XM_001096506.1| PREDICTED: Macaca mulatta cytochrome P450, subfamily XIA (LOC708065), mRNA

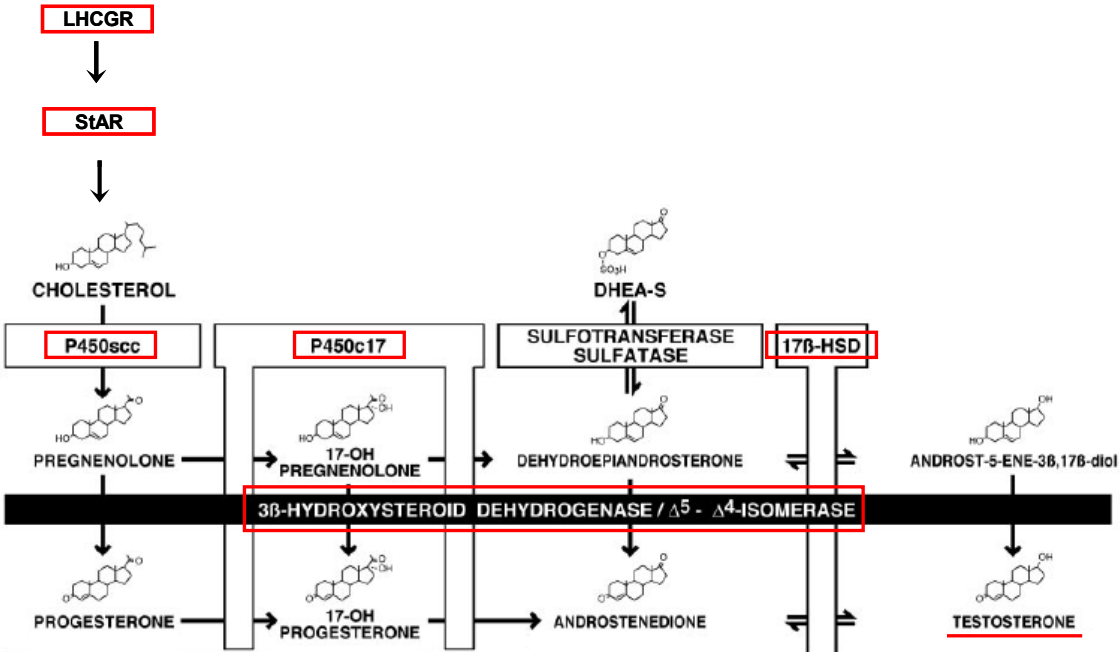

Modified from: Simard, J. et al. (2005). Molecular biology of the 3 beta-hydroxysteroid dehydrogenase/Delta(5)-Delta(4) isomerase gene family. Endocrine Reviews. *26*, 525-582.

Figure 4.7 Schematic Representation of Testosterone Biosynthesis Red (or dark grey) boxes indicate the primary components and enzymes in the Leydig cell testosterone biosynthetic pathway that were investigated. $P450_{scc}$ is also known as Cytochrome P450, family 11, subfamily A, polypeptide 1 (CYP11A1) or cholesterol side-chain cleavage. $P450_{c17}$ is the same as Cytochrome P450, family 17, subfamily A, polypeptide 1 (CYP17A1).

CHAPTER 5

EFFECTS OF MODERATE CALORIE RESTRICTION ON SELECTED MEASURES OF REPRODUCTIVE FUNCTION IN THE MALE RHESUS MACAQUE (*MACACA MULATTA*)

INTRODUCTION

Over the last 75 years calorie restriction (CR) has been established as the only proven non-genetic method of altering longevity and attenuating the biological changes associated with aging (Koubova and Guarente, 2003; Lane et al., 1999b; McCay et al., 1935). Moderate calorie restriction is believed to successfully intervene in the cascade of events that underlie normal aging, thus accounting for its advantageous health benefits. CR also exhibits great consistency across mammalian taxa and demonstrates generalized, beneficial health effects on almost every physiological system within the organism. To date this nutritional paradigm has been found to be effective in a variety of species including nematodes, spiders, flies, mollusks, rodents, dogs and possibly non-human primates, such as squirrel monkeys and cynomolgus and rhesus macaques (Ingram et al., 1990; Lane et al., 1999b; Roth et al., 1999; Weindruch and Walford, 1988). Its long history notwithstanding, however, very little is known with regard to the exact mechanism(s) of action of CR. Equally unknown is the potential impact of this nutritional paradigm on the hypothalamic-pituitary-gonadal (HPG) axis. Could moderate CR possibly improve reproductive health

parameters as it does with other systems within the body? Alternatively, could it have no impact or even unfavorable effects on reproductive outcome?

Previous work in our lab has found limited impact of CR on testicular gene expression in young adult or old adult rhesus macaques based on mRNA expression and semi-quantitative and real-time PCR data (Chapter 4). These findings suggest that CR can elicit general beneficial health effects without negative consequences on the gonadal portion of the HPG axis, meaning calorie restriction could potentially be implemented without causing problems with testicular physiology. This is especially relevant as the past two decades have seen an upward trend in the average age of couples having children (Buwe et al., 2005) with a 16-24% increase in the birth rate for U.S. fathers over age 35 years (Buwe et al., 2005; Eskenazi et al., 2003; Kidd et al., 2001). Additionally, external cues such as nutrition can have a substantial effect on the HPG axis. The recent phenomenon of increased average body mass index (BMI) experienced by the Western world has resulted in an increased incidence of obesity (Hursting et al., 2003). Obese men have lower sperm concentration and total sperm count compared to men with a BMI below obese levels (Jensen et al., 2004), while another study found an inverse relationship between BMI and total number of motile sperm cells and a positive relationship between BMI and DNA fragmentation per subject (Kort et al., 2006). The risk for increased BMI typically goes up as men get older, so that reproductive capacity is not only impacted negatively by age but also by the pathologies often associated with obesity.

Since CR is capable of reducing body mass and adiposity and improving general health parameters, it would be of great benefit to know if CR could also maintain reproductive fitness and/or attenuate age changes in the system. In contrast to our previous work which found no negative consequence of CR for testicular gene expression, other research has documented a significant effect on epididymal gene expression in Brown Norway rats (Jervis and Robaire, 2003). Changes in epididymal function could potentially lead to post-production sperm alterations.

The aim of the present study was to investigate the potential impact of moderate CR on parameters of normal sperm physiology and function in young adult rhesus macaques as measured through the use of semen collection and analysis.

MATERIALS AND METHODS

Animals and Diets

All experiments were approved for use by the Institutional Animal Care and Use Committees at the University of Maryland and the Oregon National Primate Research Center. The study consisted of 8 Young Adult (12 years) male rhesus macaques (*Macaca mulatta*) fed a control diet (CON; n=4) or calorie restricted at 30% CON (CR; n=4) for the previous 8 years post-pubertally. For plasma testosterone analysis another animal was included in each group (CON and CR; n=5). Animals were individually housed in a temperature-controlled environment under 12L:12D photoperiod (lights on 7 h -19 h) and allowed

auditory, visual and olfactory interaction with male and female conspecifics in the vivarium. Food was provided in two meals at 8 h and 15 h daily; water was available *ad libitum*.

Diet consisted of individual biscuits that had been specially formulated for this study supplemented with a daily low calorie treat (Ingram et al., 1990). The general composition of the diet was 15% protein, 5% fat and 5% fiber with a caloric content of approximately 3.7 kcal/g. Biscuits included a vitamin/mineral mix that was 40% higher than the recommended allowance for rhesus macaques by a National Research Council report (NRC, 1978), but were otherwise similar to those used in many laboratory studies of rhesus macaques. Supplementation was designed to offset any potential malnutrition in CR animals. Thus, it should be clear that the CON and CR groups were receiving exactly the same diet. Biochemical assays were performed periodically and with every new shipment to ensure diet content and quality (Black et al., 2001; Mattison et al., 2005).

The amount of food provided to CON animals was originally determined to be approximately *ad libitum* because they were observed to leave a few uneaten biscuits each day during regular measurements of food consumption. CR macaques were given 30% less than age- and body-weight matched controls. Food allotments were held constant other than as needed on a case-by-case basis when warranted by greater than acceptable changes in body weight (Lane et al., 1999b; Mattison et al., 2005).

Penile Electrostimulation

Penile electrostimulation (PES) is known to work in unanesthetized, manually restrained primates (Gould and Mann, 1988; Kholkute et al., 2000; Mastroianni and Manson, 1963). Following methods described previously (Sarason et al., 1991), PES was performed on three separate occasions for each study animal; one collection in spring (March-April) and two collections in fall (September-October). All animals were fitted with a lightweight metal alloy collar and acclimated to the collection procedure through a 17-day habituation regiment. Training involved familiarizing the animals to collared pole restraint, removal from their individual cages, restraint in the collection chair, collection, and return to their cages. To facilitate animal handling and alleviate any discomfort, animals were given 10 mg diazepam and 80 mg acetaminophen one hour prior to training or collection.

Semen Collection and Processing

Semen samples were collected into sterile collection tubes and allowed to liquefy at room temperature (RT) prior to evaluation (see Appendices K-M for detail). Ejaculate weight was obtained and exactly 30 minutes post-collection the liquid fraction of sample was transferred to a sterile centrifuge tube. Volume was recorded and aliquots were removed for osmolarity, pH and morphology determination. The remaining liquid fraction was then suspended in 15 mL warm TALP-Hepes with bovine serum albumin (BSA) and centrifuged at 130-150G for 10 minutes. After centrifugation the supernatant was immediately removed and

frozen for later seminal plasma analysis. The wash procedure was repeated twice. Following centrifugation the sperm pellet was resuspended in 1 mL warm TALP-BSA and placed in 5% CO_2/95% air at 37^{o}C. Aliquots for viability, count and concentration were taken and sperm motility was measured. The remaining sample was then used for zona pellucida binding and acrosomal staining assay (Appendices N-P), sperm chromatin structure assay, or frozen for future post-thaw analysis (Appendices Q and R). A summary of semen measurements can be found in Table 5.1.

Count, Concentration and Motility Analysis

After washing and resuspension, count and concentration were measured with phase contrast microscopy using a Neubauer hemocytometer. Percent motility was determined for fresh washed and frozen-thawed samples by visual observation at 200X magnification with duplicate counts of 100 sperm using a phase contrast microscope. Motility was measured as total movement, not just forward progress, which was accounted for with status rating (see Appendix K for details).

Viability, Osmolarity and pH Analysis

Sperm viability was determined for fresh semen samples using the hypo-osmotic swelling (HOS) assay previously described by Jeyendran (2003; for detail see Appendix L). Briefly, 5 µL of washed semen was incubated with 100 µL of HOS solution for 30 minutes in 5% CO_2/95% air at 37^{o}C. A minimum of 200

sperm were then observed with phase contrast microscopy for swelling. Results were recorded as a percent of the total count.

Osmolarity and pH were determined for freshly collected raw samples using a Vapro® Vapor Pressure Osmometer (Wescor; Logan, UT) and EMD colorpHast pH Strips (Fisher Scientific; Hampton, NH).

Morphology Analysis

Sperm morphology was scored for freshly collected raw samples as well as frozen-thawed sperm using one-step eosin-nigrosin staining (EN; IMV International Corp; Maple Grove, MN; see Appendix M for details). Briefly, smears were made by mixing equal volumes of semen and EN stain, air dried, coverslipped and examined at 1000X under oil immersion (100X bright-field). Two slides and 300 total sperm were examined for each collection. Results were recorded as percent Normal or Abnormal with abnormal sperm further subdivided into Head, Midpiece or Tail abnormality.

Seminal Plasma Assay

Accessory sex gland activity was measured via the seminal vesicle and prostate markers, fructose and citric acid, respectively. Enzymatic BioAnalysis kits were utilized with analysis performed in accordance with the manufacturer's instructions (Boehringer-Mannheim/R-Biopharm; Marshall, MI). Fructose was quantified by reaction with hexokinase and the stoichiometrically produced NADPH was measured by an increased absorbance at 340nm. Prostate gland

contribution was similarly determined utilizing an enzymatic reaction and the reduction of NADH was evaluated with an absorbance change at 340nm. The assay sensitivity limit for fructose was 0.25 µg/mL and for citric acid it was 0.2 µg/mL.

ZP Binding and AR Assay

A modified zona pellucida binding and acrosomal staining assay (Appendices N-P) was performed with all fresh sperm samples according to previously described methods (VandeVoort et al., 1992; VandeVoort et al., 1994; VandeVoort et al., 1997). Briefly, washed sperm samples in TALP-BSA (10×10^6 sperm/mL) were activated by adding dbcAMP and caffeine (Sigma-Aldrich Corp; St. Louis, MO). A total of 2-10 zona pellucida were placed in 100 µL drops of the capacitated sperm suspension under mineral oil (Sigma-Aldrich Corp) for 1 minute. Following coincubation, ZP were quickly rinsed in a series of media washes to remove any unbound sperm and immediately fixed in cold absolute ethanol. After fixation ZP were placed on 10-well Teflon-masked glass slides (Tekdon Inc; Myakka City, FL), allowed to air dry and then coverslipped. Binding and acrosomal status of sperm was determined by fluorescent microscopy using Hoescht chromatin staining and indirect immunofluorescence of a polyclonal antisperm antiserum that labels the acrosomal contents of intact sperm. Labeling was performed directly on the glass slides to allow rapid processing of ZP while minimizing the use of antisera. Acrosomal status of ZP-bound sperm is reported as the percentage of total bound sperm that are acrosome reacted. Antibodies

for labeling were generously provided by Dr. Cathi VandeVoort of the California National Primate Research Center at the University of California-Davis.

SCSA®

The sperm chromatin structure assay is a flow-cytometric test that measures the susceptibility of sperm nuclear DNA to acid-induced DNA denaturation *in situ*. The assay was used to determine the percentage of sperm with elevated levels of DNA fragmentation in washed, fresh-frozen semen. Frozen, washed sperm samples were submitted to SCSA® Diagnostics (Brookings, SD) for analysis per their laboratory specifications.

Testosterone Sampling and Analysis

Animals were surgically fitted with an indwelling subclavian vein catheter which enabled remote serial blood samples to be collected from an adjacent room without disturbing the animals (Downs and Urbanski, 2006). Blood samples (1 mL) were collected from each subject every 30 minutes over a 24-hour period. Samples were placed in EDTA-coated glass tubes and centrifuged at 4^{o}C; plasma was stored at –20^{o}C until assay for testosterone (T). Plasma testosterone concentrations were measured by radioimmunoassay (RIA) as previously described (Resko et al., 1973).

Statistical Analysis

Data for each male were averaged for three collections and then group treatment averages were determined. Data are expressed as group mean ± SEM (CON and CR; n=4) of all semen collections for each parameter measured.

Group mean testosterone values (CON and CR; n=5) were determined by taking the overall mean of the individual hormone values spanning the entire 24-hour sampling period. Group maximum T values were determined by first identifying the maximum value for an individual and then averaging it with two adjacent values on each side of the time point. The mean of those individual maximum values was then recorded. Similarly, the group minimum values were determined by taking the mean of the five adjacent lowest values for each individual.

Statistical comparisons between CON and CR groups were made by Student's *t*-test using SPSS (SPSS Inc.; Chicago, IL) or Excel (Microsoft; Redmond, WA). Tests for heterogeneity of variance for semen parameters were determined using Statistical Analysis System (SAS Institute; Cary, NC). For all analyses significant differences were accepted at $P<0.05$.

RESULTS

Circannual patterns of testicular function have been reported in the rhesus macaque with distinct seasonal variations in testicular volume, semen quality, sperm number, sexual behavior and frequency of birth rate observed in wild and captive populations, even under constant light cycles (Gould and Mann, 1988;

Gupta et al., 2000; Muehlenbein et al., 2002). Because of this potential confounding effect, we tested for seasonal differences in animals prior to continuing other analyses.

No seasonality differences in semen measurements (ejaculate weight, volume, count, concentration, motility, viability, osmolarity, pH and ZP binding) were detected in our study using a paired Student's *t*-test between spring and average fall collection values for each animal. Additionally, no correlation was detected between individual animal weight and the proportion of morphological sperm abnormalities (head, midpiece and tail). Analysis was performed using Statistical Analysis System (SAS Institute; Cary, NC) with $P<0.05$.

Standard Sperm Functionality Measures

Ejaculate weight, liquid volume of ejaculate, sperm count, sperm concentration, sperm motility, sperm viability, ejaculate osmolarity and ejaculate pH for freshly collected semen are presented in Figures 5.1 A-H and Table 5.2. No significant diet-induced changes were detected between groups in any of these parameters based on Student's *t*-test comparisons.

Examples of various morphological outcomes of sperm development can be seen in Figures 5.2 A-H. No significant diet-induced differences were detected between CON and CR groups with regards to the percentage of normal and abnormal sperm per ejaculate (Figure 5.3A). Similarly, no significant treatment differences were observed in the percentage of head, midpiece or tail

abnormalities between groups (Figure 5.3B). Data are from fresh raw semen and are presented in Table 5.3.

Two standard functional measures were taken of frozen-thawed sperm: motility and morphology. Results of frozen-thawed sperm motility outcome can be seen in Figure 5.4 and Table 5.4. Morphological characterization of the frozen-thawed samples are presented in Figures 5.5 A-B and Table 5.5. As with the freshly processed samples, no significant differences were observed between treatment groups in motility, the percentage of normal and abnormal sperm, or in the three categories of abnormalities.

Seminal Plasma Constituents

Attempts to quantify accessory sex gland contribution to the ejaculate were made using spectrophotometric enzymatic assays for fructose and citric acid. Unfortunately, it appears that the samples were too dilute due to the volume of wash buffer used during processing. Efforts will be made to concentrate the samples and quantify these markers at a later date.

ZP Binding and Acrosome Reaction

Representative images of the zona pellucida binding and acrosome reaction assay are shown in Figure 5.6. Hoescht 33,258 staining of DNA/chromatin (blue) can clearly be seen in the upper portion of the figure while the lower portion demonstrates fluorescein isothiocyanate (FITC) double-antibody staining of the sperm acrosomal membrane (green).

The results of the ZP binding AR assay are given in Table 5.6 with the mean number of sperm bound per zonae and the percentage of acrosome reacted sperm. No significant differences were detected between groups for either of these endpoints.

SCSA®

A total of 14 samples from all eight animals were submitted to SCSA® Diagnostics (Brookings, SD) for analysis. No significant differences were detected between groups; results are given in Tables 5.7 and 5.8. Each ejaculate sample proved to be of high quality with the exception of CON #22382.

Representative data sheets for the sperm chromatin structure assay (Figure 5.7) show a high quality sample (upper image) and a poor quality sample with a high DNA fragmentation index (DFI) score (lower image). A value above 30% usually indicates that the animal would experience reduced success at siring offspring, whether from intercourse, intrauterine insemination, *in vitro* fertilization or intracytoplasmic sperm injection (Bungum et al., 2004; Larson-Cook et al., 2003).

Testosterone Concentrations

Daily circulating plasma testosterone levels for both treatment groups are displayed in Figure 5.8. Each group exhibited the same general pattern of T expression over the 24-hour period. There were no significant differences in mean or maximum levels of circulating testosterone (Figure 5.9). Daily minimum

T levels, however, were significantly lower (P<0.01) in the CON group compared to CR-treated animals.

DISCUSSION

Male rhesus macaques benefit from CR with an apparent slowing of age-related changes in metabolic responses and improved overall health. Such findings seem to indicate a metabolic shift from growth and reproduction toward a strategy of life maintenance (Roth et al., 2004). The impact of moderate CR on male reproductive physiology is unclear, however, and appears to differ with degree and timing of treatment. For example, CR prior to puberty can delay the maturational increase in circulating testosterone concentrations, indicative of reproductive activation, by approximately one year (Lane et al., 1997; Roth et al., 2000).

We previously examined the impact of moderate CR on testicular gene expression in young adult rhesus macaques and found limited effects. Epididymal function, however, has a major effect on the functional capacity of sperm. Mammalian spermatozoa leaving the testis are not capable of fertilizing oocytes. During passage through the epididymis they undergo a progressive series of morphological and physiological changes in a process known as epididymal maturation. Only after these changes will sperm acquire the ability to fertilize (Elder and Dale, 2000; Harrison and Lewis, 1986). Recent findings by Jervis and Robaire (2003) have demonstrated an effect of short-term, moderate CR on epididymal gene expression in young BN rats. In addition to measuring

testicular gene expression, it becomes necessary to utilize functional assays to determine sperm vigor since changes in the epididymis could potentially lead to post-production alterations.

The aim of the present study was to investigate the potential impact of moderate CR on parameters of normal sperm physiology and function in young adult rhesus macaques. This was achieved through the use of semen collection and analysis utilizing a large number of quantifiable endpoints to provide a complete characterization of ejaculate quality and sperm health. These endpoints, though specific, were chosen in order to address three broader questions of male reproductive function: 1) Can sperm physically reach the site of fertilization? 2) Can sperm undergo physiological modifications necessary for fertilization? and 3) Can sperm initiate and sustain embryo development?

Can sperm physically reach the site of fertilization?

Assessment techniques which are robust, reliable and as easy as possible to perform are fundamental to modern basic semen analysis. Nine components of the classical spermiogram that were investigated in our study include ejaculate weight, liquid volume of ejaculate, sperm count, sperm concentration, sperm motility, sperm viability, ejaculate osmolarity, ejaculate pH and sperm morphology. Cumulatively, these measures give an indication of the probable success a male would have in mating and siring offspring. Our findings indicated no significant differences ($P<0.05$) between CON and CR groups in any of these ejaculate characteristics. Further, the means for each group appear to fall within

the normal ranges for macaque semen (Gould and Mann, 1988; Lanzendorf et al., 1990).

Ejaculate weight and volume indicate the ability to produce adequate means for sperm delivery to the female reproductive tract. These two parameters are primarily determined by accessory sex gland secretions, with low volume typically indicative of retrograde semen flow into the bladder or accessory sex gland pathology. Count and concentration demonstrate the ability of the animal to produce adequate spermatozoa to survive transport through the female tract. These parameters were not statistically significant between treatment groups, although variability was much less in the CR-treated animals as measured by SEM.

Motility is an evaluation of spontaneous sperm movement and was measured in both fresh semen and frozen-thawed samples. The ability of spermatozoa to propel themselves through the female reproductive tract following ejaculation is important if the sperm are to reach the uterine isthmus where fertilization typically occurs. Sperm motility in both treatment groups was generally good with no significant differences observed. It is important to remember, however, that although good sperm are necessarily motile, motile sperm are not necessarily fertile; thus, the need for a complete battery of tests in determining reproductive potential. From a purely observational standpoint, it seems that sperm from CR animals may have tolerated freezing slightly better as motility only dropped from 56% to 37% following post-thaw analysis compared to the CON group which went from 64% down to 25%. Again, the differences were

not statistically significant due to biological variation, and post-thaw motility was generally lower in both groups compared to values reported in the literature (Nichols and Bavister, 2006).

Spermatozoa, like all other cells, must selectively regulate the movement of molecules across their surface to maintain equilibrium between themselves and their environment. When exposed to hypo-osmotic conditions sperm will allow water to enter the cytoplasm in an attempt to reach osmotic equilibrium. It can be assumed that the capacity of sperm to swell in the presence of a hypo-osmotic solution is a sign that membrane integrity and normal functional activity are intact. Membrane viability is not only important for sperm metabolism but critically timed changes in membrane properties are required for successful sperm activation, acrosome reaction and binding to the oocyte. We chose to use the HOS assay to evaluate the functional integrity of the sperm membrane rather than the 'live-dead' EN stain which only measures whether the membrane is morphologically intact (Jeyendran et al., 1984). The assay is simple to run and demonstrates a high correlation between the percentage of sperm in an ejaculate that are capable of swelling and their ability to undergo activation and/or oocyte binding. The percentage of viable sperm was not significantly different between CON and CR animals in the present study.

Seminal plasma is derived primarily (50-80%) from seminal vesicles with a smaller fraction (13-30%) contributed by the prostate (Harraway et al., 2000; Haugen and Grotmol, 1998). Ejaculate osmolarity and pH are both dependent on the ratios of these secretions and can be influenced by the nutritional status of

the animal. Stable osmolarity and the basic pH of semen allow spermatozoa to survive in the slightly acidic environment of the vagina until they can pass through the cervix into the uterus. Our data showed no significant differences between diet groups for either of these parameters.

Morphology refers to the shape, size, and surface appearance of sperm. This can be determined with the one-step eosin-nigrosin staining technique which does not need negative phase contrast optics but instead can be run with ordinary bright-field microscopy. It includes few methodological steps to control, making it preferable in terms of standardization and quality control management. Evaluation of stained semen smears from our study, both fresh and frozen-thawed samples, showed no statistically significant diet-induced differences between treatments. There were significant differences between fresh and frozen-thawed samples, but these differences are simply an artifact of the cryopreservation and/or thawing process and not attributable to diet.

While the nine sperm parameters analyzed showed no statistically significant differences between experimental groups, it is worth noting that in every instance, with the exception of sperm viability, biological variation in the CR-treated animals was similar or less than that measured in their CON counterparts. In fact, upon analysis, CR variability was found to be significantly smaller for sperm count ($P<0.04$) and tended toward significance for three other ejaculate parameters: volume, weight and osmolarity ($P<0.06$-0.11). This may be an indication that the body has experienced a metabolic shift to a more efficient

strategy of life maintenance as these parameters appeared to be more tightly regulated in our CR-treated animals.

Additionally, we attempted to quantify the seminal plasma constituents, fructose and citric acid. This is not a component of the traditional spermiogram, but since the seminal vesicles and prostate contribute approximately 90% of the seminal plasma volume it is of great interest to determine if these glands are functioning properly (Gonzales, 2001; Owen and Katz, 2005). Seminal vesicle secretion is important for sperm metabolism, semen coagulation, sperm motility, stability of chromatin and suppression of immune activity in the female reproductive tract (Gonzales, 2001; Lewis-Jones et al., 1996). Specifically fructose, the major carbohydrate in human semen, has been reported to be a source of energy for the motile sperm (Elzanaty et al., 2002; Lewis-Jones et al., 1996). As a result, the measurement of seminal fructose has been used in most fertility labs worldwide and by the World Health Organization as a marker of seminal vesicle function (Gonzales, 2001; Harrison and Lewis, 1986). Prostate derived citrate is one of the most important anions present in human semen and is probably responsible for regulating ionized calcium levels in the seminal plasma. It may also be responsible for the high buffering capacity of semen which allows sperm to survive in the acidic vaginal environment until it can enter the neutral pH cervical mucus (Owen and Katz, 2005). Determination then of fructose and citric acid concentration becomes one of the major methods for evaluating seminal vesicle and prostatic function.

Unfortunately, the spectrophotometric enzymatic assays we used were unable to measure these constituents accurately, possibly due to the dilution of plasma during our washing of each semen collection. Previous reports of semen collection in squirrel monkeys (Yeoman et al., 1998) used only 4 mL of buffer for washing each ejaculate compared to our 15 mL. They also heated the wash supernatant to 80^{o}C for 15 minutes to stop any enzymatic reactions. We did not do this, so it is possible that our samples may have appreciably degraded in the time it took to perform the wash and get the supernatant into a -80^{o}C freezer. Future efforts will be made, however, to concentrate the samples and quantify these markers.

Taken together these data demonstrate that moderate CR had limited impact on semen quality in adult rhesus macaques based on the spermiogram parameters observed. Despite these similarities it is still possible that sperm competency could be affected at some point further along the reproductive pathway, possibly at the point of fertilization.

Can sperm undergo physiological modifications necessary for fertilization?

Fertilization is a complex process requiring the spermatozoa to undergo a cascade of events before it can fuse with the oocyte plasma membrane (Yanagimachi, 1994). The zona pellucida, a unique extracellular translucent matrix surrounding the mature oocyte, mediates critical steps in the fertilization process, including induction of sperm acrosome reaction in some species, sperm binding and establishment of block to polyspermy. Unlike other vertebrates, eutherian spermatozoa cannot penetrate the ZP immediately after ejaculation.

Instead, a final stage of maturation, termed capacitation, is required in which sperm acquire the ability to undergo the acrosome reaction (Mortimer, 1994; Yanagimachi, 1994). Capacitation regulates the induction of the acrosome reaction and is marked by hyperactivation in motility of the sperm. Using the ZP binding and AR assay we quantified the ability of collected sperm to become capacitated, bind to homologous zona pellucida and undergo the acrosome reaction.

Our results showed no statistically significant difference between experimental groups for the number of bound sperm per zonae and the percent of bound sperm which were acrosome reacted. While the variation in our samples was comparable to published reports, our mean values were considerably lower than those reported by VandeVoort et al. (1992; 1994). Using the same assay, they documented sperm binding at anywhere from 71 ($\pm$ 28) to 96.2 ($\pm$ 17) sperm per ZP. They also reported an acrosome reacted percentage of 8.2 ($\pm$0.9) to 30 ($\pm$8) in rhesus macaques as compared to our 0.4-1%.

There are a few possible reasons for these differences. First, while human sperm will spontaneously capacitate *in vitro*, rhesus macaque spermatozoa must be exposed to the activators caffeine and dbcAMP (VandeVoort et al., 1994). Once capacitated, ZP binding will occur when exposed to zona pellucida membranes, and this binding acts as a signal to induce the sperm acrosome reaction. Although activation was checked prior to coincubation with ZP, perhaps we achieved lower limits of sperm capacitation than was needed for binding. Secondly, almost all rhesus macaque sperm are acrosome intact upon ZP

binding and will only acrosome react when exposed to a homologous sperm-ZP interaction (VandeVoort et al., 1992; VandeVoort et al., 1994). Unlike humans where acrosome reacted sperm can still bind, if rhesus macaque sperm acrosome react prior to interaction with the oocyte, their binding capacity is significantly reduced (VandeVoort et al., 1997). It is possible that sperm in each of our assays was already acrosome reacted and thus was unable to fuse to the ZP. Finally, assay differences may simply be a result of animal variation. Subjects in our study were inexperienced males chosen not for their breeding success but rather because they were a part of a CR study.

Can sperm initiate and sustain embryo development?

Sperm chromatin, consisting of DNA and heterogeneous nucleoproteins, is normally a highly organized and compact structure intended to protect genetic integrity during transport through the male and female reproductive tracts. Accumulating data suggest that alterations in genomic organization of the sperm nuclei are negatively correlated with the fertility potential of sperm and its ability to maintain embryo survival. The sperm chromatin structure assay (SCSA®) measures DNA integrity, an essential component for the accurate transmission of genetic information to the offspring, via DNA fragmentation levels and has proven highly effective in predicting fertility outcome both *in vivo* and *in vitro* (Larson-Cook et al., 2003).

Recent reports by Evenson et al. (2006) have indicated that natural pregnancy is not possible when $\geq$30% of sperm DNA is damaged. It has been

suggested that sperm DNA integrity may even be a more objective measure of sperm function compared to standard semen analysis, which can be very subjective and prone to intra- and inter-observer variability (Agarwal and Said, 2003). Meta-analyses of the Georgetown Male Factor Infertility Study show that SCSA® infertility test is significantly predictive for reduced pregnancy success using intercourse, intrauterine insemination, routine *in vitro* fertilization and, to a lesser extent, intracytoplasmic sperm injection (Evenson and Wixon, 2006). Findings in the present experiment found no significant differences between treatment groups and indicate that DNA integrity was very high in all eight of the study animals. The one exception was a CON animal for which there was only one available sample for assay. In this instance, the subject demonstrated a DFI of 32.5%. It would appear that this animal would be infertile based on the one ejaculate, but it is difficult to speculate without further samples.

Finally, we know that Leydig cell-derived testosterone is the driving force behind masculinization, sperm production, and male secondary sex characteristics. There have been sporadic studies of testosterone measurement in rhesus macaques, and they are often contradictory. Some reports claim non-significant declines in testicular mass, serum T levels and pulsatile T release in aged animals (Black and Lane, 2002; Roth et al., 2004) while others show no evidence of different T levels with age (Mattison et al., 2003; Mattison et al., 2001). This can perhaps be attributed to poor sampling and/or the fact that T

levels vary widely amongst individuals, throughout the day and even from day-to-day.

Due to the extensive expertise of the ONPRC to catheterize our experimental subjects and sample remotely, we were able to obtain blood samples every 30 minutes across a 24-hour period. Such timely sampling is necessary if true T profiles are to be established, as sampling too infrequently will not allow detection of the circadian pattern of testicular T release. In our study treatment groups displayed a similar pattern of daily circulating plasma testosterone levels. Likewise, no statistically significant differences were detected between CON and CR animals for mean or maximum circulating T levels. Daily minimum levels, however, were significantly different ($P<0.01$) with CON subjects lower than their CR counterparts. The biological relevance of this is uncertain, but it may be another indication of physiological efficiency. By decreasing the daily swing between maximum and minimum levels and maintaining tighter control over T release, CR animals may be able to divert energy toward more critical functions of life maintenance. This may in turn account for the decreased variability observed in the majority of our spermiogram parameters.

Our findings may also be an indication that CR can maintain T levels, which would be of great benefit since age-related testosterone decline can cause weakened muscle function, lower bone density and loss of cognitive function. Studies in Brown Norway rats have shown that CR initiated at 4 months of age and applied continuously for 30 months results in significantly higher concentrations of serum testosterone concentration compared to controls,

suggesting that long-term CR can transiently suppress the reductions in steroidogenesis that are characteristic of aging (Chen et al., 2005). Should CR be shown to elicit the same biological response in a nonhuman primate model, it could potentially be implemented as a counterbalancing force in human aging. This could have far-reaching social consequences by improving quality of life issues including immune function, bone and muscle health, libido and cognition.

SUMMARY

In the present study we investigated the potential impact of moderate CR on parameters of normal sperm physiology and function in young adult rhesus macaques (*Macaca mulatta*). Semen samples were collected via penile electrostimulation three times over a 7-month period from 8 Young Adult (12 years) rhesus macaques fed a control diet (CON; n=4) or calorie restricted at 30% CON (CR; n=4) for the previous 8 years post-pubertally. Ejaculate weight, liquid volume of ejaculate, sperm count, sperm concentration, sperm motility, sperm viability, ejaculate osmolarity, ejaculate pH and sperm morphology for freshly collected semen were determined along with motility and morphology analysis of frozen-thawed samples. Our findings indicated no statistically significant differences ($P<0.05$) between the two groups in any of these ejaculate characteristics, although variability in CR-treated subjects tended to be lower. ZP binding and AR assay and SCSA® were conducted and also indicated no significant differences between CON and CR-treated animals. Additionally, circulating plasma testosterone levels were recorded in all test subjects along

with an additional animal in each group (CON and CR; n=5). Both groups exhibited the same general pattern of T expression over the 24-hour period with no significant differences in mean or maximum levels of circulating testosterone. Daily minimum T levels, however, were significantly lower (P<0.01) in the CON group compared to CR-treated animals. The biological relevance of this is uncertain, but it may indicate a metabolic shift toward a more efficient strategy of life maintenance. Thus, moderate CR was neither detrimental nor beneficial to semen quality in young adult rhesus macaques based on the physiological parameters observed. This study is among the first to address the effects of CR on male reproductive function in nonhuman primates. Whether CR impacts fertility in aging male macaques remains to be determined. These data represent a unique and valuable opportunity to contribute to the growing body of literature regarding the effects of caloric restriction and its impact on biological function.

ACKNOWLEDGEMENTS

Research was supported by NIA CR Grant AG21382, ART Core HD18185, ONPRC Core Grant RR00163 and NIH Grants AG-19914, HD-29186, RR-00163 and U01-AG21380-03. Additional support provided by: Research Assistantship from the Department of Animal and Avian Sciences at the University of Maryland; the Intramural Research Program of the National Institutes of Health; and the National Institute on Aging. We would also like to thank the members of the Oregon National Primate Research Center: Dr. Mary Zelinski, Maralee Lawson, Diana Takahashi, Michelle Sparman, Carrie Thomas,

Audrey Trupp, Kaleb Grund, Marci Szlavich, Norma Myers, and the late Dr. John Fanton. Technical support provided by Dr. Cathi VandeVoort and her staff at the California National Primate Research Center and Dr. Julie Long and her staff at the USDA Agricultural Research Service. We would like to thank Tia Dixon for her assistance with scoring morphology slides. Statistical support graciously provided by Erin Hoerl Leone at the University of Maryland.

Table 5.1 Summary of Semen Measurements

Measure	Rationale
Ejaculate appearance	Indicative of cell (sperm) numbers
Ejaculate weight	Indicative of accessory sex gland production and secretion
Ejaculate color	Abnormal color may indicate accessory sex gland or other clinical pathology
Ejaculate volume	Low volume may indicate retrograde semen flow into the bladder or accessory sex gland pathology
Osmolarity/osmolality	Indicative of ionic composition
pH	Indicative of ratio of alkaline seminal vesicle secretions and acidic prostatic secretions
Count	Indicative of overall spermatogenesis success
Concentration	Indicative of successful spermatogenesis and accessory sex gland production
Motility	Indicative of sperm ability to reach the ova
Morphology	Indicative of cell maturation status
Activation (capacitation)	Indicative of sperm ability to reach the ova and then penetrate the zona pellucida
Agglutination	May indicate possible surface antigen problems
Zona pellucida (ZP) binding	Sperm binding to the ZP outer surface is a prerequisite for oocyte vitelline membrane binding and penetration
Acrosome reaction	Prior to fertilization the outer acrosomal membrane fuses with the surrounding plasma membrane
Hypo-osmotic swelling assay	Indicative of intact sperm membrane. Membrane integrity can influence motility, activation, acrosome reaction and is required for successful fusion with the ova
Seminal plasma composition	Overall measure of accessory sex gland contribution
Sperm chromatin structure assay (SCSA®)	Indicative of DNA packaging and sperm development capabilities

Figures 5.1 A-H Semen Parameters in Young Adult CON and CR Rhesus Macaques Data for each male were averaged for three collections and then group treatment averages were determined for Young Adult rhesus macaques. Analyses were made between CON and CR by Student's *t*-test ($P<0.05$) using SPSS (SPSS Inc.; Chicago, IL) or Excel (Microsoft; Redmond, WA). Each point, along with SEM, represents mean data from four animals. No significant differences were detected for any of the standard sperm functionality measures.

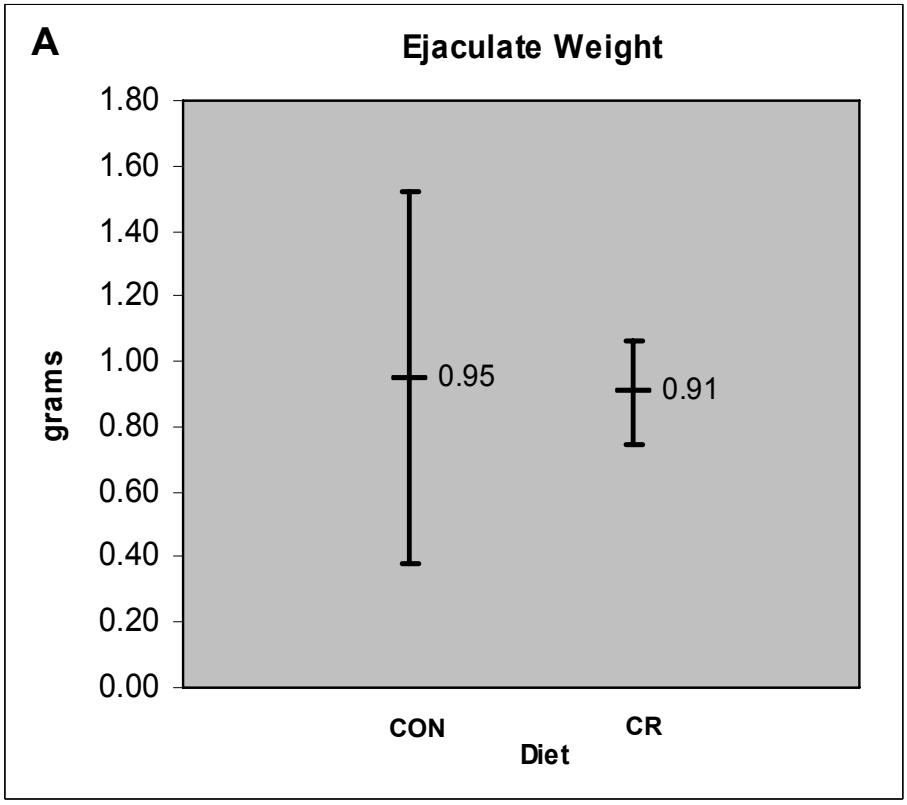
A
Ejaculate Weight
1.80
1.60
1.40
1.20
1.00
0.80
0.60
0.40
0.20
0.00
grams
0.95
0.91
CON
CR
Diet

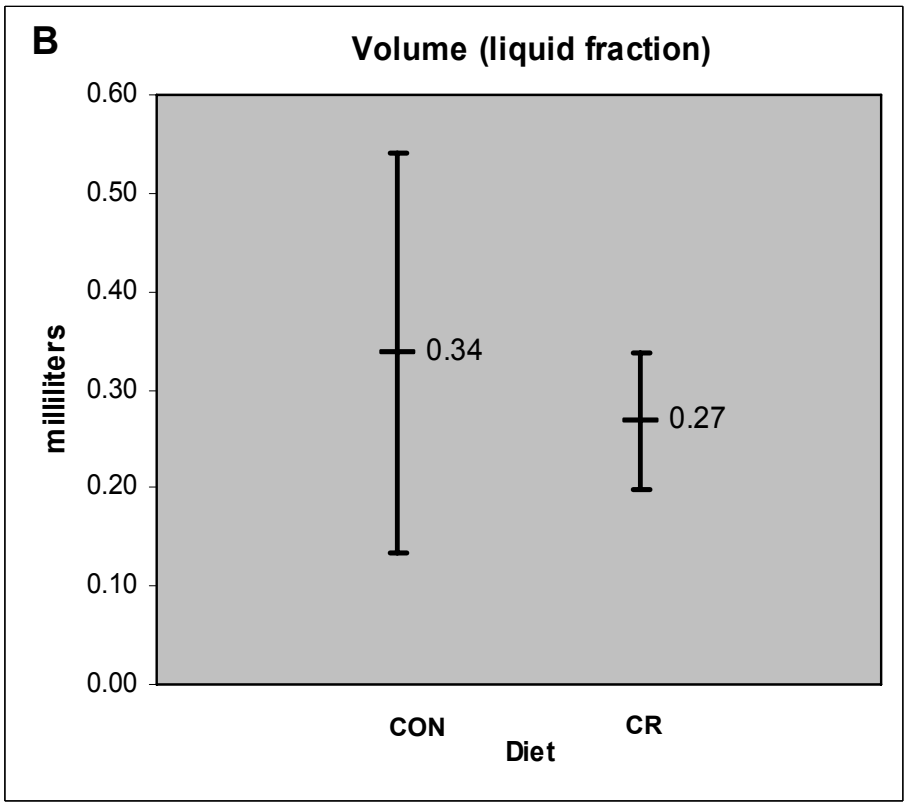
B
Volume (liquid fraction)
0.60
0.50
0.40
0.30
0.20
0.10
0.00
milliliters
0.34
0.27
CON
CR
Diet

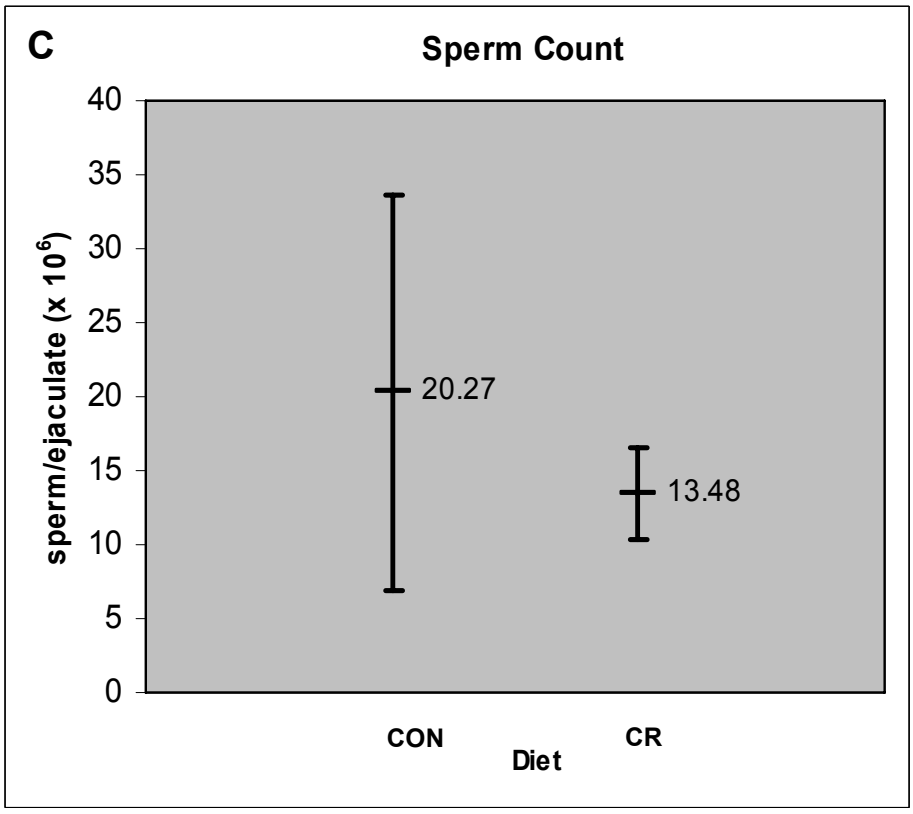
C
Sperm Count
sperm/ejaculate (x 10^6)
40
35
30
25
20
15
10
5
0
20.27
13.48
CON
CR
Diet

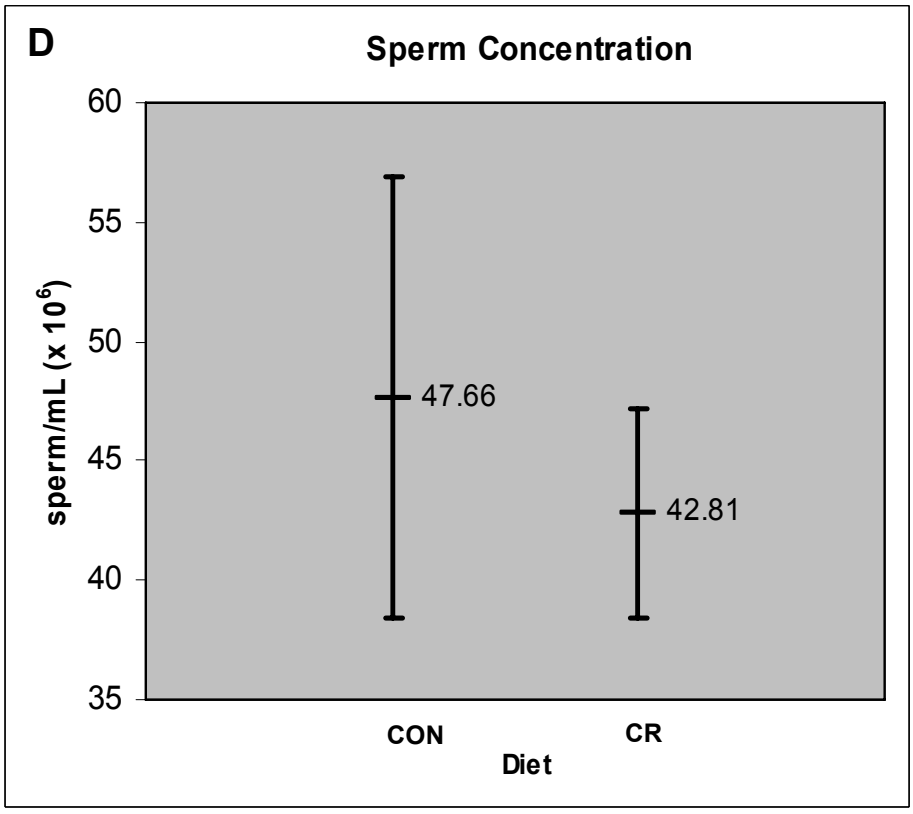
D
Sperm Concentration
sperm/mL (x 10^6)
60
55
50
45
40
35
47.66
42.81
CON
CR
Diet

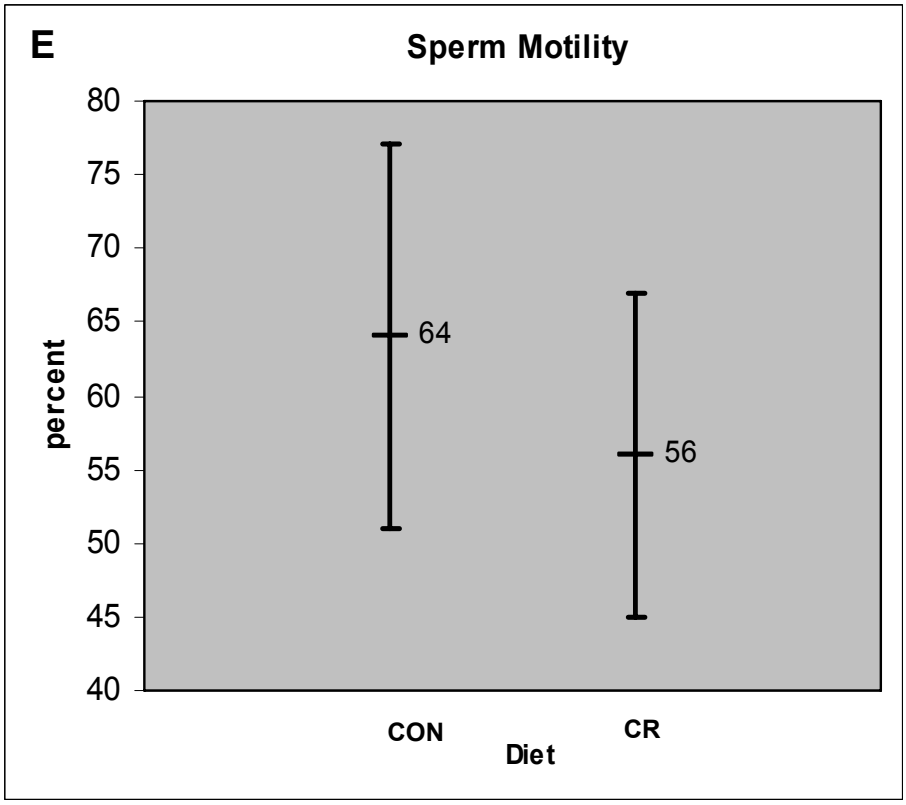
E
Sperm Motility
80
75
70
65
60
55
50
45
40
percent
64
56
CON
CR
Diet

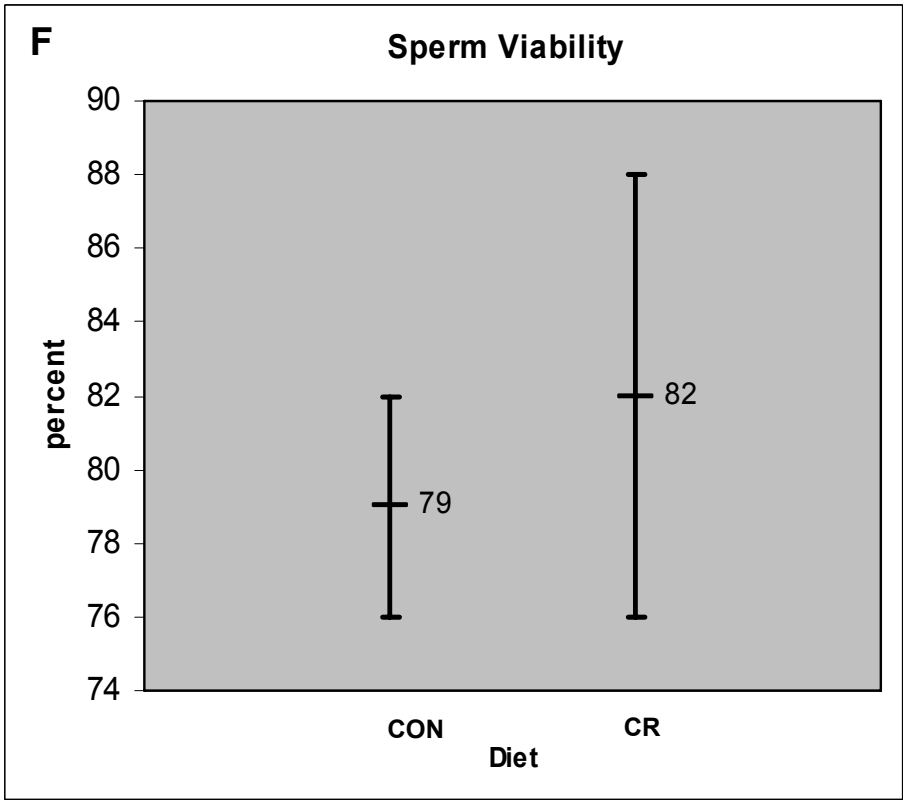
F
Sperm Viability
90
88
86
84
82
80
78
76
74
percent
82
79
CON
CR
Diet

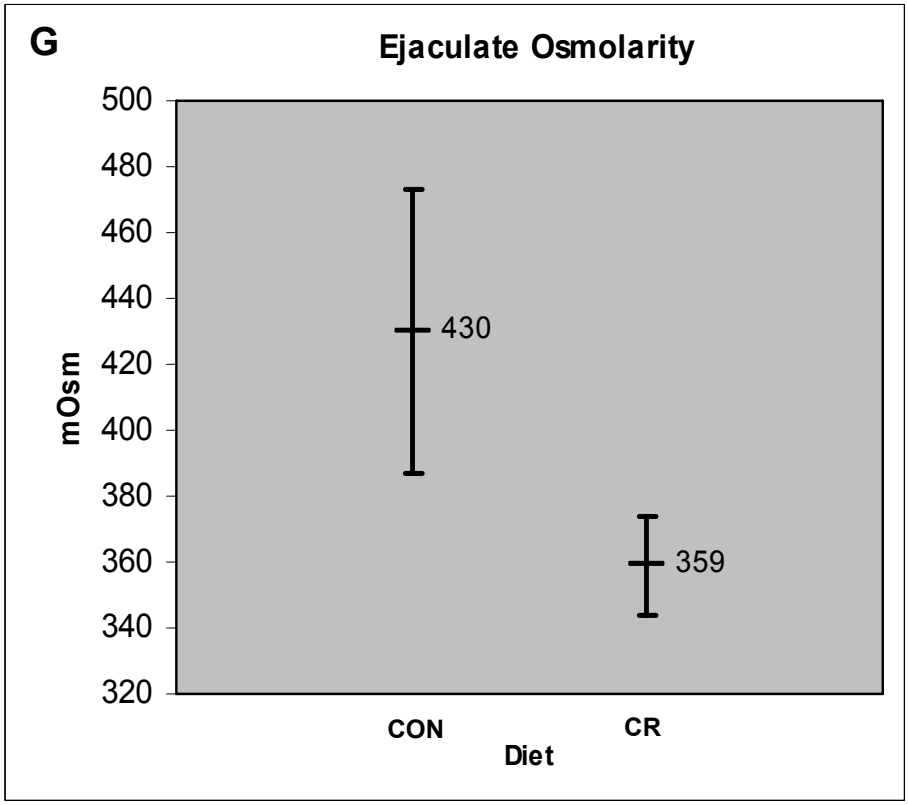
G
Ejaculate Osmolarity
500
480
460
440
420
400
380
360
340
320
mOsm
430
359
CON
CR
Diet

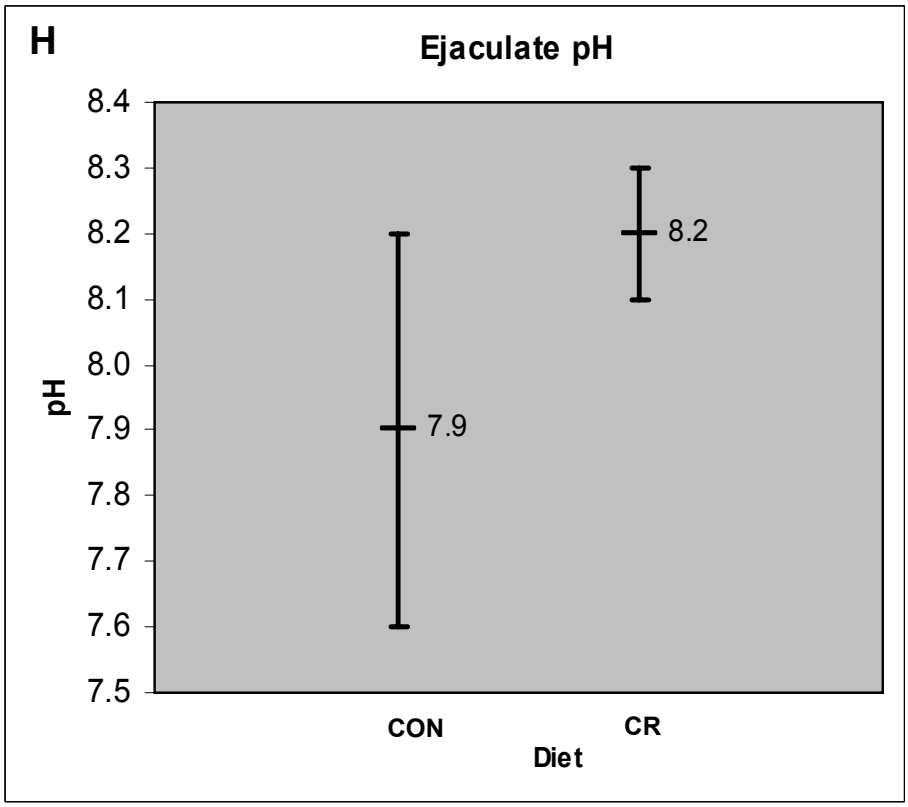
H
Ejaculate pH
8.4
8.3
8.2
8.1
8.0
7.9
7.8
7.7
7.6
7.5
pH
8.2
7.9
CON
CR
Diet

	CON	CR
ejaculate weight (g)	0.95 ± 0.57	0.91 ± 0.16
ejaculate volume (mL)	0.34 ± 0.20	0.27 ± 0.07
sperm count (x 10^6)	20.27 ± 13.4	13.48 ± 3.1
sperm concentration (per mL; x 10^6)	47.66 ± 9.21	42.81 ± 4.38
sperm motility (%)	64 ± 13	56 ± 11
sperm viability (%)	79 ± 3	82 ± 6
ejaculate osmolarity (mOsm)	430 ± 43	359 ± 15
ejaculate pH	7.9 ± 0.3	8.2 ± 0.1

Table 5.2 Semen Parameter Values in Young Adult CON and CR Rhesus Macaques Mean data (± SEM) from the preceding figures are presented in numerical form. No significant differences ($P<0.05$) were observed between the two diet groups for the ejaculate characteristics.

Variability, however, was found to be significantly smaller for CR-treated animals in sperm count ($P<0.04$) and tended toward significance for three other ejaculate parameters: volume, weight and osmolarity ($P<0.06$-0.11).

Figures 5.2 A-H Sperm Morphology Examples from Young Adult Rhesus Macaques Representative images showing normal morphology (A and B) along with various abnormalities found in sperm for CON and CR treated animals (n=4 each). Black arrows show the locations of abnormalities.

- Head abnormality: round head (C) and acrosome damage (D)
- Midpiece abnormality: thickened midpiece (E) and coiled midpiece (F)
- Tail abnormality: coiled tail (G and H)

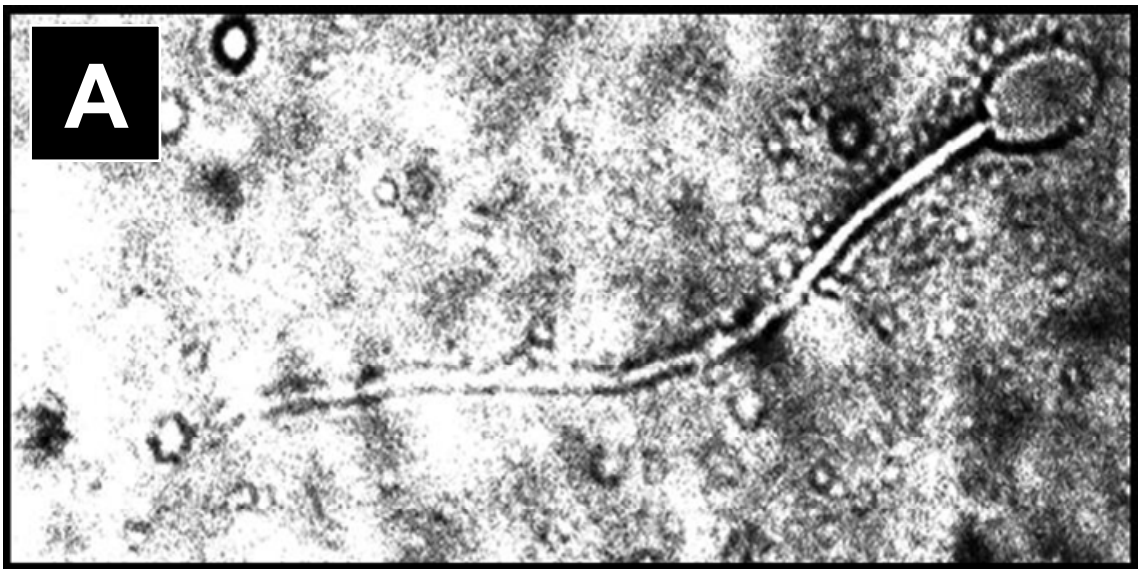

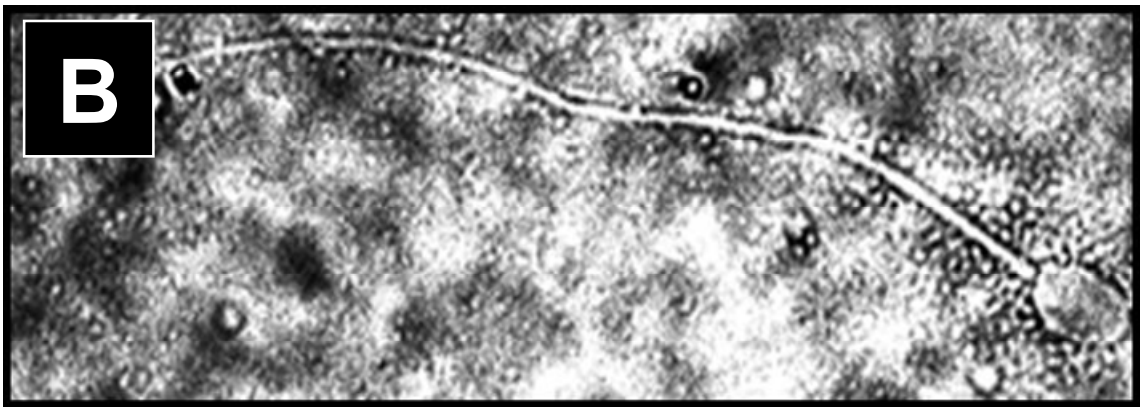

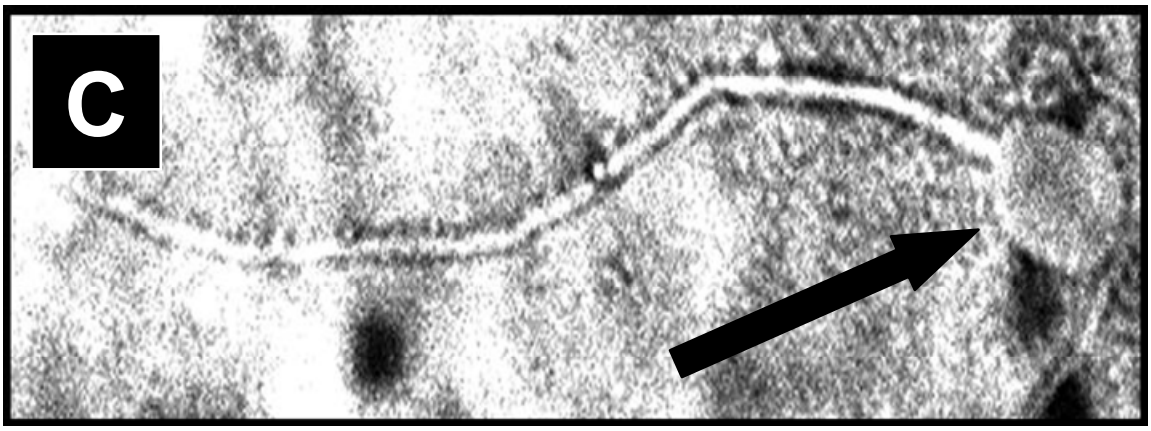
C

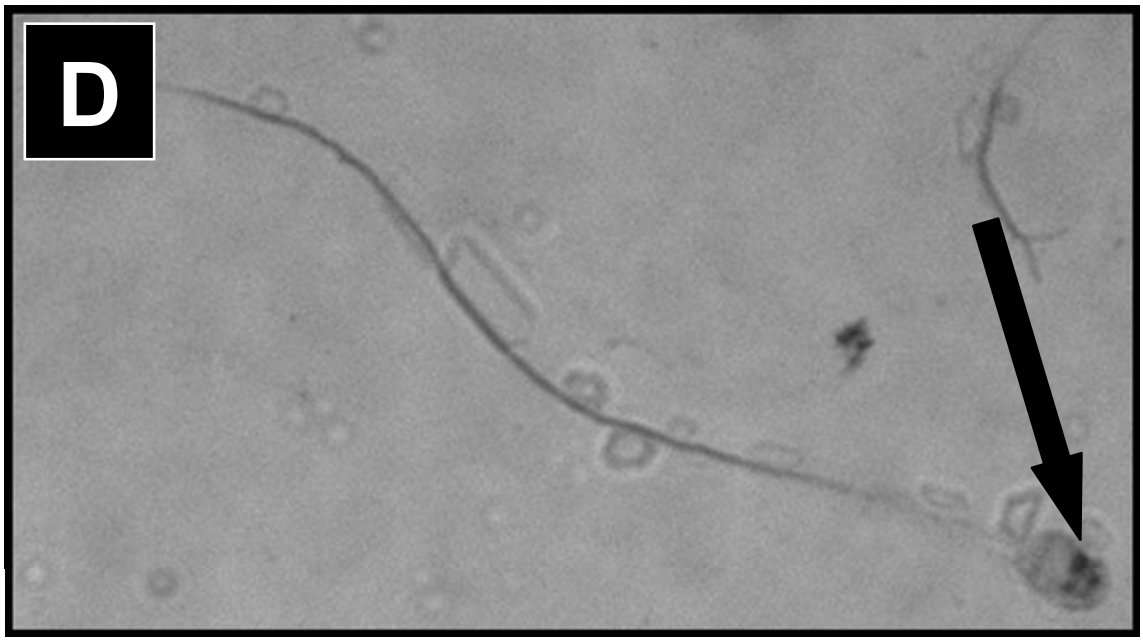
D

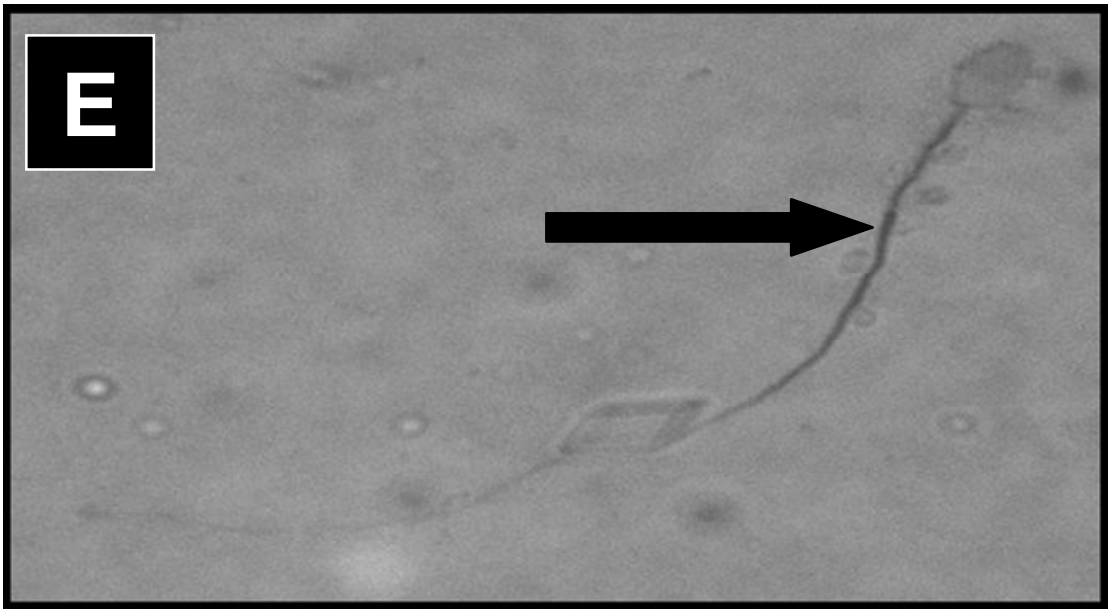
E


F

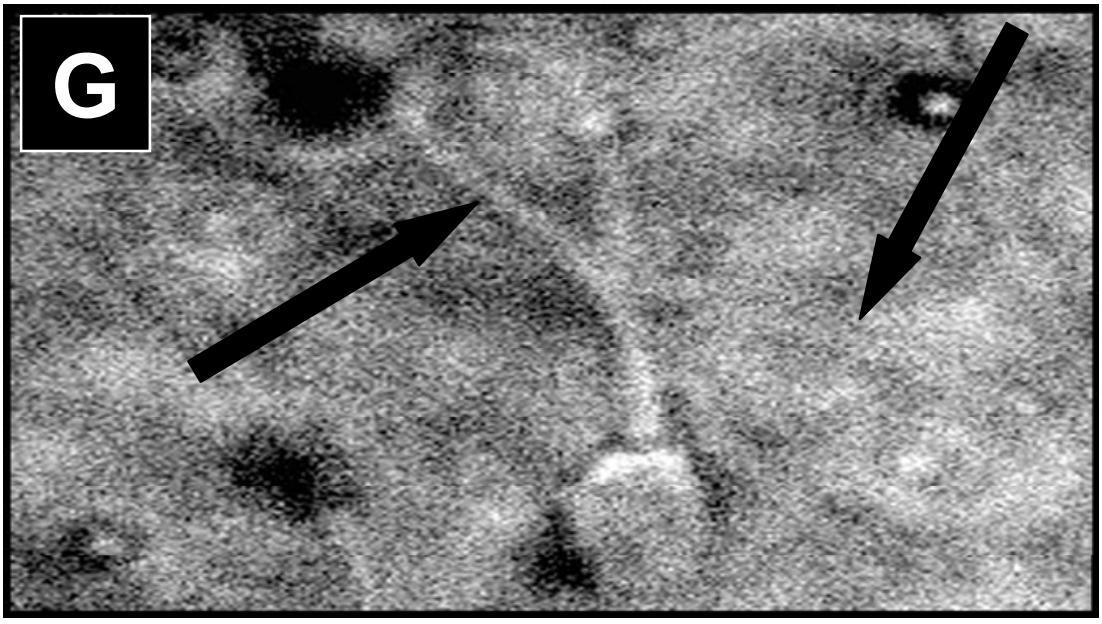
G

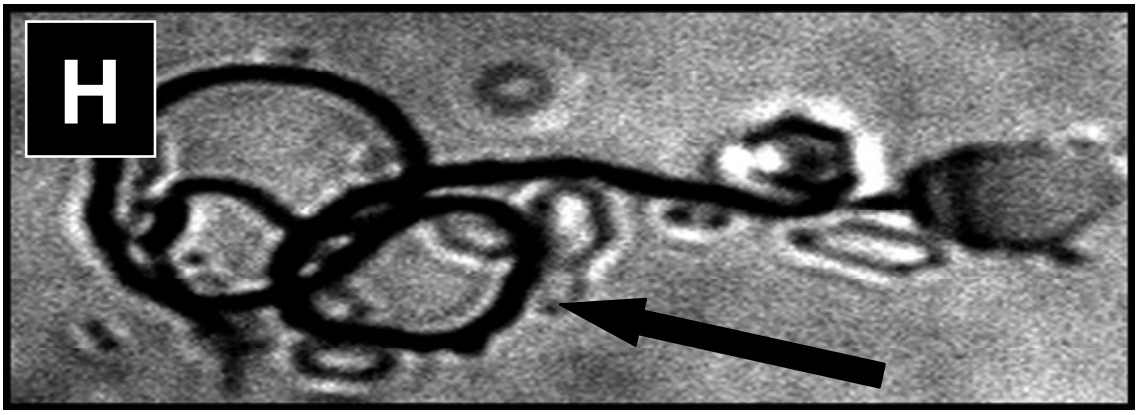
H

Figures 5.3 A-B Fresh Sperm Morphology in Young Adult CON and CR Rhesus Macaques Morphology classifications per ejaculate were normalized into percentages for all descriptive categories. Statistical comparisons were then made by Student's *t*-test ($P<0.05$) using SPSS (SPSS Inc.; Chicago, IL) Each bar, along with SEM, represents mean, normalized data from four treatment animals. In Figure A no significant diet-induced differences were observed between Normal and Abnormal sperm morphology. Figure B shows no significant treatment difference in Abnormal sperm as classified into three categories (Head, Midpiece, Tail).

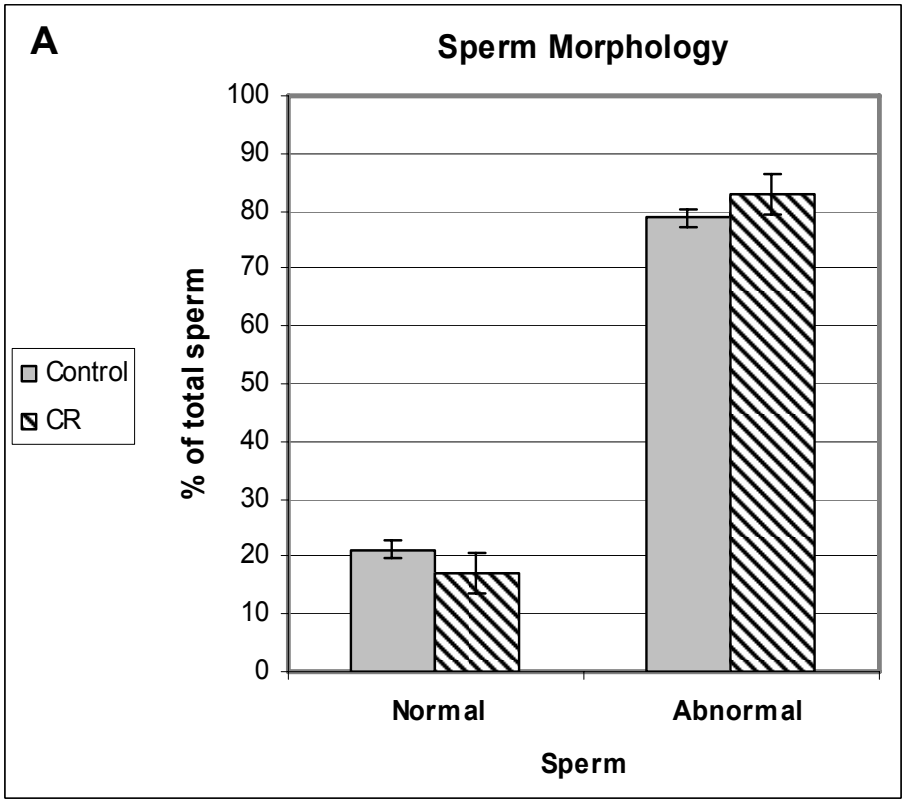
A
Sperm Morphology
100
90
80
70
60
50
40
30
20
10
0
% of total sperm
Control
CR
Normal
Abnormal
Sperm

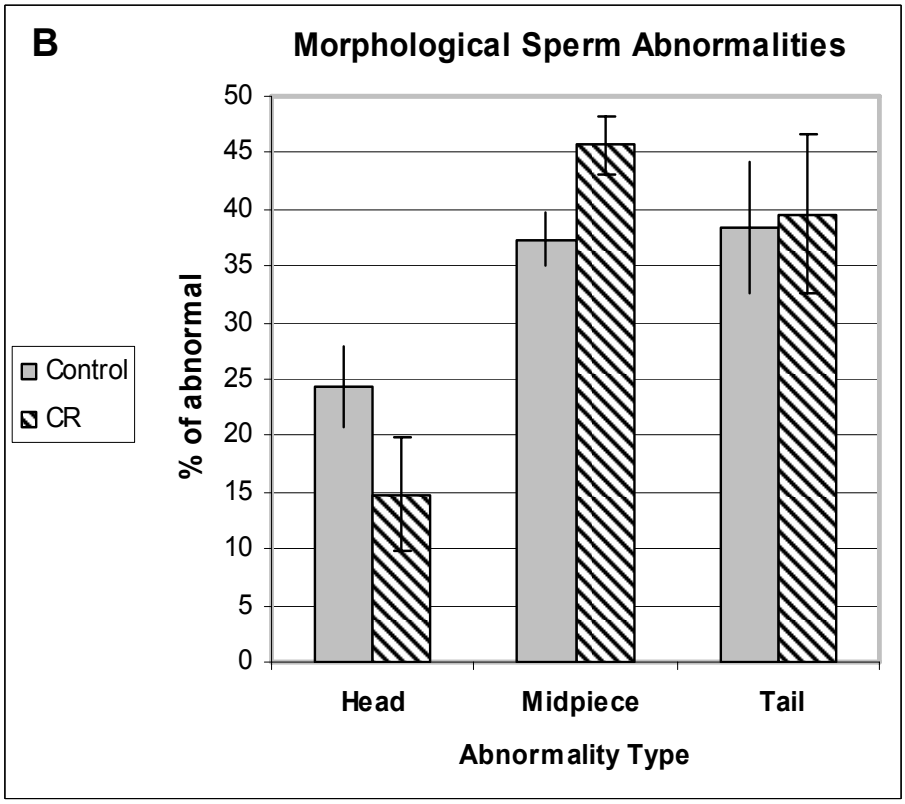
B
Morphological Sperm Abnormalities
50
45
40
35
30
25
20
15
10
5
0
% of abnormal
Control
CR
Head
Midpiece
Tail
Abnormality Type

Sperm Morphology (%)	**CON**	**CR**
Normal	21.3 ± 1.6	17.0 ± 3.6
Abnormal	78.7 ± 1.6	83.0 ± 3.6
Morphological Sperm Abnormalities (% of Abnormal)	**CON**	**CR**
Head	24.3 ± 3.5	14.8 ± 5.1
Midpiece	37.3 ± 2.4	45.7 ± 2.6
Tail	38.4 ± 5.9	39.5 ± 7.0

Table 5.3 Fresh Sperm Morphology Values in Young Adult CON and CR Rhesus Macaques Mean data (± SEM) from the preceding figures are presented in numerical form. No significant differences ($P<0.05$) were observed between the two diet groups for the morphological characteristics.

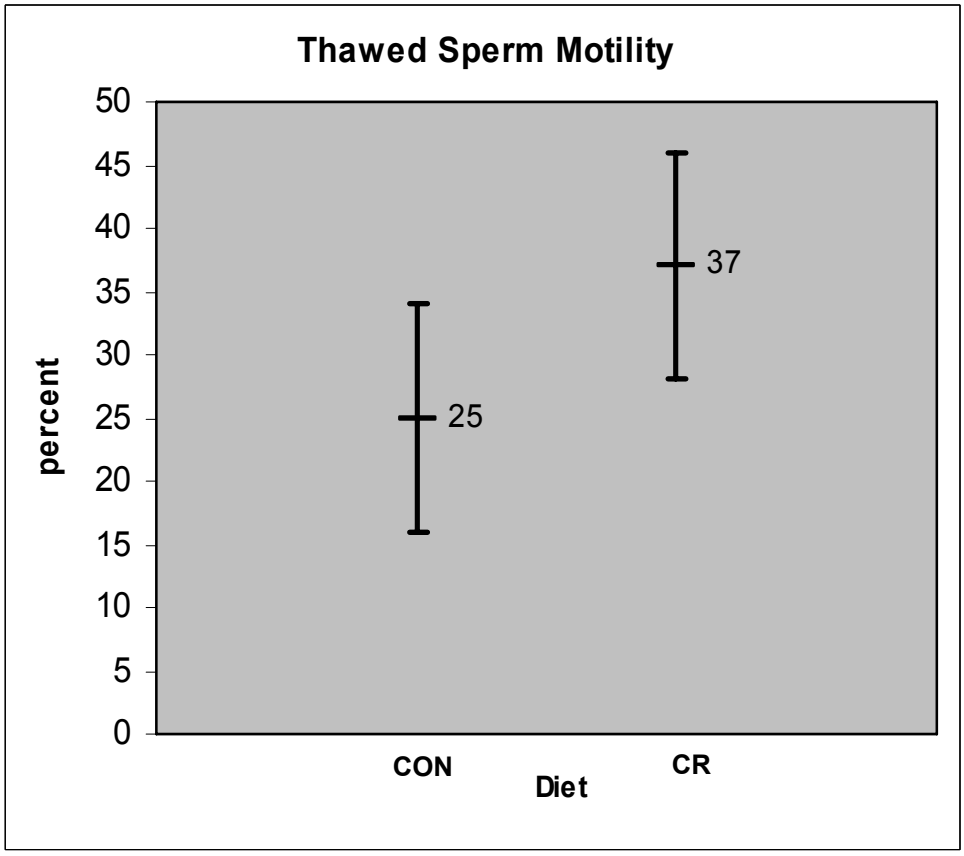

Figure 5.4 Motility of Frozen-Thawed Sperm in Young Adult CON and CR Rhesus Macaques Data for each male was averaged for three collections and then group treatment averages were determined for Young Adult rhesus macaques. Analyses were made between CON and CR by Student's *t*-test ($P<0.05$) using SPSS (SPSS Inc.; Chicago, IL) or Excel (Microsoft; Redmond, WA). Each point, along with SEM, represents mean data from four animals. No significant differences were detected for any of the standard sperm functionality measures.

Table 5.4 Frozen-Thawed Sperm Motility Values in Young Adult CON and CR Rhesus Macaques Mean data (± SEM) from the preceding figure is presented in numerical form. No significant difference ($P<0.05$) was observed between the two diet groups.

	CON	CR
motility (%)	25.0 ± 9.0	37.0 ± 9.0

Figures 5.5 A-B Frozen-Thawed Sperm Morphology in Young Adult CON and CR Rhesus Macaques Morphology classifications of frozen-thawed samples were normalized into percentages for all descriptive categories. Statistical comparisons were then made by Student's *t*-test ($P<0.05$) using SPSS (SPSS Inc.; Chicago, IL) or Excel (Microsoft; Redmond, WA). Each bar, along with SEM, represents mean, normalized data from four treatment animals. In Figure A no significant diet-induced differences were observed between Normal and Abnormal sperm morphology. Figure B shows no significant treatment difference in Abnormal sperm as classified into three categories (Head, Midpiece, Tail).

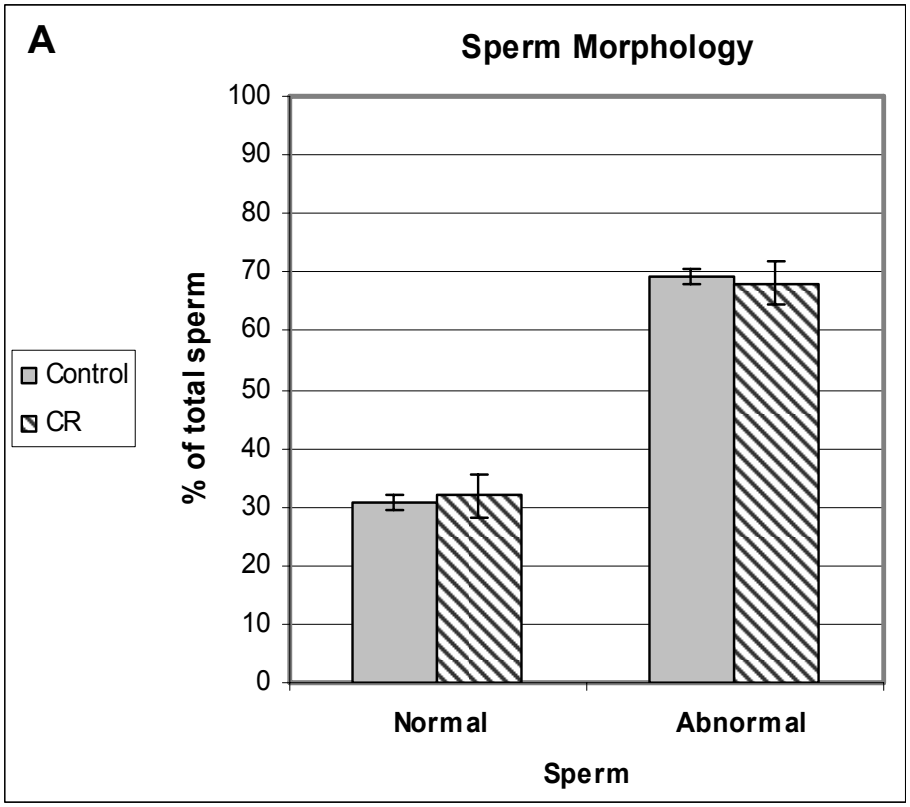
A
Sperm Morphology
100
90
80
70
60
50
40
30
20
10
0
% of total sperm
Control
CR
Normal
Abnormal
Sperm

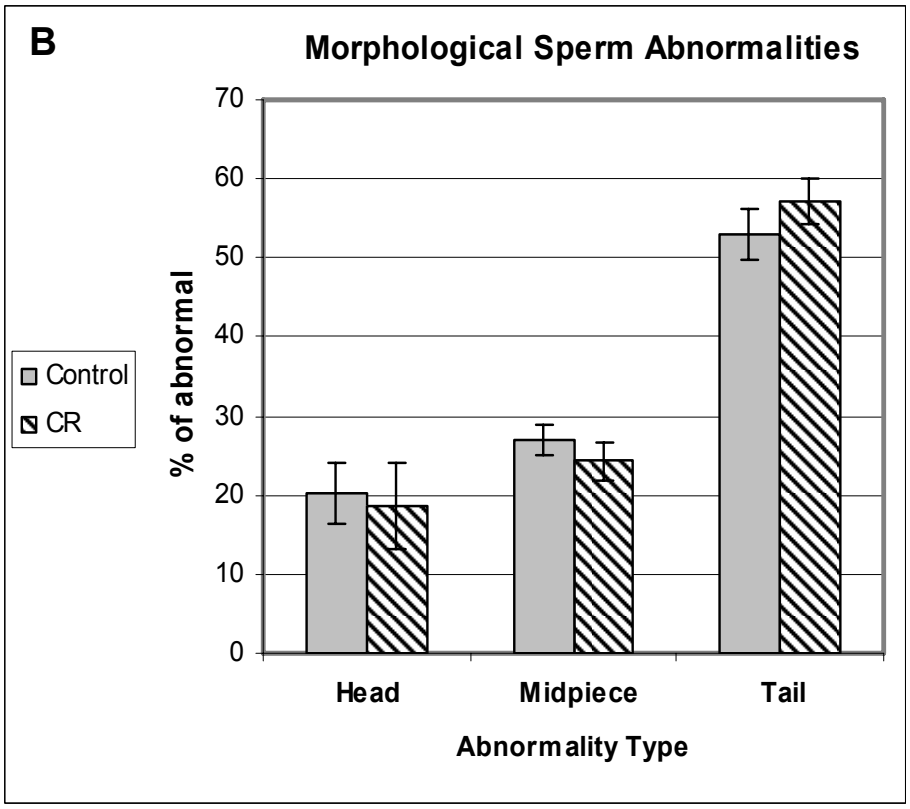
B
Morphological Sperm Abnormalities
70
60
50
40
30
20
10
0
% of abnormal
Control
CR
Head
Midpiece
Tail
Abnormality Type

Sperm Morphology (%)	**CON**	**CR**
Normal	30.6 ± 1.3	69.4 ± 1.3
Abnormal	31.9 ± 3.6	68.1 ± 3.6
Morphological Sperm Abnormalities (% of abnormal)	**CON**	**CR**
Head	20.0 ± 3.9	18.7 ± 5.5
Midpiece	27.0 ± 2.0	24.3 ± 2.5
Tail	53.0 ± 3.2	57.0 ± 3.0

Table 5.5 Frozen-Thawed Sperm Morphology Values in Young Adult CON and CR Rhesus Macaques Mean data (± SEM) from the preceding figures are presented in numerical form. No significant differences ($P<0.05$) were observed between the two diet groups for the morphological characteristics.

Figure 5.6 Example of Staining for ZP Binding and AR Assay The upper image demonstrates Hoescht 33,258 staining of DNA/chromatin. The lower image shows fluorescein isothiocyanate (FITC) double-antibody staining of the sperm acrosomal membrane. By using alternating fluorescent filters we are able to count the total number of sperm bound to each oocyte zonae and their acrosomal status. Experimental results are shown in the table below.

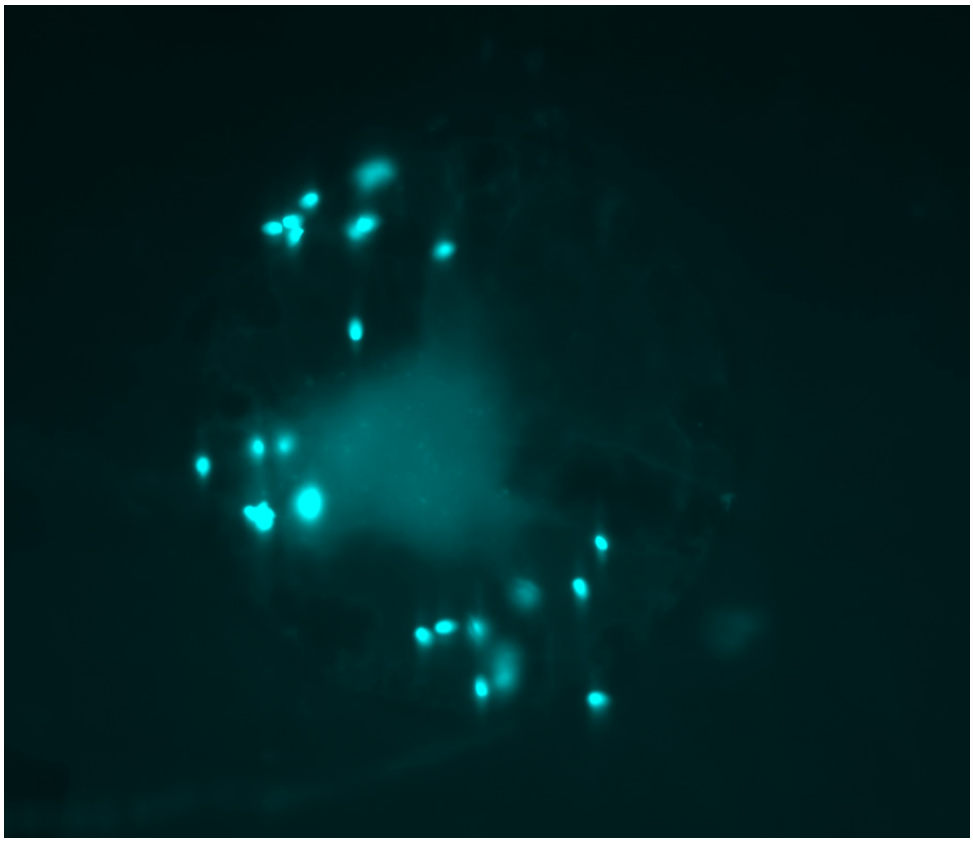

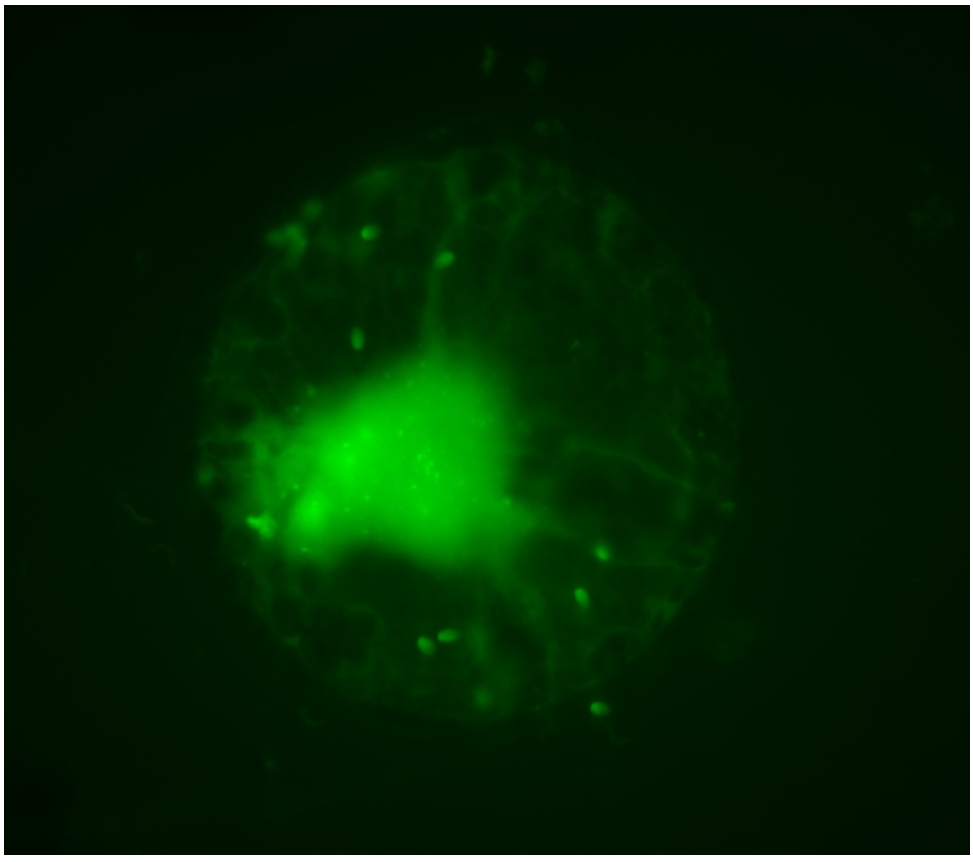

Treatment	No. of sperm/zonae	% acrosome reacted
CON	14 ± 11	0.4 ± 0.4
CR	4 ± 3	1.0 ± 0.8

Table 5.6 ZP Binding and AR Assay Results for Young Adult CON and CR Rhesus Macaques Data for each male was averaged and then group treatment averages were determined. Analyses were made between CON and CR by Student's *t*-test ($P<0.05$) using SPSS (SPSS Inc.; Chicago, IL) or Excel (Microsoft; Redmond, WA). Mean value (± SEM) are from four animals. No significant differences were detected between groups for the number of sperm bound or the percentage of sperm showing reacted acrosomes.

Table 5.7 Individual SCSA® Results for Young Adult CON and CR Rhesus Macaques Experimental findings of the sperm chromatin structure assay for Young Adult CON and CR rhesus macaques are shown. All of the animals appear to have excellent sperm with the exception of CON #22382. This animal would most likely be infertile based on the one sample obtained.

Key:
% Total: DNA Fragmentation Index (DFI; % Moderate + % High)
% Moderate: moderately damaged sperm
% High: highly damaged sperm
%HDS: High DNA Stainability or measure of immature chromatin

DNA Fragmentation Index (%DFI; % sperm cells containing damaged DNA)
a. < 15% DFI = excellent sperm DNA integrity
b. > 15 to < 30% DFI = good sperm DNA integrity
c. > 30% DFI = fair to poor sperm DNA integrity

High DNA stainability (HDS; % cells with immature chromatin)
a. < 15% HDS = normal
b. > 15% HDS = above normal

CONTROL

Sample		DNA Fragmentation Index % Total	% Moderate	% High	% HDS
22388		0.4	0.3	0.1	0.7
		0.2	0.2	0.0	0.7
	Mean	**0.3**	**0.2**	**0.1**	**0.7**
	S.D.	**0.1**	**0.1**	**0.0**	**0.0**

Sample		DNA Fragmentation Index % Total	% Moderate	% High	% HDS
22382		32.4	8.4	24.0	1.4
		32.7	8.5	24.1	2.3
	Mean	**32.5**	**8.5**	**24.1**	**1.9**
	S.D.	**0.2**	**0.1**	**0.1**	**0.6**

Sample		DNA Fragmentation Index % Total	% Moderate	% High	% HDS
22376		0.7	0.5	0.1	0.8
		0.5	0.4	0.1	1.5
	Mean	0.6	0.5	0.1	1.1
	S.D.	0.1	0.1	0.0	0.5
22376		0.6	0.5	0.1	1.4
		0.9	0.5	0.4	1.2
	Mean	0.7	0.5	0.2	1.3
	S.D.	0.2	0.0	0.2	0.1
22376	**Mean (all)**	**0.6**	**0.5**	**0.2**	**1.2**
	S.D.	**0.2**	**0.1**	**0.1**	**0.3**

Sample		DNA Fragmentation Index % Total	% Moderate	% High	% HDS
22387		0.3	0.2	0.1	0.9
		0.2	0.2	0.0	0.9
	Mean	0.2	0.2	0.1	0.9
	S.D.	0.0	0.0	0.0	0.0
22387		0.1	0.1	0.0	0.9
		0.2	0.1	0.0	1.3
	Mean	0.1	0.1	0.0	1.1
	S.D.	0.1	0.0	0.0	0.3
22387		1.2	1.2	0.0	3.2
		0.3	0.3	0.0	2.6
	Mean	0.8	0.7	0.0	2.9
	S.D.	0.6	0.6	0.0	0.4
22387	**Mean (all)**	**0.4**	**0.3**	**0.0**	**1.6**
	S.D.	**0.2**	**0.2**	**0.0**	**0.3**

CR

Sample		DNA Fragmentation Index % Total	% Moderate	% High	% HDS
22389		5.1	3.9	1.2	1.7
		5.2	4.1	1.1	1.5
	Mean	**5.2**	**4.0**	**1.2**	**1.6**
	S.D.	**0.1**	**0.2**	**0.0**	**0.2**

Sample		DNA Fragmentation Index % Total	% Moderate	% High	% HDS
22384		1.7	1.7	0.1	1.9
		1.6	1.5	0.1	1.9
	Mean	**1.7**	**1.6**	**0.1**	**1.9**
	S.D.	**0.1**	**0.1**	**0.0**	**0.0**

Sample		DNA Fragmentation Index % Total	% Moderate	% High	% HDS
22375		0.3	0.3	0.0	3.0
		0.2	0.2	0.0	2.9
	Mean	0.3	0.2	0.0	3.0
	S.D.	0.1	0.1	0.0	0.1
22375		1.0	0.8	0.3	2.1
		1.1	0.8	0.3	2.3
	Mean	**1.0**	0.8	0.3	**2.2**
	S.D.	0.0	0.0	0.0	0.2
22375	**Mean (all)**	**0.6**	**0.5**	**0.1**	**2.6**
	S.D.	**0.0**	**0.0**	**0.0**	**0.1**

Sample		DNA Fragmentation Index % Total	% Moderate	% High	% HDS
22371		0.0	0.0	0.0	0.8
		0.1	0.1	0.0	0.8
	Mean	0.1	0.1	0.0	0.8
	S.D.	0.1	0.0	0.0	0.0
22371		0.2	0.2	0.1	3.1
		0.4	0.3	0.1	4.2
	Mean	**0.3**	0.2	0.1	**3.7**
	S.D.	0.1	0.1	0.0	0.8
22371		0.3	0.2	0.1	1.2
		0.3	0.2	0.1	1.2
	Mean	**0.3**	0.2	0.1	**1.2**
	S.D.	0.0	0.0	0.0	0.0
22371	**Mean (all)**	**0.2**	**0.2**	**0.1**	**1.9**
	S.D.	**0.1**	**0.1**	**0.0**	**0.3**

Table 5.8 Mean DNA Fragmentation Index for Young Adult CON and CR Rhesus Macaques Data for each male was averaged and then group treatment averages were determined. Analyses were made between CON and CR by Student's *t*-test ($P<0.05$) using SPSS (SPSS Inc.; Chicago, IL) or Excel (Microsoft; Redmond, WA). Mean value ($\pm$ SEM) are from four animals. No significant differences were detected between groups for the sperm chromatin structure assay.

	CON	**CR**
DFI (%)	8.5 $\pm$ 8.0	1.9 $\pm$ 1.1

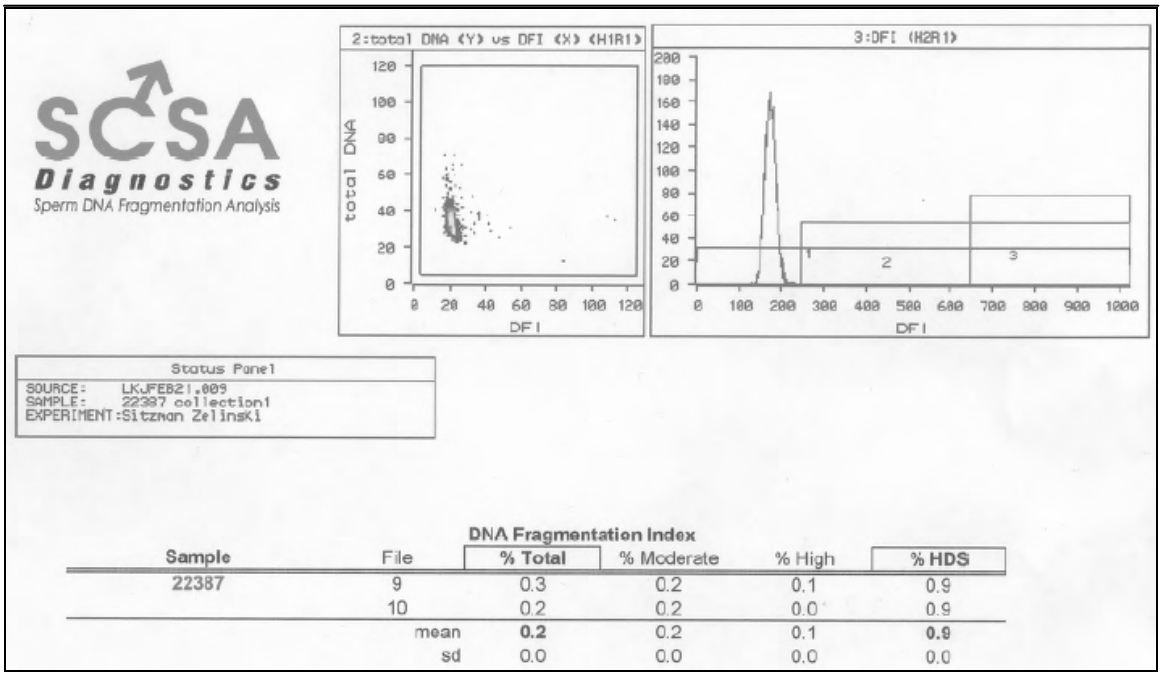

DNA Fragmentation Index

Sample	File	% Total	% Moderate	% High	% HDS
22387	9	0.3	0.2	0.1	0.9
	10	0.2	0.2	0.0	0.9
	mean	**0.2**	0.2	0.1	**0.9**
	sd	0.0	0.0	0.0	0.0

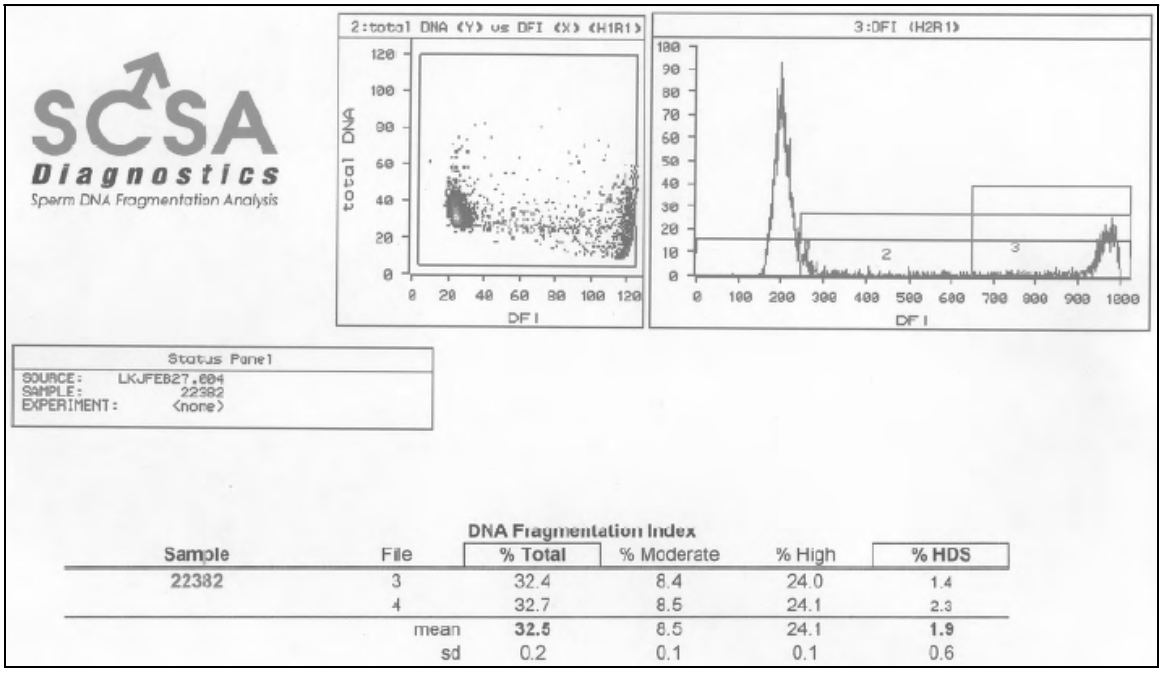

DNA Fragmentation Index

Sample	File	% Total	% Moderate	% High	% HDS
22382	3	32.4	8.4	24.0	1.4
	4	32.7	8.5	24.1	2.3
	mean	**32.5**	8.5	24.1	**1.9**
	sd	0.2	0.1	0.1	0.6

Figure 5.7 Representative Sperm Chromatin Structure Assay Output Example of output provided by SCSA® Diagnostics on two rhesus macaque sperm samples. The upper data sheet displays a high quality sample with a very low DNA Fragmentation Index (DFI). The lower data sheet shows a DFI above 30% meaning that sperm from this animal would have reduced pregnancy success whether from intercourse, intrauterine insemination, *in vitro* fertilization or intracytoplasmic sperm injection.

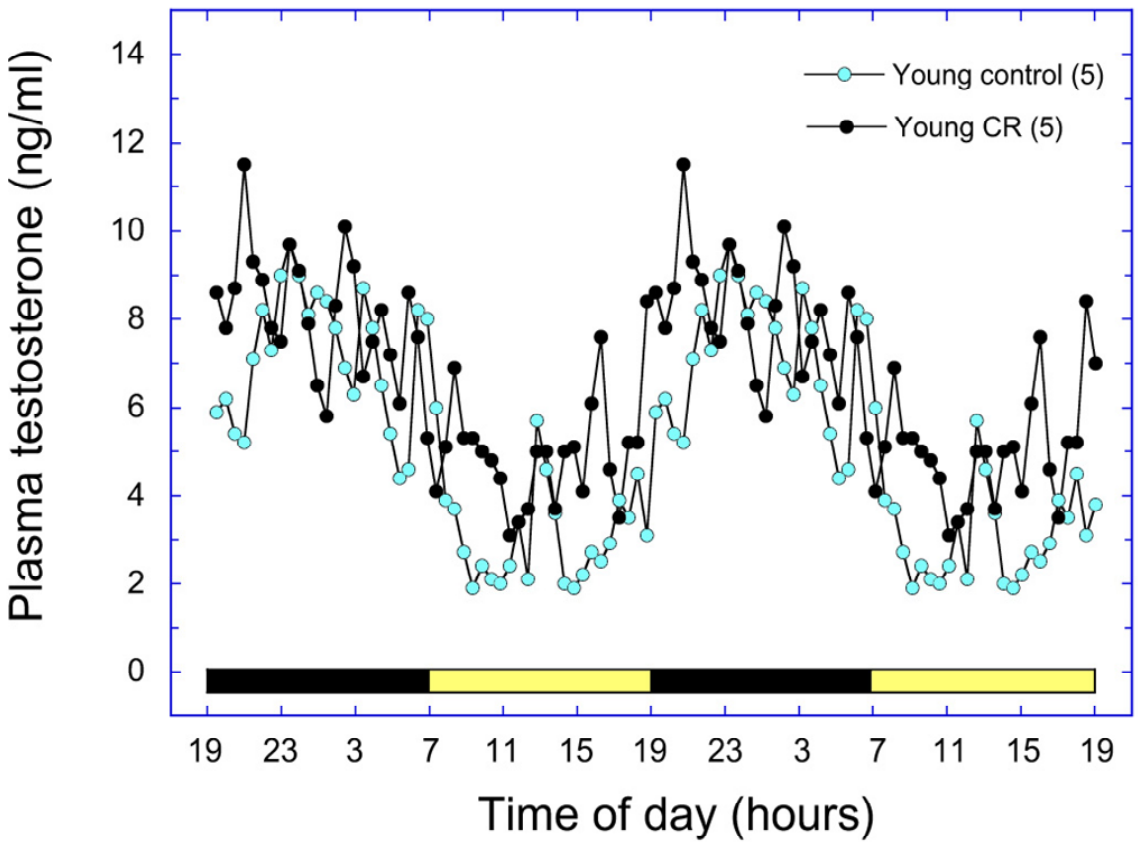

Figure 5.8 Daily Circulating Plasma Testosterone Levels for Young Adult CON and CR Rhesus Macaques Plot shows similar pattern of daily circulating testosterone in both treatment groups. Data from a single 24-hour period is double plotted in order to better visualize the circadian expression pattern.

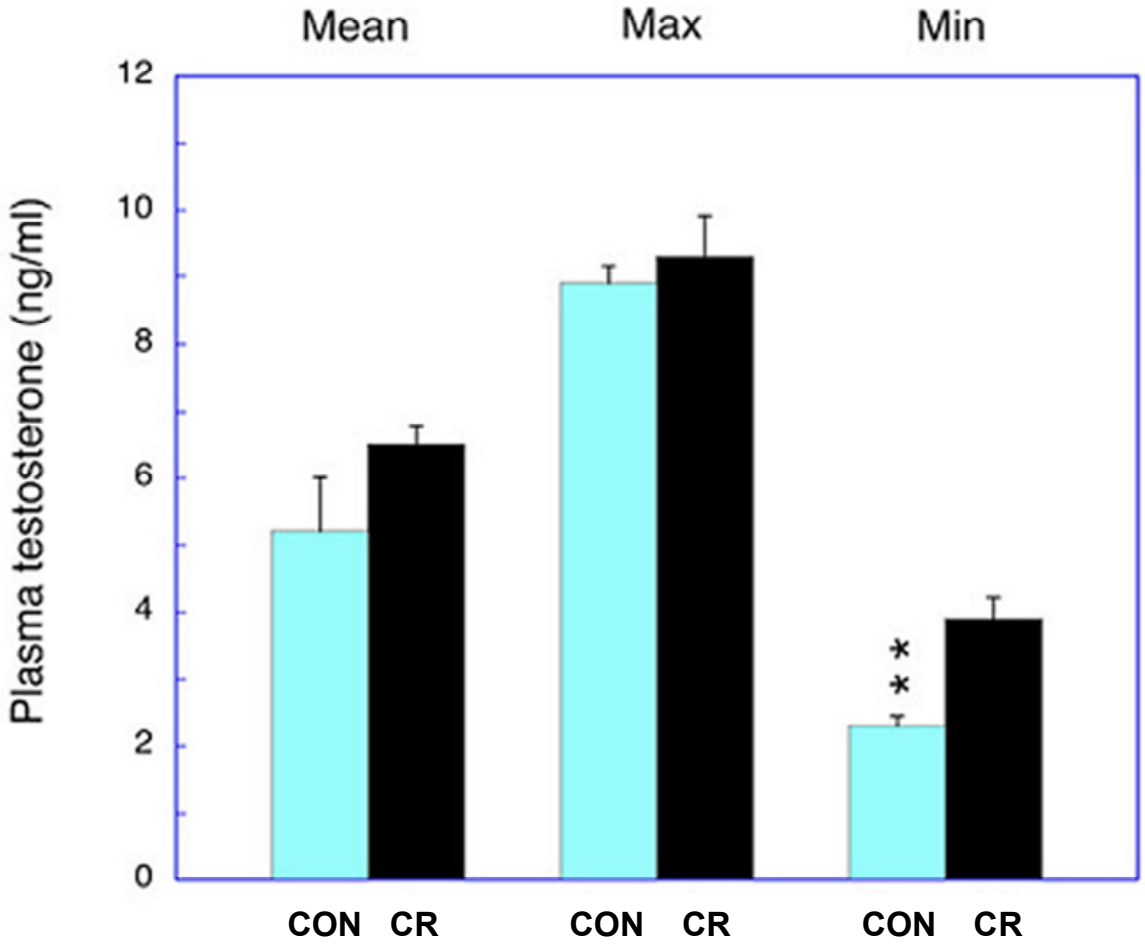

Figure 5.9 Mean, Maximum and Minimum Daily Plasma Testosterone Levels for Young Adult CON and CR Rhesus Macaques Data are expressed as group mean ± SEM with n=5 for each treatment. Statistical comparisons between CON and CR groups were made by Student's *t*-test with significant differences established at $P<0.05$. No significant differences were detected for mean or maximum circulating T levels, but minimum T levels were significantly lower ($P<0.01$) for CON animals compared to their calorie restricted counterparts.

CHAPTER 6

GENERAL DISCUSSION

Biological aging represents a complex, multifactorial cascade of events that occurs simultaneously at molecular, cellular and systemic levels, resulting in disruption of an organism's homeostatic mechanisms and ability to respond to stress. Aging thus leads to a progressive loss of function, including reproductive capacity, accompanied by increasing incidence of disease and mortality. The objectives of this project were to: 1) analyze neuroendocrine changes to the HPG axis that occur with aging and 2) evaluate the effects of moderate CR on reproductive function in male rhesus macaques.

There are many theories that attempt to explain senescence, each which may adequately describe some or all of the observed processes alone or in combination with other theories. The *Disposable Soma Theory* proposes that organisms may have the innate ability to shift metabolic resources from growth and reproduction to improved somatic maintenance and repair, effectively slowing the aging process and prolonging disease resistance and health (Kirkwood and Austad, 2000; Miller et al., 2002). The *Gene Regulation Theory* proposes that senescence results from changes in gene expression. One example of this is the identification of an insulin-like signaling pathway or its homolog that can modify lifespan in yeast, nematodes, flies and mice (Kenyon, 2001; Weinert and Timiras, 2003). The *Free Radical Theory* proposes that aging is caused by cumulative oxidative damage generated by free radical-containing

reactive oxygen species produced during normal cellular respiration (Koubova and Guarente, 2003; Weinert and Timiras, 2003). A growing body of evidence implicates mitochondrial derived ROS as a major cause of cellular decline and a direct relationship between individual age, species longevity and rate of ROS production has been documented (Gredilla and Barja, 2005; Kirkwood and Austad, 2000; Weinert and Timiras, 2003). The *Neuroendocrine Theory* proposes that aging is a result of neural and endocrine functional changes which are crucial for coordinating an organism's response to its environment and maintaining an optimal functional state to balance reproduction and survival (Weinert and Timiras, 2003).

Regardless of the causes, aging occurs in all biological systems. Over the last 75 years calorie restriction has been established as the only proven non-genetic method of altering longevity and attenuating biological changes associated with aging (Koubova and Guarente, 2003; Lane et al., 1999b; McCay et al., 1935). To date, this nutritional paradigm has been found to be effective in protozoa, yeast, rotifers, fleas, nematodes, spiders, flies, mollusks, fish, mice, rats, dogs and possibly non-human primates such as squirrel monkeys and cynomolgus and rhesus macaques (Ingram et al., 1990; Lane et al., 1999b; Roth et al., 1999; Weindruch and Walford, 1988). Not only is CR effective for extending lifespan but it also demonstrates widespread, beneficial health effects on almost every physiological system within the organism. Researchers have shown that CR can reduce body mass and adiposity, lower body temperature and blood pressure, decrease glucose and fasting plasma insulin levels while

increasing insulin sensitivity and high density lipoprotein levels, and reduce oxidative stress (Gredilla and Barja, 2005; Gresl et al., 2001; Heilbronn and Ravussin, 2003; Koubova and Guarente, 2003; Lane et al., 1997). Its long history notwithstanding, however, very little is known with regard to the exact mechanism(s) of CR action.

The potential health benefits of CR could be very valuable, especially in developed societies where life expectancy is increasing and demographics are shifting to an older population. Many reports from scientific and mainstream sources in the United States warn of an impending healthcare crisis and financial difficulties of dealing with an aging population and the medical challenges that inevitably follow. Additionally, the recent phenomenon of increased average body mass index (BMI) experienced by the Western world has resulted in an increased incidence of obesity and manifestations of poor health including type II diabetes, heart disease, stroke and high blood pressure. The consequences of increased BMI negatively impact reproductive potential as well, with men experiencing lower sperm concentrations and total sperm counts (Jensen et al., 2004), while also demonstrating an inverse relationship between BMI and total number of motile sperm cells and a positive relationship between BMI and sperm DNA fragmentation per subject (Kort et al., 2006).

These kinds of statistics and data do not bode well for a population that has delayed child-bearing for a number of socioeconomic reasons. Since 1980, in the United States, there has been an upward trend in the average age of couples having children (Buwe et al., 2005) with a 16-24% increase in the birth

rate for fathers over age 35 years (Buwe et al., 2005; Eskenazi et al., 2003; Kidd et al., 2001). One consequence of reproductive decline is infertility with approximately 25-50% of conception difficulties attributable to male factors, making it the single most common cause of infertility in clinical cases (Agarwal and Said, 2003; Eskenazi et al., 2003; Kidd et al., 2001; Larson-Cook et al., 2003).

Reproductive aging in men typically follows a gradual course where decline may be due to functional deterioration at several sites including reduced testosterone production, decreased hypothalamic gonadotropin-releasing hormone and altered pituitary gland release of gonadotropins (Harman et al., 2001; Moffat et al., 2002; Ottinger, 1998). In men testosterone is responsible for regulation of gonadotropin secretion by the hypothalamic-pituitary system and predominantly drives spermatozoa production. Although the impact of its decline on reproductive senescence is not completely understood, there is the potential for a cascade effect to the entire reproductive system with its fall. Testosterone loss can also result in weakened muscle function, decreased bone density and degradation of other physiological parameters related to overall aging (Harman et al., 2001; Moffat et al., 2002). Also of importance is the neurological impact of testosterone decline. Men with Alzheimer's disease (AD) have significantly lower T levels than aged men without AD. Importantly, testosterone depletion appears to occur before clinical and pathological diagnosis of AD, suggesting that low T contributes to AD pathogenesis rather than results from it (Rosario et al., 2006).

Other parameters of reproductive function and fertility in elderly men have traditionally focused on semen analysis. For conventional spermiogram measures the weight of scientific evidence suggests that increased male age is associated with undesirable changes in reproductive potential such as decreased semen volume (Henkel et al., 2005; Kidd et al., 2001), increased DNA fragmentation (Evenson and Wixon, 2006), lower sperm motility (Eskenazi et al., 2003; Zubkova and Robaire, 2006) and increased sperm abnormalities (Kidd et al., 2001; Zubkova and Robaire, 2006). In general, however, most measures of male reproductive health exhibit no evidence of an age 'threshold' but rather display gradual changes over time (Eskenazi et al., 2003).

Since calorie restriction is capable of reducing body mass and adiposity and improving general health parameters, it would be of great benefit to know if CR could also maintain reproductive fitness and attenuate age-related changes. The National Institute on Aging's study of CR in rhesus macaques (Ingram et al., 1990) has shown positive health effects paralleling those observed in other species. Could moderate CR, which was implemented in these animals post-pubertally, also improve male reproductive health parameters? Alternatively, could it have no impact or even an unfavorable effect on reproductive outcome or the neuroendocrine system?

Throughout life and during specific mammalian life stages the HPG axis is responsible for a number of circadian activities including rhythmic release of GnRH, ACTH, luteinizing hormone and growth hormone (Griffin and Ojeda, 2000; Knobil et al., 1994). In fact, the levels of most reproductive hormones, such

as testosterone, are regulated in a circadian fashion in mammals (Jilg et al., 2005; Sehgal, 2004). Pituitary gland gene expression profiling and semi-quantitative RT-PCR in our first experiment showed circadian clock mechanism components present in Juvenile, Young Adult and Old Adult macaques and demonstrated age differences in *Per2* expression. This is an important finding since there are well documented alterations in circadian organization during aging, including changes in hormonal rhythms, core body temperature, sleep/wake cycles, activity and locomotor patterns, behavioral responses, and response to the phase-shifting effects of light (Asai et al., 2001; Hofman and Swaab, 2006; Oster et al., 2003). Despite these overt signs, however, the physiological underpinnings for the circadian dysregulation remain unclear. Due to its unique position in the HPG axis, age-related changes in the pituitary gland and its clock components could be responsible for many of these physiological manifestations.

Pituitary gland gene expression profiles of Young Adult CON and CR macaques in our study detected potential differential expression in <150 probesets. Changes in *TSHR* and *CGA* expression, as measured by sqRT-PCR, were observed resulting in lower levels for both genes in CR-treated animals. Other genes associated with reproduction, metabolism and oxidative stress showed no treatment effects. The biological relevance of these observations is unknown, but it may be connected to two well-documented CR-induced metabolic adjustments, lower core-body temperature (Heilbronn et al., 2006; Lane et al., 1996; Mattison et al., 2003; Roth et al., 2000; Weindruch and

Walford, 1988) and suppression of the thyroid axis as measured by lower TSH and thyroid hormone levels (Gredilla and Barja, 2005; Heilbronn and Ravussin, 2003; Koubova and Guarente, 2003; Mattison et al., 2001).

These two phenomena may be linked, as a depression in body temperature often indicates a reduction in the rate of oxygen consumption. The hypometabolic state imposed by CR is reflected by the approximately 50% reduction in serum triiodothyronine hormone concentrations (Weindruch and Sohal, 1997). Because calorie restriction is a nutritional paradigm, impact on an animal's metabolism is a likely mode of action. In fact, several hypotheses related to the mechanisms of CR's biological effects are linked to reduced (or more efficient) processing of energy (Heilbronn and Ravussin, 2003; Mattison et al., 2003; Weinert and Timiras, 2003). The changes in TSHR and CGA mRNA expression in our CR animals indicate a modification of the metabolic pathway and could potentially correlate with these kinds of physiological responses. While the changes may have been subtle, this line of investigation is still very important since mRNA expression has the potential to cause or inhibit temporal dysregulation of gene expression, a principal factor in cellular malfunction and disease.

Our third experiment profiled testicular gene expression in Young Adult CON and CR animals and found diet-related changes in <300 probesets, although mRNA expression was not altered based on sqRT-PCR and real-time RT-PCR for a large group of selected genes. Having found limited impact of CR in Young Adult subjects, we retrospectively analyzed the effect of CR on gene

expression in an aging series of rhesus macaque testicular tissue. Here we observed age-related and/or diet-induced changes in *HSD17β3*, *INSL3*, *CSNK1E* and *CGA* expression with *CGA* in Old Adult CR subjects returning to youthful levels. This matched results of our pituitary gland gene expression experiment where significantly different levels of *CGA* were observed between treatment groups. In both instances the CR-treated group exhibited lower levels of expression, and in the case of the Old Adult CR subjects, testicular *CGA* was restored to the level of Juvenile and Young Adult expression. Unlike the connection to *TSHR* in the pituitary gland, however, *CGA* in the testis may be playing a role as a paracine factor of gonadal function where differences in expression may indicate a more tightly regulated feedback mechanism. Most importantly there were no observable differences in expression levels between Old Adult animals and their age-matched CR-treated counterparts. These results suggest that CR can elicit general beneficial health effects without negative consequences on the gonadal portion of the HPG axis.

Normal spermiogram measures, ZP binding, AR assay and SCSA® for Young Adult CON and CR macaques indicated no differences between groups. It is worth noting that in every instance, with the exception of sperm viability, biological variation in the CR-treated animals was similar or less than that measured in their CON counterparts. In fact, upon analysis, variation was found to be significantly different for sperm count (P<0.04) and trended toward significance for three other ejaculate parameters: volume, weight and osmolarity (P<0.06-0.11). This may be an indication that the body has experienced a

metabolic shift to a more efficient strategy of life maintenance as these parameters appeared to be more tightly regulated in our CR-treated animals. Both groups exhibited similar daily testosterone profiles with no difference in mean or maximum levels, however, daily minimum testosterone levels were lower in the CON group. The biological relevance of this is uncertain, but it may be another indication of physiological efficiency. By decreasing the daily swing between maximum and minimum levels and maintaining tighter control over T release, CR animals may be able to divert energy toward more critical functions of life maintenance. This may in turn account for the decreased variability observed in the majority of our spermiogram parameters. Taken together, our data demonstrate that moderate CR was not detrimental to semen quality in adult rhesus macaques based on the spermiogram parameters observed; thus, CR could potentially be executed without causing problems with testicular physiology.

The more promising aspect of our study could be in regard to the observed CR-modified testosterone levels. Because declining testosterone may cause weakened muscle function, lower bone density and loss of cognitive function, it would be of great benefit if CR were shown to maintain T levels. Studies in Brown Norway rats have shown that CR initiated at 4 months of age and applied continuously for 30 months results in significantly higher concentrations of serum testosterone concentration compared to controls, suggesting that long-term CR can transiently suppress the reductions in steroidogenesis that are characteristic of aging (Chen et al., 2005). Should CR

be shown to elicit the same biological response in a nonhuman primate model, it could potentially be implemented as a counterbalancing force in human aging. This could have far-reaching social consequences by improving quality of life issues including immune function, bone and muscle health, libido and cognition.

Animals in our study previously demonstrated CR-induced attenuations of age-related changes and improved health parameters (Mattison et al., 2003; Roth et al., 2002). Findings even suggest a metabolic shift from growth and reproduction toward a strategy of life maintenance (Roth et al., 2004). In all of our studies, we found negligible impact of CR on neuroendocrine or reproductive function in the male rhesus macaque. The observed changes in gene expression and T levels, however, may be regulating diverse physiological responses due to their key location in the HPG axis and their critical functional importance. As to how these variations are connected, the answer may come from the study of toxicology.

Hormesis, in a toxicological context, implies that small doses of toxin may have long term benefits in conditioning an organism's enhanced stress responses. Biologically, the Hormesis Hypothesis states that CR is not simply a passive effect of nutrient deprivation, but a highly conserved active defense response that appeared early in evolutionary history to increase an organism's chance of surviving adversity (Sinclair, 2005). Without discerning the specific mechanisms behind it, the hypothesis asserts that low calorie intake is a mildly stressful condition that provokes a positive compensatory response enabling the

organism to survive environmental perturbations by altering metabolism and increasing defenses against aging.

The appeal of the Hormesis Hypothesis is that it explains so many different observations about CR, ranging from the ability of CR cells/animals to withstand stress, to the finding that lower organisms have conserved stress response pathways that lengthen lifespan, to the link between CR and the endocrine system. It may even be that many of the current hypotheses of aging and CR stem from researchers attempting to describe different parts of the same phenomenon. In this regard the Hormesis Hypothesis may be able to unite disparate parts of other hypotheses that have until now not been connected.

One example of a possible hormetic response in our studies may be the real-time PCR results for testicular StAR expression. An age-related decline in StAR mRNA and protein in the testis has been observed in rodents (Luo et al., 2001). We observed a similar age-related decline in mRNA expression from Juvenile to Young Adult and Old Adult macaques. Our study also included Old Adult subjects that had been calorie restricted for the previous five years. These animals appeared to have StAR levels similar to the Juvenile group, but also exhibited a great deal of variability in expression. This variability confounded the results, thus providing no significant differences between any of the groups. Is it possible, however, that CR was triggering a hormetic response in the OACR group and as a result StAR was returning to more youthful levels? Was the true biological response to CR execution simply masked by the late age of CR onset in our subjects? One way to truly determine what was occurring is to track a large

cohort of macaques over time using the measures utilized in our experiments. This is difficult to do, however, due to expense and the large number of animals required for sampling at multiple timepoints.

The downside of the Hormesis Hypothesis is that it does not determine the proximal causes of senescence but instead targets longevity regulators which in turn counter aging. It is similar to putting gas in a car to go somewhere, but having no idea or care that there is a combustion engine driving the process. Most people may not need to have a functional understanding of the machinery, but science doesn't work that way; it needs to understand the driving forces behind phenomena. This is especially true with CR because even if advantageous health benefits can be achieved without negative consequences to the male HPG axis, it is unlikely that most people could adhere to the strict dietary regimen. Thus, an understanding of the biological mechanisms responsible for its effects is necessary if we are to develop alternative strategies of implementation. For that reason it would be an exciting possibility to undertake a collaborative relationship with the Pennington Biomedical Research Center in Louisiana and their ongoing human studies. In doing so we could monitor the possible effects of CR on male reproduction in a population adhering to a diet which is feasible for most people.

Based on our studies, pituitary gland and testicular gene expression and gonadal function appear resistant to CR-induced changes. Such stability may correlate with lifetime reproductive strategies and species-specific life histories and is not necessarily unexpected as it would be disconcerting for components of

a primary axis, such as the HPG, to be fluctuating too broadly under anything less than pathological conditions. With CR, however, there may be a few key components that are carefully modified in such a way as to affect multiple physiological responses simultaneously. Calorie restricted animals may, in effect, be walking a finer biological tightrope between somatic maintenance and reproduction than that experienced by free-feeding animals. In the case of males, where the energy investment in continuous reproductive capacity is minimal, it may be more efficient to fine-tune rather than cease sperm production completely due to the time and energy requirements necessary to restart the system. Ultimately I hope this work will have contributed in some small way to the eventual understanding of calorie restriction and its relevance to male reproductive aging.

There is only one thing for it then - to learn.
Learn why the world wags and what wags it.

- T.H. White, 1906 -1964

Appendix A: Protocol for RNA Extraction of Pituitary Gland and Testes Tissue

1. Set up for the area where extraction is to be performed is extremely important. Use a biological safety cabinet that can be maintained as RNA/RNase free as possible. Use the ultraviolet light for 10 minutes prior to using the hood in order to destroy any RNase from mold or bacteria.
2. It is extremely important to clean all equipment before extraction with RNase Zap® and to change/spray gloves regularly. Using filtered pipet tips will also help limit potential contamination.
3. The homogenizer should be cleaned prior to use and between samples by running the blade in the following:
    a. DEPC water (diethylpyrocarbonate, one 50 mL volume)
    b. 70% EtOH (one 50 mL volume)
    c. chloroform (one 50 mL volume)
    d. Probe should be wiped and dried with tissue between each step
4. Determine the tissue to be used and how it was harvested, stabilized, and stored. If necessary excise the sample from the complete tissue. How this is done will depend on how the tissue was stored (i.e. RNAlater or LNO_2). LNO_2 preserved tissue can be cut on an aluminum foil-wrapped block of dry ice while RNAlater tissue can be cut at room temperature (RT, although the dry ice method is preferred).
5. Determine the starting amount of sample/tissue and record.
6. Place the tissue in a 2 mL flat-bottom microcentrifuge tube and add the appropriate volume of Buffer RLT lyses solution. The buffer is supplied in the Qiagen RNeasy Mini Kit but must have β-mercaptoethanol added to it prior to use (10 µL 14.3M β-ME / mL Buffer RLT). Solution is stable for one month at RT.
    a. < 20 mg 350-600 µL RLT (600 µL if tissue was in RNAlater)
    b. 20-50 mg 600 µL RLT
7. Homogenize tissue immediately for 20-40 seconds using a Rotor-stator homogenizer. Do not load all tissue samples and then homogenize.
8. Spin lysate in tabletop microcentrifuge for 5 minutes at maximum speed (13,000RPM) with tabs out.
9. After centrifugation pipet the supernatant to a new 2 mL flat-bottom microcentrifuge tube. Be careful to avoid transferring the pellet or any lipid layer that may be on the surface of the supernatant.
10. Add 1 volume of molecular grade 70% ethanol (ex. add 600 µL EtOH if 600 µL RLT was used). Mix by pipeting and continue immediately.
11. Apply up to 700 µL of sample to the Qiagen column placed inside a 2 mL collection tube. Centrifuge for 30 seconds >8000G (>10,000RPM). If the original sample was in a volume >700 µL this step will have to be repeated using the same column (i.e. elute-centrifuge-elute-centrifuge-continue).
12. Move filter to a new 2 mL collection tube and discard the flowthrough tube.
13. Add 700 µL of Buffer RW1 to the RNeasy column. Allow to sit for two minutes at RT with lid closed.

14. Centrifuge for 30 seconds at >8000G to wash the column.
15. Move filter to a new 2 mL collection tube and discard the flowthrough tube.
16. Add 500 µL Buffer RPE to the RNeasy column. Allow to sit for 5 minutes at RT with lid closed.
17. Centrifuge for 30 seconds at >8000G.
18. Move filter to a new 2 mL collection tube and discard the flowthrough tube.
19. Add another 500 µL Buffer RPE and centrifuge for 1 minute at >8000G.
20. Move filter to a new 2 mL collection tube and discard the flowthrough tube.
21. Centrifuge again for 2 minutes to eliminate the RPE buffer completely.
22. Transfer column to a final 2 mL collection tube. This tube will be used for storage so it should be labeled clearly. Leave the cap off the column and open for 5 minutes so as to completely dry the filter.
23. To elute the RNA pipet 40 µL of RNase-free water directly onto the membrane. Allow to sit for 2-3 minutes at RT.
24. Centrifuge for 1 minute at >8000G.
25. Place total RNA extract on ice as quickly as possible.
26. RNA quality and concentration can be analyzed by microcapillary electrophoresis (bioanalyzer) prior to being used for microarray hybridization. A good quality RNA sample will have two ribosomal peaks on the bioanalyzer output at 18S (first peak) and 28S. The graph should have a low, constant baseline with sharp peaks; a degraded sample will show an abnormal profile. The next page shows an example of successful extraction results from our experiments as determined by model 2100 Agilent Bioanalyzer (Santa Clara, CA).

Bio_Sizing_Total-RNA-Nano_2005-09-13_18-28-08 Page 1

Assay: Eukaryote Total RNA Nano
Data Path: C:\Program Files\Agilent 2100 Bioanalyzer\Bio Sizing\Data

Read: 9/13/2005 6:28:08 PM (A.02.12 SI292)
Modified: 9/13/2005 6:52:25 PM (A.02.12 SI292)

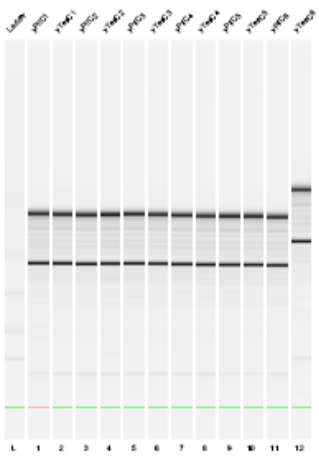

Instrument: G2938B, Serial# DE24802791, Firmware Version A.01.16
Assay: C:\Program Files\Agilent 2100 Bioanalyzer\Bio Sizing\Assays\RNA\Eukaryote Total RNA Nano.asy
Title: Eukaryote Total RNA Nano
Version: 1.4
Comments: Copyright 1999 - 2002 Caliper Technologies Corp.

Ladder Concentration:	150 ng/ul	Baseline:	19 Seconds
Min Peak Height:	0.5 (above baseline)	Filter Width:	1 Seconds
Slope Threshold:	0.8 /Second	Baseline Plateau:	0.5 Seconds
Min Peak Width:	0.5 Seconds	Polynomial Order:	6
Start Time:	20 Seconds		
End Time:	69 Seconds		

Notes:

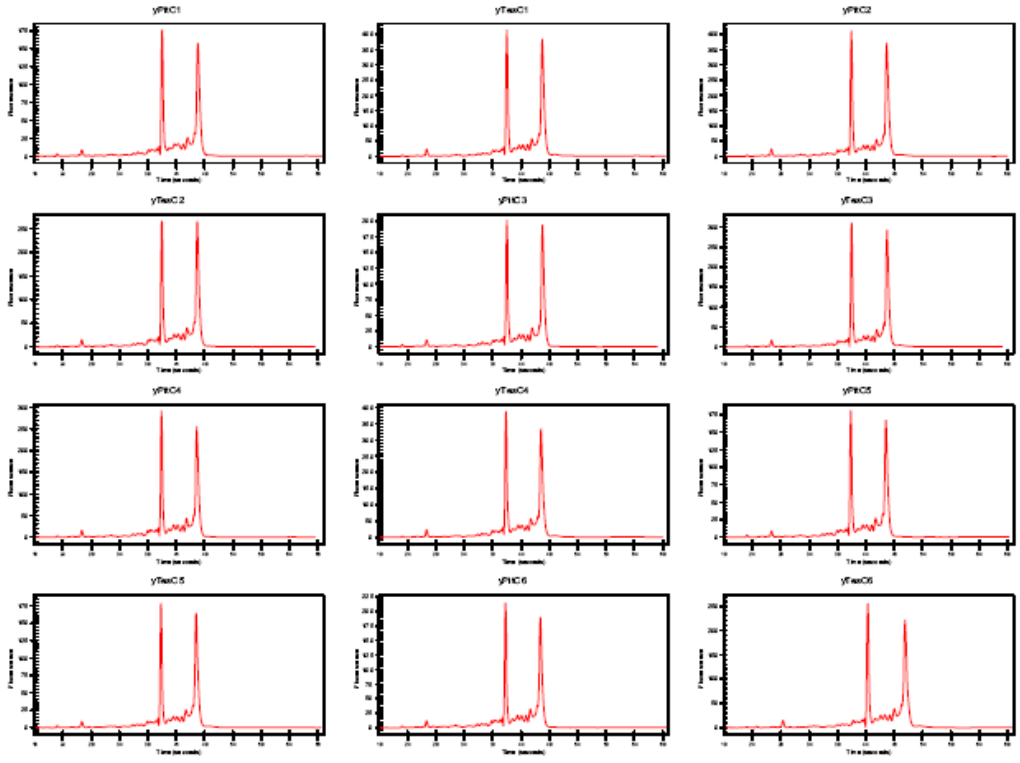

Agilent Technologies 2100 Bioanalyzer - Bio Sizing (Version A.02.12 SI292) Printed: 9/13/2005 7:34:51 PM

Appendix B: Protocol for Use of Genesifter® Software

1. Once you have received the data files from the microarray experiments, select the .CEL files to be analyzed and compress them for uploading
2. Login to GeneSifter®: Import Data: Upload Tools
3. Run Advanced Upload Methods
    a. Select: Method → GCRMA. RMA normalizes data across a group of arrays while MAS5 normalizes within individual chips. We chose RMA because we expected fewer mismatches with rhesus tissue on the GeneChip® Rhesus Macaque Genome Arrays (Affymetrix)
    b. Array → Rhesus macaque
4. Select Data File: Find the zip compressed file on the hard drive
    a. Target Creation → how many Groups are in the study
5. Name the Data set. Be descriptive and add notes as needed. Name the study Groups and assign individual data files to a Group
6. Data is now uploaded and in the GeneSifter® server
7. Analysis is run
8. Go to Analysis: Pairwise and click on the magnifying glass next to the Array of interest
9. Select/Assign experiments to a Group
10. Advanced Analysis Settings (RMA) – the following options need to be set by the user depending on their preferences
    a. Normalization: None (this has already been done with the Affymetrix software algorithms in Step 3)
    b. Statistics: *t*-test (in our case or ANOVA if more than two Groups)
    c. Quality (Signal): choose level of sensitivity to cutoff/exclude weaker signals. We left this as N/A initially since we filtered by hand later
    d. √ box for Exclude Control Probes: these were only needed by the Core during hybridization as a quality control check
    e. √ box for Show Genes that are Upregulated
    f. √ box for Show Genes that are Downregulated
    g. Threshold: Lower – None, Upper – None: this way fold-changes are ignored and only statistically significant *P*-values are used. This allowed us to set and sort a fold-change threshold later in Excel
    h. Correction:
        i. Bonferroni – may incur too many false negatives as it is the most conservative
        ii. Holm – moderately conservative
        iii. Westfall and Young – moderately conservative
        iv. Benjamini and Hochberg – least conservative, corrects error rate by estimating the false discovery rate (FDR). There is still the possibility of false discovery error
    i. Data is already log transformed
11. Analyze - For our samples we ran pairwise comparisons (Student's *t*-test) with Benjamini and Hochberg post-hoc correction. The result was 1018 pituitary and 1452 testis genes showing a change between treatments.

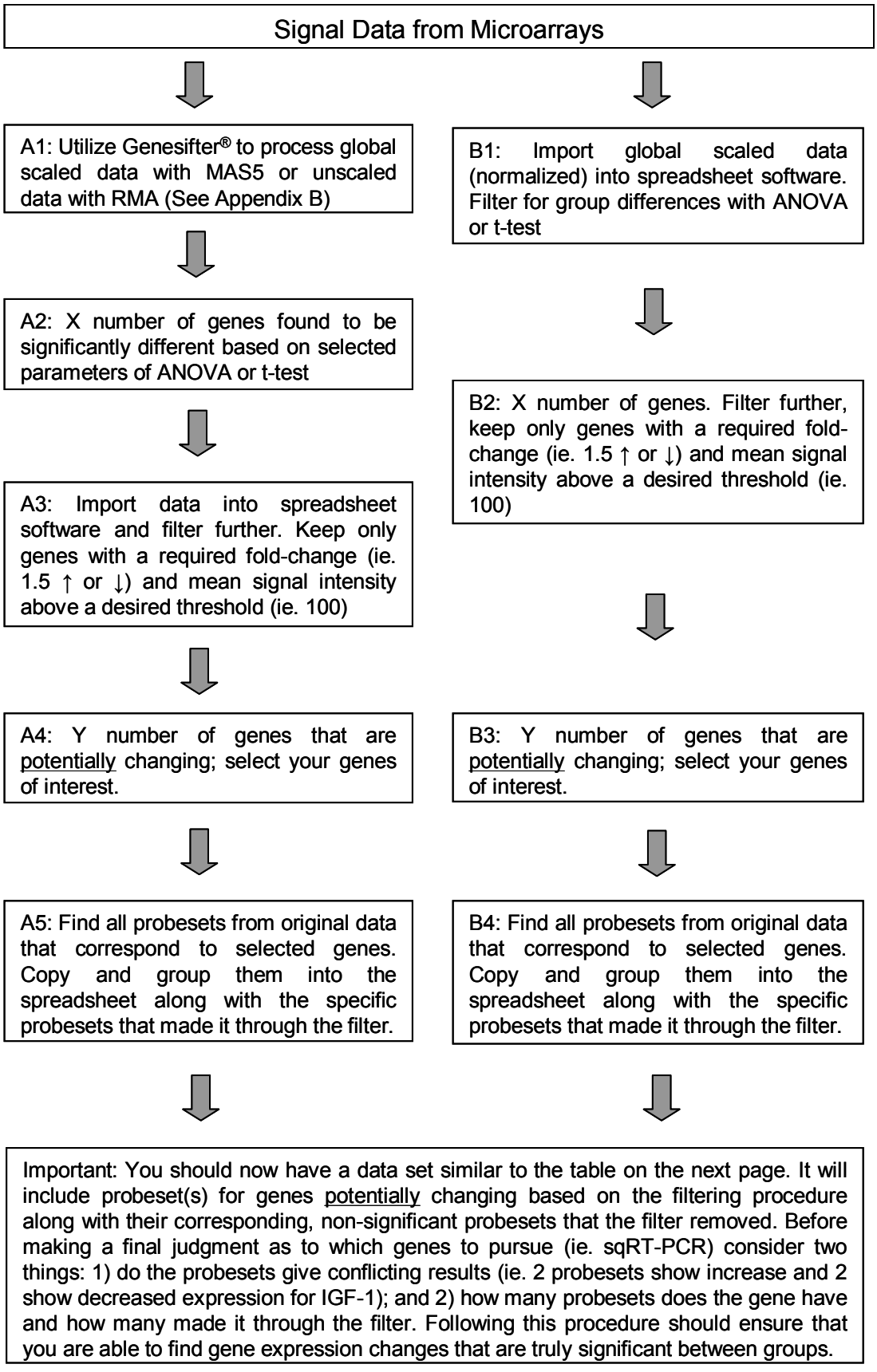
Signal Data from Microarrays
A1: Utilize Genesifter® to process global scaled data with MAS5 or unscaled data with RMA (See Appendix B)
A2: X number of genes found to be significantly different based on selected parameters of ANOVA or t-test
A3: Import data into spreadsheet software and filter further. Keep only genes with a required fold-change (ie. 1.5 ↑ or ↓) and mean signal intensity above a desired threshold (ie. 100)
A4: Y number of genes that are potentially changing; select your genes of interest.
A5: Find all probesets from original data that correspond to selected genes. Copy and group them into the spreadsheet along with the specific probesets that made it through the filter.
B1: Import global scaled data (normalized) into spreadsheet software. Filter for group differences with ANOVA or t-test
B2: X number of genes. Filter further, keep only genes with a required fold-change (ie. 1.5 ↑ or ↓) and mean signal intensity above a desired threshold (ie. 100)
B3: Y number of genes that are potentially changing; select your genes of interest.
B4: Find all probesets from original data that correspond to selected genes. Copy and group them into the spreadsheet along with the specific probesets that made it through the filter.
Important: You should now have a data set similar to the table on the next page. It will include probeset(s) for genes potentially changing based on the filtering procedure along with their corresponding, non-significant probesets that the filter removed. Before making a final judgment as to which genes to pursue (ie. sqRT-PCR) consider two things: 1) do the probesets give conflicting results (ie. 2 probesets show increase and 2 show decreased expression for IGF-1); and 2) how many probesets does the gene have and how many made it through the filter. Following this procedure should ensure that you are able to find gene expression changes that are truly significant between groups.

Appendix C: Flow diagram (previous page) of two possible methods for filtering microarray data. Option A utilizes Genesifter® software which provides faster analysis and embedded links for each gene to multiple databases. Option B is more labor intensive and requires effort later to search databases for genes. Both methods should work equally well but will not always give matching results. In addition to finding potentially significant genes you can add in other genes of interest by doing a keyword search of the raw microarray data.

The table below is an example of the type of results achieved after filtering the microarray data with the two methods described above.

Method A: the signal data is $\log_2$ transformed

Gene Title	Other ID / Probeset	Gene ID	mean 1	mean 2	SEM 1	SEM 2	Stats
ATP binding domain 4	MmugDNA.6466.1.S1_at	ATPBD4	3.3299	4.3619	0.1401	0.2519	0.0232
RYK receptor-like tyrosine kinase	MmugDNA.30524.1.S1_at	RYK	3.5830	4.6055	0.1863	0.1976	0.0197
Growth hormone inducible transmembrane protein	MmugDNA.32920.1.S1_at	GHITM	8.2073	9.2208	0.1172	0.1842	0.0097
Zinc finger protein 492	MmugDNA.17791.1.S1_at	ZNF492	5.3034	6.3061	0.2812	0.1673	0.0375
Nuclear receptor subfamily 4, group A, member 2	MmugDNA.20818.1.S1_s_at	NR4A2	10.7475	9.7416	0.2854	0.2136	0.0477
Secreted frizzled-related protein 1	MmugDNA.34907.1.S1_at	SFRP1	4.3145	3.2463	0.1004	0.0836	0.0012
MCF.2 cell line derived transforming sequence-like	MmugDNA.33725.1.S1_at	MCF2L	7.2038	6.1219	0.2920	0.2452	0.0470
Serine/threonine/tyrosine kinase 1	MmugDNA.2954.1.S1_at	STYK1	5.2432	4.1279	0.2216	0.1714	0.0164
Lix1 homolog (mouse)	MmugDNA.26440.1.S1_at	LIX1	5.5621	4.4434	0.1858	0.2106	0.0163
Collagen, type II, alpha 1 (primary osteoarthritis, spondyloepiphyseal dysplasia)	MmugDNA.24005.1.S1_at	COL2A1	6.8697	5.6806	0.2909	0.2099	0.0295
ATPase, Na+/K+ transporting, beta 1 polypeptide	MmugDNA.24357.1.S1_at	ATP1B1	10.4057	9.2054	0.2621	0.1448	0.0160
Oculocutaneous albinism II (pink-eye dilution homolog, mouse)	MmugDNA.21826.1.S1_at	OCA2	6.8704	5.5854	0.2734	0.1333	0.0134

Method B: retains the original signal data and mean

Other ID / Probeset	CON 1	Call	CON 2	Call	CON 3	Call	Gene ID	CR 1	Call	CR 2	Call	CR 3	Call		CON mean	CON SEM	CR mean	CR SEM		Fold Change
MmugDNA.13551.1.S1_at	68.2	P	85.7	P	71.7	M	PLCB	39.8	A	54.2	A	40.2	A		75.20	5.35	44.73	4.73		0.59
MmugDNA.40784.1.S1_at	189	P	216.1	P	163.1	P		200.2	P	206.4	P	179.4	P		189.40	15.30	195.33	8.17		1.03
MmugDNA.16826.1.S1_s_at	3337.8	P	3308.7	P	2853.3	P	CROP	3091.2	P	3184.5	P	3138.1	P		3166.60	156.88	3137.93	26.93		0.99
MmugDNA.33064.1.S1_x_at	215.1	P	257.9	P	273	P		90.4	P	394.9	P	188.7	P		248.67	17.34	224.67	89.72		0.90
MmugDNA.33064.1.S1_at	214.2	P	198.1	P	187.7	P		124.9	P	405	P	230.6	P		200.00	7.71	253.50	81.66		1.27
MmugDNA.24030.1.S1_at	364.7	P	345.5	P	345.5	P	SOD2	420	P	353.8	P	345.6	P		351.90	6.40	373.13	23.55		1.06
MmugDNA.19007.1.S1_at	254.1	P	134.6	P	184.9	P	CAT	191.7	P	221.1	P	239.4	P		191.20	34.64	217.40	13.89		1.14
MmugDNA.32721.1.S1_at	41.4	A	55.3	A	23.6	A		29.2	A	26.9	A	43.9	A		40.10	9.17	33.33	5.32		0.83

Appendix D: Genesifter® filtering of our experimental groups (Young Adult CON, n=3; Young Adult CR, n=3). Screening was determined with *t*-test (*P*<0.05) and Benjamini-Hochberg correction followed by hand filtering for 1.5 fold-change. The result was 145 probesets indicating potential differences in pituitary gland gene expression.

Gene Title	Gene ID	Other ID / Probeset	CON mean	CON SEM	CR mean	CR SEM	*t*-test
Phospholipase C, beta 1 (phosphoinositide-specific)	**PLCB1**	**MmugDNA.13551.1.S1_at**	**4.0000**	**0.0277**	**3.3777**	**0.0471**	**0.0003**
Fibronectin type III domain containing 3B	FNDC3B	MmugDNA.38842.1.S1_at	4.7213	0.0302	4.0216	0.0661	0.0007
POU domain, class 2, transcription factor 2	POU2F2	MmugDNA.2090.1.S1_at	4.2572	0.0619	3.5024	0.0484	0.0007
Secreted frizzled-related protein 1	SFRP1	MmugDNA.34907.1.S1_at	4.3145	0.1004	3.2463	0.0836	0.0012
Adenosine A2b receptor	ADORA2B	MmugDNA.35810.1.S1_at	3.2735	0.0098	3.8923	0.0852	0.0020
not provided	-	MmugDNA.42299.1.S1_at	4.0021	0.0249	4.8205	0.1126	0.0021
Fibroblast growth factor 10	FGF10	MmugDNA.19579.1.S1_at	4.3279	0.0302	5.1306	0.1131	0.0024
Guanine nucleotide binding protein (G protein), alpha 14	GNA14	MmugDNA.41403.1.S1_at	5.3485	0.0571	4.4196	0.1294	0.0028
Potassium voltage-gated channel, subfamily H (eag-related), member 2	KCNH2	MmugDNA.8632.1.S1_at	6.7130	0.0369	6.1132	0.0859	0.0030
1-acylglycerol-3-phosphate O-acyltransferase 3	**AGPAT3**	**MmugDNA.39097.1.S1_at**	**9.5874**	**0.0423**	**8.9716**	**0.0919**	**0.0037**
Snf2-related CBP activator protein	SRCAP	MmugDNA.23155.1.S1_at	4.2016	0.0823	3.5607	0.0669	0.0038
not provided	-	MmugDNA.16026.1.S1_at	8.6620	0.3274	4.6756	0.6049	0.0044
Lectin, galactoside-binding, soluble, 8 (galectin 8)	LGALS8	MmugDNA.28010.1.S1_at	3.6676	0.0643	4.3105	0.0923	0.0046
Filamin A interacting protein 1	FILIP1	MmugDNA.17551.1.S1_at	4.2554	0.0962	4.9825	0.0855	0.0048
not provided	-	MmugDNA.27855.1.S1_at	4.8568	0.0112	5.6371	0.1421	0.0054
Chloride intracellular channel 4	CLIC4	MmugDNA.28843.1.S1_at	9.0570	0.0451	9.6855	0.1065	0.0056
Suppression of tumorigenicity 18 (breast carcinoma) (zinc finger protein)	ST18	MmugDNA.30345.1.S1_at	5.8635	0.1323	5.1176	0.0510	0.0062
Zinc finger protein 506	ZNF506	MmugDNA.31196.1.S1_at	7.8758	0.0984	7.2061	0.0830	0.0065
RNA-binding protein	FLJ20273	MmugDNA.20089.1.S1_at	5.9644	0.1003	6.6234	0.0805	0.0069
Nipped-B homolog (Drosophila)	NIPBL	MmugDNA.24065.1.S1_at	8.6000	0.0891	7.9614	0.0903	0.0073
PDZ and LIM domain 3	PDLIM3	MmugDNA.18347.1.S1_at	8.8537	0.0302	8.0691	0.1576	0.0081
gb:CO646781 DB_XREF=gi:50568275 DB_XREF=ILLUMIGEN_MCQ_39627 CLONE=IBIUW:23193 TID=Mmu.9549.1 CNT=6 FEA=EST TIER=ConsEnd STK=0 NOTE=sequence(s) clustered along genome	-	Mmu.9549.1.S1_at	5.8398	0.1664	6.7684	0.0943	0.0083
Transcribed locus	-	MmugDNA.42157.1.S1_at	3.7717	0.2795	5.2529	0.1280	0.0085
Thyroid stimulating hormone receptor	**TSHR**	**MmugDNA.32655.1.S1_at**	**3.28999**	**0.111393**	**2.631527**	**0.029322**	**0.0086**
CDNA FLJ36663 fis, clone UTERU2002826	-	MmugDNA.28098.1.S1_at	8.4939	0.1188	9.1459	0.0663	0.0087
Neuron navigator 1	NAV1	MmugDNA.32339.1.S1_at	6.6341	0.1022	5.8121	0.1379	0.0087
Protein geranylgeranyltransferase type I, beta subunit	PGGT1B	MmugDNA.10009.1.S1_at	5.5542	0.0135	6.1714	0.1286	0.0088
Solute carrier family 20 (phosphate transporter), member 1	SLC20A1	MmugDNA.16839.1.S1_at	9.5518	0.0901	8.8813	0.1104	0.0093
Chromosome 10 open reading frame 49	C10orf49	MmugDNA.27226.1.S1_at	8.3836	0.2234	7.0708	0.1672	0.0093
Immunoglobulin kappa constant	IGKC	MmugDNA.23504.1.S1_s_at	6.6961	0.1399	7.3692	0.0316	0.0094
Growth hormone inducible transmembrane protein	GHITM	MmugDNA.32920.1.S1_at	8.2073	0.1172	9.2208	0.1842	0.0097
Syntaxin 3	STX3	MmugDNA.3869.1.S1_at	4.7479	0.0546	5.8603	0.2376	0.0103
Hypothetical protein LOC645721	LOC645721	MmugDNA.23383.1.S1_at	6.7367	0.1057	7.5044	0.1322	0.0105
KIAA0513	KIAA0513	MmugDNA.16133.1.S1_at	4.8186	0.1223	5.5726	0.1132	0.0106
not provided	-	MmugDNA.40550.1.S1_at	3.6893	0.0091	4.2770	0.1349	0.0122
gi:59676429 DEF=SCN4B_3456.2 Rhesus macaque genomic DNA Macaca mulatta STS genomic clone MMA3456.2, sequence tagged site	-	MmuSTS.1023.1.S1_at	5.2869	0.3679	6.9707	0.1215	0.0122
Osteomodulin	OMD	MmugDNA.17909.1.S1_at	7.3038	0.2263	8.4702	0.1485	0.0126
Oculocutaneous albinism II (pink-eye dilution homolog, mouse)	OCA2	MmugDNA.21826.1.S1_at	6.8704	0.2734	5.5854	0.1333	0.0134
Immediate early response 2	IER2	MmugDNA.26855.1.S1_at	11.1255	0.1334	10.3051	0.1499	0.0150
Tescalcin	TESC	MmugDNA.30872.1.S1_at	10.2908	0.1063	9.6995	0.1006	0.0156
AP2 associated kinase 1	AAK1	MmugDNA.26429.1.S1_at	5.9302	0.1546	6.6435	0.0873	0.0159
ATPase, Na+/K+ transporting, beta 1 polypeptide	ATP1B1	MmugDNA.24357.1.S1_at	10.4057	0.2621	9.2054	0.1448	0.0160
Lix1 homolog (mouse)	LIX1	MmugDNA.26440.1.S1_at	5.5621	0.1858	4.4434	0.2106	0.0163
Serine/threonine/tyrosine kinase 1	STYK1	MmugDNA.2954.1.S1_at	5.2432	0.2216	4.1279	0.1714	0.0164

Gene Title	Gene ID	Other ID / Probeset	CON mean	CON SEM	CR mean	CR SEM	*t*-test
Hypothetical protein FLJ12505	VASH2	MmugDNA.30454.1.S1_at	6.0800	0.1744	5.3214	0.0773	0.0165
DPH5 homolog (S. cerevisiae)	DPH5	MmugDNA.14615.1.S1_s_at	4.6256	0.1914	5.3904	0.0218	0.0165
NHP2 non-histone chromosome protein 2-like 1 (S. cerevisiae)	NHP2L1	MmugDNA.3458.1.S1_at	6.4103	0.4512	4.6511	0.0509	0.0179
Ankyrin repeat and SOCS box-containing 8	ASB8	MmugDNA.19994.1.S1_at	8.5876	0.1735	7.7784	0.1174	0.0181
Potassium channel, subfamily K, member 1	KCNK1	MmugDNA.12778.1.S1_at	7.2444	0.1290	7.8345	0.0822	0.0182
IQ motif containing GTPase activating protein 1	IQGAP1	MmugDNA.19813.1.S1_at	9.7648	0.1529	9.1677	0.0250	0.0183
gi:51853714 DEF=CTSL2_2905 Rhesus macaque genomic DNA Macaca mulatta STS genomic clone MMA2905, sequence tagged site. GEN=CTSL2 PROD=cathepsin L2	-	MmuSTS.4178.1.S1_at	10.1170	0.1756	9.3704	0.0819	0.0183
Formin 2	FMN2	MmugDNA.20444.1.S1_at	6.2923	0.1181	6.9622	0.1289	0.0186
Transcribed locus	-	MmugDNA.29329.1.S1_at	8.2406	0.1084	7.3737	0.1992	0.0187
Chondroitin sulfate proteoglycan 5 (neuroglycan C)	CSPG5	MmugDNA.14190.1.S1_at	7.1158	0.1326	6.5157	0.0853	0.0190
CDNA FLJ41934 fis, clone PERIC2005111	-	MmugDNA.18540.1.S1_at	5.4854	0.0981	6.2115	0.1641	0.0191
Syntrophin, beta 1 (dystrophin-associated protein A1, 59kDa, basic component 1)	SNTB1	MmugDNA.18390.1.S1_at	5.0557	0.0851	5.8128	0.1804	0.0192
RYK receptor-like tyrosine kinase	RYK	MmugDNA.30524.1.S1_at	3.5830	0.1863	4.6055	0.1976	0.0197
gb:CO580930 DB_XREF=gi:50412176 DB_XREF=ILLUMIGEN_MCQ_48010 CLONE=IBIUW:17041 TID=Mmu.2883.1 CNT=2 FEA=EST TIER=ConsEnd STK=0 NOTE=sequence(s) clustered along genome	-	Mmu.2883.1.S1_at	7.8018	0.0642	8.3908	0.1445	0.0204
ATPase, Na+/K+ transporting, beta 1 polypeptide	ATP1B1	MmugDNA.26322.1.S1_s_at	12.6125	0.1254	11.9742	0.1179	0.0207
Chromosome 2 open reading frame 34	C2orf34	MmugDNA.31052.1.S1_at	4.5103	0.1638	3.9038	0.0223	0.0214
Transmembrane protein 20	TMEM20	MmugDNA.31724.1.S1_at	4.4162	0.1931	5.1812	0.0796	0.0215
gi:47776948 DEF=PCDH20_1029 Rhesus macaque genomic DNA Macaca mulatta STS genomic clone MMA1029, sequence tagged site. GEN=PCDH20 PROD=protocadherin 20	-	MmuSTS.2010.1.S1_at	3.8353	0.0154	4.9254	0.2976	0.0216
Chromosome 6 open reading frame 194	C6orf194	MmugDNA.16575.1.S1_at	4.4463	0.1039	5.1675	0.1678	0.0217
Carbohydrate (chondroitin 4) sulfotransferase 11	CHST11	MmugDNA.9039.1.S1_at	5.9585	0.1472	6.8940	0.2106	0.0220
Within bgcn homolog (Drosophila)	WIBG	MmugDNA.35808.1.S1_at	7.1137	0.1508	6.1556	0.2162	0.0221
gi:49533512 DEF=SFRP1_1897 Rhesus macaque genomic DNA Macaca mulatta STS genomic clone MMA1897, sequence tagged site. GEN=SFRP1 PROD=secreted frizzled-related protein 1	-	MmuSTS.4330.1.S1_at	8.3461	0.2762	6.9961	0.2483	0.0221
Transcribed locus	-	MmugDNA.15702.1.S1_at	6.2726	0.0586	6.9522	0.1783	0.0223
Small glutamine-rich tetratricopeptide repeat (TPR)-containing, beta	SGTB	MmugDNA.17918.1.S1_at	3.3096	0.1460	3.9542	0.1021	0.0224
CDNA clone IMAGE:3934193	-	MmugDNA.21342.1.S1_at	4.1907	0.1995	5.2372	0.2108	0.0226
Transmembrane 4 L six family member 18	TM4SF18	MmugDNA.6970.1.S1_at	6.0288	0.1647	5.4149	0.0459	0.0229
ATP binding domain 4	ATPBD4	MmugDNA.6466.1.S1_at	3.3299	0.1401	4.3619	0.2519	0.0232
Tripartite motif-containing 4	TRIM4	MmugDNA.4424.1.S1_at	5.5035	0.2025	4.6816	0.1090	0.0233
Myosin heavy chain Myr 8	RP11-54H7.1	MmugDNA.15890.1.S1_at	6.5733	0.1367	7.2763	0.1439	0.0240
ADP-ribosylation factor-like 11	ARL11	MmugDNA.28111.1.S1_at	7.8023	0.2037	8.6869	0.1459	0.0242
gi:47777234 DEF=VCAM1_385 Rhesus macaque genomic DNA Macaca mulatta STS genomic clone MMA385, sequence tagged site. GEN=VCAM1 PROD=vascular cell adhesion molecule 1	-	MmuSTS.4697.1.S1_at	5.9631	0.4055	7.4657	0.1450	0.0251
Ataxin 1	ATXN1	MmugDNA.32588.1.S1_at	5.9401	0.2022	5.0616	0.1520	0.0255
Dipeptidyl-peptidase 6	DPP6	MmugDNA.37049.1.S1_at	11.0942	0.2255	10.1948	0.1277	0.0256
RALBP1 associated Eps domain containing 2	REPS2	MmugDNA.39023.1.S1_at	5.8124	0.0465	6.5195	0.1985	0.0256
Poly (ADP-ribose) polymerase family, member 15	PARP15	MmugDNA.22391.1.S1_at	4.5930	0.3627	6.2920	0.3326	0.0260

Gene Title	Gene ID	Other ID / Probeset	CON mean	CON SEM	CR mean	CR SEM	*t*-test
Calpain 1, (mu/I) large subunit	CAPN1	MmugDNA.8965.1.S1_at	4.9625	0.1892	4.3125	0.0157	0.0267
Poly(rC) binding protein 2	PCBP2	MmugDNA.4665.1.S1_at	7.0127	0.1483	6.4209	0.0909	0.0272
Indolethylamine N-methyltransferase	INMT	MmugDNA.27753.1.S1_at	4.6948	0.2624	6.2542	0.3777	0.0275
Transmembrane protein 116	TMEM116	MmugDNA.23118.1.S1_at	5.1113	0.2260	4.3352	0.0396	0.0277
not provided	-	MmugDNA.32599.1.S1_at	4.5153	0.2464	3.6473	0.0805	0.0286
Blood vessel epicardial substance	BVES	MmugDNA.8035.1.S1_at	4.3093	0.1635	5.0116	0.1322	0.0288
Trophoblast-derived noncoding RNA	TncRNA	MmugDNA.13964.1.S1_at	4.2395	0.1993	5.1667	0.1933	0.0289
Transcribed locus, moderately similar to NP_061913.2 elongation protein 4 homolog; PAX6 neighbor gene; chromosome 11 open rea	-	MmugDNA.6193.1.S1_at	9.5222	0.1369	8.9273	0.1150	0.0292
Collagen, type II, alpha 1 (primary osteoarthritis, spondyloepiphyseal dysplasia, congenital)	COL2A1	MmugDNA.24005.1.S1_at	6.8697	0.2909	5.6806	0.2099	0.0295
gi:60301119 DEF=ASS_8219 Rhesus macaque genomic DNA Macaca mulatta STS genomic clone MMA8219, sequence tagged site	-	MmuSTS.2126.1.S1_s_at	9.9162	0.1866	9.0997	0.1618	0.0298
gi:47777053 DEF=RGS1_1489 Rhesus macaque genomic DNA Macaca mulatta STS genomic clone MMA1489, sequence tagged site. GEN=RGS1 PROD=regulator of G-protein signalling 1	-	MmuSTS.3131.1.S1_at	4.8501	0.2503	6.0279	0.2559	0.0302
gi:47776742 DEF=IGF1_1346 Rhesus macaque genomic DNA Macaca mulatta STS genomic clone MMA1346, sequence tagged site. GEN=IGF1 PROD=insulin-like growth factor 1	-	MmuSTS.628.1.S1_at	5.7329	0.3015	4.7445	0.0147	0.0307
Hypothetical protein LOC162073	LOC162073	MmugDNA.32218.1.S1_at	7.7181	0.0949	7.1191	0.1571	0.0310
GRAM domain containing 1A	GRAMD1A	MmugDNA.33477.1.S1_at	3.3993	0.1945	4.1954	0.1517	0.0321
Protease, serine, 1 (trypsin 1)	PRSS1	MmugDNA.10752.1.S1_at	4.6141	0.1789	5.3448	0.1415	0.0328
KIAA0495	KIAA0495	MmugDNA.18652.1.S1_at	6.2333	0.1905	7.0399	0.1655	0.0330
Aldo-keto reductase family 7, member A3 (aflatoxin aldehyde reductase)	AKR7A3	MmugDNA.13635.1.S1_s_at	5.3546	0.1777	4.5856	0.1652	0.0339
RAB2, member RAS oncogene family	RAB2	MmugDNA.15882.1.S1_at	7.4699	0.1193	5.7666	0.5254	0.0341
not provided	-	MmugDNA.6966.1.S1_at	4.2398	0.1735	4.8971	0.1146	0.0342
Sidekick homolog 2 (chicken)	SDK2	MmugDNA.38063.1.S1_at	8.4958	0.0764	7.7463	0.2253	0.0345
ADP-ribosylation factor-like 11	ARL11	MmugDNA.28111.1.S1_x_at	7.7983	0.1849	8.5799	0.1671	0.0350
Hypothetical protein LOC90784	LOC90784	MmugDNA.19148.1.S1_at	4.4512	0.0407	5.0870	0.2022	0.0368
Collagen, type XII, alpha 1	COL12A1	MmugDNA.27864.1.S1_at	5.8450	0.3217	7.0218	0.2056	0.0368
gi:53828476 DEF=TM7SF3 _5273 Rhesus macaque genomic DNA Macaca mulatta STS genomic clone MMA5273, sequence tagged site. GEN=TM7SF3 PROD=transmembrane 7 superfamily member 3	-	MmuSTS.944.1.S1_at	8.4411	0.1776	7.5302	0.2363	0.0369
gi:59676223 DEF=GPC4 _7535 Rhesus macaque genomic DNA Macaca mulatta STS genomic clone MMA7535, sequence tagged site	-	MmuSTS.4265.1.S1_at	11.4041	0.1576	10.7802	0.1274	0.0370
Zinc finger protein 492	ZNF492	MmugDNA.17791.1.S1_at	5.3034	0.2812	6.3061	0.1673	0.0375
Alpha-methylacyl-CoA racemase	AMACR	MmugDNA.36476.1.S1_at	5.8645	0.2074	6.6364	0.1450	0.0380
not provided	-	MmugDNA.35833.1.S1_at	5.7849	0.1157	6.3890	0.1618	0.0385
gi:47776569 DEF=EDNRB_607 Rhesus macaque genomic DNA Macaca mulatta STS genomic clone MMA607, sequence tagged site. GEN=EDNRB PROD=endothelin receptor type B	-	MmuSTS.4094.1.S1_at	7.7539	0.0200	8.5533	0.2624	0.0385
221745_at WD-repeat protein	-	MmugDNA.4928.1.S1_at	7.3792	0.1676	6.7388	0.1343	0.0407
Hypothetical protein LOC339457	LOC339457	MmugDNA.36513.1.S1_at	6.5849	0.2235	5.6815	0.2049	0.0408
NMD3 homolog (S. cerevisiae)	NMD3	MmugDNA.36304.1.S1_at	6.1956	0.2332	7.5240	0.3810	0.0410
Acyl-CoA synthetase medium-chain family member 3	ACSM3	MmugDNA.7137.1.S1_s_at	3.8922	0.0986	3.1942	0.2135	0.0412
Hypothetical protein BC009732	LOC133308	MmugDNA.3901.1.S1_at	5.6485	0.1823	6.2631	0.0984	0.0413
Vacuolar protein sorting 13B (yeast)	VPS13B	MmugDNA.5302.1.S1_at	7.1431	0.1849	6.1740	0.2713	0.0419

Gene Title	Gene ID	Other ID / Probeset	CON mean	CON SEM	CR mean	CR SEM	*t*-test
Calcium channel, voltage-dependent, alpha 1G subunit	CACNA1G	MmugDNA.30662.1.S1_at	5.4910	0.2007	4.8688	0.0650	0.0420
MYC induced nuclear antigen	MINA	MmugDNA.26614.1.S1_at	7.9115	0.1953	8.5429	0.0878	0.0420
Annexin A4	ANXA4	MmugDNA.28580.1.S1_at	11.3659	0.2073	10.6760	0.1086	0.0421
gi:55960839 DEF=OMD _6110 Rhesus macaque genomic DNA Macaca mulatta STS genomic clone MMA6110, sequence tagged site. GEN=OMD PROD=osteomodulin	-	MmuSTS.722.1.S1_at	7.3262	0.2861	8.3701	0.2117	0.0427
Ankyrin repeat domain 10	ANKRD10	MmugDNA.2810.1.S1_at	5.6822	0.2940	6.5818	0.0885	0.0428
CDNA clone IMAGE:5263455	-	MmugDNA.10813.1.S1_at	6.6621	0.1462	5.8084	0.2522	0.0429
Syntaxin 3	STX3	MmugDNA.23304.1.S1_at	8.3230	0.2249	9.3101	0.2515	0.0430
gb:CO582780 DB_XREF=gi:50414838 DB_XREF=ILLUMIGEN_MCQ_43967 CLONE=IBIUW:16462 TID=Mmu.8925.1 CNT=2 FEA=EST TIER=ConsEnd STK=0 NOTE=sequence(s) clustered along genome	-	Mmu.8925.1.S1_at	9.4828	0.1748	10.1069	0.1246	0.0438
Muscleblind-like (Drosophila)	MBNL1	MmugDNA.23132.1.S1_s_at	7.6985	0.0581	8.3211	0.2061	0.0438
CDNA clone IMAGE:4814184	-	MmugDNA.21664.1.S1_at	6.2720	0.5587	7.9498	0.1457	0.0439
gi:52626966 DEF=DMRT3 _4753 Rhesus macaque genomic DNA Macaca mulatta STS genomic clone MMA4753, sequence tagged site. GEN=DMRT3 PROD=doublesex and mab-3 related transcription factor 3	-	MmuSTS.1310.1.S1_at	8.2976	0.4411	6.5404	0.4150	0.0441
CDNA clone IMAGE:4799094	-	MmugDNA.8934.1.S1_at	6.8264	0.2437	6.0371	0.1218	0.0442
Reticulon 4	RTN4	MmugDNA.11786.1.S1_at	6.6544	0.4249	8.4994	0.4757	0.0445
gi:49533179 DEF=F3_45.3 Rhesus macaque genomic DNA Macaca mulatta STS genomic clone MMA45.3, sequence tagged site. GEN=F3 PROD=coagulation factor III	-	MmuSTS.1925.1.S1_at	8.2253	0.2931	9.2072	0.1718	0.0446
CDNA clone IMAGE:4814184	-	MmugDNA.17794.1.S1_at	5.1248	0.4666	6.6045	0.2125	0.0447
Tripartite motif-containing 33	TRIM33	MmugDNA.20660.1.S1_at	6.9196	0.0569	6.1954	0.2465	0.0458
matrix metallopeptidase 23A	-	MmugDNA.29748.1.S1_at	7.2641	0.2434	6.4869	0.1204	0.0458
gi:60301337 DEF=MYOC_8491 Rhesus macaque genomic DNA Macaca mulatta STS genomic clone MMA8491, sequence tagged site	-	MmuSTS.3230.1.S1_at	4.3538	0.2149	6.2356	0.6229	0.0461
Carboxypeptidase M	CPM	MmugDNA.37694.1.S1_at	7.6415	0.0941	8.2837	0.2045	0.0463
gb:CB553954 DB_XREF=gi:31303149 DB_XREF=MMSP0046_B11 TID=Mmu.14068.2 CNT=1 FEA=EST TIER=ConsEnd STK=1 NOTE=sequence(s) clustered along genome	-	Mmu.14068.2.A1_at	3.7368	0.2114	4.3811	0.0796	0.0463
gb:CN645072 DB_XREF=gi:47158515 DB_XREF=ILLUMIGEN_MCQ_11205 CLONE=IBIUW:9888 TID=Mmu.2050.1 CNT=5 FEA=EST TIER=ConsEnd STK=0 NOTE=sequence(s) clustered along gene	-	Mmu.2050.1.S1_s_at	10.0760	0.1487	11.0569	0.3104	0.0464
Transcribed locus	-	MmugDNA.17471.1.S1_at	7.6247	0.1224	6.6648	0.3143	0.0466
not provided	-	MmugDNA.104.1.S1_at	5.9002	0.1740	6.5154	0.1283	0.0466
MCF.2 cell line derived transforming sequence-like	MCF2L	MmugDNA.33725.1.S1_at	7.2038	0.2920	6.1219	0.2452	0.0470
Nuclear receptor subfamily 4, group A, member 2	NR4A2	MmugDNA.20818.1.S1_s_at	10.7475	0.2854	9.7416	0.2136	0.0477
gb:CB308356 DB_XREF=gi:28831066 DB_XREF=AGENCOURT_11818364 CLONE=IMAGE:6882119 TID=Mmu.12441.1 CNT=11 FEA=EST TIER=ConsEnd STK=0 NOTE=sequence(s) clustered along gene	-	Mmu.12441.1.S1_at	10.6749	0.2808	11.5230	0.1083	0.0479
not provided	-	MmugDNA.33118.1.S1_s_at	6.5648	0.1075	5.7987	0.2512	0.0486
not provided	-	MmugDNA.27103.1.S1_at	3.2195	0.1453	4.5172	0.4403	0.0489
gi:49533147 DEF=CXCL14 _2459 Rhesus macaque genomic DNA Macaca mulatta STS genomic clone MMA2459, sequence tagged site. GEN=CXCL14 PROD=chemokine (C-X-C motif) ligand 14	-	MmuSTS.1894.1.S1_at	5.4121	0.3638	6.8856	0.3820	0.0491
2'-5'-oligoadenylate synthetase 3, 100kDa	OAS3	MmugDNA.20819.1.S1_at	7.5521	0.2107	6.8187	0.1590	0.0499
CDNA FLJ45742 fis, clone KIDNE2016327	-	MmugDNA.22044.1.S1_at	8.6085	0.2972	7.6606	0.1679	0.0500

Appendix E: Genesifter® filtering of our experimental groups (Young Adult CON, n=3; Young Adult CR, n=3). Screening was determined with *t*-test (*P*<0.05) and Benjamini-Hochberg correction followed by hand filtering for 1.5 fold-change. The result was 260 probesets indicating potential differences in testicular gene expression.

Gene Title	Gene ID	Other ID / Probeset	CON mean	CON SEM	CR mean	CR SEM	*t*-test
gi:59676458 DEF=SLC7A1_7877 Rhesus macaque genomic DNA Macaca mulatta STS genomic clone MMA7877, sequence tagged site	-	MmuSTS.1093.1.S1_at	10.5008	0.0324	11.1026	0.0165	0.0001
Dipeptidyl-peptidase 4 (CD26, adenosine deaminase complexing protein 2)	DPP4	MmugDNA.5046.1.S1_at	7.7196	0.0390	6.9920	0.0379	0.0002
Transducin (beta)-like 1Y-linked	TBL1Y	MmugDNA.25035.1.S1_s_at	6.8790	0.0631	5.8355	0.0583	0.0003
newRS.gi:21071024 DEF=Orthologous to gi:21071024 Homo sapiens histone 1, H4c (HIST1H4C), mRNA. GEN=HIST1H4C PROD=H4 histone family, member G	-	MmunewRS.661.1.S1_at	13.0693	0.0573	11.0048	0.1744	0.0004
Heat shock 60kDa protein 1 (chaperonin)	HSPD1	MmugDNA.36856.1.S1_at	10.6129	0.0396	9.8421	0.0685	0.0006
not provided	-	MmugDNA.16026.1.S1_at	6.9346	0.3259	3.8948	0.1351	0.0010
gi:53828476 DEF=TM7SF3 _5273 Rhesus macaque genomic DNA Macaca mulatta STS genomic clone MMA5273, sequence tagged site. GEN=TM7SF3 PROD=transmembrane 7 superfamily member 3	-	MmuSTS.944.1.S1_at	6.6577	0.0676	5.9359	0.0519	0.0011
Establishment of cohesion 1 homolog 1 (S. cerevisiae)	ESCO1	MmugDNA.42000.1.S1_at	8.7018	0.0851	7.5326	0.1205	0.0014
Staphylococcal nuclease domain containing 1	SND1	MmugDNA.1637.1.S1_at	3.5476	0.0878	4.3499	0.0548	0.0015
Exocyst complex component 6	EXOC6	MmugDNA.25604.1.S1_at	6.7695	0.0559	6.1550	0.0566	0.0015
UDP glycosyltransferase 3 family, polypeptide A1	UGT3A1	MmugDNA.16619.1.S1_at	3.3092	0.0712	5.1200	0.2237	0.0015
Syntaxin 6	STX6	MmugDNA.34574.1.S1_at	4.9534	0.0903	4.2759	0.0127	0.0017
Glycosyltransferase 8 domain containing 3	GLT8D3	MmugDNA.30383.1.S1_at	5.2723	0.1966	3.7824	0.0646	0.0020
gDNA.Hs.103915.0.S1 FEA=U133PSR GEN=JMJD3 DEF=Orthologous to 213146_at jumonji domain containing 3	-	MmugDNA.6170.1.S1_at	8.4101	0.0861	9.2090	0.0713	0.0020
Sperm specific antigen 2	**SSFA2**	**MmugDNA.26522.1.S1_at**	**7.6727**	**0.2266**	**5.8902**	**0.1146**	**0.0022**
gi:60301372 DEF=PEG10_8006 Rhesus macaque genomic DNA Macaca mulatta STS genomic clone MMA8006, sequence tagged site	-	MmuSTS.3365.1.S1_at	8.6675	0.0479	7.9190	0.0975	0.0023
Transcribed locus	-	MmugDNA.13576.1.S1_at	5.8685	0.1112	5.1016	0.0219	0.0025
Enolase superfamily member 1	ENOSF1	MmugDNA.32608.1.S1_at	7.5035	0.0985	8.3245	0.0768	0.0028
Bruno-like 4, RNA binding protein (Drosophila)	BRUNOL4	MmugDNA.5472.1.S1_at	4.3843	0.0330	5.2330	0.1254	0.0028
gi:52626809 DEF=ADRA2A _4205 Rhesus macaque genomic DNA Macaca mulatta STS genomic clone MMA4205, sequence tagged site. GEN=ADRA2A PROD=adrenergic, alpha-2A-, receptor	-	MmuSTS.417.1.S1_at	7.7602	0.0739	6.5727	0.1659	0.0028
gi:60301103 DEF=AMPH_8202 Rhesus macaque genomic DNA Macaca mulatta STS genomic clone MMA8202, sequence tagged site	-	MmuSTS.2085.1.S1_at	5.1151	0.0846	4.4983	0.0524	0.0034
gb:CN646290 DB_XREF=gi:47159733 DB_XREF=ILLUMIGEN_MCQ_25961 CLONE=IBIUW:8718 TID=Mmu.12457.1 CNT=4 FEA=EST TIER=ConsEnd STK=0 NOTE=sequence(s) clustered along gene	-	Mmu.12457.1.S1_s_at	11.6796	0.1142	10.8799	0.0669	0.0038
gi:51854151 DEF=SPP1_3239 Rhesus macaque genomic DNA Macaca mulatta STS genomic clone MMA3239, sequence tagged site. GEN=SPP1 PROD=secreted phosphoprotein 1	-	MmuSTS.2862.1.S1_at	4.8351	0.0801	5.9989	0.1778	0.0040
gb:CN644246 DB_XREF=gi:47157689 DB_XREF=ILLUMIGEN_MCQ_9960 CLONE=IBIUW:9053 TID=Mmu.5363.1 CNT=5 FEA=EST TIER=ConsEnd STK=0 NOTE=sequence(s) clustered along genome	-	Mmu.5363.1.S1_at	7.4558	0.0805	6.7895	0.0802	0.0042
Cell division cycle 2, G1 to S and G2 to M	CDC2	MmugDNA.42865.1.S1_at	10.5137	0.1037	9.5826	0.1208	0.0043
gDNA.g8923837 FEA=U133PSR GEN=KIAA1212 DEF=Orthologous to 219387_at KIAA1212	-	MmugDNA.33282.1.S1_at	9.8410	0.0542	9.0441	0.1258	0.0043
not provided	-	MmugDNA.10943.1.S1_at	5.9061	0.0957	5.2080	0.0727	0.0044
gi:62000413 DEF=TNFSF4_270 Rhesus macaque genomic DNA Macaca mulatta STS genomic clone MMA270, sequence tagged site	-	MmuSTS.2557.1.S1_at	6.0067	0.0808	5.4085	0.0640	0.0044
Chromosome 20 open reading frame 108	C20orf108	MmugDNA.39842.1.S1_at	10.0649	0.1198	9.1384	0.1066	0.0045

Gene Title	Gene ID	Other ID / Probeset	CON mean	CON SEM	CR mean	CR SEM	*t*-test
Heat shock 70kDa protein 4	HSPA4	MmugDNA.37971.1.S1_at	10.1530	0.1230	9.4399	0.0143	0.0045
Transcribed locus	-	MmugDNA.27647.1.S1_at	8.1009	0.3290	6.0113	0.1552	0.0046
not provided	-	MmugDNA.42703.1.S1_at	8.6371	0.0947	8.0351	0.0475	0.0047
gDNA.Hs.247828.1.A1 FEA=U133PSR DEF=Orthologous to 222225_at Similar to bA476I15.3 (novel protein similar to septin)	-	MmugDNA.37161.1.S1_at	7.2867	0.0951	8.0101	0.0848	0.0047
Spectrin repeat containing, nuclear envelope 2	SYNE2	MmugDNA.12872.1.S1_at	5.1372	0.1236	4.2410	0.1008	0.0049
Transcribed locus	-	MmugDNA.11482.1.S1_at	5.7666	0.1528	6.8194	0.1149	0.0053
Plexin C1	PLXNC1	MmugDNA.8622.1.S1_at	8.5547	0.0731	7.5028	0.1794	0.0056
not provided	-	MmugDNA.14737.1.S1_at	6.5964	0.1236	5.8465	0.0619	0.0056
gi:60301269 DEF=HSPA4_7803 Rhesus macaque genomic DNA Macaca mulatta STS genomic clone MMA7803, sequence tagged site	-	MmuSTS.2729.1.S1_s_at	8.9122	0.1264	8.1920	0.0428	0.0057
gi:62000459 DEF=ZNF423_9303 Rhesus macaque genomic DNA Macaca mulatta STS genomic clone MMA9303, sequence tagged site	-	MmuSTS.2633.1.S1_at	7.1432	0.1233	8.1035	0.1344	0.0062
Cleavage stimulation factor, 3' pre-RNA, subunit 2, 64kDa, tau variant	CSTF2T	MmugDNA.23306.1.S1_at	7.7477	0.1024	8.4670	0.0931	0.0065
Transcribed locus	-	MmugDNA.12213.1.S1_at	7.6909	0.0512	8.3272	0.1118	0.0066
Chloride channel, nucleotide-sensitive, 1A	CLNS1A	MmugDNA.3618.1.S1_at	6.7181	0.1122	5.7922	0.1399	0.0067
ST3 beta-galactoside alpha-2,3-sialyltransferase 6	ST3GAL6	MmugDNA.10160.1.S1_at	7.2071	0.0362	6.5296	0.1265	0.0067
SAM domain containing 1	RP5-875H10.1	MmugDNA.15856.1.S1_at	3.9788	0.0983	3.3526	0.0721	0.0068
Lymphocyte antigen 96	LY96	MmugDNA.11614.1.S1_at	6.2554	0.1831	7.4623	0.1503	0.0070
gi:49533548 DEF=SPTBN4_2491 Rhesus macaque genomic DNA Macaca mulatta STS genomic clone MMA2491, sequence tagged site. GEN=SPTBN4 PROD=spectrin, beta, non-erythrocytic 4	-	MmuSTS.4490.1.S1_at	7.1692	0.0962	6.5768	0.0677	0.0073
BAT2 domain containing 1	BAT2D1	MmugDNA.11808.1.S1_at	9.9701	0.0881	9.3661	0.0813	0.0073
gDNA.Hs.192907.0.A1 FEA=U133PSR GEN=TTN DEF=Orthologous to 241791_at titin	-	MmugDNA.20569.1.S1_at	7.1424	0.1124	6.2145	0.1461	0.0073
POU domain, class 6, transcription factor 1	POU6F1	MmugDNA.3065.1.S1_at	6.3275	0.1158	7.4267	0.1858	0.0074
Sulfide quinone reductase-like (yeast)	SQRDL	MmugDNA.36497.1.S1_at	8.4300	0.0940	9.0379	0.0774	0.0075
not provided	-	MmugDNA.24287.1.S1_at	9.7570	0.1863	10.6978	0.0406	0.0078
gi:55167870 DEF=VHL _5065 Rhesus macaque genomic DNA Macaca mulatta STS genomic clone MMA5065, sequence tagged site. GEN=VHL PROD=von Hippel-Lindau syndrome	-	MmuSTS.1838.1.S1_at	7.1866	0.1417	6.3004	0.1108	0.0079
not provided	-	MmugDNA.42299.1.S1_at	3.3925	0.1259	4.3587	0.1511	0.0080
Chromosome 20 open reading frame 108	C20orf108	MmugDNA.39842.1.S1_s_at	10.2930	0.0759	9.5570	0.1313	0.0083
Transmembrane protein 56	TMEM56	MmugDNA.37454.1.S1_at	6.0535	0.1447	5.3385	0.0291	0.0084
STS genomic clone MMA37, sequence tagged site. GEN=ENO2 PROD=enolase 2	-	MmuSTS.4136.1.S1_at	6.1931	0.1449	7.0973	0.1208	0.0087
Prickle-like 1 (Drosophila)	PRICKLE1	MmugDNA.23051.1.S1_at	6.6279	0.1305	5.8955	0.0798	0.0087
gDNA.Hs.7218.0.A1 FEA=U133PSR GEN=ACAS2L DEF=Orthologous to 224882_at acetyl-Coenzyme A synthetase 2 (AMP forming)-like	-	MmugDNA.26367.1.S1_at	8.6648	0.1191	8.0076	0.0694	0.0089
Ferredoxin 1	FDX1	MmugDNA.29297.1.S1_at	10.4396	0.0995	11.0691	0.0878	0.0090
Protein kinase C, beta 1	PRKCB1	MmugDNA.30839.1.S1_at	6.1771	0.1209	5.3960	0.1130	0.0092
Heat shock 60kDa protein 1 (chaperonin)	HSPD1	MmugDNA.36856.1.S1_s_at	10.6783	0.1238	9.9986	0.0736	0.0092
Zinc finger protein 161	ZNF161	MmugDNA.3735.1.S1_at	7.6860	0.0805	6.7856	0.1750	0.0095
Hypothetical protein LOC283075	LOC283075	MmugDNA.26953.1.S1_at	5.6705	0.0524	4.8837	0.1612	0.0097
gDNA.Hs.44024.0.A1 FEA=U133PSR DEF=Orthologous to 238448_at Transcribed locus	-	MmugDNA.42707.1.S1_at	4.0113	0.1407	3.2119	0.1000	0.0098
Dihydrolipoamide dehydrogenase	DLD	MmugDNA.19688.1.S1_at	6.8485	0.1605	5.5378	0.2357	0.0101

Gene Title	Gene ID	Other ID / Probeset	CON mean	CON SEM	CR mean	CR SEM	*t*-test
gi:60301269 DEF=HSPA4_7803 Rhesus macaque genomic DNA Macaca mulatta STS genomic clone MMA7803, sequence tagged site	-	MmuSTS.2729.1.S1_at	7.5492	0.1579	6.7368	0.0812	0.0102
Cullin 4B	CUL4B	MmugDNA.20224.1.S1_at	9.2914	0.1687	8.5063	0.0347	0.0104
Family with sequence similarity 19 (chemokine (C-C motif)-like), member A5	FAM19A5	MmugDNA.41812.1.S1_at	7.2179	0.1082	6.4622	0.1270	0.0106
Mucosa associated lymphoid tissue lymphoma translocation gene 1	MALT1	MmugDNA.522.1.S1_at	6.4061	0.2094	5.2875	0.1321	0.0107
Jumonji domain containing 1C	JMJD1C	MmugDNA.34169.1.S1_at	9.9346	0.0215	9.2575	0.1493	0.0109
Chromosome 1 open reading frame 148	C1orf148	MmugDNA.9726.1.S1_at	5.9856	0.0686	6.6578	0.1335	0.0110
Casein kinase 1, alpha 1	CSNK1A1	MmugDNA.39332.1.S1_at	4.9273	0.0982	4.3288	0.0918	0.0112
Family with sequence similarity 107, member B	FAM107B	MmugDNA.38951.1.S1_at	8.3467	0.1042	7.4412	0.1766	0.0116
Chromosome 10 open reading frame 118	C10orf118	MmugDNA.9437.1.S1_at	9.9865	0.1511	9.1508	0.1144	0.0116
gb:CN646290 DB_XREF=gi:47159733 DB_XREF=ILLUMIGEN_MCQ_25961 CLONE=IBIUW:8718 TID=Mmu.12457.1 CNT=4 FEA=EST TIER=ConsEnd STK=0 NOTE=sequence(s) clustered along genome	-	Mmu.12457.1.S1_at	10.6076	0.1454	9.9400	0.0429	0.0117
Plexin A1	PLXNA1	MmugDNA.2754.1.S1_at	6.9930	0.1221	6.3544	0.0788	0.0117
ELK1, member of ETS oncogene family	ELK1	MmugDNA.38775.1.S1_at	6.8850	0.1283	6.1899	0.0948	0.0121
gDNA.Hs.296695.0.S1 FEA=U133PSR GEN=LOC154761 DEF=Orthologous to 234088_at Hypothetical protein LOC154761	-	MmugDNA.26631.1.S1_at	3.1632	0.0496	3.7598	0.1285	0.0123
SET and MYND domain containing 2	SMYD2	MmugDNA.16584.1.S1_at	6.2211	0.0639	5.2070	0.2264	0.0125
Chromosome 1 open reading frame 95	C1orf95	MmugDNA.34555.1.S1_at	3.8890	0.0796	4.4895	0.1150	0.0127
Ellis van Creveld syndrome	EVC	MmugDNA.9242.1.S1_at	6.4712	0.1436	7.1238	0.0509	0.0128
Peroxisomal LON protease like	LONPL	MmugDNA.30130.1.S1_at	9.7886	0.1396	10.4850	0.0842	0.0129
RAB2, member RAS oncogene family	RAB2	MmugDNA.15882.1.S1_at	5.4311	0.1376	4.5867	0.1447	0.0134
Musashi homolog 2 (Drosophila)	MSI2	MmugDNA.9375.1.S1_at	6.5067	0.1862	7.3411	0.0686	0.0136
Limb region 1 homolog (mouse)	LMBR1	MmugDNA.29113.1.S1_at	6.8757	0.0943	6.2881	0.1035	0.0137
gDNA.Hs.247711.1.S1 FEA=U133PSR GEN=FLJ20557 DEF=Orthologous to 234902_s_at hypothetical protein FLJ20557	-	MmugDNA.7226.1.S1_at	9.8919	0.1055	10.4955	0.0988	0.0140
not provided	-	MmugDNA.34944.1.S1_at	5.0858	0.1775	6.1944	0.1986	0.0141
ROD1 regulator of differentiation 1 (S. pombe)	ROD1	MmugDNA.26968.1.S1_s_at	9.1956	0.1452	8.5319	0.0665	0.0142
Amino-terminal enhancer of split	AES	MmugDNA.43210.1.S1_at	9.6832	0.1463	9.0721	0.0219	0.0145
Family with sequence similarity 84, member A	FAM84A	MmugDNA.26517.1.S1_at	7.3498	0.1530	6.2011	0.2325	0.0145
CUB and Sushi multiple domains 1	CSMD1	MmugDNA.451.1.S1_at	4.5191	0.1911	5.9661	0.2964	0.0148
gi:55167728 DEF=PDP2 _5850 Rhesus macaque genomic DNA Macaca mulatta STS genomic clone MMA5850, sequence tagged site. GEN=PDP2 PROD=pyruvate dehydrogenase phosphatase isoenzyme 2	-	MmuSTS.1131.1.S1_at	6.2131	0.2659	5.0315	0.1122	0.0149
gDNA.g12053092 FEA=U133PSR GEN=FLJ35934 DEF=Orthologous to 224172_at FLJ35934 protein	-	MmugDNA.6975.1.S1_at	5.4800	0.0604	6.6391	0.2786	0.0153
Receptor accessory protein 1	REEP1	MmugDNA.31866.1.S1_at	10.1940	0.1402	9.4957	0.1006	0.0155
Neuroblastoma-amplified protein	NAG	MmugDNA.34091.1.S1_s_at	5.2048	0.0848	4.5865	0.1273	0.0156
Zinc finger protein 160	ZNF160	MmugDNA.32096.1.S1_at	6.4504	0.1676	7.1756	0.0652	0.0157
D4, zinc and double PHD fingers, family 3	DPF3	MmugDNA.29362.1.S1_at	4.8769	0.0313	4.0744	0.1972	0.0159
Dynein, axonemal, heavy polypeptide 9	DNAH9	MmugDNA.25552.1.S1_at	8.6953	0.2080	9.7519	0.1619	0.0160
Hypothetical protein LOC641515	LOC641515	MmugDNA.29680.1.S1_at	7.4748	0.1650	8.3303	0.1376	0.0164
gi:47776372 DEF=ALDH1B1_1553 Rhesus macaque genomic DNA Macaca mulatta STS genomic clone MMA1553, sequence tagged site. GEN=ALDH1B1 PROD=aldehyde dehydrogenase 1 family, member B1	-	MmuSTS.2796.1.S1_at	7.0657	0.0854	6.4241	0.1367	0.0164
gi:49533200 DEF=GAB3_1528 Rhesus macaque genomic DNA Macaca mulatta STS genomic clone MMA1528, sequence tagged site. GEN=GAB3 PROD=GRB2-associated binding protein 3	-	MmuSTS.2384.1.S1_at	6.2121	0.1411	5.6223	0.0454	0.0164

Gene Title	Gene ID	Other ID / Probeset	CON mean	CON SEM	CR mean	CR SEM	*t*-test
PCTAIRE protein kinase 2	PCTK2	MmugDNA.870.1.S1_at	5.3887	0.1334	4.7421	0.0935	0.0165
NudE nuclear distribution gene E homolog like 1 (A. nidulans)	NDEL1	MmugDNA.17067.1.S1_at	5.0310	0.1348	4.3395	0.1109	0.0167
Protein tyrosine phosphatase, non-receptor type 5 (striatum-enriched)	PTPN5	MmugDNA.3314.1.S1_at	6.4709	0.1819	5.6748	0.0870	0.0168
gi:62000083 DEF=ASGR1_8213 Rhesus macaque genomic DNA Macaca mulatta STS genomic clone MMA8213, sequence tagged site	-	MmuSTS.107.1.S1_at	6.1331	0.1375	7.2140	0.2378	0.0170
gi:59676473 DEF=SNTA1 _6874 Rhesus macaque genomic DNA Macaca mulatta STS genomic clone MMA6874, sequence tagged site	-	MmuSTS.1146.1.S1_at	7.3237	0.1592	6.6903	0.0268	0.0172
gi:47776604 DEF=F11R_1772 Rhesus macaque genomic DNA Macaca mulatta STS genomic clone MMA1772, sequence tagged site. GEN=F11R PROD=F11 receptor	-	MmuSTS.4739.1.S1_at	7.3580	0.2044	6.4596	0.1039	0.0173
Cisplatin resistance-associated overexpressed protein	**CROP**	**MmugDNA.33064.1.S1_x_at**	**6.7473**	**0.0591**	**6.1355**	**0.1463**	**0.0179**
Establishment of cohesion 1 homolog 1 (S. cerevisiae)	ESCO1	MmugDNA.16962.1.S1_at	8.3590	0.1634	7.5770	0.1183	0.0179
Cofactor required for Sp1 transcriptional activation, subunit 3, 130kDa	CRSP3	MmugDNA.42284.1.S1_s_at	6.5749	0.0742	7.2011	0.1440	0.0181
Epithelial stromal interaction 1 (breast)	EPSTI1	MmugDNA.15476.1.S1_at	5.4452	0.0956	4.7518	0.1520	0.0181
Calcitonin-related polypeptide, beta	CALCB	MmugDNA.4167.1.S1_at	4.0314	0.2125	4.9053	0.0805	0.0184
Adenylate cyclase 8 (brain)	ADCY8	MmugDNA.17241.1.S1_at	4.1835	0.0267	4.8553	0.1727	0.0184
Transcribed locus	-	MmugDNA.38168.1.S1_at	6.8319	0.1693	6.0785	0.0994	0.0185
Multiple substrate lipid kinase	MULK	MmugDNA.3836.1.S1_at	7.6641	0.1006	7.0477	0.1254	0.0185
Solute carrier family 9 (sodium/hydrogen exchanger), member 9	SLC9A9	MmugDNA.5028.1.S1_at	4.4886	0.3068	5.8454	0.1762	0.0185
gb:CN644288 DB_XREF=gi:47157731 DB_XREF=ILLUMIGEN_MCQ_10067 CLONE=IBIUW:9095 TID=Mmu.15849.1 CNT=2 FEA=EST TIER=ConsEnd STK=0 NOTE=sequence(s) clustered along gene	-	Mmu.15849.1.S1_a_at	7.8242	0.1596	7.0580	0.1202	0.0186
Olfactomedin 3	OLFM3	MmugDNA.36167.1.S1_at	4.3905	0.3578	3.0147	0.0282	0.0186
Oxysterol binding protein-like 6	OSBPL6	MmugDNA.37149.1.S1_s_at	5.8482	0.1293	5.2241	0.1012	0.0191
gb:CD767529 DB_XREF=gi:32426031 DB_XREF=AGENCOURT_14716309 CLONE=IMAGE:6973283 TID=Mmu.12628.1 CNT=2 FEA=EST TIER=ConsEnd STK=0 NOTE=sequence(s) clustered along gene	-	Mmu.12628.1.S1_at	6.5116	0.1789	5.7429	0.0947	0.0191
gDNA.Hs.158154.0.A1 FEA=U133PSR GEN=MGC2610 DEF=Orthologous to 217505_at hypothetical protein MGC2610	-	MmugDNA.25118.1.S1_at	5.9151	0.2485	4.9584	0.0608	0.0201
gb:CO583226 DB_XREF=gi:50415879 DB_XREF=ILLUMIGEN_MCQ_44565 CLONE=IBIUW:17369 TID=Mmu.6559.1 CNT=3 FEA=EST TIER=ConsEnd STK=0 NOTE=sequence(s) clustered along genome	-	Mmu.6559.1.S1_s_at	8.3684	0.0811	7.7670	0.1396	0.0204
Solute carrier family 39 (zinc transporter), member 14	SLC39A14	MmugDNA.34818.1.S1_at	4.9687	0.1222	4.2645	0.1455	0.0207
gb:BM423033 DB_XREF=gi:18392527 DB_XREF=PLATE1_C06 TID=Mmu.4039.1 CNT=2 FEA=EST TIER=ConsEnd STK=0 NOTE=sequence(s) clustered along genome	-	Mmu.4039.1.S1_at	7.7714	0.2287	5.8782	0.4578	0.0208
Hexose-6-phosphate dehydrogenase (glucose 1-dehydrogenase)	H6PD	MmugDNA.28426.1.S1_at	6.1390	0.1371	5.3745	0.1562	0.0212
gi:55774112 DEF=ZNF6 _4707 Rhesus macaque genomic DNA Macaca mulatta STS genomic clone MMA4707, sequence tagged site. GEN=ZNF6 PROD=zinc finger protein 6 (CMPX1)	-	MmuSTS.2203.1.S1_at	7.8938	0.2169	6.9363	0.1444	0.0213
CAMP-binding guanine nucleotide exchange factor IV (cAMP-GEFIV) mRNA, clone W15, partial sequence	-	MmugDNA.28928.1.S1_at	6.5383	0.0361	5.9160	0.1664	0.0217
Zinc finger protein 584	ZNF584	MmugDNA.26148.1.S1_at	8.1669	0.1497	8.8167	0.0960	0.0217
Tousled-like kinase 1	TLK1	MmugDNA.30536.1.S1_x_at	4.3725	0.1642	3.6994	0.0854	0.0220
Chromosome 5 open reading frame 5	C5orf5	MmugDNA.29493.1.S1_at	5.6106	0.1638	5.0088	0.0265	0.0222
Solute carrier family 25, member 36	SLC25A36	MmugDNA.9919.1.S1_at	8.5665	0.1561	7.6372	0.2040	0.0224

Gene Title	Gene ID	Other ID / Probeset	CON mean	CON SEM	CR mean	CR SEM	*t*-test
Euchromatic histone-lysine N-methyltransferase 1	EHMT1	MmugDNA.42551.1.S1_at	7.9316	0.1483	7.2713	0.1075	0.0227
Transcribed locus	-	MmugDNA.5319.1.S1_at	5.6535	0.0569	6.4317	0.2083	0.0227
gi:51854088 DEF=S100B_3127 Rhesus macaque genomic DNA Macaca mulatta STS genomic clone MMA3127, sequence tagged site. GEN=S100B PROD=S100 calcium binding protein, beta	-	MmuSTS.2362.1.S1_at	5.1274	0.2787	7.5689	0.6184	0.0228
ATPase, Na+/K+ transporting, beta 1 polypeptide	ATP1B1	MmugDNA.24357.1.S1_at	8.4481	0.2432	7.2352	0.2337	0.0228
Peroxisomal biogenesis factor 5-like	PEX5L	MmugDNA.5498.1.S1_at	8.3821	0.1203	7.6284	0.1722	0.0230
gb:BV208356.1 DB_XREF=gi:49533039 GEN=ABCG2 TID=Mmu.1351.1 CNT=5 FEA=STS TIER=ConsEnd STK=0 NOTE=sequence(s) clustered along genome DEF=ABCG2_1993 Rhesus macaque genomic DNA Macaca mulatta STS genomic clone MMA1993, sequence tagged site. PR	-	Mmu.1351.1.S1_at	6.2243	0.0974	5.5181	0.1713	0.0231
newRS.gi:46409363 DEF=Orthologous to gi:46409363 Homo sapiens FLJ44060 protein (FLJ44060), mRNA. GEN=FLJ44060 PROD=FLJ44060 protein	-	MmunewRS.1007.1.S1_at	9.8142	0.1613	9.1633	0.0846	0.0233
KRR1, small subunit (SSU) processome component, homolog (yeast)	KRR1	MmugDNA.35.1.S1_at	7.9282	0.2960	6.8408	0.0839	0.0241
not provided	-	MmugDNA.29708.1.S1_at	4.8866	0.1591	5.6544	0.1496	0.0246
Transcribed locus	-	MmugDNA.12201.1.S1_at	8.1665	0.1627	8.8032	0.0814	0.0249
MCF.2 cell line derived transforming sequence	MCF2	MmugDNA.1622.1.S1_at	7.3565	0.1724	6.4158	0.2069	0.0251
gi:47777150 DEF=SOX4_1527 Rhesus macaque genomic DNA Macaca mulatta STS genomic clone MMA1527, sequence tagged site. GEN=SOX4 PROD=SRY (sex determining region Y)-box 4	-	MmuSTS.3908.1.S1_at	10.1262	0.2094	9.2194	0.1536	0.0251
Cullin 5	CUL5	MmugDNA.25803.1.S1_at	7.3527	0.0602	6.6848	0.1818	0.0252
SUB1 homolog (S. cerevisiae)	SUB1	MmugDNA.24125.1.S1_s_at	6.9946	0.1202	6.3908	0.1246	0.0252
Small trans-membrane and glycosylated protein	LOC57228	MmugDNA.6744.1.S1_at	6.5225	0.1667	7.3464	0.1675	0.0252
Phosphatidylinositol 4-kinase type II	PI4KII	MmugDNA.18437.1.S1_at	5.3380	0.0498	4.5207	0.2293	0.0253
Phosphodiesterase 11A	PDE11A	MmugDNA.39988.1.S1_at	4.5772	0.1160	3.8399	0.1778	0.0255
Splicing factor, arginine/serine-rich 3	SFRS3	MmugDNA.15838.1.S1_at	7.6545	0.1581	6.9486	0.1289	0.0258
Esophageal cancer related gene 4 protein	ECRG4	MmugDNA.4152.1.S1_at	10.7997	0.0892	11.8221	0.2818	0.0258
gb:CO580468 DB_XREF=gi:50411618 DB_XREF=ILLUMIGEN_MCQ_48638 CLONE=IBIUW:16483 TID=Mmu.8587.1 CNT=4 FEA=EST TIER=ConsEnd STK=0 NOTE=sequence(s) clustered along genome	-	Mmu.8587.1.S1_at	6.8402	0.1645	6.2203	0.0713	0.0259
not provided	-	MmugDNA.23280.1.S1_at	7.0199	0.1713	6.3198	0.1092	0.0261
Similar to ECT2 protein (Epithelial cell transforming sequence 2 oncogene)	RP3-509I19.5	MmugDNA.16841.1.S1_at	3.9156	0.2687	4.8509	0.0431	0.0264
gi:47776533 DEF=CYP1B1_568 Rhesus macaque genomic DNA Macaca mulatta STS genomic clone MMA568, sequence tagged site. GEN=CYP1B1 PROD=cytochrome P450, family 1, subfamily B, polypeptide 1	-	MmuSTS.4020.1.S1_at	7.2963	0.1087	8.0887	0.2036	0.0264
Centrosomal protein 350kDa	CEP350	MmugDNA.33476.1.S1_at	9.1591	0.1467	8.3638	0.1799	0.0267
Ubiquitin specific peptidase 34	USP34	MmugDNA.23342.1.S1_at	10.0012	0.1253	9.4156	0.1165	0.0267
Par-3 partitioning defective 3 homolog (C. elegans)	PARD3	MmugDNA.4680.1.S1_s_at	7.0125	0.1546	6.3857	0.0990	0.0269
Oxysterol binding protein-like 6	OSBPL6	MmugDNA.6874.1.S1_at	7.5631	0.1991	6.6665	0.1731	0.0273
gi:47776614 DEF=FBXO21_1269 Rhesus macaque genomic DNA Macaca mulatta STS genomic clone MMA1269, sequence tagged site. GEN=FBXO21 PROD=F-box only protein 21	-	MmuSTS.4759.1.S1_at	10.7364	0.1657	9.9634	0.1559	0.0273
gi:47777086 DEF=SEMA3C_394 Rhesus macaque genomic DNA Macaca mulatta STS genomic clone MMA394, sequence tagged site. GEN=SEMA3C PROD=sema domain, immunoglobulin domain (Ig), short basic domain, sec, ted,	-	MmuSTS.3255.1.S1_at	7.6108	0.1702	7.0023	0.0558	0.0273
N-acylsphingosine amidohydrolase (acid ceramidase)-like	ASAHL	MmugDNA.11678.1.S1_at	5.9533	0.1244	6.9067	0.2523	0.0275

Gene Title	Gene ID	Other ID / Probeset	CON mean	CON SEM	CR mean	CR SEM	*t*-test
NPC1 (Niemann-Pick disease, type C1, gene)-like 1	NPC1L1	MmugDNA.43041.1.S1_at	7.0910	0.2876	8.1632	0.1336	0.0278
Calpastatin	CAST	MmugDNA.13716.1.S1_s_at	10.2139	0.0976	9.5638	0.1667	0.0282
Oxysterol binding protein-like 8	OSBPL8	MmugDNA.31287.1.S1_at	6.6312	0.1499	5.6748	0.2419	0.0283
Amnionless homolog (mouse)	AMN	MmugDNA.40561.1.S1_at	4.8819	0.1900	5.6050	0.1032	0.0287
Ankyrin repeat and SOCS box-containing 13	ASB13	MmugDNA.43105.1.S1_at	3.9196	0.0570	4.6475	0.2104	0.0288
1-acylglycerol-3-phosphate O-acyltransferase 3	**AGPAT3**	**MmugDNA.24842.1.S1_at**	**6.9155**	**0.1831**	**5.8291**	**0.2697**	**0.0290**
not provided	-	MmugDNA.40445.1.S1_at	6.2120	0.1735	5.0962	0.2870	0.0292
CD200 molecule	CD200	MmugDNA.3834.1.S1_at	5.9106	0.0617	6.6426	0.2115	0.0293
Ryanodine receptor 3	RYR3	MmugDNA.26610.1.S1_at	6.1387	0.1838	7.0617	0.2084	0.0293
AF4/FMR2 family, member 2	AFF2	MmugDNA.39958.1.S1_at	7.4549	0.1776	6.8099	0.0803	0.0296
Male sterility domain containing 1	MLSTD1	MmugDNA.5167.1.S1_at	3.3113	0.2361	4.6192	0.3193	0.0301
Hypothetical protein FLJ14503	RP11-393H10.2	MmugDNA.40188.1.S1_at	7.8088	0.2102	7.0808	0.0694	0.0303
Hypothetical protein LOC147646	LOC147646	MmugDNA.21637.1.S1_at	6.7120	0.1521	6.0935	0.1111	0.0304
gi:49533243 DEF=GPR48_2097 Rhesus macaque genomic DNA Macaca mulatta STS genomic clone MMA2097, sequence tagged site. GEN=GPR48 PROD=G protein-coupled receptor 48	-	MmuSTS.2467.1.S1_at	9.7143	0.1453	9.1038	0.1164	0.0305
Adaptor-related protein complex 3, beta 1 subunit	AP3B1	MmugDNA.31519.1.S1_at	5.0789	0.1826	4.3062	0.1489	0.0305
Integrin, alpha 9	ITGA9	MmugDNA.23640.1.S1_at	3.5743	0.3401	4.9898	0.2696	0.0310
Hypothetical protein LOC283666	LOC283666	MmugDNA.35151.1.S1_at	5.4552	0.1064	4.7350	0.1936	0.0311
Full length insert cDNA clone ZE05E03	-	MmugDNA.35572.1.S1_at	5.4967	0.1231	4.6539	0.2277	0.0312
Discs, large homolog 2, chapsyn-110 (Drosophila)	DLG2	MmugDNA.19569.1.S1_at	8.7637	0.1660	9.4064	0.1094	0.0319
Latrophilin 3	LPHN3	MmugDNA.42945.1.S1_at	6.3277	0.2196	5.4846	0.1412	0.0320
gi:60301433 DEF=SH3GL2_8623 Rhesus macaque genomic DNA Macaca mulatta STS genomic clone MMA8623, sequence tagged site	-	MmuSTS.3981.1.S1_at	7.0450	0.2134	6.2084	0.1470	0.0320
mitogen activated protein kinase binding protein 1	-	MmugDNA.40041.1.S1_at	5.6704	0.1154	5.0614	0.1501	0.0324
Inter-alpha (globulin) inhibitor H5	ITIH5	MmugDNA.27539.1.S1_at	7.8735	0.1647	7.1019	0.1748	0.0325
Kelch-like 23 (Drosophila)	KLHL23	MmugDNA.37133.1.S1_at	8.1791	0.1364	7.3495	0.2194	0.0326
AFFX-HS-5-8SrRNA TID=MmurRNA.1.1 CNT=1 FEA=rRNA DEF=gi|555853:6623-6779 Human 5.8S ribosomal RNA	-	MmurRNA.1.1.S1_at	8.2973	0.0911	10.8682	0.7965	0.0327
Hypothetical protein LOC285429	LOC285429	MmugDNA.31358.1.S1_s_at	9.5724	0.2104	8.8892	0.0352	0.0328
Cardiomyopathy associated 3	CMYA3	MmugDNA.32217.1.S1_at	8.5775	0.1996	6.2651	0.6969	0.0332
Phospholipase A2, group IB (pancreas)	PLA2G1B	MmugDNA.2316.1.S1_s_at	9.2994	0.2387	8.4885	0.0903	0.0336
Poly (ADP-ribose) polymerase family, member 15	PARP15	MmugDNA.22391.1.S1_at	7.0326	0.4052	9.9686	0.8337	0.0339
gi:51853642 DEF=BST1_2659 Rhesus macaque genomic DNA Macaca mulatta STS genomic clone MMA2659, sequence tagged site. GEN=BST1 PROD=bone marrow stromal cell antigen 1	-	MmuSTS.3501.1.S1_at	6.9889	0.3283	8.1578	0.1693	0.0340
Complement factor H-related 1	CFHR1	MmugDNA.30885.1.S1_at	5.7228	0.2227	6.5195	0.1187	0.0343
NGFI-A binding protein 1 (EGR1 binding protein 1)	NAB1	MmugDNA.37875.1.S1_at	6.6894	0.1488	6.0586	0.1348	0.0348
SH3 domain protein D19	SH3D19	MmugDNA.30001.1.S1_at	5.7559	0.1439	5.0655	0.1673	0.0352
Dipeptidyl-peptidase 7	DPP7	MmugDNA.28618.1.S1_at	7.3914	0.1817	6.7120	0.1189	0.0352
Dickkopf homolog 3 (Xenopus laevis)	DKK3	MmugDNA.42302.1.S1_at	10.2406	0.1728	9.4762	0.1729	0.0353
gi:62000495 DEF=GCN5L2_3982 Rhesus macaque genomic DNA Macaca mulatta STS genomic clone MMA3982, sequence tagged site	-	MmuSTS.2728.1.S1_at	7.6650	0.1756	7.0604	0.0818	0.0355
not provided	-	MmugDNA.4020.1.S1_at	5.2273	0.0793	4.3190	0.2802	0.0355
AF4/FMR2 family, member 2	AFF2	MmugDNA.34251.1.S1_at	4.3383	0.2101	3.6269	0.0909	0.0359

Gene Title	Gene ID	Other ID / Probeset	CON mean	CON SEM	CR mean	CR SEM	*t*-test
CTP synthase II	CTPS2	MmugDNA.43.1.S1_at	6.7734	0.1987	6.0962	0.0944	0.0370
gDNA.Hs.247712.0.S1 FEA=U133PSR GEN=LOC284307 DEF=Orthologous to 232774_x_at Hypothetical protein LOC284307	-	MmugDNA.18660.1.S1_at	7.8014	0.1788	8.6348	0.2033	0.0370
gDNA.Hs2.406180.1.S1 FEA=U133PSR GEN=KIAA2018 DEF=Orthologous to 1559601_at similar to K06A9.1b.p	-	MmugDNA.9948.1.S1_at	5.4410	0.1190	6.0381	0.1544	0.0375
gi:47776812 DEF=KCNK13_1417 Rhesus macaque genomic DNA Macaca mulatta STS genomic clone MMA1417, sequence tagged site. GEN=KCNK13 PROD=potassium channel, subfamily K, member 13	-	MmuSTS.1405.1.S1_at	6.6483	0.1254	6.0109	0.1670	0.0379
SRY (sex determining region Y)-box 5	SOX5	MmugDNA.25319.1.S1_at	7.5083	0.0843	8.1046	0.1764	0.0381
Dynein, axonemal, heavy polypeptide 9	DNAH9	MmugDNA.4110.1.S1_at	6.5010	0.2004	7.1663	0.0910	0.0390
Fibrinogen-like 1	FGL1	MmugDNA.26990.1.S1_at	6.2877	0.0248	7.3872	0.3649	0.0397
Glycosyltransferase-like domain containing 1	GTDC1	MmugDNA.37449.1.S1_s_at	5.0769	0.3033	4.1588	0.0367	0.0397
RAN binding protein 2	RANBP2	MmugDNA.31162.1.S1_at	8.4340	0.1563	7.8471	0.1172	0.0398
Erythrocyte membrane protein band 4.1 like 5	EPB41L5	MmugDNA.6620.1.S1_at	3.9813	0.2498	4.8147	0.1222	0.0401
gi:62000188 DEF=FPGT_8857 Rhesus macaque genomic DNA Macaca mulatta STS genomic clone MMA8857, sequence tagged site	-	MmuSTS.948.1.S1_at	6.7846	0.1356	6.1880	0.1462	0.0403
1-acylglycerol-3-phosphate O-acyltransferase 3	**AGPAT3**	**MmugDNA.39097.1.S1_at**	**9.2073**	**0.1725**	**8.5831**	**0.1190**	**0.0408**
Collagen, type I, alpha 1	COL1A1	MmugDNA.26445.1.S1_at	7.8845	0.1683	9.0522	0.3543	0.0409
TAF9B RNA polymerase II, TATA box binding protein (TBP)-associated factor,	TAF9B	MmugDNA.20363.1.S1_at	6.3241	0.0789	5.7144	0.1897	0.0412
not provided	-	MmugDNA.13529.1.S1_at	6.5464	0.1785	7.5959	0.3056	0.0413
Phosphoglucomutase 2	PGM2	MmugDNA.21887.1.S1_at	5.9704	0.1712	5.3474	0.1225	0.0416
gb:AF227555.1 DB_XREF=gi:8132802 TID=Mmu.10994.1 CNT=1 FEA=mRNA TIER=ConsEnd STK=0 NOTE=sequence(s) clustered along genome DEF=Macaca mulatta interleukin-6 signal transducer receptor (IL-6) mRNA, partial	-	Mmu.10994.1.S1_at	7.2277	0.1929	6.4760	0.1661	0.0418
gDNA.Hs.307059.0.S1 FEA=U133PSR DEF=Orthologous to 234748_x_at KRMP1 mRNA for mitotic kinesin-related protein, partial cds, alternative exon	-	MmugDNA.8037.1.S1_at	7.3903	0.1380	8.1461	0.2159	0.0420
Transcribed locus	-	MmugDNA.23580.1.S1_at	11.5090	0.1967	10.9060	0.0558	0.0420
Hypothetical protein LOC162993	LOC162993	MmugDNA.20052.1.S1_at	10.1147	0.2435	10.9494	0.1461	0.0424
Exocyst complex component 7	EXOC7	MmugDNA.37506.1.S1_at	6.1641	0.2049	5.4692	0.1183	0.0425
Chromosome 9 open reading frame 105	C9orf105	MmugDNA.22984.1.S1_at	5.6417	0.2063	4.9362	0.1239	0.0427
KIAA1109	KIAA1109	MmugDNA.30700.1.S1_at	7.6424	0.1675	7.0336	0.1233	0.0429
Nipsnap homolog 3B (C. elegans)	NIPSNAP3B	MmugDNA.9183.1.S1_at	4.7201	0.2458	3.8620	0.1630	0.0437
Collagen, type I, alpha 1	COL1A1	MmugDNA.34995.1.S1_s_at	10.0242	0.1009	11.0927	0.3535	0.0438
TRAF2 and NCK interacting kinase	TNIK	MmugDNA.28110.1.S1_at	7.2035	0.1315	6.6138	0.1549	0.0440
gDNA.Hs.72115.0.A1 FEA=U133PSR GEN=C6orf105 DEF=Orthologous to 229070_at chromosome 6 open reading frame 105	-	MmugDNA.28889.1.S1_at	7.0522	0.1242	7.6716	0.1736	0.0440
Roundabout, axon guidance receptor, homolog 1 (Drosophila)	ROBO1	MmugDNA.22252.1.S1_at	7.2392	0.1413	7.9087	0.1833	0.0444
gDNA.Hs.28391.0.A1 FEA=U133PSR GEN=LPHN3 DEF=Orthologous to 242186_x_at latrophilin 3	-	MmugDNA.4650.1.S1_at	5.9853	0.0192	5.3396	0.2229	0.0447
Phosphotriesterase related	PTER	MmugDNA.38414.1.S1_at	5.4088	0.2256	6.0679	0.0363	0.0448
Deleted in lymphocytic leukemia 8	DLEU8	MmugDNA.25512.1.S1_at	4.5146	0.2223	5.2799	0.1452	0.0449
gb:AF235162.1 DB_XREF=gi:9408532 TID=Mmu.12516.1 CNT=1 FEA=mRNA TIER=ConsEnd STK=0 NOTE=sequence(s) clustered along genome DEF=Macaca mulatta Flt-1 mRNA, partial cds.	-	Mmu.12516.1.S1_at	5.9339	0.1010	6.5218	0.1779	0.0453
Chromosome 21 open reading frame 57	C21orf57	MmugDNA.1454.1.S1_at	8.9070	0.3355	10.0495	0.2134	0.0453
LSM11, U7 small nuclear RNA associated	LSM11	MmugDNA.7409.1.S1_at	7.4848	0.0644	8.5287	0.3582	0.0455
Adaptor-related protein complex 1, sigma 2 subunit	AP1S2	MmugDNA.12168.1.S1_at	5.8100	0.1096	4.8826	0.3049	0.0458

Gene Title	Gene ID	Other ID / Probeset	CON mean	CON SEM	CR mean	CR SEM	*t*-test
chromosome 10 open reading frame 25	-	MmugDNA.26101.1.S1_at	6.4484	0.1779	7.1141	0.1501	0.0459
Transcribed locus, strongly similar to NP_061844.1 G protein-coupled receptor 27; super conserved receptor expressed in brain	-	MmugDNA.28513.1.S1_at	9.1433	0.2187	8.2940	0.2008	0.0459
gi:56089251 DEF=SPG6 _5293 Rhesus macaque genomic DNA in pCR-XL-TOPO Macaca mulatta STS genomic clone MMA5293, sequence tagged site. GEN=SPG6 PROD=spastic paraplegia 6 (autosomal dominant)	-	MmuSTS.255.1.S1_at	7.8828	0.0897	6.8970	0.3329	0.0460
Kallikrein 10	KLK10	MmugDNA.23514.1.S1_at	4.6574	0.1688	4.0477	0.1306	0.0461
G elongation factor, mitochondrial 1	GFM1	MmugDNA.14779.1.S1_at	4.5263	0.2249	3.8640	0.0583	0.0464
Leucine rich repeat containing 58	LRRC58	MmugDNA.946.1.S1_at	5.5232	0.2720	4.7373	0.0532	0.0470
Ankyrin repeat and SOCS box-containing 8	ASB8	MmugDNA.19994.1.S1_at	7.6021	0.2271	6.7681	0.1870	0.0471
Solute carrier family 5 (low affinity glucose cotransporter), member 4	SLC5A4	MmugDNA.17537.1.S1_at	7.0746	0.2239	7.9148	0.1951	0.0474
Within bgcn homolog (Drosophila)	WIBG	MmugDNA.35808.1.S1_at	7.3735	0.2805	6.4234	0.1848	0.0474
S100 calcium binding protein A13	S100A13	MmugDNA.37998.1.S1_s_at	6.6918	0.0944	7.4735	0.2597	0.0474
Solute carrier family 44, member 1	SLC44A1	MmugDNA.39116.1.S1_at	5.5614	0.1652	4.9679	0.1305	0.0478
Solute carrier family 7 (cationic amino acid transporter, y+ system), member 1	SLC7A1	MmugDNA.6417.1.S1_at	5.5375	0.2163	6.1928	0.0855	0.0479
not provided	-	MmugDNA.11903.1.S1_at	6.8654	0.1373	6.0274	0.2649	0.0484
Ankyrin repeat and SOCS box-containing 5	ASB5	MmugDNA.38981.1.S1_at	8.3716	0.2172	9.1670	0.1820	0.0485
gi:60301528 DEF=WIF1_7996 Rhesus macaque genomic DNA Macaca mulatta STS genomic clone MMA7996, sequence tagged site	-	MmuSTS.4753.1.S1_at	5.4693	0.1497	6.3067	0.2583	0.0486
Protein phosphatase 1, regulatory (inhibitor) subunit 1A	PPP1R1A	MmugDNA.14104.1.S1_at	5.8026	0.2228	5.0828	0.1275	0.0486
TRAF2 and NCK interacting kinase	TNIK	MmugDNA.3074.1.S1_at	4.7422	0.0838	4.1238	0.2042	0.0487
Luteinizing hormone/choriogonadotropin receptor	**LHCGR**	**MmugDNA.21104.1.S1_at**	**7.5216**	**0.2428**	**8.3359**	**0.1602**	**0.0488**
Ankyrin repeat and IBR domain containing 1	ANKIB1	MmugDNA.26186.1.S1_at	5.3457	0.1029	4.7170	0.2000	0.0490
CNKSR family member 3	CNKSR3	MmugDNA.14645.1.S1_s_at	4.4822	0.1831	3.8883	0.1078	0.0490
Cysteine conjugate-beta lyase; cytoplasmic (glutamine transaminase K,	CCBL1	MmugDNA.31015.1.S1_at	8.6614	0.2176	7.9950	0.0976	0.0491
DCN1, defective in cullin neddylation 1, domain containing 4 (S. cerevisiae)	DCUN1D4	MmugDNA.36638.1.S1_at	5.5776	0.1367	4.9894	0.1601	0.0491
gb:CB230611 DB_XREF=gi:28282189 DB_XREF=AGENCOURT_11467541 CLONE=IMAGE:6883556 TID=Mmu.12981.1 CNT=13 FEA=EST TIER=ConsEnd STK=0 NOTE=sequence(s) clustered along genome	-	Mmu.12981.1.S1_at	9.1237	0.2359	8.0945	0.2831	0.0491
gb:CN647784 DB_XREF=gi:47161227 DB_XREF=ILLUMIGEN_MCQ_29068 CLONE=IBIUW:7248 TID=Mmu.12423.1 CNT=3 FEA=EST TIER=ConsEnd STK=0 NOTE=sequence(s) clustered along genome	-	Mmu.12423.1.S1_at	4.8968	0.1833	4.1725	0.1842	0.0494
gb:CB230611 DB_XREF=gi:28282189 DB_XREF=AGENCOURT_11467541 CLONE=IMAGE:6883556 TID=Mmu.12981.1 CNT=13 FEA=EST TIER=ConsEnd STK=0 NOTE=sequence(s) clustered along genome	-	Mmu.12981.1.S1_s_at	9.7647	0.1485	8.5300	0.4185	0.0498
Transporter 2, ATP-binding cassette, sub-family B (MDR/TAP)	TAP2	MmugDNA.3066.1.S1_at	6.8936	0.1462	6.2929	0.1592	0.0498

Appendix F: Compiled list of genes considered for investigation after screening microarray data for our experimental groups (Young Adult CON, n=3; Young Adult CR, n=3). The table includes pituitary gland and testis genes that showed a significant and non-significant change in gene expression based on our filtering parameters.

Pituitary genes (Filtered with Genesifter: t-test (P<0.05) and 1.5 fold-change: 145 probesets)			Signal means have been log2 transformed					
Gene Title	**Gene ID**	**Other ID / Probeset**	**CON mean**	**CON SEM**	**CR mean**	**CR SEM**	**Ratio/Direction**	***t*-test**
1-acylglycerol-3-phosphate O-acyltransferase 3	AGPAT3	MmugDNA.39097.1.S1_at	9.59	0.04	8.97	0.09	1.53 / Down	0.0037
Phospholipase C, beta 1 (phosphoinositide-specific)	PLCB1	MmugDNA.13551.1.S1_at	4.00	0.03	3.38	0.05	1.54 / Down	0.0003
Thyroid stimulating hormone receptor	TSHR	MmugDNA.32655.1.S1_at	3.29	0.11	2.63	0.03	1.58 / Down	0.0046
Pituitary genes (not significantly different but potentially worth investigating)								
Gene Title	**Gene ID**	**Other ID / Probeset**	**CON mean**	**CON SEM**	**CR mean**	**CR SEM**	**Ratio**	**Direction**
Glycoprotein hormones, alpha polypeptide	CGA	MmugDNA.4648.1.S1_at	9.88	0.44	6.68	1.82	9.15	Down
Glycoprotein hormone alpha 2	GPHA2	MmugDNA.19830.1.S1_at	3.01	0.01	2.98	0.03	1.02	Down
Glycoprotein hormone beta 5	GPHB5	MmugDNA.39443.1.S1_at	3.52	0.01	3.54	0.02	1.01	Up
Uncoupling protein 2 (mitochondrial, proton carrier)	UCP2	MmugDNA.16174.1.S1_at	9.33	0.17	9.43	0.02	1.06	Up
Thyroid stimulating hormone, beta	TSHB	MmuSTS.968.1.S1_at	14.05	0.13	14.39	0.03	1.26	Up
Macaca mulatta chorionic gonadotropin beta subunit mRNA	CGB	Mmu.13013.1.S1_at	10.51	0.19	10.43	0.04	1.06	Down
Prolactin releasing hormone	Prolactin	MmuSTS.2319.1.S1_at	15.43	0.05	15.43	0.04	1.00	Up
Proopiomelanocortin	POMC	MmugDNA.3018.1.S1_at	15.41	0.05	15.52	0.04	1.08	Up
Monkey growth hormone mRNA	GH	Mmu.15973.2.S1_x_at	6.56	0.04	6.41	0.08	1.12	Down
Follicle stimulating hormone, beta polypeptide	FSHB	MmugDNA.37655.1.S1_at	9.68	0.35	9.39	0.43	1.22	Down
Luteinizing hormone, beta subunit and Adrenocorticotropin hormone	LHB and ACTH	Do not exist on microarray						
Testicular genes (Filtered with Genesifter: t-test (P<0.05) and 1.5 fold-change: 260 probesets)			Signal means have been log2 transformed					
Gene Title	**Gene ID**	**Other ID / Probeset**	**CON mean**	**CR mean**	**CON SEM**	**CR SEM**	**Ratio/Direction**	***t*-test**
Cisplatin resistance-associated overexpressed protein	CROP	MmugDNA.33064.1.S1_x_at	6.75	6.14	0.06	0.15	1.53 / Down	0.0179
1-acylglycerol-3-phosphate O-acyltransferase 3	AGPAT3	MmugDNA.39097.1.S1_at	9.21	8.58	0.17	0.12	1.54 / Down	0.0408
Luteinizing hormone/choriogonadotropin receptor	LHCGR	MmugDNA.21104.1.S1_at	7.52	8.34	0.24	0.16	1.76 / Up	0.0488
Sperm specific antigen 2	SSFA2	MmugDNA.26522.1.S1_at	7.67	5.89	0.23	0.11	3.44 / Down	0.0022
Testicular genes (not significantly different but potentially worth investigating)								
Gene Title	**Gene ID**	**Other ID / Probeset**	**CON mean**	**CON SEM**	**CR mean**	**CR SEM**	**Ratio**	**Direction**
Glycoprotein hormones, alpha polypeptide	CGA	MmugDNA.29263.1.S1_at	9.30	0.07	9.46	0.14	1.12	Up
Glycoprotein hormone alpha 2	GPHA2	MmugDNA.19830.1.S1_at	3.18	0.03	3.23	0.06	1.03	Up
Glycoprotein hormone beta 5	GPHB5	MmugDNA.39443.1.S1_at	5.14	0.13	5.00	0.09	1.10	Down
Steroidogenic acute regulatory protein	StAR	MmuSTS.4519.1.S1_at	7.89	0.40	7.97	0.74	1.06	Up
Prostaglandin-endoperoxide synthase 2 (prostaglandin G/H synthase and cyclooxygenase)	PTGS2	MmugDNA.4494.1.S1_at	2.00	0.03	2.01	0.05	1.00	Up
Superoxide dismutase 2, mitochondrial	SOD2	MmugDNA.24030.1.S1_at	12.99	0.17	13.01	0.04	1.01	Up
Catalase	CAT	MmugDNA.19007.1.S1_at	7.15	0.07	7.74	0.31	1.50	Up
Glutathione peroxidase 5 (epididymal androgen-related protein)	GPX5	MmugDNA.34442.1.S1_at	5.16	0.02	5.36	0.16	1.15	Up
Insulin-like 3 (Leydig cell)	INSL3	MmugDNA.29281.1.S1_s_at	11.78	0.36	12.58	0.66	1.74	Up
Hydroxysteroid (17-beta) dehydrogenase 3	HSD17B3	MmugDNA.20457.1.S1_at	10.75	0.44	10.52	0.59	1.18	Down
Hydroxy-delta-5-steroid dehydrogenase, 3 beta- and steroid delta, somerase 2	HSD3B2	MmuSTS.601.1.S1_at	2.74	0.01	2.67	0.05	1.05	Down
Cytochrome P450, family 17, subfamily A, polypeptide 1	CYP17A1	MmuSTS.4193.1.S1_at	7.46	0.47	8.23	0.81	1.71	Up
Cytochrome P450, family 11, subfamily A, polypeptide 1	CYP11A1	MmuSTS.4192.1.S1_at	5.95	0.43	6.09	0.68	1.10	Up
Thyroid stimulating hormone, beta	TSHB	MmuSTS.968.1.S1_at	5.16	0.35	5.09	0.13	1.05	Down
Macaca mulatta chorionic gonadotropin beta subunit mRNA	CGB	Mmu.13013.1.S1_at	7.88	0.06	7.85	0.14	1.02	Down
Prolactin releasing hormone	Prolactin	MmuSTS.2319.1.S1_at	8.96	0.55	8.94	0.58	1.01	Down
Proopiomelanocortin	POMC	MmugDNA.3018.1.S1_at	10.53	0.17	10.72	0.10	1.14	Up
Monkey growth hormone mRNA	GH	Mmu.15973.2.S1_x_at	6.14	0.32	6.02	0.24	1.08	Down
Follicle stimulating hormone, beta polypeptide	FSHB	MmugDNA.37655.1.S1_at	3.15	0.06	3.18	0.10	1.02	Up
Luteinizing hormone, beta subunit and Adrenocorticotropin hormone	LHB and ACTH	Do not exist on microarray						

Appendix G: Protocol for Use of PrimerExpress® Software

The following is the general protocol for designing PCR primers using the PrimerExpress® software. There are other software options available or alternatively you can design primers by hand using calculations based on melting temperatures. Although this is the system used for designing our primers it is intended only as a general example and adjustments can be made as needed.

1. Choose the gene(s) of interest based on microarray results
2. Go to NCBI (www.ncbi.nlm.hih.gov)
3. Select: All Databases from menu options then: Nucleotide: sequence database
4. Under Search: Nuceotide▼: for _____ enter in a search term. The best is the Gene Identifier from the microarray output. Other terms such as Gene Title, Gene ID or a common name are also useful
5. Choose the best result option, preferably one that has the complete mRNA sequence in your species of choice. Try to avoid clones and partial mRNA, different species and STS fragments which could be either an intron or exon and won't be good for primer design. A list of all the genes in the NCBI database that we used for designing our primers is included at the end of this protocol.
6. Some important components of the Results Page:
    a. Locus – should be same as Gene Identifier
    b. Definition – tells common name and if complete or partial mRNA, clone, cDNA, etc.
    c. Source Organism – from where the sequence was derived
    d. References – links to relevant PubMed articles
    e. Features: Source – organ or tissue source and possibly who/where sequence discovered/posted into the database
    f. CDS – coding sequence from 'start' to 'stop' codon; protein/amino acid sequence
    g. Gene – location and length
    h. Origin – actual base pair (bp) sequence
7. There are many other options for each search result and NCBI is continually adding new tools to the database. It's now possible to automatically receive the reverse complemented strand, search for STS only, export the results to text files, and many more options.
8. There are roughly three possible search result outcomes.
    a. Complete mRNA sequence from your species of interest is shown. This is the best case scenario.
    b. Partial mRNA or clone from your species of interest
    c. Complete or partial mRNA or clone from another species (ortholog) is given. With the last two options you will need to BLAST the ortholog sequence to possibly find a better sequence in another species or listing.
9. If you need to BLAST then open NCBI again in another window

10. Click on BLAST and under Nucleotide select Option: nucleotide-nucleotide BLAST (blastn). Also on this page is the option to compare two sequences in order to compare homology [Under Special select Option: Align two sequences (bl2seq)].
11. Copy the gene sequence (Origin) from your previous results and paste into the Search box on the newly opened BLASTn window
12. Now hit the BLAST! button followed by FORMAT! button
13. Scroll down to: Sequences producing significant alignments.
14. Want to look for: high score, low E value, species of interest and mRNA
15. By clicking on score you can see a comparison of the GeneChip® sequence you BLASTed with the new sequence you want to use. It shows Identities (how many base pairs match) and Gaps (mismatches).
16. Click on new gene that you will now use for PrimerExpress®. If there is no ideal match then BLAST the two sequences to see how much homology there is between the two. For example, human LHβ and mouse LHβ are almost identical meaning that the gene is relatively conserved across species. From this you could infer that it would be possible to use the human sequence of LHβ in order to design primers intended for use in rhesus macaque tissue.
17. Copy the final sequence to be used for primer design into a word processing file of some kind.
18. Open the PrimerExpress® software.
19. Click on File: New: RT-PCR Document (sqRT-PCR) or Taqman® Probe and Primer Design (qRT-PCR).
20. Open the word processing file with the sequence and Copy and Paste it into Sequence window.
21. Go to Params tab and enter the following guidelines, adjust as necessary:
    for sqRT-PCR:
    a. T_m Requirements: Min 55-57^oC Max 65-68^oC Opt 60^oC Max Diff 2 (T_m is melting temperature while T_a is annealing temperature)
    b. GC Content: Min 40-45 Max 55-60 Clamp 0-2
    c. Length: Min 19 Max 24 Opt 22
    d. 5' Tail: ignore this option
    e. Amplicon: Min 70 Max 90 (T_m) Min 300 Max 500 (Length)

    for qRT-PCR primer and probe parameters:
    a. Min GC: 40% Max GC: 80%
    b. Min length: 18 Max length: 25 (Targeting 20)
    c. Amplicon Min: 100 bp Amplicon Max: 150 bp
    d. We allowed ourselves a penalty between 9-11 and wanted to have more C than G bases. If there were more G than C in the probe we used the complementary strand instead. For example, if the software returned a probe 5' ATCGGCGTCTGG 3' then the complementary 3' TAGCCGCAGACC 5' would become 5' CCAGACGCCGAT 3' for the preferred probe to use.
    e. Probe had to be < 30 bp with the shortest possibility preferred
    f. 3' end of primers could not have more than 2 C or G in the last 5 bp

g. T_m between primers and probe had to be > 10°C (9°C is tolerable)
h. Kept penalty low

22. Click on Primers tab. Then on top menu select Options: Find Primers Now
23. What you will get is a list of potential primers. You want to select the primers that have the best combination of the following: low penalty, few base pair repeats, appropriate lengths for primers and amplicon, similar T_m for both primers, good % of G/C content and limited A/T content.

Designing primers by hand

1. Target the 3' end of the mRNA sequence
2. 20-23 base pairs in length
3. T_a: 65-72°C (which is the mean of the T_m for both primers)
4. 60% G/C content
5. Finish with GC, CG, CC or GG with A/T in the middle (ie. CAG, GTC)
6. 300-500 bp for amplicon length
7. Forward and Reverse primers should have approximately equal T_m
8. No more than four C or G in a row

Use the calculation: $T_m = 4(G+C) + 2(A+T)$

When producing cDNA from mRNA you can either work with oligo dNTP hexamers or random dNTP hexamers. Oligos will attach only at the 3' PolyAAA tail end of the mRNA sequence whereas random hexamers will attach anywhere along the sequence. If you choose to produce cDNA with random dNTP hexamers then the primer can be anywhere in the sequence because you typically get longer translated genes. If you choose to produce cDNA with oligo dNTP hexamers then you should limit the primer design sequence to the 3' PolyAAA tail end of your mRNA. The translated genes will be more similar to each other but length may vary as transcriptase falls off. These non-specific amplified products are of different lengths and is why higher/specific temperatures help eliminate 'ghost' bands. We designed all our probes and primers to the 3' end of the mRNA sequence so that they would function with oligo or random dNTP hexamer derived cDNA.

Here is the complete list of genes we used for designing our sqRT-PCR and qRT-PCR primers and probes used in Chapters 3 and 4. They can be found in the National Center for Biotechnology Information (NCBI) Entrez Nucleotide database, a collection of sequences from several sources. The only exception was StAR primers and probe for qRT-PCR which were graciously supplied by Dr. Jon Hennebold at the Oregon National Primate Research Center.

1. LOCUS: XM_001090917; 628 bp mRNA linear
   DEFINITION PREDICTED: Macaca mulatta similar to Glycoprotein hormones alpha chain precursor (Anterior pituitary glycoprotein hormones common alpha subunit) (Follitropin alpha chain) (Follicle-stimulating hormone alpha chain) (FSH-alpha) (Lutropin alpha chain) (Luteinizing hormone alpha …), mRNA

2. LOCUS: XM_001104839; 4420 bp mRNA linear
   DEFINITION PREDICTED: Macaca mulatta thyroid stimulating hormone receptor, transcript variant 2 (TSHR), mRNA
3. LOCUS: XM_001104367; 6316 bp mRNA linear
   DEFINITION PREDICTED: Macaca mulatta 1-acylglycerol-3-phosphate O-acyltransferase 3 (AGPAT3), mRNA
4. LOCUS: XM_001115559; 2094 bp mRNA linear
   DEFINITION PREDICTED: Macaca mulatta uncoupling protein 2 (UCP2), mRNA
5. LOCUS: XM_001101290; 4965 bp mRNA linear
   DEFINITION PREDICTED: Macaca mulatta similar to sperm specific antigen 2, mRNA.
6. LOCUS: XM_001093672; 2103 bp mRNA linear
   DEFINITION PREDICTED: Macaca mulatta casein kinase 1 epsilon (CSNK1E), mRNA
7. LOCUS: XM_001107538; 5111 bp mRNA linear
   DEFINITION PREDICTED: Macaca mulatta prostaglandin-endoperoxide synthase 2 (PTGS2, COX2), mRNA.
8. LOCUS: XM_001114090; 3041 bp mRNA linear
   DEFINITION PREDICTED: Macaca mulatta luteinizing hormone/ choriogonadotropin receptor (LHCGR), mRNA
9. LOCUS: XM_001090472; 2343 bp mRNA linear
   DEFINITION PREDICTED: Macaca mulatta similar to steroidogenic acute regulator isoform 1, transcript variant 3, mRNA (sqRT-PCR only)
10. LOCUS: XM_001105829; 1131 bp mRNA linear
    DEFINITION PREDICTED: Macaca mulatta estradiol 17 beta-dehydrogenase 3, transcript variant 2 (HSD17B3), mRNA.
11. LOCUS: DR769273; 549 bp mRNA linear
    DEFINITION ILLUMIGEN_MCQ_62609 Katze_MMTE Macaca mulatta cDNA clone IBIUW:34171 5' similar to Bases 6 to 449 highly similar to human INSL3 (Hs.37062), mRNA sequence
12. LOCUS: XM_001113717; 1815 bp mRNA linear
    DEFINITION PREDICTED: Macaca mulatta hydroxy-delta-5-steroid dehydrogenase, 3 beta- and steroid delta-isomerase 2, transcript variant 1 (HSD3B2), mRNA.

Two other primer sets were designed for earlier work with macaque adrenals by Dr. Urbanski's staff. They used the following human sequences:

1. LOCUS: NM_000102; 1755 bp mRNA linear
   DEFINITION Homo sapiens cytochrome P450, family 17, subfamily A, polypeptide 1 (CYP17A1), mRNA
2. LOCUS: NM_000781; 1821 bp mRNA linear
   DEFINITION Homo sapiens cytochrome P450, family 11, subfamily A, polypeptide 1 (CYP11A1), nuclear gene encoding mitochondrial protein, mRNA

Appendix H: Protocol for RT-PCR and Gel Imaging

Reverse Transcription (RT)

1. Prepare one batch of RT-MasterMix in a tube. Always prepare mix for n+0.5 (or n+1) where n = number of samples. For each sample you will need (in this order):
   - 4.0 µl of 10X RT Buffer
   - 2.4 µl of 25 mM $MgCl_2$
   - 2.0 µl of 5 mM dNTPs
   - 2.0 µl of RNAsin (RNase inhibitor; 10 units / µL)
   - 1.0 µl of Reverse Transcriptase
   - 3.6 µl of DEPC H_20
   - Total of 15 µL final volume
2. Separately, prepare RNA samples for denaturing and oligo $d(T)_{15}$ annealing. For each RNA sample you will need:
   - 1 µl of oligo $d(T)_{15}$ (could also use random hexamers if desired)
   - X µl of sample containing 1 µg of RNA (no more than 4 µl)
   - Y µl of H_20 (volume needed to complete 5 µl)
   - Total of 5 µl final volume
3. Heat RNA samples in thermocycler to denature the RNA: 5 min @ 70°C
4. Quickly cool the sample tubes down on ice: 5 min @ 4°C
5. Add the enzyme-containing RT-MasterMix to the treated RNA samples.
6. Load the 20 µL RNA/MasterMix tubes and run an RT program on the thermocycler: 5 min @ 25°C → 60 min @ 37°C → 15 min @ 70°C
7. Place cDNA on ice immediately and store at -20°C if not using right away.

Primer Preparation

Primers arrive in a lyophilized form and must be rehydrated:

1. Take the primers out of the -20°C freezer and place at RT for 10 minutes
2. Spin them down to make sure all the powder is at the bottom of the vial
3. From the spec sheet supplied with each primer find the number of nmoles of product. Multiply the value by 10 and add this amount of water or TE buffer (µL) in order to obtain a 100 µM stock. Vortex.
4. Store stock at -20°C; remove aliquots as needed to make 25 µM working dilutions (1:4 dilution)

Polymerase Chain Reaction Protocol (PCR)

1. Prepare one batch of PCR-MasterMix per set of primers in a tube. Always prepare mix for n+0.5 (or n+1) where n = number of samples.
2. For each sample you will need (in this order):
   - 2.5 µL of 10X PCR buffer (containing 15mM $MgCl_2$)
   - 0.5 µL of dNTPs (10mM concentration, or random hexamers)
   - 0.5 µL of 5' forward primer (25-50µM)
   - 0.5 µL of 3' reverse primer (25-50µM)
   - 0.15 µL of HotStarTaq® DNA Polymerase
   - 19.85 of µL dH_20

Total of 24 µL final volume

3. Add 1 µL of cDNA sample to 24 µL of PCR-MasterMix. Spin down sample if needed before loading in thermocycler.
4. Load the 25 µL cDNA/MasterMix tubes and run a PCR amplification program on the thermocycler:
    a) 15 min at 95°C – activation of HotStarTaq® DNA Polymerase
    b) 1 min at 94°C – denaturation of cDNA
    c) 1 min at specific annealing temperature for the primer pair
    d) 1 min at 72°C – amplification/extension
    e) Repeat for # of cycles specific to each primer pair
5. Place amplified cDNA on ice immediately and store @ -20°C if not running a detection gel right away.

DNA Detection Protocol using Agarose Gel

1) Prepare 1 L of stock 10X TBE Buffer (Tris-Borate-EDTA)
    a. 1 g NaOH (to speed the reaction)
    b. 108 g Tris base (Trizma, $C_4H_{11}NO_3$, F.W. 121.1)
    c. 55 g boric acid (H_3BO_3, F.W. 61.8)
    d. 7.4 g EDTA-disodium salt (F.W. 372.2) OR 9.3 g EDTA-monosodium salt (F.W. X)
    e. Add dH_20 to 1 Liter
    f. pH is 8.3 and requires no adjustment
2) Prepare 2 L of stock 1X TBE Buffer (200 mL 10X stock + 1800 mL dH_2O)
3) Prepare agarose gel at the appropriate % (2% for our studies)
4) 100 mL 1X TBE Buffer + 2 g agarose
5) Heat in microwave, swirling occasionally, until agarose is dissolved.
6) Cool under tap water and add 1 µL of ethidium bromide [50 µg / mL] to achieve a final concentration of 0.5 µg / mL.
7) Pour into electrophoresis mold and insert combs.
8) Once the gel has set remove combs and place gel in the electrophoresis chamber. Cover with 1X buffer.
9) Mix 1µL of DNA loading buffer with 7µL of sample.
10) Load samples into gel wells and load 1.5 µL MassRuler DNA Ladder Low Range (Feremantas) in first column.
11) Run electrophoresis at 90 volts (lower for higher resolution).
12) Visualize the gel using QuantityOne software and GelDoc. Save images as .tiff files for importing into photo software later.

Appendix I: Troubleshooting Microarray Data, Primer Design, RT-PCR and Gel Imaging

During the course of events leading from microarray data to successful quantification of gene expression there are a number of potential pitfalls. I had to overcome many of them during my research so I thought it useful to document some of the solutions I found to these problems. In addition, there are a number of background details I discovered along the way which others may find valuable to their own research. The comments, though relevant to them, don't really belong in any of the earlier chapters so I've compiled them here.

Finally, I encourage anyone performing microarray experiments for the first time to extensively mine the company website of the array platform they are using. It will have a wealth of information which will only help you as you work through proper experimental design and analysis.

Affymetrix Microarrays

The raw signal data point in a global scaled (normalized) dataset represents the amount of RNA bound to the microarray chip. It is one arbitrary value for the signal intensity of that one particular probeset for a gene. The probeset consists of 11-16 matching probe pairs as well as 11-16 mismatched probe pairs; each probe is 25 base pairs long. This setup allows the chip/algorigthm to check for errors/mismatches/false positives and to globally scale the data to its own chip or across a series of chips. All matching probe pair sequences are designed to target the 3' untranslated region (UTR) of mRNA. Information on all probesets and their probe pair sequences can be found at the Affymetrix website (www.affymetrix.com) where, in the case of the Rhesus Macaque Genome Array, they list ~600,000 probe (~300,000 probe pair) sequences. These are only the matches, however, so there are actually 1.2 x 10^6 probe (600,000 probe pair) sequences. Each probeset for a given gene has its probe pairs scattered across the microarray chip in a grid. The instrument system knows where the sequences are based on their position and consolidates the signals to give one average/scaled intensity value (arbitrary units). Each gene can have anywhere from 1-8+ probesets on the chip. That is why, for example, that StAR has 1 probeset while LHCGR has 3 and AGPAT has 7. There are 52,000+ probesets on the rhesus macaque chip representing 47,000+ transcripts/genes. The image below is taken from the Affymetrix manual: Data Analysis and Fundamentals. It shows a probeset which includes 10 probe pairs. For simplicity the probe pairs are shown grouped together, but on the actual GeneChip® they would be scattered around the array.

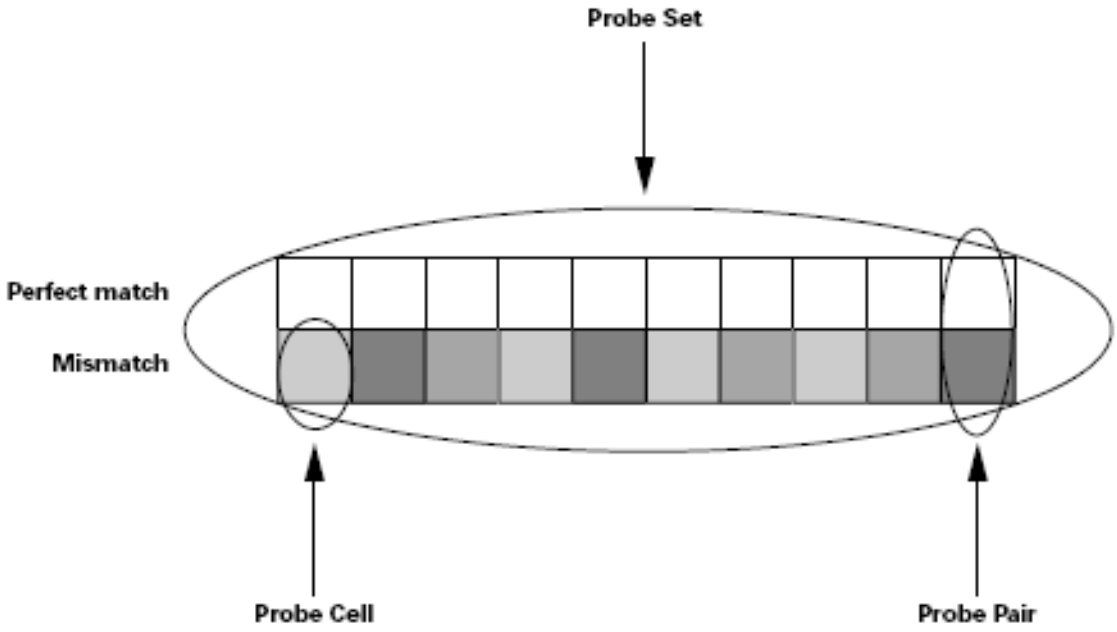

So where do these gene sequences come from? At the time of our experiments, the sequences on the Affymetrix GeneChip® Rhesus Macaque Genome Array came from the University of Nebraska and the Baylor School of Medicine. These two facilities are working to determine the entire rhesus macaque genome, including introns and exons. They shared their data with Affymetrix for use in their array system. Affymetrix then attached a GeneID to each probeset so that it can be found in the NCBI Entrez Nucleotide database (National Center for Biotechnology Information; www.ncbi.nlm.nih.gov). When you search for these probesets, however, the link will take you to a human ortholog for the gene. Why? It seems that Nebraska/Baylor have not yet entered the sequences into the NCBI GeneBank. Instead they are posting their data at the Ensembl project (www.ensembl.org) with some additional sequences available at (http://rhesusgenechip.unomaha.edu). Baylor also has its own website but it's not as user-friendly as Ensembl and in theory should be identical. Since the sequences are not in NCBI, Affymetrix did the next best thing and connected to all the human orthologs. This is not a problem as long as you are aware of it and take the extra step to find the rhesus macaque mRNA sequence. What we did was to BLAST the human ortholog sequence for our genes of interest at the NCBI website so as to get the best fitting, alternative sequences. In every case, except INSL3 and LHβ, we were able to find a predicted rhesus macaque sequence. (We eventually found a cloned mRNA sequence for INSL3 which we used in our primer design). The predicted sequences are from the Southwest National Primate Research Center in San Antonio, TX. They have been using Baylor's genomic sequences (including introns and exons) and computational comparing them to other species in order to make a best fit prediction as to the actual rhesus macaque sequences. Without understanding these details a

researcher may mistakenly think the rhesus macaque array is simply using human orthologs and may end up designing PCR primers against the wrong sequences.

sqRT-PCR

Although elegant in its simplicity, the fundamental technique of reverse-transcription polymerase chain reaction (sqRT-PCR) is fraught with challenges. Even though the methodology is identical for each gene investigated, it is the subtle nuances that can determine success or failure.

First, for each pair of primers we determined the optimal annealing temperature and linear range of amplification. This involved preparing a pooled sample of cDNA to run with the primers. Then, using a lower temperature and higher number of cycles, we ran the PCR to see if any single band amplicons were detected. From the initial run we were able to make a judgment as to the need for temperature and cycle adjustments. We always investigated β-actin first because it is a highly expressed housekeeping gene, showed even expression on the microarray data and would demonstrate that the cDNA was of good quality. Usually if adjustments had to be made for the PCR it meant raising the annealing temperature of the run.

Once we had a rough idea of the ideal temperature setting we kept the temperature constant and pulled samples at various cycles of the reaction. By doing this and running the products on a gel we were able to determine the linear range of amplification for each gene. We were now ready to run individual samples at the appropriate temperature and cycle count for each pair of primers. Even though we were fairly fortunate and ran these trials very carefully, it still took multiple reactions to get each gene to work properly.

One of the biggest problems we had with a number of primers was the presence of a double band on the electrophoresis gel. There are a few possibilities as to the cause of multiple bands on a gel. It could be that the cDNA is not good. In our case this did not seem to be the problem because the results of our β-actin PCR were very clean. It could also be a reagent problem, but again this seemed unlikely as other researchers in the lab were having success with the same materials. It could be that the gene was being expressed differentially in individual animals (i.e. splice variants). This too seemed unlikely, but we reconfirmed our primer design to make sure we were picking up our desired genes. It seemed the most likely explanation was a temperature issue. The secondary bands we were seeing were most likely caused by poorly annealing primers that were replicating smaller amplicons randomly. Ultimately, the way to determine what was going on was to increase annealing temperatures during the PCR run. In doing so we hoped to eliminate any nonspecific primer binding and achieve only one nice, clean band for our gel images.

Below are gel images from two of our experiments. Image A shows TSHβ during linear range amplification trials. As you can see there are two distinct bands. Unfortunately, even with increased annealing temperatures, this was one of the primer pairs that we were unable to completely correct. Although it may have been possible to get them working by further adjustments or redesigning new primers, the decision was made to discontinue our investigation of this gene (discussed in Chapter 2).

Images B and C show experimental results of StAR detection. Our initial trials, seen in Image B, resulted in nonspecific binding and double bands. In this instance we were able to achieve results by raising the annealing temperature and adjusting the number of cycles. We confirmed proper PCR amplification by sequencing the resulting amplicons.

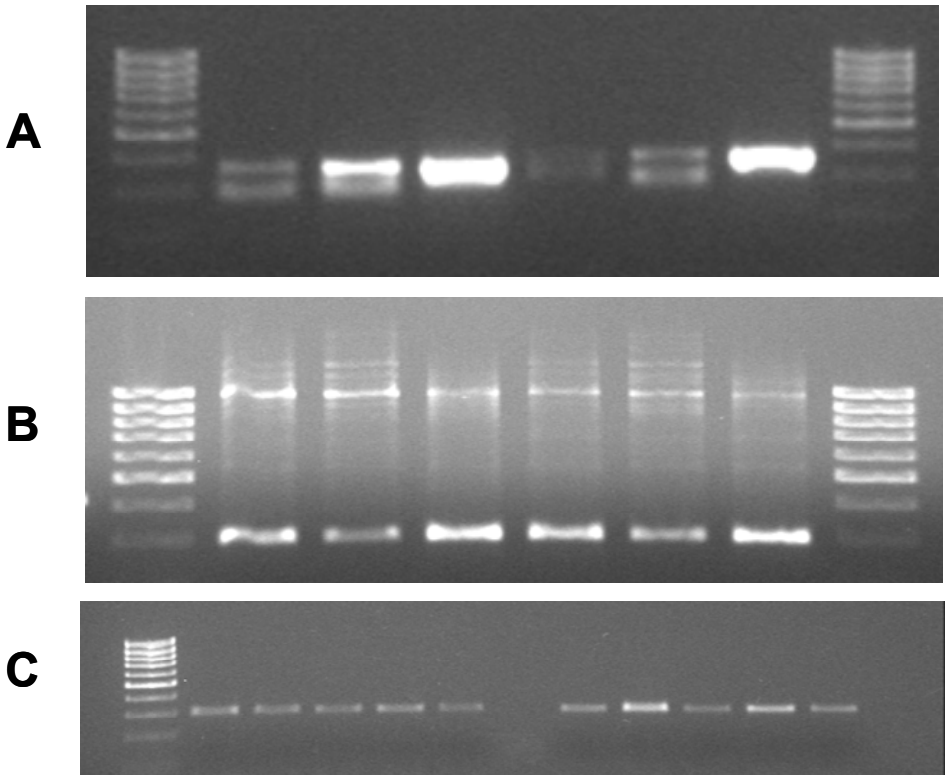

Appendix J: Protocol for Microwave Antigen Retrieval (MAR) and Immunohistochemistry (IHC)[1]

Day 1

1) Procedure has been optimized for free floating tissue sections.
2) Place sectioned tissue into a six-well plate and rinse sections 2 X 10 minutes in 0.02M KPBS at room temperature (RT) on an orbital shaker. Rather than transferring tissue keep sections in one plate as long as possible by suctioning out solutions. Alternatively, use individual mesh screen cups for each well so all tissues can be transferred together. This is the best method for microwave antigen retrieval (MAR) because it allows for a quick and efficient transfer during heating.
3) Microwave antigen retrieval:
    a. Prepare 60 mL of 2X Antigen Retrieval Citra (BioGenex; San Ramon, CA) from stock and bring to RT.
    b. Irradiate* the beaker of retrieval solution at full power (level 10) for ~60 seconds until the buffer boils**. Once it boils, quickly pour the solution into a six-well plate. Transfer the tissue from the wash plate to the retrieval solution. Heat the tissue at power level 4 for 20 seconds so as to maintain the buffer at ~80^{o}C. When finished remove plate and place on countertop so as to cool slowly to RT.
    c. After antigen retrieval a check of tissue integrity can be performed. Mount the treated sections onto slides and allow to air dry. Stain tissue with a contrasting stain (such as eosin-Y), dehydrate, and coverslip. Look at tissue under the microscope to determine if it has been damaged (i.e. holes, cellular degradation, etc).
4) After cooling, transfer the tissue back to the six-well plate and wash 2 X 10 minutes in 0.02M KPBS at RT on an orbital shaker.
5) Optional step: Elimination of endogenous peroxidases.
    a. Transfer tissue into 0.3-2% hydrogen peroxide in absolute methanol for 20-60 minutes at room temperature (adjust % and time based on the nature of the tissue being stained). Incubation time will be reduced as you increase % of H_2O_2. When doing ICC for GnRH do not use methanol. Instead treat for 30 minutes in 1% hydrogen peroxidase made in 0.02M KPBS.
    b. Wash sections 2 X 10 minutes in KPBS at RT on an orbital shaker.
    c. In the case of the pituitary gland the nature of the tissue makes it too fragile to withstand incubation in hydrogen peroxide.
6) Block non-specific binding sites by incubating sections in KPBS-B for 90 minutes at RT using orbital shaker.
7) Wash sections 2 X 10 minutes in 0.02M KPBS at RT on an orbital shaker.

[1]From Dr. Henryk Urbanski's lab. Modification of original protocol from Dr. Susan Smith's lab at ONPRC. The key to good antigen retrieval and IHC depends on three things: is the tissue mounted or free floating, what type of tissue is it, and what antibody is being used. This protocol should serve as a guideline and can be modified to fit the situation depending on those three variables.

8) Incubate sections in 1^{o} antibody (Ab) diluted in KPBS-B (1:500) for 60 minutes at RT followed by 24-48 hours at 4^{o}C on orbital shaker.

Day 2

1. After incubation with the 1^{o} Ab, wash tissue 4 X 10 minutes in 0.02M KPBS at RT on an orbital shaker.
2. Dilute biotinylated 2^{o} Ab 1:250 in KPBS-A.
3. Incubate sections with biotinylated Ab for 60 minutes at RT on an orbital shaker.
4. Wash tissue 4 X 10 minutes in 0.02M KPBS at RT on an orbital shaker.
5. Incubate sections in Avidin: Biotinylated enzyme Complex (VECTASTAIN ABC System; Vector Laboratories; Burlingame, CA) made in KPBS-A for 60 minutes at RT. Prepare the solution at least 1 hour prior to incubation.
6. After ABC incubation wash sections 4 X 10 minutes in 0.02M KPBS at RT on an orbital shaker.
7. Follow this with 2 X 10 minute rinses in 150 mM sodium acetate.
8. While rinsing prepare the diaminobenzidine solution (DAB; Sigma; St. Louis, MO) under a fume hood.
9. Just before using add 15 µL 30% H_2O_2 to the filtered 30 mL DAB. The DAB is now activated and must be used under a hood. DAB is extremely carcinogenic and mutagenic so use carefully.
10. Aliquot appropriate volume of DAB into each well and observe. The reaction will usually go very quickly.
11. As sections turn brown transfer them back into sodium acetate and observe. If more staining is needed return to DAB, otherwise move tissue to 0.02M KPBS to arrest the DAB reaction.
12. When all sections are out of the DAB, wash 3 X 10 minutes in 0.02M KPBS at RT on an orbital shaker.
    - Treat all DAB exposed equipment with excess bleach. Dumping and/or spraying bleach directly onto equipment will deactivate the DAB. It can then be soaked in bleach water and left to stand for at least an hour. Pour fluid down drain and wash equipment.
13. Mount sections onto glass slides and allow to air dry for 1-2 hours. Label slides with HistoPrep pen in advance so information doesn't come off during dehydrating and mounting.
14. Dehydrate slides in ethanol series (70%, 90%, 100%) for 10 minutes per concentration. Skip the 70% wash if slides were allowed to dry overnight.
15. Continue dehydrating slides through two stages of xylene for 10 minutes each.
16. Coverslip each slide as it is removed from the final xylene wash. Slides can be left in the wash until ready to coverslip.
17. Allow slides to air dry minimum of two hours.

*Settings for the microwave in Dr. Urbanski's lab:
Specifications - 800 watt output, 1.25 KW power consumption, high frequency output from 80W to 800W at 10 power levels, Samsung (Model No. MW 5700W)

**To standardize timer and power level settings for different microwaves:

1. Prepare beaker of retrieval solution as normal.
2. Irradiate at maximal power level and register the time necessary to boil.
3. Once buffer boils quickly distribute it evenly among a six well plate. Turn power level to 2/3/4/5 and irradiate for 30-60 seconds (depending on tissue and antibody to be used). Monitor to make sure buffer does not boil and check temperature after each trial. If temperature tends to decrease repeat procedure with the next increasing power level.
4. Proceed only when power, irradiation times, and liquid volume have been established for a given temperature.
5. To obtain repetitive results remember to maintain the same total volume of liquid in the wells each time.

Media/Buffers/Solutions

<u>0.12M KPBS Stock Solution</u>
1.47 g KH_2PO_4
8.59 g K_2HPO_4
27.0 g NaCl
Add DEPC water to 400 mL. Adjust pH to 7.4 and complete volume to 500 mL. Autoclave. Adjust recipe for larger volumes.

<u>0.02M KPBS</u>
Dilute from 0.12M KPBS stock solution

<u>KPBS-A</u>
497.5 mL 0.02M KPBS
\+ 2.5 mL Triton X-100 (final concentration of 0.5%)
Has a very long shelf life when stored at 4^{o}C

<u>KPBS-B</u>
487.5 mL 0.02M KPBS
2.5 mL Triton X-100 (final concentration of 0.5%)
\+ 10 mL heat inactivated (56^{o}C for 30 minutes) 2% normal donkey serum
Has a very long shelf life when stored at 4^{o}C

<u>ABC</u> (VECTASTAIN ABC System; Vector Laboratories; Burlingame, CA)
10 mL KPBS
20 µL Solution A
\+ 20 µL Solution B
Make at least one hour prior to use

<u>1% H_2O_2</u>
29 mL 0.02M KPBS
\+ 1 mL 30% H_2O_2

150 mM sodium acetate

136.1 g sodium acetate in 1 L water (1 M)
75 mL of 1 M sodium acetate to total volume of 500 mL of water

DAB (Sigma; St. Louis, MO)

30 mL of 150 mM sodium acetate
\+ One 10 mg DAB tablet
Dissolve completely by stirring (protect from light while doing this)
Add 15 µL of 30% H_2O_2 to activate solution

1^o Ab → rabbit anti-REV-ERBα (Lifespan Biosciences; Seattle, WA)
2^o Ab → donkey anti-rabbit I_gG

Tissue fixation prevents diffusion of soluble components and cellular decomposition, but is itself a major artifact when contemplating immunocytochemistry (IHC). Of main concern is masking of potential tissue antigens. When aldehyde-based fixatives are used (in our case paraformaldehyde), methylene bridges are formed between reactive sites on different portions of the same molecule or adjacent proteins. Fixation does not, however, alter the secondary protein structure. Consequently, the antigen is presumed to be masked in the fixed tissue rather than destroyed by the paraformaldehyde fixative making it possible to utilize microwave oven-boiled slides/tissue for IHC.

The two most important factors influencing MAR effectiveness are the heating conditions (time and temperature) and pH value of the MAR solution. Although the exact chemical reaction is not clear, the mechanism of MAR-IHC appears to involve a renaturation of the structure of fixed proteins through a series of conformational changes, including the possible hydrolysis of formalin-induced cross-linkages (Shi et al., 2001). It appears that 0.01M citrate or bicarbonate buffer (pH 6.0) and 6M urea are superior as bath solutions during boiling (Cattoretti et al., 1993).

Appendix K: Protocol for Fresh Sperm Processing[2]

Caution: Primate semen potentially carries Herpes B virus. Lab coat, gloves, mask, and goggles (or face shield) must be worn when handling primate semen samples. Also remember to dispose of all biomaterial and/or equipment in the appropriate biohazard containers or treat with bleach.

Note: TALP-Hepes w/ BSA should be equilibrated to 37^{o}C, pH 7.4. TALP w/ BSA should be equilibrated to 37^{o}C, 5% CO_2, pH 7.4. Check pH prior to use. Sperm and TALP w/ BSA should be kept in loosely capped 15 mL conical centrifuge tube in the 37^{o}C, 5% CO_2, incubator as much as possible.

1. Samples are collected into pre-weighed, sterile, plastic collection tubes. Animal ID#, date, animal technicians, sedative, stimulations, time of collection (T=0), and other comments are noted on the collection sheet.
2. Sample (and tube) is weighed and placed in biosafety hood at room temperature in order to allow semen to exude from the contracting coagulum. Exudate will eventually be reabsorbed by coagulum if allowed to sit too long. Note appearance of whole sample on data sheet.
3. Exactly 30 minutes (T=30) post-collection the liquid fraction of sample is transferred to a sterile 15 mL conical centrifuge tube using a P200 or P1000 pipetman. (One piece plastic pipets and serological pipets are toxic to sperm. Never use these). Avoid transferring any coagulum. Volume is recorded to the nearest 0.01 mL. Remember to dispose of all equipment in the appropriate biohazard container or treat with bleach.
4. While transferring make two 5 µL eosin-nigrosin (EN) morphology/viability slides for later analysis. Also note color of liquid fraction on data sheet.
    a. If volume is sufficient, the following measures should be taken, in descending order of importance:
        i. 5 µL into 100 µL HOS solution
        ii. pH using 5 µL and pH paper
        iii. osmolarity using 5 µL and osmometer
5. Add 5 mL warm TALP-Hepes w/ BSA to the sample and gently mix using a pipetman. Avoid vigorous trituration as it can damage the sperm. Then add the remaining 10 mL of media.It is **VERY IMPORTANT** that the sample is thoroughly mixed for all washes in order to remove anti-capacitation factors and debris. **DO NOT** wash coagulum.
6. Sample is centrifuged at 130-150G for 10 minutes at room temperature (RT). Make sure the centrifuge is balanced with 15 mL water. Record color and weight of coagulum (and tube).
7. After centrifugation the supernatant is immediately removed using a P1000 and/or P200 pipetman and clean tip. **SAVE THIS FIRST WASH FOR ANALYSIS.** Place wash in another clean 15 mL conical centrifuge tube. Label with animal number and date and place in –80^{o}C freezer for later analysis.

[2] Modified from ONPRC ART Core protocol and Dr. Cathi VandeVoort's lab at CNPRC

8. Add 5 mL warm TALP-Hepes w/ BSA to tube and gently resuspend sperm pellet with pipetman. Add another 10 mL of media. Centrifuge again at 130-150G for 10 minutes.
9. Repeat steps 7 and 8 for a total of three washes. Do not save the supernatant, instead dispose of it in a container with 10% bleach solution. After 20 minutes this can be dumped down the drain.
10. After final centrifugation the pellet is carefully resuspended in 1 mL warm TALP w/ BSA using a P1000 pipetman.
11. Count and concentration can be determined immediately and recorded on data sheet. While doing this the washed sperm should be placed loosely capped in the 37^{o}C, 5% CO_2 incubator.
12. Check results of HOS test. This added time will allow the sperm to continue warming in the incubator after so much time washing at RT.
13. Check motility and status. While checking motility also make note of agglutination and non-sperm cellular components (NSCC).
14. Determine the volume of washed sample containing ~10 x 10^6 sperm. Aliquot this amount into a 15 mL conical centrifuge tube and bring to 1 mL in warm TALP w/ BSA. Place loosely capped in incubator at 37^{o}C, 5% CO_2 and record on data sheet. This dilution is needed for the Sperm-Zona Binding and Acrosomal Staining assay. (Depending on original concentration it may not be possible to have ~10 x 10^6 sperm/mL.)
15. Depending on remaining washed sample volume, ~200 µL aliquots should be made for ROS, SCSA®, and membrane assays. Label screw-top cryovials with animal number, volume, and date and place in –80^{o}C freezer for later analysis. Record volumes on data sheet.
16. The remainder of the sample should be frozen in TEST-yolk extender with cryoprotectant. If needed, reduce the volume aliquoted for assays in step 16 in order to have an adequate concentration for freezing. Record volume on data sheet.

Count and Concentration

1. 190 µL milliQ H_2O and 10 µL of sperm dilution from step 10 are combined into a 0.6 mL microcentrifuge tube.
2. 10 µL of the mix is added to each side of a Neubauer or other hemocytometer with affixed cover slip. Let hemocytometer sit for 5 minutes to make counting easier, but do not let fluid dry out. Sperm are counted using a phase contrast microscope. Make appropriate calculation corrections for the hemocytometer (if necessary) and average the results. Concentration is recorded in million sperm/mL (x 10^6 sperm/mL).
3. If counts differ by >10% between sides then recount using fresh sample until <10%. Average results.

Motility and Status

1. 190 µL warm TALP w/ BSA is aliquoted into a 0.6 mL microcentrifuge tube. 10 µL of sperm suspension from step 10 is added (1:20 dilution) and mixed gently but thoroughly.
2. A 20 µL pipetman is used to place 10 µL of dilution onto a warm microscope slide. A coverslip is carefully added.
3. Motility is determined by counting 100 sperm using a phase contrast microscope (with stage warmer or warm room if possible).
4. Status is determined by giving the sample an average score based on the following scale:
   0 = all dead
   1 = slight side-to-side, no forward progress
   2 = rapid side-to-side, no forward progress
   3 = rapid side-to-side, forward progress in spurts
   4 = slow, steady forward progress
   5 = rapid, steady forward progress

Media/Buffers/Solutions

TALP (w/ BSA)

157 mM NaCl	9.2 g / 1000 mL	
166 mM KCl	12.4 g / 1000 mL	(2.48 g / 200 mL)
120 mM $CaCl_2 + 2H_2O$	17.6 g / 1000 mL	(3.52 g / 200 mL)
120 mM $MgCl_2 + 6H_2O$	24.4 g / 1000 mL	(4.88 g / 200 mL)
167 mM $NaHCO_3$	14.0 g / 1000 mL	(2.80 g / 200 mL)
295 mM glucose	53.1 g / 1000 mL	(26.55 g / 500 mL)

1. Pour 500 mL NaCl stock solution into 1500 mL beaker.
2. Add 10 mg (0.01 g) phenol red.
3. Make sodium lactate solution from 60% syrup [1:35 v/v (ex. 2 mL + 70 mL milliQ water)]. Add 67 mL to beaker.
4. Add 1 mL gentamicin (50 mg/mL solution).
5. Add the following stock solutions:
   a. KCl 19 mL
   b. $CaCl_2 + 2H_2O$ 17 mL
   c. $MgCl_2 + 6H_2O$ 4.1 mL
   d. $NaHCO_3$ 150 mL
6. Dissolve 280 mg $NaH_2PO_4 + H_2O$ in 100 mL glucose stock. Add 17 mL of this solution to beaker. Add slowly in a dropwise fashion.
7. Add 0.006 g (6 mg) sodium pyruvate.
8. Add NaCl stock to bring final volume to 970 mL.
9. Check osmolarity (between 285-295 mOsm). Adjust with NaCl stock solution as needed.
10. Sterile filter and store at 4^oC for one week.

Prior to use:

1. Place 100 mL TALP stock in beaker.
2. Add 0.3 g (0.3%) BSA. Let dissolve, do not stir.
3. Sterile filter and store TALP w/ BSA in 37°C, 5% CO_2, incubator for no more than one day.

TALP-Hepes (w/ BSA)

Combine the following ingredients into 1000 mL milliQ water

NaCl	6.660 g
KCl	0.239 g
$CaCl_2 + 2H_2O$	0.294 g
$MgCl_2 + 6H_2O$	0.102 g
Na_2HPO_4	0.048 g
glucose	0.900 g
sodium lactate	1.87 mL
phenol red	0.010 g
$NaHCO_3$	0.168 g
gentamicin sulftate	0.050 g
Hepes	2.603 g
sodium pyruvate	0.060 g

pH to 7.3-7.5 with osmolarity 275-290. Discard media if below 275 mOsm or above 300 mOsm. If in the target range, use following formula to adjust:

[initial reading – desired (280)] / initial reading = final volume

Sterile filter and store at 4°C for one month.

Prior to use:

1. Place 100 mL TALP-Hepes stock in beaker.
2. Add 0.3 g (300 mg / 0.3%) BSA. Let dissolve, do not stir.
3. Sterile filter and store TALP-Hepes w/ BSA in 37°C, 5% CO_2, incubator for no more than one day.

Expirations
With Hepes = one month in refrigerator
Without Hepes = one week in refrigerator
Anything with BSA = one or two days

MACAQUE SEMEN COLLECTION RECORD

Species: Rhesus macaque ID: 22371 (CR) Date: 10-6-04

Birthdate/age: 3-2-93 Weight (Date taken): 11.0 kg (Target 10.5 kg) (8-31-04)

Collecting technician: Kaleb Marci **Jen** Norma Assisting technician: Kaleb Marci Jen **Norma**

Sedative: 10 mg valium Start time (out of cage): 1:18pm End time (return to cage): blood draw

Stimulation 1: Start time: 1:27pm End time: 1:27pm Last voltage: 17

Stimulation 2: Start time: End time: Last voltage:

Stimulation 3: Start time: End time: Last voltage:

Time collected (0): 1:27pm Comments: Very relaxed

Post-liquefaction (30 minutes) PROCESSOR: Brandon

Raw liquid fraction

Appearance: transparent / **translucent** / opaque

Color: grey-white / **pearl-white** / yellow / pink-red /brown

Volume: 610 µL

Morphology[2] (N/Ab): (/) % normal

HOS (NS/S): (11 / 189) 94.5 % swollen

HOS (NS/S): (22 / 178) 86 % swollen

pH: ~7.7 (7.6-7.8) mOsm: 337

Washed fraction (in TALP-Hepes w/ BSA)

Concentration: 52.25 x 10^5 sperm/mL

Motility: 80 %

Agglutination: NS / SS none

Coagulum

Weight (collection tube + ejac): 8.37 g

Weight (collection tube + coag): 7.72 g

Weight (collection tube): 6.56 g

Weight (ejaculate): 1.81 g

Weight (coagulum): 1.16 g

Weight (liquid fraction): 0.65 g

Color: grey-white / **prl-white** / yellow / pink-red / brown

Count: (47 / 57 / 61 / 44) 52.25 avg

Status[1]: 0 1 2 3 **4** 5

NSCC: present / **absent**

Disposition (raw)

Morphology: 2x5 µL (10 µL) HOS: 2 x 2.5 µL (5 µL)

pH: 5 µL mOsm: 5 µL

NOTES (continued on back if necessary): SCSA, ROS, and membrane samples are all frozen at –80°C. Pellets are frozen in LN_2.

Disposition (washed, in 1 mL TALP w/ BSA)

Conc/count: 10 µL

Motility/status: 10 µL

SCSA: 175 µL

ROS: 175 µL

Membrane: 175 µL

Bind/AR: 192 µL

Diluted to: ~10 x 10^5 sperm/mL

Freezing: 263 µL

Starting conc: ~13.7 x 10^5 sperm/mL

Frozen conc: ~0.68 x 10^5 sperm/plt

pellets frozen: 23 (2 vialsx8, 1 vialx7)

Change if other volumes are collected.

[1]0=all dead 1=slight side-to-side, no forward progress 2=rapid side-to-side, no forward progress

3=rapid side-to-side, forward progress in spurts 4=slow, steady, forward progress 5=rapid, steady, forward progress

Example of a data sheet used for semen collection and processing

Appendix L: Protocol for Sperm Hypo-osmotic Swelling Assay (HOS)

Caution: Primate semen potentially carries Herpes B virus. Lab coat, gloves, mask, and goggles (or face shield) must be worn when handling primate semen samples. Also remember to dispose of all biomaterial and/or equipment in the appropriate biohazard containers or treat with bleach.

1. Incubate microcentrifuge tube containing 100 µL of HOS stock solution at 37°C, 5% CO_2, for 10 minutes.
2. Add 5 µL of well-mixed, liquefied, raw semen to HOS solution and mix.
3. Incubate semen/HOS solution mixture for at least 30 minutes, but not more than 3 hours, at 37°C, 5% CO_2.
4. After incubation place drop of well-mixed semen/HOS sample on a microscope slide and coverslip.
5. Observe under phase contrast for sperm swelling.
6. Count at least 100 (preferably 200) sperm per sample.
7. Classify sperm as swollen or non-swollen and report as % swollen.

Sperm swelling criteria

1. Non-swollen – normal appearance
2. Swollen – abnormal appearance
    a. Tip – tip of the tail is swollen, but the rest of the tail is normal
    b. Hairpin swelling – tail swells at midpiece and mainpiece junction
        i. with tip swelling
        ii. without tip swelling
    c. Shortened and thickened tail – tail swells, constricting surface and causing shortening
    d. Partly/completely enveloped sperm tail – tail balloons from swelling

Results

Normal – ≥60% Equivocal – 50-60% Abnormal – <50%

Media/Buffers/Solutions

Stock solutions for HOS solution

1.5 mM fructose (MW 180.16)	2.70 g / 100 mL milliQ water
1.5 mM sodium citrate + $2H_2O$ (MW 294.1)	1.47 g / 100 mL milliQ water

HOS stock

1. Mix both solutions (fructose + sodium citrate) for final volume of 200 mL.
2. Pipet 100 µL aliquots into disposable microcentrifuge tubes.
3. Freeze at –80°C until ready to use.

Appendix M: Protocol for Sperm Morphology Staining

Caution: Primate semen potentially carries Herpes B virus. Lab coat, gloves, mask, and goggles (or face shield) must be worn when handling primate semen samples. Also remember to dispose of all biomaterial and/or equipment in the appropriate biohazard containers or treat with bleach.

1. Label a frosted slide with animal number, date, and researchers initials.
2. Prewarm slides and stain to 37^{o}C.
3. Pipet 5 µL raw semen sample and 5 µL eosin-nigrosin stain onto 2 slides.
4. Mix together with wooden end of swab.
5. Using a second slide, pull the droplet along the first slide to form a smooth, even smear.
6. Dry the slide rapidly by placing on a slide warmer.
7. Read immediately using phase contrast microscope as crystals and ferning start to appear if slide sits too long.
8. Alternatively, slides can usually be read later if they are coverslipped with Permount mounting media to eliminate cracking.

Criteria for scoring

1. Live
    a. normal live sperm – unstained and morphologically normal
    b. abnormal live sperm – unstained but morphologically abnormal
2. Dead
    a. normal dead sperm – stained but morphologically normal
    b. abnormal dead sperm – stained and morphologically abnormal

Abnormalities should be noted as primarily of the Head, Midpiece or Tail

Appendix N: Protocol for Harvesting and Freezing Primate Oocytes for ZP Binding and Acrosomal Staining[3]

Caution: All procedures should be done wearing a facemask to protect from potential Herpes B exposure from aerosols.

1. Drain off the excess DPBS and transfer the ovaries to the 60 mm petri dish. Add enough fresh DPBS to keep the ovaries dampened. Remove excess tissue if needed.
2. Holding the ovary with the forceps, bisect each ovary with the razor blade.
3. Using the 1 cc syringe with 25 ga needle, puncture and tear all visible follicles on both ovaries. Turn ovaries over and repeat on the other side. Continue to shred the ovaries with the needles until no additional oocytes can be retrieved.

OR

1. Stimulated ovaries are aspirated laparoscopically into 15 mL conical centrifuge tubes containing heparin and TALP-Hepes w/ BSA.
2. Aspirates are taken to the ART Core for processing.
3. Two days post-collection extra oocytes, of varying stages, are given to our lab in a four-well plate containing HECM-9 maturation medium.
4. Remove the oocytes from the 60 mm petri dish or four-well plate using a micropipet and stripper tip. Place the oocytes into a 35 mm petri dish containing 2 mL fresh DPBS.
5. Add 2 mL of 4M DMSO (becomes 4 mL of 2M DMSO). Add the DMSO slowly, swirling the dish constantly. If needed the 35 mm dish can be placed in the refrigerator for up to 24 hours although this is not optimal.
6. Using a micropipet with a capillary tube adapter, load intact oocytes into the capillary tube. Load 5-10 oocytes into each tube
7. Draw the column of fluid containing the oocytes up into the capillary tube so that there is an air gap of at least 5 mm at each end. Seal the end of the capillary tube with CritoSeal and remove from the micropipet. Seal the remaining end and place in a 15 mL conical centrifuge tube labeled with the animal ID, date, and your initials.
8. Note on the centrifuge tube the total number of straws. Store the tube in the appropriately labeled box at –80^{o}C.

Media/Buffers/Solutions

4M DMSO in Dulbecco's Phosphate Buffered Saline (DPBS)
2.8 mL DMSO + 7.2 mL sterile filtered DPBS without calcium chloride
Store at room temperature for 1 month

[3] Modified from Cathi VandeVoort's lab at CNPRC

Appendix O: Protocol for Sperm Activation (Capacitation) for Zona Pellucida Binding and Acrosomal Staining[4]

Caution: Primate semen potentially carries Herpes B virus. Lab coat, gloves, mask, and goggles (or face shield) must be worn when handling primate semen samples. Also remember to dispose of all biomaterial and/or equipment in the appropriate biohazard containers or treat with bleach.

1. Weigh[5] 194 mg caffeine into labeled sterile 15 mL conical centrifuge tube. Add 10 mL milliQ water and vortex to dissolve.
2. Weigh[4] 49 mg dbcAMP into labeled 15 mL conical centrifuge tube.
3. Add 1 mL caffeine solution to dbcAMP and vortex to dissolve.
4. Dilute the sperm to ~10 x 10^6 sperm/mL in warm TALP w/ BSA. This may already be done if the sperm was freshly processed. If different concentration make sure to note on data sheet.
5. Pipet 1 mL diluted sperm into sterile 15 mL conical centrifuge tube.
6. Add 10 µL of dbcAMP/caffeine solution to the 1 mL aliquot of diluted sperm. Incubate at 37^{o}C, 5% CO_2 with lid loosely capped for 15-30 min.
7. Pipet 20 µL of activated sperm suspension onto a slide and quickly coverslip. Observe for activation and motility. If properly activated the sperm heads should have a distinct side-to-side movement.
8. Make note of capacitation results on data sheet.

[4] Modified from Cathi VandeVoort's lab at CNPRC

[5] There are multiple ways to make these solutions depending on how many mL are needed. The important thing is to have a final concentration of 20 mM for each.

Appendix P: Protocol for Sperm-Zona Pellucida Binding and Acrosomal Staining[6]

Binding

1. Setup five 35 mm petri dishes with 3-5 mL DPBS near the dissecting microscope. These will be used to wash the DMSO from the oocytes. It may be useful to draw small circular targets on the underside of the plates to help keep track of the oocytes.
2. Place a 75 µL drop of TALP w/ BSA in the middle of a 35 mm petri dish, fill dish with mineral oil, label 'zona' and place in 37°C, 5% CO_2 incubator.
3. Prepare a dish for each male to be used by drawing a 10µL 'disk' of TALP w/ BSA on the bottom of a labeled 35 mm petri dish. Add ~3mL of mineral oil and place in the 37°C, 5% CO_2 incubator.
4. Label the frosted end of a 10-well Teflon-masked slide with the male ID #, date, and your initials and place on the left rear of the dissecting microscope stage.
5. Oocytes are kept frozen at –80°C in capillary tubes (5-10 oocytes/tube). Remove the needed number of tubes from the freezer and allow to thaw at RT. Carefully score and break off the ends of the tube just below the CritoSeal and use the capillary tube adapter and micropipet to expel the tube's contents into the first 35 mm petri dish of DPBS. Repeat if needed, placing all the oocytes into the same dish. It may be necessary to rinse the tube with the well solution in order to free all the oocytes.
6. Using a micropipet and stripper tip, transfer oocytes through the remaining dishes to wash off the freezing medium. Check that all cumulus cells have been removed from the oocytes and remove any that might be remaining.
7. Transfer the rinsed oocytes to the 75 µL drop of TALP w/ BSA in the 35 mm petri dish labeled 'zona'. Return it to the 37°C, 5% CO_2 incubator until needed. Dispose of the washing plates.
8. Prepare the activated sperm according to protocol at a dilution of ~10 x 10^6 sperm/mL.
9. During activation place the Boerner 9-well glass plate near the dissecting microscope. Fill each well with ~500 µL DPBS. These will be used to rinse the oocytes after binding. Place a 35 mm petri dish at the upper left of the microscope on a Kimwipe-covered ice pack and pipet 2-3 mL of ice-cold ethanol into the dish. Immediately before sperm activation is complete place the 'zona' dish on the rear right of the microscope.
10. After activation pipet 90 µL of sperm through the oil of the appropriate petri dish, adding to the 10 µL disk to create a 100 µL dome. (Try to avoid making a bubble that can trap oocytes later).
11. Using a micropipet and stripper tip, transfer the desired number of oocytes from the 'zona' dish into the activated sperm drop. Incubate for EXACTLY the predetermined time (i.e. 30 seconds) and then transfer into the DPBS in the Boerner plate.

[6] Modified from Cathi VandeVoort's lab at CNPRC

12. Transfer the oocytes through four more wells to wash off any unbound sperm before moving the oocytes to the petri dish of iced ethanol. Remember to use one of the extra DPBS wells to flush the pipet tip between transfers.
13. The oocytes and bound sperm are now fixed and can be mounted to a 10-well Teflon-masked slide. Transfer them to the appropriately labeled well.
14. Allow the slide to dry VERY WELL then place in a slide box at –20°C or –80°C (non-frostfree) until staining. They should not be left more than a few weeks before staining. If the slide is to be stained immediately pipet ~30 µL of 4% paraformaldehyde onto each used well and allow to incubate for 10 minutes.

Staining

1. If the slide(s) has been frozen, warm to room temperature and then pipet 30 µL of 4% paraformaldehyde onto each used well. Make sure slide is completely warm or oocytes may come loose during processing. Incubate for 10 minutes. Move the slide to a 100 mm petri dish containing a small water-soaked pad to maintain humidity. Rinse each well with 30 µL DPBS for 5 minutes. While observing the slide on the dissecting microscope remove the DPBS with a micropipet and stripper tip, being careful to remove as much as possible without disturbing the oocytes. This technique should be used for all subsequent washes/removals to avoid freeing the oocytes from the slide and ultimately losing or destroying them. Repeat two more times.
2. Pipet 30 µL of BSA blocking solution onto each well used and incubate at RT for 15 minutes. Prepare the 1:30 RAS dilution (10 µL RAS + 290 µL blocking solution) during this incubation.
3. Pipet 30 µl of RAS onto each well used. Cover the petri dish and place in incubator at 37°C for 60 minutes.
4. Remove the RAS solution with micropipet and stripper tip. Add 30 µl of BSA blocking solution to each well used in order to wash off the excess RAS. Incubate at room temperature for 5 minutes and then remove blocking solution. Repeat two more times. During the last RAS wash prepare the FGAR dilution (1 µL FGAR + 49 µL blocking solution).
5. ALL REMAINING STEPS ARE DONE WITH THE ROOM DARK. A red filter can be placed over the microscope light source in order to protect the stain from photobleaching.
6. After removing the last wash from the slide, pipet 30 µL of the FGAR dilution onto each well used. Cover and place in the incubator at 37°C for 60 minutes.
7. Remove the FGAR solution with micropipet and stripper tip. Wash off the excess FGAR by pipetting 30 µl of BSA blocking solution to each well used. Incubate at RT for 5 minutes and then remove blocking solution. Repeat two more times. During the third wash dilute the Hoescht 33,258 in DPBS (10 µL Hoescht stock + 190 µL DPBS).
8. After removing the last blocking solution wash add 30 µL of diluted H258

to each well used. Place in the 37°C incubator, covered, for 20 minutes.

9. Remove the H258 with micropipet and stripper tip. Wash off the excess H258 by pipetting 30 µL of DPBS to each well used. Incubate at RT for 5 minutes under an inverted slide box. Remove the DPBS. Repeat once.
10. After the final wash allow the slide to dry at RT under a slide box to block out light. Once dry place a 5 µL drop of Permount mounting medium on each well used and cover with a coverslip. Carefully remove excess bubbles with a pipet tip pressed against the coverslip.
11. Observe on the fluorescence microscope. If needed, slides can be stored in a slide box at 4°C until viewed. They should not be left more than a few weeks before reading.

Criteria for Scoring

1. Using the filter for Hoescht 33,258, first count the total number of sperm bound to the oocyte zona. Start at the top of the oocyte and work down to the bottom of the slide. Hoescht is a DNA/chromatin stain that is able to penetrate the sperm and oocyte due to the ethanol fixation step.
2. Next begin taking a count of the total number of sperm for which an acrosomal status can be determined. It will be less than the total bound because the double Ab staining cannot penetrate to the sperm trapped between the oocyte and slide. This is done by switching to the FITC filter and moving away from the slide.
3. When the first clearly stained FITC sperm is observed alternate between the Hoescht and FITC filters. If a sperm's acrosome is intact it will appear as a ¾ head. If a sperm is seen under H258 and disappears with FITC then it is acrosomally reacted.

Media/Buffers/Solutions

<u>4% paraformaldehyde in Dulbecco's Phosphate Buffered Saline (DPBS)</u>
10.8 mL of 37% paraformaldahyde + 89.2 mL sterile filtered DPBS without calcium chloride
Aliquot into 1.6 mL tubes (leaving very little air) and store at –20°C indefinitely
Thaw with hot water when ready to use (making sure crystals go into solution)

<u>blocking solution</u>
10mg/mL (1%) BSA in DPBS. Freeze 1 mL aliquots and store at –20°C

- rabbit antiserum (RAS) [freshly diluted to 1:30 in blocking solution]
- FITC-goat anti-rabbit IgG (FGAR) [freshly diluted 1:50 in blocking solution]
- bisbenzimide fluorochrome (Hoescht 33,258) [freshly diluted 1:20 in DPBS from frozen 10µg/mL stock[7]]

[7] bisbenzimide fluorochrome stock: 1mg bisbenzimide dissolved in 1mL distilled water. Store 1mg/ml <u>concentrate</u> at –20°C in an amber vial or wrapped in foil. Dilute 10µl concentrate with 0.99ml DPBS to make a 10µg/ml <u>stock</u>. Store at 4°C in an amber vial or wrapped in foil.

Appendix Q: Protocol for Sperm Cryopreservation[8]

Caution: Primate semen potentially carries Herpes B virus. Lab coat, gloves, mask, and goggles (or face shield) must be worn when handling primate semen samples. Also remember to dispose of all biomaterial and/or equipment in the appropriate biohazard containers or treat with bleach.

1. Begin with a washed and prepared sample in TALP w/ BSA.
2. If not already, place the specimen in a 15 mL conical centrifuge tube and centrifuge at 130-150G for 10 minutes.
3. While centrifuging add 60 µL glycerol (cryoprotectant) to 940 µL TEST-yolk extender and vortex. Refrigerate the 6% glycerol solution until needed
4. After centrifuging remove supernatant and discard in 10% bleach solution. Resuspend pellet in the second vial of TEST-yolk extender to 1 mL.
5. Place the tube in a beaker filled with cool water. Slowly add 330 µL of glycerol solution dropwise to extended sperm, mixing after every few drops.
6. Place the beaker containing the specimen into the refrigerator for 10 min.
7. Add another 330 µL of glycerol solution to the sample, gently mix in the same way, and return to refrigerator for 10 minutes.
8. Add the last third of the glycerol, mixing gently, and return to refrigerator for 60 minutes.
9. Prelabel enough Nalgene screw-top cryovials to hold all the pellets to be made (vials can hold about fifteen 50 µL pellets). Place vials and caps in a shallow bucket containing liquid nitrogen until needed.
10. Set up small block of dry ice on lid of styrofoam container. Create small depressions in the dry ice with the connected end of a pair of forceps or other tool. Clean the item before using it to make the depressions.
11. When 60 minute cooling is complete, mix sperm gently with pipet and begin aliquoting 50 µL drops directly onto the dry ice. Pellets should freeze in ~1 minute.
12. Within 1-3 minutes remove pellets from dry ice by dumping them into shallow bucket of LN_2 (the pellets should look like cooked egg yolks). Be careful as the pellets slide off very easily. If the LN_2 is too deep it will be hard to see the pellets and load them properly.
13. Use forceps to hold cryovials under the liquid nitrogen while loading pellets with another pair of forceps. Seal the vials tightly with liquid nitrogen still in them.
14. Return capped cryovials to liquid nitrogen bucket until all pellets are loaded. Quickly load vials into canes and store in designated LN_2 tank.
15. Record animal ID#, date, motility, concentration, number of pellets per vial, and number of vials on data sheet.

[8] Modified from ONPRC ART Core

Media/Buffers/Solutions

TEST-yolk extender

	g/100 mL		
TES	4.326	penicillin G/streptomycin sulfate	1.000 mL
Trizma base	1.027	fresh egg yolk	60 mL
(D+)glucose	1.000	skim milk	40 mL

Day 1

1. Bring the first three ingredients to 100 mL with milliQ water.
2. Adjust pH to 7.4 with 1.0M NaOH or 1.0M HCl.
3. If needed, sterile filter the buffer and store in refrigerator overnight. Otherwise continue with next step.
4. Combine 60 mL egg yolk with 40 mL skim milk and mix well.
5. Combine the buffer solution with 25 mL of the egg-milk mixture.
6. Inactivate the solution (125 mL) at 56^{o}C for 30-60 minutes while stirring. This can be done by submersing an Erlenmeyer flask into a larger beaker of water. Place the beaker on a hot plate. Monitor water temperature, adding ice whenever it becomes too hot.
7. Cool to less than 20^{o}C in the refrigerator.
8. Add 1 mL pen/strep.
9. Store in refrigerator overnight. This is supposedly to allow some sedimentation to occur, but it seems to be very minimal. Centrifugation later will take care of most of the protein sediment. If needed this step can be skipped and continue with step 10 immediately.

Day 2

10. The next day do not resuspend the solution, but instead remove supernatant and transfer to an appropriate centrifuge tube(s).
11. Centrifuge for 4 hours at 100,000G. Use the Beckman Ultracentrifuge (L7-65, rotor SW-28) with the Molecular Core in the Cooley Building. Spin at 27,000 RPM to get close to 100,000G. Should be able to spin three ~35 mL tubes of cryoprotectant (and one water blank) at one time.
12. Remove and save supernatant. Centrifuge supernatant for 2 more hours at 100,000G.
13. Remove supernatant and measure pH (7.4) and osmolarity (?). Adjust if necessary.
14. Filter through 0.45 µM syringe filters (in ART Core). A fresh filter is required for every ~10 mL of extender or whenever it becomes too difficult to filter properly.
15. Freeze in 1 mL aliquots at –80^{o}C in cryovials for one month.

To use TEST-yolk extender

Thaw two vials of extender, centrifuge at 14,000G for 5 minutes and use the supernatant.

Appendix R: Protocol for Frozen/Thawed Sperm Processing[9]

Caution: Primate semen potentially carries Herpes B virus. Lab coat, gloves, mask, and goggles (or face shield) must be worn when handling primate semen samples. Also remember to dispose of all biomaterial and/or equipment in the appropriate biohazard containers or treat with bleach.

1. Sperm pellets are kept in cryovials in liquid nitrogen tank. Pellets should be at a concentration of ~0.5-1 x 10^6 sperm/pellet, but this should be verified by looking at the freezing record that corresponds to the sample. Place appropriate number of pellets in a sterile 15 mL conical centrifuge tube (without any media). We want ~1-2 x 10^6 total sperm for analysis.
2. Place the capped centrifuge tube in a 37^{o}C water bath for 40 seconds (warming rate of 350^{o}C/minute).
3. After thawing note pellet volume to nearest 0.05 mL with pipet. Add 15 mL warm TALP-Hepes w/ BSA to the tube and resuspend the pellet(s) by gently triturating using the pipetman. Take care to avoid vigorous mixing as it can damage the sperm.
4. Centrifuge the sperm suspension at 130-150G for 8 minutes. Make sure the centrifuge is balanced with 15 mL water.
5. After centrifuging remove supernatant and discard in 10% bleach solution. Add warm TALP w/ BSA to pellet to achieve a concentration of ~1-2 x 10^6 sperm/mL (100µL) and gently resuspend. Count and concentration can be determined and morphology slides can be made at this point if desired.
6. The washed sperm should be placed in the 37^{o}C, 5% CO_2, incubator (loosely capped) for 30 minutes before checking motility and status again.

Count and Concentration

1. 190 µL milliQ H_2O and 10 µL of sperm suspension are combined into a 0.6 mL microcentrifuge tube (1:20 dilution) and mixed gently but thoroughly.
2. 10 µL of the mix is added to each side of a Neubauer or other hemocytometer with affixed cover slip. Let hemocytometer sit for 5 minutes to make counting easier, but do not let fluid dry out. Sperm are counted using a phase contrast microscope. Make appropriate calculation corrections for the hemocytometer (if necessary) and average the results. Concentration is recorded in million sperm/mL (x 10^6 sperm/mL).
3. If counts differ by >10% between sides then recount using fresh sample until <10%. Average results.

[9] Modified from ONPRC ART Core protocol and Dr. Cathi VandeVoort's lab at CNPRC

Motility and Status

1. A 20 µL pipetman is used to place 10 µL of washed sperm suspension onto a warm microscope slide. A coverslip is carefully added.
2. Motility is determined by counting 100 sperm using a phase contrast microscope (with stage warmer or warm room if possible).
3. Status is determined by giving the sample an average score based on the following scale:
    0 = all dead
    1 = slight side-to-side, no forward progess
    2 = rapid side-to-side, no forward progress
    3 = rapid side-to-side, forward progress in spurts
    4 = slow, steady forward progress
    5 = rapid, steady forward progress

References

Abizaid, A., Horvath, B., Keefe, D. L., Leranth, C. and Horvath, T. L. (2004). Direct visual and circadian pathways target neuroendocrine cells in primates. European Journal of Neuroscience *20*, 2767-2776.

Agarwal, A. and Said, T. M. (2003). Role of sperm chromatin abnormalities and DNA damage in male infertility. Human Reproduction Update *9*, 331-345.

Alvarez, J. D., Chen, D. C., Storer, E. and Sehgal, A. (2003). Non-cyclic and developmental stage-specific expression of circadian clock proteins during murine spermatogenesis. Biology of Reproduction *69*, 81-91.

Asai, M., Yoshinobu, Y., Kaneko, S., Mori, A., Nikaido, T., Moriya, T., Akiyama, M. and Shibata, S. (2001). Circadian profile of Per gene mRNA expression in the suprachiasmatic nucleus, paraventricular nucleus, and pineal body of aged rats. Journal of Neuroscience Research *66*, 1133-1139.

Ascoli, M., Fanelli, F. and Segaloff, D. L. (2002). The lutropin/choriocrctnadotropin receptor, a 2002 perspective. Endocrine Reviews *23*, 141-174.

Austad, S. N. (2001). An experimental paradigm for the study of slowly aging organisms. Experimental Gerontology *36*, 599-605.

Balsalobre, A. (2002). Clock genes in mammalian peripheral tissues. Cell and Tissue Research *309*, 193-199.

Balsalobre, A., Damiola, F. and Schibler, U. (1998). A serum shock induces circadian gene expression in mammalian tissue culture cells. Cell *93*, 929-937.

Black, A., Allison, D. B., Shapses, S. A., Tilmont, E. M., Handy, A. M., Ingram, D. K., Roth, G. S. and Lane, M. A. (2001). Calorie restriction and skeletal mass in rhesus monkeys (*Macaca mulatta*): Evidence for an effect mediated through changes in body size. Journals of Gerontology Series a-Biological Sciences and Medical Sciences *56*, B98-B107.

Black, A. and Lane, M. A. (2002). Nonhuman primate models of skeletal and reproductive aging. Gerontology *48*, 72-80.

Bungum, M., Humaidan, P., Spano, M., Jepson, K., Bungum, L. and Giwercman, A. (2004). The predictive value of sperm chromatin structure assay (SCSA) parameters for the outcome of intrauterine insemination, IVF, and ICSI. Human Reproduction *19*, 1401-1408.

Buwe, A., Guttenbach, M. and Schmid, M. (2005). Effect of paternal age on the frequency of cytogenetic abnormalities in human spermatozoa. Cytogenetic and Genome Research *111*, 213-228.

Cattoretti, G., Pileri, S., Parravicini, C., Becker, M. H. G., Poggi, S., Bifulco, C., Key, G., Damato, L., Sabattini, E., Feudale, E., Reynolds, F., Gerdes, J. and Rilke, F. (1993). Antigen unmasking on formalin-fixed, paraffin-embedded tissue sections. Journal of Pathology *171*, 83-98.

Chappell, P. E., White, R. S. and Mellon, P. L. (2003). Circadian gene expression regulates pulsatile gonadotropin-releasing hormone (GnRH) secretory patterns in the hypothalamic GnRH-secreting GT1-7 cell line. Journal of Neuroscience *23*, 11202-11213.

Chen, H. L. (2004). Gene expression by the anterior pituitary gland: effects of age and caloric restriction. Molecular and Cellular Endocrinology *222*, 21-31.

Chen, H. L., Cangello, D., Benson, S., Folmer, J., Zhu, H., Trush, M. A. and Zirkin, B. R. (2001). Age-related increase in mitochondrial superoxide generation in the testosterone-producing cells of Brown Norway rat testes: relationship to reduced steroidogenic function? Experimental Gerontology *36*, 1361-1373.

Chen, H. L., Hardy, M. P. and Zirkin, B. R. (2002). Age-related decreases in Leydig cell testosterone production are not restored by exposure to LH in vitro. Endocrinology *143*, 1637-1642.

Chen, H. L., Huhtaniemi, I. and Zirkin, B. R. (1996). Depletion and repopulation of Leydig cells in the testes of aging Brown Norway rats. Endocrinology *137*, 3447-3452.

Chen, H. L., Irizarry, R. A., Luo, L. D. and Zirkin, B. R. (2004). Leydig cell gene expression: effects of age and caloric restriction. Experimental Gerontology *39*, 31-43.

Chen, H. L., Luo, L. D., Liu, J., Brown, T. and Zirkin, B. R. (2005). Aging and caloric restriction: Effects on Leydig cell steroidogenesis. Experimental Gerontology *40*, 498-505.

Chen, H. L. and Zirkin, B. R. (1999). Long-term suppression of Leydig cell steroidogenesis prevents Leydig cell aging. Proceedings of the National Academy of Sciences of the United States of America *96*, 14877-14881.

Dey, J., Carr, A. J. F., Cagampang, F. R. A., Semikhodskii, A. S., Loudon, A. S. I., Hastings, M. H. and Maywood, E. S. (2005). The tau mutation in the Syrian hamster differentially reprograms the circadian clock in the SCN and peripheral tissues. Journal of Biological Rhythms *20*, 99-110.

Dhahbi, J. M., Kim, H.-J., Mote, P. L., Beaver, R. J. and Spindler, S. R. (2004). Temporal linkage between the phenotypic and genomic responses to caloric restriction. Proceedings of the National Academy of Sciences of the United States of America *101*, 5524-5529.

Diano, S., Urbanski, H. F., Horvath, B., Bechmann, I., Kagiya, A., Nemeth, G., Naftolin, F., Warden, C. H. and Horvath, T. L. (2000). Mitochondrial uncoupling protein 2 (UCP2) in the nonhuman primate brain and pituitary. Endocrinology *141*, 4226-4238.

Dillman, J. F. and Phillips, C. S. (2005). Comparison of non-human primate and human whole blood tissue gene expression profiles. Toxicological Sciences *87*, 306-314.

Downs, J. L. and Urbanski, H. F. (2006). Neuroendocrine changes in the aging reproductive axis of female rhesus macaques (Macaca mulatta). Biology of Reproduction *75*, 539-546.

Dufau, M. L. (1998). The luteinizing hormone receptor. Annual Review of Physiology *60*, 461-496.

Eide, E. J. and Virshup, D. M. (2001). Casein kinase I: Another cog in the circadian clockworks. Chronobiology International *18*, 389-398.

Elder, K. and Dale, B. (2000). In vitro fertilization. (Cambridge, UK:Cambridge University Press).

Elzanaty, S., Richthoff, J., Malm, J. and Giwercman, A. (2002). The impact of epididymal and accessory sex gland function on sperm motility. Human Reproduction *17*, 2904-2911.

Eskenazi, B., Wyrobek, A. J., Sloter, E., Kidd, S. A., Moore, L., Young, S. and Moore, D. (2003). The association of age and semen quality in healthy men. Human Reproduction *18*, 447-454.

Evenson, D. P. and Wixon, R. L. (2006). Use of the sperm chromatin structure assay (SCSA) as a diagnostic tool in the human infertility clinic. Fertility Magazine *4*, 15-18.

Everett, J. W. (1994). Pituitary and Hypothalamus: Perspectives and Overview, in The Physiology of Reproduction, E. Knobil, J. D. Neill, et al., eds. (New York:Raven Press), 1509-1526.

Fejes, I., Koloszar, S., Szollodsi, J., Zavaczki, Z. and Pal, A. (2005). Is semen quality affected by male body fat distribution? Andrologia *37*, 155-159.

Foresta, C., Bettella, A., Vinanzi, C., Dabrilli, P., Meriggiola, M. C., Garolla, A. and Ferlin, A. (2004). Insulin-like factor 3: A novel circulating hormone of testis origin in humans. Journal of Clinical Endocrinology and Metabolism *89*, 5952-5958.

Gibbs, R. A., Rogers, J., Katze, M. G., Bumgarner, R., Gibbs, R. A. and Weinstock, G. M. (2007). Evolutionary and biomedical insights from the rhesus macaque genome. Science *316*, 222-234.

Gillespie, J. M. A., Chan, B. P. K., Roy, D., Cai, F. and Belsham, D. D. (2003). Expression of circadian rhythm genes in gonadotropin-releasing hormone-secreting GT1-7 neurons. Endocrinology *144*, 5285-5292.

Glossop, N. R. J. and Hardin, P. E. (2002). Central and peripheral circadian oscillator mechanisms in flies and mammals. Journal of Cell Science *115*, 3369-3377.

Gonzales, G. F. (2001). Function of seminal vesicles and their role on male fertility. Asian Journal of Andrology *3*, 251-258.

Gould, K. G. and Mann, D. R. (1988). Comparison of electrostimulation methods for semen recovery in the rhesus monkey (*Macaca mulatta*). Journal of Medical Primatology *17*, 95-103.

Gredilla, R. and Barja, G. (2005). Minireview: The role of oxidative stress in relation to caloric restriction and longevity. Endocrinology *146*, 3713-3717.

Gresl, T. A., Colman, R. J., Roecker, E. B., Havighurst, T. C., Huang, Z., Allison, D. B., Bergman, R. N. and Kemnitz, J. W. (2001). Dietary restriction and glucose regulation in aging rhesus monkeys: A follow-up report at 8.5 yr. American Journal of Physiology-Endocrinology and Metabolism *281*, E757-E765.

Griffin, J. E. and Ojeda, S. R., eds. (2000). Textbook of Endocrine Physiology (New York:Oxford University Press, Inc.).

Guillaumond, F., Dardente, H., Giguere, V. and Cermakian, N. (2005). Differential control of Bmal1 circadian transcription by REV-ERB and ROR nuclear receptors. Journal of Biological Rhythms *20*, 391-403.

Gupta, G., Maikhuri, J., Setty, B. and Dhar, J. D. (2000). Seasonal variations in daily sperm production rate of rhesus and bonnet monkeys. Journal of Medical Primatology *29*, 411-414.

Hardy, M. P. and Schlegel, P. N. (2004). Testosterone production in the aging male: Where does the slowdown occur? Endocrinology *145*, 4439-4440.

Harman, S. M., Metter, E. J., Tobin, J. D., Pearson, J. and Blackman, M. R. (2001). Longitudinal effects of aging on serum total and free testosterone levels in healthy men. Journal of Clinical Endocrinology and Metabolism *86*, 724-731.

Harraway, C., Berger, N. G. and Dubin, N. H. (2000). Semen pH in patients with normal versus abnormal sperm characteristics. American Journal of Obstetrics and Gynecology *182*, 1045-1047.

Harrison, R. M. and Lewis, R. W. (1986). The male reproductive tract and its fluids, in Comparative Primate Biology: Reproduction and Development, W. R. Dukelow and J. Erwin, eds. (New York:Alan R. Liss, Inc.), 101-148.

Haugen, T. B. and Grotmol, T. (1998). pH of human semen. International Journal of Andrology *21*, 105-108.

He, Z. P., Chan, W. Y. and Dym, M. (2006). Microarray technology offers a novel tool for the diagnosis and identification of therapeutic targets for male infertility. Reproduction *132*, 11-19.

Heilbronn, L. K., de Jonge, L., Frisard, M. I., DeLany, J. P., Larson-Meyer, D. E., Rood, J., Nguyen, T., Martin, C. K., Volaufova, J., Most, M. M., Greenway, F. L., Smith, S. R., Deutsch, W. A., Williamson, D. A. and Ravussin, E.

(2006). Effect of 6-month calorie restriction on biomarkers of longevity, metabolic adaptation, and oxidative stress in overweight individuals: A randomized controlled trial. Journal of the American Medical Association *295*, 2482-2482.

Heilbronn, L. K. and Ravussin, E. (2003). Calorie restriction and aging: review of the literature and implications for studies in humans. American Journal of Clinical Nutrition *78*, 361-369.

Henkel, R., Maass, G., Schuppe, H. C., Jung, A., Schubert, J. and Schill, W. B. (2005). Molecular aspects of declining sperm motility in older men. Fertility and Sterility *84*, 1430-1437.

Hochberg, Y. (1988). A sharper Bonferroni procedure for multiple tests of significance. Biometrika *75*, 800-802.

Hofman, M. A. and Swaab, D. F. (2006). Living by the clock: The circadian pacemaker in older people. Ageing Research Reviews *5*, 33-51.

Holehan, A. M. and Merry, B. J. (1985). The control of puberty in the dietary restricted female rat. Mechanisms of Ageing and Development *32*, 179-191.

Huang, H. and Manton, K. G. (2004). The role of oxidative damage in mitochondria during aging: A review. Frontiers in Bioscience *9*, 1100-1117.

Hursting, S. D., Lavigne, J. A., Berrigan, D., Perkins, S. N. and Barrett, J. C. (2003). Calorie restriction, aging, and cancer prevention: Mechanisms of

action and a applicability to humans. Annual Review of Medicine-Selected Topics in the Clinical Sciences *54*, 131-152.

Ingram, D. K., Cutler, R. G., Weindruch, R., Renquist, D. M., Knapka, J. J., April, M., Belcher, C. T., Clark, M. A., Hatcherson, C. D., Marriott, B. M. and Roth, G. S. (1990). Dietary restriction and aging - the initiation of a primate study. Journals of Gerontology *45*, B148-B163.

Irizarry, R. A., Hobbs, B., Collin, F., Beazer-Barclay, Y. D., Antonellis, K. J., Scherf, U. and Speed, T. P. (2003). Exploration, normalization, and summaries of high density oligonucleotide array probe level data. Biostatistics *4*, 249-264.

Ivell, R. and Bathgate, R. A. D. (2002). Reproductive biology of the relaxin-like factor (RLF/INSL3). Biology of Reproduction *67*, 699-705.

Ivell, R., Hartung, S. and Anand-Ivell, R. (2005). Insulin-like factor 3: Where are we now? Annals of the New York Academy of Sciences *1041*, 486-496.

Jensen, T. K., Andersson, A. M., Jorgensen, N., Andersen, A. G., Carlsen, E., Petersen, J. H. and Skakkebaek, N. E. (2004). Body mass index in relation to semen quality and reproductive hormones among 1,558 Danish men. Fertility and Sterility *82*, 863-870.

Jervis, K. M. and Robaire, B. (2003). Effects of caloric restriction on gene expression along the epididymis of the Brown Norway rat during aging. Experimental Gerontology *38*, 549-560.

Jeyendran, R. S. (2003). Protocols for Semen Analysis in Clinical Diagnosis. (New York:Parthenon Publishing Group).

Jeyendran, R. S., Vanderven, H. H., Perezpelaez, M., Crabo, B. G. and Zaneveld, L. J. D. (1984). Development of an assay to assess the functional integrity of the human-sperm membrane and its relationship to other semen characteristics. Journal of Reproduction and Fertility *70*, 219-&.

Ji, W. Z., He, X. C., Wang, H., Bavister, B. D. and Li, X. L. (2001). Semen parameters and cryopreservation of spermatozoa of Assamese macaque (*Macaca assamensis*). Biology of Reproduction *64 Suppl 1*, 312.

Jilg, A., Moek, J., Weaver, D. R., Korf, H. W., Stehle, J. H. and von Gall, C. (2005). Rhythms in clock proteins in the mouse pars tuberalis depend on MT1 melatonin receptor signalling. European Journal of Neuroscience *22*, 2845-2854.

Kappeler, L., Gourdji, D., Zizzari, P., Bluet-Pajot, M. T. and Epelbaum, J. (2003). Age-associated changes in hypothalamic and pituitary neuroendocrine gene expression in the rat. Journal of Neuroendocrinology *15*, 592-601.

Kenyon, C. (2001). A conserved regulatory system for aging. Cell *105*, 165-168.

Kholkute, S. D., Gopalkrishnan, K. and Puri, C. P. (2000). Variations in seminal parameters over a 12-month period in captive bonnet monkeys. Primates *41*, 393-405.

Kidd, S. A., Eskenazi, B. and Wyrobek, A. J. (2001). Effects of male age on semen quality and fertility: a review of the literature. Fertility and Sterility *75*, 237-248.

Kimura, M., Itoh, N., Takagi, S., Sasao, T., Takahashi, A., Masumori, N. and Tsukamoto, T. (2003). Balance of apoptosis and proliferation of germ cells related to spermatogenesis in aged men. Journal of Andrology *24*, 185-191.

Kirkwood, T. B. L. and Austad, S. N. (2000). Why do we age? Nature *408*, 233-238.

Knobil, E., Neill, J. D., Greenwald, G. S., Markert, C. L. and Pfaff, D. W., eds. (1994). The Physiology of Reproduction (New York:Raven Press).

Kolker, D. E., Fukuyama, H., Huang, D. S., Takahashi, J. S., Horton, T. H. and Turek, F. W. (2003). Aging alters circadian and light-induced expression of clock genes in golden hamsters. Journal of Biological Rhythms *18*, 159-169.

Kolker, D. E., Vitaterna, M. H., Fruechte, E. M., Takahashi, J. S. and Turek, F. W. (2004). Effects of age on circadian rhythms are similar in wild-type and heterozygous Clock mutant mice. Neurobiology of Aging *25*, 517-523.

Kort, H. I., Massey, J. B., Elsner, C. W., Mitchell-Leef, D., Shapiro, D. B., Witt, M. A. and Roudebush, W. E. (2006). Impact of body mass index values on sperm quantity and quality. Journal of Andrology *27*, 450-452.

Koubova, J. and Guarente, L. (2003). How does calorie restriction work? Genes & Development *17*, 313-321.

Kunieda, T., Minamino, T., Katsuno, T., Tateno, K., Nishi, J., Miyauchi, H., Orimo, M., Okada, S. and Komuro, I. (2006). Cellular senescence impairs

circadian expression of clock genes in vitro and in vivo. Circulation Research *98*, 532-539.

Lane, M. A., Baer, D. J., Rumpler, W. V., Weindruch, R., Ingram, D. K., Tilmont, E. M., Cutler, R. G. and Roth, G. S. (1996). Calorie restriction lowers body temperature in rhesus monkeys, consistent with a postulated anti-aging mechanism in rodents. Proceedings of the National Academy of Sciences of the United States of America *93*, 4159-4164.

Lane, M. A., Baer, D. J., Tilmont, E. M., Rumpler, W. V., Ingram, D. K., Roth, G. S. and Cutler, R. G. (1995). Energy balance in rhesus monkeys (*Macaca mulatta*) subjected to long term dietary restriction. Journals of Gerontology Series a-Biological Sciences and Medical Sciences *50*, B295-B302.

Lane, M. A., Black, A., Handy, A. M., Shapses, S. A., Tilmont, E. M., Kiefer, T. L., Ingram, D. K. and Roth, G. S. (2001). Energy restriction does not alter bone mineral metabolism or reproductive cycling and hormones in female rhesus monkeys. Journal of Nutrition *131*, 820-827.

Lane, M. A., Ingram, D. K. and Roth, G. S. (1997). Beyond the rodent model: Calorie restriction in rhesus monkeys. Age *20*, 45-56.

Lane, M. A., Ingram, D. K. and Roth, G. S. (1999a). Calorie restriction in nonhuman primates: Effects on diabetes and cardiovascular disease risk. Toxicological Sciences *52*, 41-48.

Lane, M. A., Tilmont, E. M., De Angelis, H., Handy, A., Ingram, D. K., Kemnitz, J. W. and Roth, G. S. (1999b). Short-term calorie restriction improves

disease-related markers in older male rhesus monkeys (*Macaca mulatta*). Mechanisms of Ageing and Development *112*, 185-196.

Lanzendorf, S. E., Gliessman, P. M., Archibong, A. E., Alexander, M. and Wolf, D. P. (1990). Collection and quality of rhesus monkey semen. Molecular Reproduction and Development *25*, 61-66.

Larson-Cook, K. L., Brannian, J. D., Hansen, K. A., Kasperson, K. M., Aamold, E. T. and Evenson, D. P. (2003). Relationship between the outcomes of assisted reproductive techniques and sperm DNA fragmentation as measured by the sperm chromatin structure assay. Fertility and Sterility *80*, 895-902.

Lemos, D. R., Downs, J. L. and Urbanski, H. F. (2006). Twenty-four-hour rhythmic gene expression in the rhesus macaque adrenal gland. Molecular Endocrinology *20*, 1164-1176.

Lewis-Jones, D. I., Aird, I. A., Biljan, M. M. and Kingsland, C. R. (1996). Effects of sperm activity on zinc and fructose concentrations in seminal plasma. Human Reproduction *11*, 2465-2467.

Lewy, H., Ashkenazi, I. E. and Touitou, Y. (2005). Prolactin rhythms-oscillators' response to photoperiodic cues is age and circadian time dependent. Neurobiology of Aging *26*, 125-133.

Lewy, H., Naor, Z. and Ashkenazi, I. E. (1996). Rhythmicity of luteinizing hormone secretion expressed in vitro. European Journal of Endocrinology *135*, 455-463.

Lowrey, P. L. and Takahashi, J. S. (2004). Mammalian circadian biology: Elucidating genome-wide levels of temporal organization. Annual Review of Genomics and Human Genetics *5*, 407-441.

Luo, L. D., Chen, H. L. and Zirkin, B. R. (1996). Are Leydig cell steroidogenic enzymes differentially regulated with aging? Journal of Andrology *17*, 509-515.

Luo, L. D., Chen, H. L. and Zirkin, B. R. (2001). Leydig cell aging: Steroidogenic acute regulatory protein (StAR) and cholesterol side-chain cleavage enzyme. Journal of Andrology *22*, 149-156.

Markkula, M., Kananen, K., Klemi, P. and Huhtaniemi, I. (1996). Pituitary and ovarian expression of the endogenous follicle-stimulating hormone (FSH) subunit genes and an FSH beta-subunit promoter-driven herpes simplex virus thymidine kinase gene in transgenic mice: Specific partial ablation of FSH-producing cells by antiherpes treatment. Journal of Endocrinology *150*, 265-273.

Mastroianni, L. and Manson, W. A. (1963). Collection of monkey semen by electroejaculation. Proceedings of the Society for Experimental Biology and Medicine *112*, 1025-&.

Mattison, J. A., Black, A., Huck, J., Moscrip, T., Handy, A., Tilmont, E., Roth, G. S., Lane, M. A. and Ingram, D. K. (2005). Age-related decline in caloric intake and motivation for food in rhesus monkeys. Neurobiology of Aging *26*, 1117-1127.

Mattison, J. A., Lane, M. A., Roth, G. S. and Ingram, D. K. (2003). Calorie restriction in rhesus monkeys. Experimental Gerontology *38*, 35-46.

Mattison, J. A., Roth, G. S., Ingram, D. K. and Lane, M. A. (2001). Endocrine effects of dietary restriction and aging: The National Institute on Aging study. Journal of Anti-Aging Medicine *4*, 215-223.

McCay, C. M., Crowell, M. F. and Maynard, L. A. (1935). The effect of retarded growth upon the length of the life span and upon the ultimate body size. Journal of Nutrition *10*, 63-70.

McShane, T. M. and Wise, P. M. (1996). Life-long moderate caloric restriction prolongs reproductive life span in rats without interrupting estrous cyclicity: Effects on the gonadotropin-releasing hormone luteinizing hormone axis. Biology of Reproduction *54*, 70-75.

Merry, B. J. (2002). Molecular mechanisms linking calorie restriction and longevity. International Journal of Biochemistry & Cell Biology *34*, 1340-1354.

Merry, B. J. (2004). Oxidative stress and mitochondrial function with aging - the effects of calorie restriction. Aging Cell *3*, 7-12.

Miller, R. A., Harper, J. M., Dysko, R. C., Durkee, S. J. and Austad, S. N. (2002). Longer life spans and delayed maturation in wild-derived mice. Experimental Biology and Medicine *227*, 500-508.

Moffat, S. D., Zonderman, A. B., Metter, E. J., Blackman, M. R., Harman, S. M. and Resnick, S. M. (2002). Longitudinal assessment of serum free testosterone concentration predicts memory performance and cognitive

status in elderly men. Journal of Clinical Endocrinology and Metabolism *87*, 5001-5007.

Morrell, J. M. (1997). Cryopreservation of marmoset sperm (*Callithrix jacchus*). Cryo-Letters *18*, 45-54.

Morse, D., Cermakian, N., Brancorsini, S., Parvinen, M. and Sassone-Corsi, P. (2003). No circadian rhythms in testis: Period1 expression is clock independent and developmentally regulated in the mouse. Molecular Endocrinology *17*, 141-151.

Morse, D. and Sassone-Corsi, P. (2002). Time after time: inputs to and outputs from the mammalian circadian oscillators. Trends in Neurosciences *25*, 632-637.

Mortimer, D. (1994). Practical Laboratory Andrology. (New York:Oxford University Press, Inc.).

Muehlenbein, M. P., Campbell, B. C., Murchison, M. A. and Phillippi, K. M. (2002). Morphological and hormonal parameters in two species of macaques: Impact of seasonal breeding. American Journal of Physical Anthropology *117*, 218-227.

Naz, R. K. (1999). Vaccine for contraception targeting sperm. Immunological Reviews *171*, 193-202.

Naz, R. K. and Wolf, D. P. (1994). Antibodies to sperm-specific human Fa-1 inhibit in vitro fertilization in rhesus monkeys: Development of a simian model for testing of anti-Fa-1 contraceptive vaccine. Journal of Reproductive Immunology *27*, 111-121.

Nichols, S. M. and Bavister, B. D. (2006). Comparison of protocols for cryopreservation of rhesus monkey spermatozoa by post-thaw motility recovery and hyperactivation. Reproduction Fertility and Development *18*, 777-780.

NRC. 1978. Nutrient requirements of nonhuman primates. Committee on Animal Nutrition, Agricultural Board. Washington, D.C.: National Academy of Sciences.

Okamura, H., Yamaguchi, S. and Yagita, K. (2002). Molecular machinery of the circadian clock in mammals. Cell and Tissue Research *309*, 47-56.

Oster, H., Baeriswyl, S., van der Horst, G. T. J. and Albrecht, U. (2003). Loss of circadian rhythmicity in aging mPer1(-/-) mCry2(-/-) mutant mice. Genes & Development *17*, 1366-1379.

Ottinger, M. A. (1998). Male reproduction: Testosterone, gonadotropins, and aging, in Interdisciplinary Topics in Gerontology: Functional endocrinology of aging., C. V. Mobbs and P. R. Hof, eds. (New York:S. Karger AG), 105-126.

Owen, D. H. and Katz, D. F. (2005). A review of the physical and chemical properties of human semen and the formulation of a semen simulant. Journal of Andrology *26*, 459-469.

Packer, C., Tatar, M. and Collins, A. (1998). Reproductive cessation in female mammals. Nature *392*, 807-811.

Plas, E., Berger, P., Hermann, M. and Pfluger, H. (2000). Effects of aging on male fertility? Experimental Gerontology *35*, 543-551.

Platz, C. C., Jr., Wildt, D. E., Bridges, C. H., Seager, S. W. and Whitlock, B. S. (1980). Electroejaculation and semen analysis in a male lowland gorilla, *Gorilla gorilla gorilla*. Primates *21*, 130-132.

Prummel, M. F., Brokken, L. J. S. and Wiersinga, W. M. (2004). Ultra short-loop feedback control of thyrotropin secretion. Thyroid *14*, 825-829.

Ramesh, V., Ramachandra, S. G., Krishnamurthy, H. N. and Rao, A. J. (1998). Electroejaculation and seminal parameters in bonnet monkeys (*Macaca radiata*). Andrologia *30*, 97-100.

Refinetti, R. (2005). Circadian Physiology. (Boca Raton:CRC Press).

Reppert, S. M. and Weaver, D. R. (2002). Coordination of circadian timing in mammals. Nature *418*, 935-941.

Resko, J. A., Malley, A., Begley, D. and Hess, D. L. (1973). Radioimmunoassay of testosterone during fetal development of the rhesus monkey. Endocrinology *93*, 156-161.

Rosario, E. R., Carroll, J. C., Oddo, S., LaFerla, F. M. and Pike, C. J. (2006). Androgens regulate the development of neuropathology in a triple transgenic mouse model of Alzheimer's disease. The Journal of Neuroscience *26*, 13384-13389.

Roth, G. S., Ingram, D. K., Black, A. and Lane, M. A. (2000). Effects of reduced energy intake on the biology of aging: the primate model. European Journal of Clinical Nutrition *54*, S15-S20.

Roth, G. S., Ingram, D. K. and Lane, M. A. (1999). Calorie restriction in primates: Will it work and how will we know? Journal of the American Geriatrics Society *47*, 896-903.

Roth, G. S., Lane, M. A., Ingram, D. K., Mattison, J. A., Elahi, D., Tobin, J. D., Muller, D. and Metter, E. J. (2002). Biomarkers of caloric restriction may predict longevity in humans. Science *297*, 811-811.

Roth, G. S., Mattison, J. A., Ottinger, M. A., Chachich, M. E., Lane, M. A. and Ingram, D. K. (2004). Aging in rhesus monkeys: Relevance to human health interventions. Science *305*, 1423-1426.

Rutllant, J., Pommer, A. C. and Meyers, S. A. (2003). Osmotic tolerance limits and properties of rhesus monkey (*Macaca mulatta*) spermatozoa. Journal of Andrology *24*, 534-541.

Sarason, R. L., Vandevoort, C. A., Mader, D. R. and Overstreet, J. W. (1991). The use of nonmetal electrodes in electroejaculation of restrained but unanesthetized macaques. Journal of Medical Primatology *20*, 122-125.

Schaffer, N. E., McCarthy, T. J., Fazleabas, A. T. and Jeyendran, R. S. (1992). Assessment of semen quality in a baboon (*Papio anubis*) breeding colony. Journal of Medical Primatology *21*, 47-48.

Sehgal, A., ed. (2004). Molecular Biology of Circadian Rhythms Wiley-Liss).

Selman, C., Kerrison, N. D., Cooray, A., Piper, M. D. W., Lingard, S. J., Barton, R. H., Schuster, E. F., Blanc, E., Gems, D., Nicholson, J. K., Thornton, J. M., Partridge, L. and Withers, D. J. (2006). Coordinated multitissue

transcriptional and plasma metabonomic profiles following acute caloric restriction in mice. Physiology of Genomics *27*, 187-200.

Shi, S. R., Cote, R. J. and Taylor, C. R. (2001). Antigen retrieval techniques: Current perspectives. Journal Of Histochemistry & Cytochemistry *49*, 931-937.

Shieh, K. R. (2003). Distribution of the rhythm-related genes rPERIOD1, rPERIOD2, and rCLOCK, in the rat brain. Neuroscience *118*, 831-843.

Sinclair, D. A. (2005). Toward a unified theory of caloric restriction and longevity regulation. Mechanisms of Ageing and Development *126*, 987-1002.

Slama, R., Bouyer, J., Windham, G., Fenster, L., Werwatz, A. and Swan, S. H. (2005). Influence of paternal age on the risk of spontaneous abortion. American Journal of Epidemiology *161*, 816-823.

Smith, E. E., Hennebold, J. D., Young, K. A. and Stouffer, R. L. (2002). Temporal expression of StAR and steroidogenic enzyme mRNAs in the macaque corpus luteum during the menstrual cycle. Biology of Reproduction *66*, 264-264.

Smucny, D. A., Allison, D. B., Ingram, D. K., Roth, G. S., Kemnitz, J. W., Kohama, S. G. and Lane, M. A. (2001). Changes in blood chemistry and hematology variables during aging in captive rhesus macaques (*Macaca mulatta*). Journal of Medical Primatology *30*, 161-173.

Stehle, J. H., von Gall, C. and Korf, H. W. (2003). Melatonin: A clock-output, a clock-input. Journal Of Neuroendocrinology *15*, 383-389.

Stocco, D. M. and Wang, X. J. (2006). The role of COX2 in steroidogenesis in the aging Leydig cell. 39th Annual Meeting of the Society for the Study of Reproduction; Omaha, NE: 64.

Syntin, P., Chen, H. L., Zirkin, B. R. and Robaire, B. (2001). Gene expression in brown Norway rat Leydig cells: Effects of age and of age-related germ cell loss. Endocrinology *142*, 5277-5285.

Takahashi, J. S., Turek, F. W. and Moore, R. Y., eds. (2001). Circadian Clocks (New York:Kluwer Academic/Plenum Publishers).

Tesarik, J., Mendoza-Tesarik, R. and Mendoza, C. (2006). Sperm nuclear DNA damage: update on the mechanism, diagnosis and treatment. Reproductive Biomedicine Online *12*, 715-721.

Thacker, P. D. (2004). Biological clock ticks for men, too: Genetic defects linked to sperm of older fathers. Journal of the American Medical Association *291*, 1683-1685.

Thompson, H. J., Zhu, Z. J. and Jiang, W. Q. (2002). Protection against cancer by energy restriction: All experimental approaches are not equal. Journal of Nutrition *132*, 1047-1049.

Tollner, T. L., Vandevoort, C. A., Overstreet, J. W. and Drobnis, E. Z. (1990). Cryopreservation of spermatozoa from cynomolgus monkeys (*Macaca fascicularis*). Journal of Reproduction and Fertility *90*, 347-352.

VandeVoort, C. A., Neville, L. E., Tollner, T. L. and Field, L. P. (1993). Noninvasive semen collection from an adult orangutan. Zoo Biology *12*, 257-265.

VandeVoort, C. A., Tollner, T. L. and Overstreet, J. W. (1992). Sperm zona pellucida interaction in cynomolgus and rhesus macaques. Journal of Andrology *13*, 428-432.

VandeVoort, C. A., Tollner, T. L. and Overstreet, J. W. (1994). Separate effects of caffeine and dbcAMP on macaque sperm motility and interaction with the zona pellucida. Molecular Reproduction and Development *37*, 299-304.

VandeVoort, C. A., Yudin, A. I. and Overstreet, J. W. (1997). Interaction of acrosome-reacted macaque sperm with the macaque zona pellucida. Biology of Reproduction *56*, 1307-1316.

von Gall, C., Garabette, M. L., Kell, C. A., Frenzel, S., Dehghani, F., Schumm-Draeger, P. M., Weaver, D. R., Korf, H. W., Hastings, M. H. and Stehle, J. H. (2002). Rhythmic gene expression in pituitary depends on heterologous sensitization by the neurohormone melatonin. Nature Neuroscience *5*, 234-238.

Wang, Z. N., Lewis, M. G., Nau, M. E., Arnold, A. and Vahey, M. T. (2004). Identification and utilization of inter-species conserved (ISC) probesets on Affymetrix human GeneChip platforms for the optimization of the assessment of expression patterns in non human primate (NHP) samples. Bmc Bioinformatics *5*, 165.

Weindruch, R. and Sohal, R. S. (1997). Caloric intake and aging. New England Journal of Medicine *337*, 986-994.

Weindruch, R. and Walford, R. L. (1988). The retardation of aging and disease by dietary restriction. (Springfield, IL:Charles C. Thomas).

Weinert, B. T. and Timiras, P. S. (2003). Theories of aging. Journal of Applied Physiology *95*, 1706-1716.

Wrobel, G. and Primig, M. (2005). Mammalian male germ cells are fertile ground for expression profiling of sexual reproduction. Reproduction *129*, 1-7.

Wu, J. W. (2006). Effects of moderate calorie restriction on ovarian function and decline in rhesus monkeys. Animal and Avian Sciences, University of Maryland, College Park, MD: 235, http://hdl.handle.net/1903/3497.

Yamazaki, S., Straume, M., Tei, H., Sakaki, Y., Menaker, M. and Block, G. D. (2002). Effects of aging on central and peripheral mammalian clocks. Proceedings of the National Academy of Sciences of the United States of America *99*, 10801-10806.

Yanagimachi, R. (1994). Mammalian Fertilization, in The Physiology of Reproduction, E. Knobil, J. D. Neill, et al., eds. (New York:Raven Press),

Yeoman, R. R., Ricker, R. B. and Williams, L. E. (1997). Vibrostimulation of ejaculation yields increased motile spermatozoa compared with electroejaculation in squirrel monkeys (*Saimiri boliviensis*). Contemporary Topics in Laboratory Animal Science *35*, 62-64.

Yeoman, R. R., Sonksen, J., Gibson, S. V., Rizk, B. M. and Abee, C. R. (1998). Penile vibratory stimulation yields increased spermatozoa and accessory gland production compared with rectal electroejaculation in a

neurologically intact primate (*Saimiri boliviensis*). Human Reproduction *13*, 2527-2531.

Zhang, F. P., Markkula, M., Toppari, J. and Huhtaniemi, I. (1995). Novel expression of luteinizing hormone subunit genes in the rat testis. Endocrinology *136*, 2904-2912.

Zirkin, B. R. (2006). Steroidogenic decline in aging Leydig cells: The roles of cAMP and reactive oxygen-induced damage. 39th Annual Meeting of the Society for the Study of Reproduction; Omaha, NE: 63.

Zirkin, B. R. and Chen, H. L. (2000). Regulation of Leydig cell steroidogenic function during aging. Biology of Reproduction *63*, 977-981.

Zubkova, E. V. and Robaire, B. (2006). Effects of ageing on spermatozoal chromatin and its sensitivity to in vivo and in vitro oxidative challenge in the Brown Norway rat. Human Reproduction *21*, 2901-2910.